

Abyssal fauna of polymetallic nodule exploration areas, eastern Clarion-Clipperton Zone, central Pacific Ocean: Annelida: Capitellidae, Opheliidae, Scalibregmatidae, and Traviisiidae

Helena Wiklund^{1,3,4}, Lenka Neal¹, Adrian G. Glover¹, Regan Drennan¹,
Muriel Rabone¹, Thomas G. Dahlgren^{2,3,4}

1 Life Sciences Department, Natural History Museum, London SW7 5BD, UK **2** NORCE Norwegian Research Centre, Bergen, Norway **3** Department of Marine Sciences, University of Gothenburg, Box 463, 40530 Gothenburg, Sweden **4** Gothenburg Global Biodiversity Centre, Box 463, 40530 Gothenburg, Sweden

Corresponding author: *Thomas G. Dahlgren* (thda@norceresearch.no)

Academic editor: *Chris Glasby* | Received 14 May 2019 | Accepted 2 September 2019 | Published 28 October 2019

<http://zoobank.org/7ABDE7F0-DD42-4B96-8A13-80E1E59B1515>

Citation: Wiklund H, Neal L, Glover AG, Drennan R, Rabone M, Dahlgren TG (2019) Abyssal fauna of polymetallic nodule exploration areas, eastern Clarion-Clipperton Zone, central Pacific Ocean: Annelida: Capitellidae, Opheliidae, Scalibregmatidae, and Traviisiidae. ZooKeys 883: 1–82. <https://doi.org/10.3897/zookeys.883.36193>

Abstract

We present DNA taxonomy of abyssal polychaete worms from the eastern Clarion-Clipperton Zone (CCZ), central Pacific Ocean, using material collected as part of the Abyssal Baseline (ABYSSLINE) environmental survey cruises ‘AB01’ and ‘AB02’ to the UK Seabed Resources Ltd (UKSRL) polymetallic nodule exploration contract area ‘UK-1’, the Ocean Mineral Singapore exploration contract area ‘OMS-1’ and an Area of Particular Environmental Interest, ‘APEI-6’. This is the fourth paper in a series to provide regional taxonomic data with previous papers reporting on Cnidaria, Echinodermata and Mollusca. Taxonomic data are presented for 23 species from 85 records within four polychaete families: Capitellidae, Opheliidae, Scalibregmatidae and Traviisiidae, identified by a combination of morphological and genetic data, including molecular phylogenetic analyses. Two taxa (genetically separated from one another) morphologically matched the same known cosmopolitan species, *Ophelina abbranchiata* that has a type locality in a different ocean basin and depth from where no genetic data was available. These two species were assigned the open nomenclature ‘cf.’ as a precautionary approach in taxon assignments to avoid over-estimating species ranges. Twelve (12) taxa are here described as new species, *Ammotrypanella keenani* **sp. nov.**, *Ammotrypanella kersteni* **sp. nov.**, *Ophelina curli* **sp. nov.**, *Ophelina ganae* **sp. nov.**, *Ophelina juhazi* **sp. nov.**, *Ophelina martinezarbizui* **sp. nov.**, *Ophelina meyerae* **sp. nov.**, *Ophelina nunnallyi* **sp. nov.**, *Oligobregma brasienae* **sp. nov.**, *Oligobregma tani* **sp. nov.**, *Oligobregma whaleyi* **sp. nov.** and *Travisia zieglerae*

sp. nov. For the remaining nine taxa, we have determined them to be potentially new species, for which we make the raw data, imagery and vouchers available for future taxonomic study. The CCZ is a region undergoing intense exploration for potential deep-sea mineral extraction from polymetallic nodules. We present these data to facilitate future taxonomic and environmental impact study by making both data and voucher materials available through curated and accessible biological collections.

Keywords

CCZ, deep-sea mining, molecular phylogeny, new species, Polychaeta, Scolecida, 18S, 16S, COI

Table of contents

Introduction.....	3
Materials and methods	5
Fieldwork.....	5
Laboratory work	6
Data handling.....	6
Taxonomic assignments.....	7
Systematics.....	11
Annelida	11
Capitellidae Grube, 1862.....	11
Capitellidae sp. (NHM_1486)	11
<i>Notomastus</i> M. Sars, 1851	14
<i>Notomastus</i> sp. (NHM_162).....	14
Opheliidae Malmgren, 1867	16
<i>Ammotrypanella</i> McIntosh, 1878	16
<i>Ammotrypanella keenani</i> sp. nov.	19
<i>Ammotrypanella kersteni</i> sp. nov.	20
<i>Ammotrypanella</i> sp. (NHM_1653)	23
<i>Ammotrypanella</i> sp. (NHM_2114)	25
<i>Ophelina</i> Ørsted, 1843.....	28
<i>Ophelina curli</i> sp. nov.....	28
<i>Ophelina ganae</i> sp. nov.....	30
<i>Ophelina juhazi</i> sp. nov.....	33
<i>Ophelina martinezarbizui</i> sp. nov.	35
<i>Ophelina meyeræ</i> sp. nov.....	39
<i>Ophelina nunnallyi</i> sp. nov.....	40
<i>Ophelina</i> cf. <i>abranchiata</i> Støp-Bowitz, 1948	44
<i>Ophelina</i> cf. <i>abranchiata</i> (NHM_1769)	46
<i>Ophelina</i> cf. <i>abranchiata</i> sp. (NHM_2017).....	46
<i>Ophelina</i> sp. (NHM_689)	49
<i>Ophelina</i> sp. (NHM_1068)	49
<i>Ophelina</i> sp. (NHM_1331)	51

Scalibregmatidae Malmgren, 1867	54
<i>Oligobregma brasierae</i> sp. nov.	56
<i>Oligobregma tani</i> sp. nov.	60
<i>Oligobregma whaleyi</i> sp. nov.	63
Scalibregmatidae sp. (NHM_2308)	65
Travisiidae Hartmann-Schröder, 1971.....	66
<i>Travisia</i> Johnston, 1840	66
<i>Travisia zieglerae</i> sp. nov.	68
<i>Travisia</i> sp. (NHM_1244)	71
Discussion.....	75
Acknowledgements.....	75
References	76

Introduction

In the last decades there has been rapid growth in the commercial exploration of the abyssal deep sea for mineral resources (Gollner et al. 2017). One area that has received particular attention is the Clarion-Clipperton Zone (CCZ) in the central Pacific Ocean which is extremely rich in high-grade polymetallic nodules (Baker and Beaudoin 2013; Hein et al. 2013). There is no strict definition of the region, which lies in international waters, but it has come to be regarded as the area between the Clarion and Clipperton Fracture Zones. Exploration licenses issued by the International Seabed Authority (ISA 2017) extend from 115°W (the easternmost extent of the UK-1 claim) to approximately 158°W (the westernmost extent of the COMRA claim). As such we use from hereafter a working definition of the CCZ as the box: 13°N, 158°W; 18°N, 118°W; 10°N, 112°W; 2°N, 155°W. This is an area of almost 6 million km², approximately 1.4% of the ocean's surface, that is undergoing intense deep-sea mineral exploration for high-grade polymetallic nodules regulated by Sponsoring States (nation states that support a contractor) and the International Seabed Authority.

Annelida is one of the most abundant macrofauna groups on soft bottoms at abyssal depths (e.g. Hessler and Jumars 1974), and in the deep sea the annelid species diversity is generally high even when abundance is low. Quantitative comparisons provide evidence that the central Pacific abyss harbors the highest known deep-sea annelid diversity (Neal et al. 2011), and a recent review of global taxonomic records reported 276 species at depths between 4000 and 5000 m (Paterson et al. 2009). Online database sources prior to 2018 listed only 12 annelid records within or adjacent to the entire 6 million km² of CCZ as defined above (OBIS 2018). Nine of these records are identified to family only as they were observed from remotely operated vehicle (ROV) footage (Amon et al. 2017). Two records have their type locality within the CCZ, *Prionospio branchilucida* Altamira, Glover & Paterson in Paterson et al. 2016 and *Kirkegaardia fragilis* Blake, 2016. The last of these records, collected in

1899 just northwest of CCZ, is *Eunice antillensis* Ehlers, 1887, although the identity of that record is dubious as the type locality for that species is in Gulf of Mexico at 185 m depth (Ehlers 1887).

In terms of recent molecular studies, Janssen et al. (2015) published 556 COI sequences from polychaetes collected in the German and French license areas, but most taxa were identified to family or genus level or in a few cases tentative species names using ‘cf.’ to register similarity but with a precautionary approach. In a paper based on samples collected in the easternmost part of the CCZ, 278 specimens of polynoid polychaetes are reported belonging to ~80 molecular operational taxonomic units (MOTU), including the formal description of 17 new species and four new genera (Bonifácio and Menot 2018). Thus, despite a large number of both mineral exploration and purely scientific expeditions to the CCZ area, not much of the collected macrofauna have been properly identified and entered in publicly accessible museums and biogeographic databases. This is in part due to the fact that most of the species are new to science (e.g. Glover et al. 2002), and the lack of taxonomic guides leads to published species lists that record, for example, only ‘sp. A’, ‘sp. B’, etc., which makes species-level comparisons over a larger area infeasible and presents major issues for the long-term iterative improvement of taxonomic knowledge (Glover et al. 2018).

The DNA taxonomy part of the UK Seabed Resources (UKSR) program aims to fill some gaps in our knowledge and make data publicly available that will eventually allow for a complete taxonomic synthesis of the CCZ supported by openly available molecular and morphological data. We present results from a DNA taxonomy survey of abyssal benthic annelids collected as part of the UKSR ABYSSLINE cruises ‘AB01’ and ‘AB02’ to the UK Seabed Resources Ltd (UKSRL) polymetallic nodule exploration contract area ‘UK-1’, Ocean Mineral Singapore contract area ‘OMS-1’, and an Area of Particular Environmental Interest, ‘APEI-6’, (Fig. 1) in the eastern CCZ (Smith et al. 2013, 2015). Here we provide the first part of the Annelida taxonomic synthesis consisting of taxon records, images, genetic data and morphological descriptions from the first research cruise (AB01) aboard the RV *Melville* in October 2013 and the second (AB02) aboard the RV *Thomas G. Thompson* in February and March 2015. This part contains the families Capitellidae, Opheliidae, Scalibregmatidae and Traviisiidae, and includes 12 new species descriptions. The etymology of the new taxon names is based on a randomised list of members (crew and scientists) of the two research cruises to recognise the team effort involved in this extensive sampling program. This publication is supported by similar data publications on other taxa from the CCZ. The published papers include Echinodermata (Glover et al. 2016b), Cnidaria (Dahlgren et al. 2016), and Mollusca (Wiklund et al. 2017), while other taxa are in preparation, forming a suite of taxonomic syntheses of biodiversity in the region, supported by a contract between the UKSRL, the Natural History Museum, London and NORCE Norwegian Research Centre, Bergen.

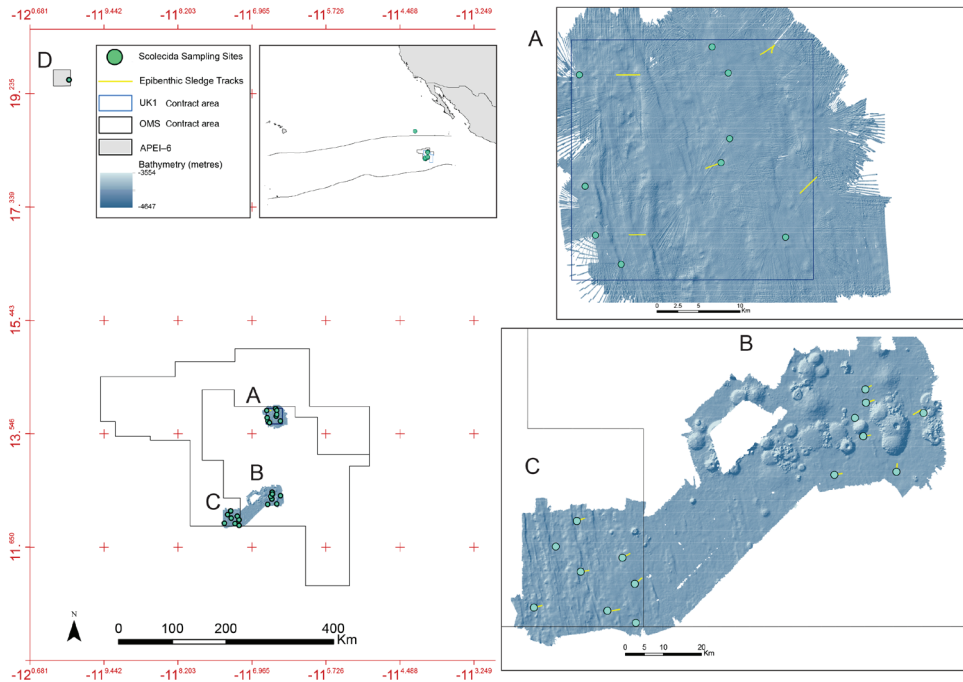


Figure 1. Map over sampling sites. **A** UK-1 Stratum-A **B** UK-1 Stratum-B study areas, both within the UK Seabed Resources UK-1 exploration contract area **C** OMS Stratum-A study area, in the Ocean Mineral Singapore (OMS) polymetallic nodule exploration contract area **D** Area of Particular Interest APEI-6. Inset map showing location of Clarion-Clipperton Fracture Zone. Bathymetric survey and sample localities from the AB01 2013 RV *Melville* survey cruise and AB02 2015 *Thomas G. Thompson* survey cruise, data courtesy Craig R. Smith (University of Hawaii), UK Seabed Resources Ltd and Seafloor Investigations, LLC.

Materials and methods

Fieldwork

The first UKSR ABYSSLINE cruise (AB01), sampling the UK-1 exploration contract area, took place in October 2013 aboard the RV *Melville*, and the second cruise (AB02), sampling the UK-1 and OMS-1 exploration contract areas and APEI-6, took place in February-March 2015 onboard RV *Thomas G. Thompson*.

A comprehensive description of our DNA taxonomy pipeline is provided in Glover et al. (2016a). In summary, deep-sea benthic specimens from the UK-1, OMS-1 and APEI-6 areas were collected using a range of oceanographic sampling gear including box core, epibenthic sledge (EBS), ROV and multiple core. Geographic data from sampling activities were recorded on a central GIS database (Fig. 1). Live-sorting of specimen samples was carried out aboard both vessels in a ‘cold-chain’ pipeline, in which material was constantly maintained in chilled, filtered seawater held at 2–4 °C. Specimens were preliminar-

ily identified at sea and imaged live using stereo microscopes with attached digital cameras (Glover et al. 2016a). The specimens were then stored in individual microtube vials containing an aqueous solution of 80% non-denatured ethanol, numbered and barcoded into a database and kept chilled until return to the Natural History Museum, London, UK.

Laboratory work

In the laboratory, specimens were re-examined using stereo and compound microscopes, identified and described to the best possible taxonomic level with key morphological features photographed with digital cameras and a small tissue-sample taken for DNA extraction. Shirlastain A and Methyl Green stain were used during the morphological examination on some specimens, in order to better observe certain characters. Methyl Green stain was limited to Capitellidae, as the staining pattern is considered of value in capitellid taxonomy (e.g. Blake 2009). The other taxa were stained exclusively with Shirlastain A. Scanning electron microscopy (SEM) using a SEM FEI Quanta 650 was conducted on several whole specimens, following a preparation of graded ethanol dehydration, critical point drying, and gold coating. Figures were assembled using Adobe Photoshop CS6 software. A fine white or black line was used to outline and highlight particular morphological features where such features were unclear from images alone.

Extraction of DNA was done with DNeasy Blood and Tissue Kit (Qiagen) using a Hamilton Microlab STAR Robotic Workstation. About 1800 bp of 18S, 450 bp of 16S, and 650 bp of cytochrome c oxidase subunit I (COI) were amplified using primers listed in Table 1. PCR mixtures contained 1 µl of each primer (10 µM), 2 µl template DNA and 21 µl of Red Taq DNA Polymerase 1.1X MasterMix (VWR) in a mixture of total 25 µl. The PCR amplification profile consisted of initial denaturation at 95 °C for 5 min, 35 cycles of denaturation at 94 °C for 45 s, annealing at 55 °C for 45 s, extension at 72 °C for 2 min, and a final extension at 72 °C for 10 min. PCR products were purified using Millipore Multiscreen 96-well PCR Purification System, and sequencing was performed on an ABI 3730XL DNA Analyser (Applied Biosystems) at The Natural History Museum Sequencing Facility, using the same primers as in the PCR reactions plus two internal primers for 18S (Table 1). Overlapping sequence fragments were merged into consensus sequences using Geneious (Kearse et al. 2012) and aligned using MAFFT (Kato et al. 2002) for 18S and 16S, and MUSCLE (Edgar 2004) for COI, both programs used as plugins in Geneious, with default settings. Bayesian phylogenetic analyses were conducted with MrBayes 3.2.6 (Ronquist et al. 2012). Analyses were run for 10–30 million generations, of which the first 25% generations were discarded as burn-in.

Data handling

The field and laboratory work created a series of databases and sample sets that are integrated into a data-management pipeline. This includes the transfer and management of data and samples between a central collections database, a molecular

Table 1. Primers used for PCR and sequencing of 18S, COI and 16S.

Primer	Sequence 5'-3'	Reference
18S		
18SA	AYCTGGTTGATCCTGCCAGT	Medlin et al. 1988
18SB	ACCTTGTACGACTTTTACTTCCTC	Nygren and Sundberg 2003
620F	TAAAGYTGYTGACAGTTAAA	Nygren and Sundberg 2003
1324R	CGGCCATGCACCACC	Cohen et al. 1998
COI		
LCO1490	GGTCAACAAATCATAAAGATATTGG	Folmer et al. 1994
HCO2198	TAAACTTCAGGGTGACCAAAAAATCA	Folmer et al. 1994
COI-E	TATACTTCTGGGTGTCCGAAGAATCA	Bely and Wray 2004
polyLCO	GAYTATWTTCAACAAATCATAAAGATATTGG	Carr et al. 2011
polyHCO	TAMACTTCWGGGTGACCAARAATCA	Carr et al. 2011
16S		
ann16SF	CGGGTATCCTGACCGTRCWAAGGTA	Sjölin et al. 2005
16SbrH	CCGGTCTGAACTCAGATCACGT	Palumbi 1996

collections database and external repositories (GenBank, WoRMS, OBIS, GBIF, GGBN, ZooBank) through DarwinCore archives and usage of the GGBN data standard (Droege et al. 2014). This provides a robust data framework to support DNA taxonomy, in which openly available data and voucher material is key to quality data standards. A further elaboration of the data pipeline is published in Glover et al. (2016a).

Taxonomic assignments

Future studies of biogeographic and bathymetric ranges, gene-flow, extinction risks, natural history, reproductive ecology, functional ecology and geochemical interactions of CCZ species are dependent on accurate taxonomic identifications. This taxonomy is dependent on a sound theoretical underpinning—a species concept—coupled with the availability of both raw data and voucher samples. Here we use a phylogenetic species concept sensu Donoghue (1985) with species determined by DNA-based phylogenetic analysis. For those taxa where the morphological data that allows description of a new species is missing, we provide the lowest-level taxonomic name possible aided by phylogenetic information. In these cases, we use an informal naming system where the best available voucher specimen number is used as the informal species name, for example *Notomastus* sp. (NHM_162) is the informal species name for all specimens that are the same species as the specimen number NHM_162. This avoids confusion with the use of sp. A, B, C, etc. where informal and confusing synonyms can easily arise. Type material, DNA specimen vouchers and DNA extractions are deposited at the Natural History Museum, London. A full list of all taxa including Natural History Museum Accession Numbers (NHMUK), NHM Molecular Collection Facility (NHM-MCF), and NCBI GenBank accession numbers is provided in Table 2.

Table 2. Taxon treatments presented in this paper. Includes family, DNA taxonomy ID (a species-level identification based on combined DNA and morphological evidence), GUID (Global Unique Identifier link to data record at <http://data.nhm.ac.uk>), ABYSSLINE record number, NHM accession number, NHM Molecular Collection Facility (MCF) sample ID number (NHMUK_MCF#) and NCBI GenBank accession number (Genbank#) for successfully sequenced genetic markers. GenBank numbers for phylogenetic analysis data downloaded from GenBank are presented in Supplementary material 1.

Family	DNA taxonomy ID	ABYSSLINE record	GUID	NHMUK Record no.	NHMUK MCF no.	Genbank no.
Capitellidae	Capitellidae sp. (NHM_1486)	NHM_613	bc34eb86-fc0c-411c-8eb9-e86774c6515a	2019.7105	0109494702	MN217415 MN217495
		NHM_1486	05d46c60-8b4d-4623-b7ff-2e8089453d7e	2019.7106	0109494649	MN217416 MN217496
	<i>Notomastus</i> sp. (NHM_162)	NHM_162	f34e2921-7b6d-4c14-b217-690d9315f073	2019.7100	0109494624	MN217417 MN217497
		NHM_915B	98291a2a-c89a-4ff62-bde5-91171368c749	2019.7101	0109494712	MN217418
		NHM_1025D	3e34e783-a51b-4a84-bc2e-6a19bac82b4e	2019.7102	0109494679	MN217419
		NHM_1200	2612dd53-ccc5-47b9-aeed-c321bda6c3d8	2019.7103	0109494687	MN217420
		NHM_1948J	24374a21-17b6-4de5-8436-18c160aa5c8d	2019.7104	0109494636	MN217421
Opheliidae	<i>Ammotrypanella keenani</i> sp. nov.	NHM_1166C	483c6faa-0338-4cf5-a21d-6f448c72f4aa	2019.7109	0109494704	MN217408 MN217513
		NHM_1250 (holotype)	1514d25d-b485-4b90-8981-3e84381bf250	2019.7110	0109494644	MN217409 MN217491 MN217514
		NHM_1871 (paratype)	d93680b5-a3a3-4623-afc4-17062e1a1a58	2019.7111	0109494707	MN217410
		NHM_1949	cff2696d-06ab-42a1-843e-6ef894872f32	2019.7112	0109494683	MN217411
	<i>Ammotrypanella kersteni</i> sp. nov.	NHM_254 (holotype)	3441cd68-7432-4dec-8415-966b104c3077	2019.7107	0109494672	MN217412 MN217492 MN217515
	<i>Ammotrypanella</i> sp. (NHM_1653)	NHM_1653	a2f7ed04-7275-4a57-a058-bd750cacc715	2019.7108	0109494685	MN217413 MN217493 MN217516
	<i>Ammotrypanella</i> sp. (NHM_2114)	NHM_2114	f4492dd1-8088-47c6-97d9-32e43ae99552	2019.7113	0109494699	MN217414 MN217494
	<i>Ophelina curli</i> sp. nov.	NHM_2112 (holotype)	c1554f01-2324-4d8d-b775-dca42f5918e7	2019.7131	0109494716	MN217435 MN217502
	<i>Ophelina ganax</i> sp. nov.	NHM_245	3a34b9cb-504b-48a3-a8e9-93077ec69520	2019.7140	0109494696	MN217436 MN217503 MN217521
		NHM_248	e67f7724-8c9f-4463-943e-7cda20441728	2019.7141	0109494197	MN217437
		NHM_473	79dcab18-936b-430e-b770-6aab60d285c5	2019.7142	0109494671	MN217438 MN217522
		NHM_598 (paratype)	2fa20a59-8bb3-4ef8-b2e9-efccbe2c9414	2019.7143	0109494713	MN217439
		NHM_708	2077c6c6-0e3e-4dfa-97a0-16d6c386ff07	2019.7144	0109494665	MN217440
NHM_1098		5661fb64-83a2-4e9a-b3c3-a8405705ed1a	2019.7145	0109494631	MN217441	
NHM_1137 (holotype)		11616c16-bdb5-4813-9d17-7170bb62702b	2019.7146	0109494711	MN217442	
NHM_1309 (paratype)		1ff41b52-9801-4b2e-8e01-ea34597b708d	2019.7147	0109494639	MN217523	

Family	DNA taxonomy ID	ABYSSLINE record	GUID	NHMK Record no.	NHMK MCF no.	Genbank no.
Opheliidae	<i>Ophelina jubazi</i> sp. nov.	NHM_1073 (holotype)	f7330230-224b-49e7-aa80-41e8654ea087	2019.7132	0109494655	MN217443 MN217504
	<i>Ophelina martinezarbizui</i> sp. nov.	NHM_681 (holotype)	0de17415-a8bf-4461-a663-dea9a3e6a2b9	2019.7116	0109494717	MN217444 MN217505 MN217524
		NHM_718	f6e2fa9b-a479-4e0d-aec6-57efff6987b2	2019.7117	0109494693	MN217445 MN217525
		NHM_883	d9a3a3b3-c16e-4359-8eb0-f09deed98401	2019.7118	0109494627	MN217446 MN217526
		NHM_994	4f6d2b7a-169f-46a9-8b3b-5d91a021aa34	2019.7119	0109494626	MN217447
		NHM_1066	972f9cb1-79d7-4296-a6d6-e04543c9105c	2019.7120	0109494664	MN217448
		NHM_1766 (paratype)	dc754b1c-e66b-4a58-a93e-796ebfd32f6a	2019.7121	0109494658	MN217449 MN217527
		NHM_1870	b6247e8d-d155-4646-87d7-e5358ada5352	2019.7122	0109494708	MN217450
		NHM_2088	7dd04f2c-435b-44b1-a85f-3b05dd3014d7	2019.7123	0109494669	MN217451
		NHM_2092	1a095836-fa97-48b8-ad4c-07ed28356ceb	2019.7124	0109494650	MN217528
		NHM_2102	93e91313-61a3-4cd7-8221-66bf20232f14	2019.7125	0109494645	MN217452 MN217529
		NHM_2116 (paratype)	d439156e-657d-4dd5-8bb5-3531e150961e	2019.7126	0109494692	MN217453 MN217530
		NHM_2144	79767cab-eb56-4ef1-acd0-5067ec3736de	2019.7127	0109494668	MN217454
		NHM_2149	1caa9eb3-3281-4ed6-8424-dfaebcf1e20b	2019.7128	0109494675	MN217455
		NHM_2150	993f577c-ee86-4660-b2d9-af0146606f92	2019.7129	0109494651	MN217456 MN217531
	<i>Ophelina meyerana</i> sp. nov.	NHM_1241 (holotype)	920d8670-507e-4126-a42b-6e208bbe66d3	2019.7130	0109494220	MN217457 MN217506
	<i>Ophelina numallyi</i> sp. nov.	NHM_683 (holotype)	220fa671-4576-45b7-930d-efde148f223f	2019.7133	0109494235	MN217458 MN217507 MN217532
		NHM_700 (paratype)	63115f48-bcf1-4b3b-9c2e-c339b97845bd	2019.7134	0109494678	MN217459
		NHM_783F	376a42db-0497-4b4a-851b-c1d5e07bd2b6	2019.7135	0109494630	MN217460
		NHM_1273 (paratype)	a3540563-8a0c-475b-96b5-12969fb8c2ba	2019.7136	0109494663	MN217461 MN217533
		NHM_1309A	25066e63-ec9-439a-9907-eaeab72e78c	2019.7137	0109494656	MN217462 MN217534 MN217433
	<i>Ophelina</i> cf. <i>abranchiata</i> sp. (NHM_1769)	NHM_1769	8a2cbe4f-277d-4355-a34f-0b53c797bef0	2019.7148	0109494637	MN217501 MN217520
	<i>Ophelina</i> cf. <i>abranchiata</i> sp. (NHM_2017)	NHM_2017	9ebcd947-c53b-4616-81d4-da42afaeca03	2019.7149	0109494660	MN217434
	<i>Ophelina</i> sp. (NHM_689)	NHM_689	6755d584-a20a-4ce5-a4f1-32ce0965128e	2019.7114	0109494689	MN217463 MN217508
	<i>Ophelina</i> sp. (NHM_1068)	NHM_1068	b28fd52f-5717-45e3-b0cc-369172a690e5	2019.7138	0109494646	MN217464 MN217509
		NHM_1874	c3ffe5f4-6ca3-4816-966c-25ec98bbb003	2019.7139	0109494684	MN217466
	<i>Ophelina</i> sp. (NHM_1331)	NHM_1331	06d48d7f-7339-4cc5-8445-b51a980e4e0f	2019.7115	0109494710	MN217465 MN217510

Family	DNA taxonomy ID	ABYSSLINE record	GUID	NHMUK Record no.	NHMUK MCF no.	Genbank no.	
Scalibregmatidae	<i>Oligobregma brasierae</i> sp. nov.	NHM_032	43545746-b8ad-43a8-92b7-53637dd131d6	2019.7150	0109494647	MN217422	
		NHM_404	5fda0cac-0a77-4ec7-a2fa-5cd529548a19	2019.7151	0109494694	MN217423	
		NHM_684 (paratype)	d84c37ed-138e-4064-a11d-a11a2470dfdf	2019.7152	0109494698	MN217424 MN217498 MN217517	
		NHM_823 (holotype)	74781dbb-1f65-4839-a766-24d6cde63ed0	2019.7153	0109494676	MN217425	
		NHM_1423 (paratype)	d949e987-6e03-4092-8492-c51dd7fcf4d7	2019.7154	0109494681	MN217426	
		NHM_1895	02aaa9c0-837a-4836-8b34-5c68296c958e	2019.7155	0109494643	MN217427	
	<i>Oligobregma tani</i> sp. nov.	NHM_773A (paratype)	4b673a6a-9090-4c24-a4eb-231190507b60	2019.7156	0109494629	MN217428 MN217499 MN217518	
		NHM_1454 (holotype)	67d3f58a-9c13-423e-93b7-3ddcf98a361e	2019.7157	0109494662	MN217429	
		NHM_1480	d47f17aa-c0c1-44f0-a448-d3f3c395fc47	2019.7158	0109494633	MN217430	
		NHM_1665 (paratype)	eca166ae-3fe0-4367-860f-08c7410165dd	2019.7159	0109494661	MN217431 MN217519	
	<i>Oligobregma whaleyi</i> sp. nov.	NHM_822 (holotype)	dde1c8f9-f87a-430b-be9d-5e34685772bb	2019.7160	0109494667	MN217432 MN217500	
	Scalibregmatidae sp. (NHM_2308)	NHM_2308	7b9d4ab8-4b7b-45c4-9cf4-6fd6b1229f48	2019.7161	0109494623	MN217467	
	Travisiidae	<i>Travisia zieglerae</i> sp. nov.	NHM_140 (paratype)	ed10356b-32a0-4b45-9fe3-c56fbc696e87	2019.7162	0109494719	MN217470 MN217512
			NHM_188	c8a0ef70-e7f7-4605-bf78-dc54ed9151eb	2019.7170	0109494718	MN217471
			NHM_241	5c0ac0b7-60cc-473e-a23b-2f49a40540f4	2019.7163	0109494648	MN217472
			NHM_356	8d2cbf0e-6522-403d-a58a-905fb13c70d6	2019.7164	0109494697	MN217473
			NHM_364	ef6e520f-7ef5-4ff9-87b5-985b8576271f	2019.7165	0109494673	MN217474
			NHM_748B (paratype)	db527676-1030-4bf0-b28d-2382825bc6bf	2019.7166	0109494654	MN217475
NHM_753			393203b1-cb80-4185-9e40-fca6e1b6fe34	2019.7167	0109494715	MN217476	
NHM_760			d3e8ec3c-d7f3-4908-b315-84f3758aacc1	2019.7168	0109494691	MN217477	
NHM_792			5d30a61b-5894-484f-b79a-df1cd4268ec1	2019.7169	0109494641	MN217478	
NHM_909 (paratype)			5f570dab-4b56-4f74-b126-ed6ceab344e3	2019.7171	0109494670	MN217479	
NHM_970			4ccb364c-35f4-458c-9c71-6f77e71493ca	2019.7172	0109494703	MN217480	
NHM_1097			939ba16d-b844-49ca-a740-bb42f039cc11	2019.7173	0109494625	MN217481	
NHM_1310			16844478-de27-448c-9acb-057835026447	2019.7174	0109494690	MN217482	
NHM_1311			192cbbb3-680b-4bcd-9cc4-a420f42af578	2019.7175	0109494700	MN217483	
NHM_1431 (holotype)			fd6bab0e-0cda-4b42-808f-a6006d409535	2019.7176	0109494211	MN217484	
NHM_1543 (paratype)	c78cc5fd-ca98-43b0-a0fb-8804fb606c71	2019.7177	0109494628	MN217485			

Family	DNA taxonomy ID	ABYSSLINE record	GUID	NHMUK Record no.	NHMUK MCF no.	Genbank no.
Travisiidae	<i>Travisia zieglerae</i> sp. nov.	NHM_1873	24409a12-2a50-4689-80dc-902cdeb5af69	2019.7178	0109494642	MN217486
		NHM_1883	9e8c22f7-a94b-45ed-a1d0-cae287a7ac2d	2019.7179	0109494666	MN217487
		NHM_1911	489dd5a6-2c68-416b-9a06-ed773d4791d6	2019.7180	0109494632	MN217488
		NHM_2019	2684a5f8-b4d4-4bcb-b386-65775506cf87	2019.7181	0109494659	MN217489
		NHM_2024	cf54f81e-5836-4684-94dc-151f589ebab4	2019.7182	0109494653	MN217490
	<i>Travisia</i> sp. (NHM_1244)	NHM_1244	f6906eae-67ec-4d37-83c6-590f3c53df76	2019.7183	0109494714	MN217468
		NHM_1863	fa708aca-6dd1-4b53-8d54-c76a93f43363	2019.7184	0109494652	MN217469 MN217511

Systematics

Annelida

Capitellidae Grube, 1862

Notes. Capitellidae represent an important group of polychaetes owing to their use as indicators of environmental health (e.g., Tomassetti and Porrello 2005). Despite their importance, capitellids have a confused and unresolved taxonomy, with a large number of often monotypic genera and the presence of species complexes. Capitellid genera are distinguished largely on chaetal distribution in anterior segments and the number of thoracic segments (see e.g., Blake 2000a; Fauchald 1972). The need for revision of the family has been deemed necessary by several authors (e.g., Fauchald 1977; Ewing 1991; Blake 2000a), as it has been observed that chaetal distribution, particularly in the posterior thorax, may change with age (e.g., Ewing 1982; 1984; Blake 2000a). Green (2002) provided a useful overview of characters used in capitellid taxonomy.

At least two species were recognised in the UKSR material, five poorly preserved representatives of a species in the diverse genus *Notomastus*, and two specimens of a species representing a new genus based on morphological and genetic data. However, given the caveats of generic definitions given above, we choose not to provide the formal description of this species and genus, and make these data and vouchers available for future revision.

Capitellidae sp. (NHM_1486)

Fig. 2A–G

Material examined. NHM_613 NHMUK ANEA 2019.7105, coll. 17 Feb. 2015, 12°23.175N, 116°32.92W, 4202 m <http://data.nhm.ac.uk/object/be34eb86-fc0c-411c-8eb9-e86774c6515a>; NHM_1486 NHMUK ANEA 2019.7106, coll. 04 Mar.

2015, 12°29.70N, 116°39.01W, 4260 m <http://data.nhm.ac.uk/object/05d46c60-8b4d-4623-b7ff-2e8089453d7e>.

Description. Species represented by one anterior fragment and one body fragment only. Specimen NHM_1486 posteriorly incomplete, 8 mm long and 0.6 mm wide for about 22 chaetigers (posterior part of fragment is damaged). Preserved specimens creamy white in ethanol (Fig. 2A); live specimens creamy yellow to white semi-translucent (Fig. 2B). Epithelium smooth (Fig. 2).

Prostomium conical, anteriorly broadly rounded, slightly longer than wide (Fig. 2C). Eyespots not observed. Nuchal organs everted, lightly pigmented, located at posterior border of prostomium. Peristomium as a narrow, smooth, achateous ring.

Chaetigers 1–10 (= thorax) with capillaries only. First chaetiger with chaetae in notopodia only, subsequent nine chaetigers with chaetae in both noto- and neuropodia. All thoracic chaetae slender, bilimbate capillaries (Fig. 2D), arranged in two rows, with alternating longer and shorter capillaries, about 10 chaetae per ramus. Genital pores or lateral organs not observed under light microscopy.

Chaetigers 11–12 are considered transitional between thorax and abdomen marked by appearance of hooded hooks only in neuropodia, but segments are of similar thickness to those in anterior part of body (Fig. 2E).

Abdominal segments enlarged (inflated), without lobe (Fig. 2A). All abdominal chaetigers with capillary chaetae only in notopodia and hooded hooks only in neuropodia. Abdominal capillaries similar to those in thorax, about 15 per ramus. Hooded hooks with long and slender shaft, with swelling around mid-point of shaft; with a main fang and about three rows of small teeth (Fig. 2F); about 15 hooks per ramus. Remainder of body unknown.

Methyl green stain. Prostomium, chaetigers 4–6 and abdominal chaetigers do not stain (or at best stain very lightly). Peristomium, chaetigers 1–3 and 7–12/13 stain more strongly (Fig. 2G).

Genetic data. GenBank MN217415–MN217416 for 16S and MN217495–MN217496 for 18S. COI was unsuccessful for this species, no identical matches on GenBank for 16S or 18S. The species is distinct from all other specimens in this study and in our phylogenetic analyses forms an unresolved clade with *Barantolla lepte* Hutchings, 1974, three *Notomastus* M. Sars, 1851 and one *Heteromastus* Eisig, 1887 species (Fig. 4).

Remarks. This species is unusual amongst Capitellidae due to its large number of mixed segments (with capillaries only in notopodia and hooded hooks only in neuropodia). Usually, the abdominal chaetigers in Capitellidae bear hooded hooks only, or there are a small number of posterior thoracic and/or anterior abdominal segments that bear both capillaries and hooks. Of the known genera, only *Promastobranchnus* Gallardo, 1968 shows such chaetal distribution. However, it can be distinguished from the other UKSR-collected species in having the first chaetiger with both noto- and neurochaetae and possessing 12 to 13 instead of 10 chaetigers with capillary chaetae in both rami. Therefore, this material represents not only a new species, but based on current

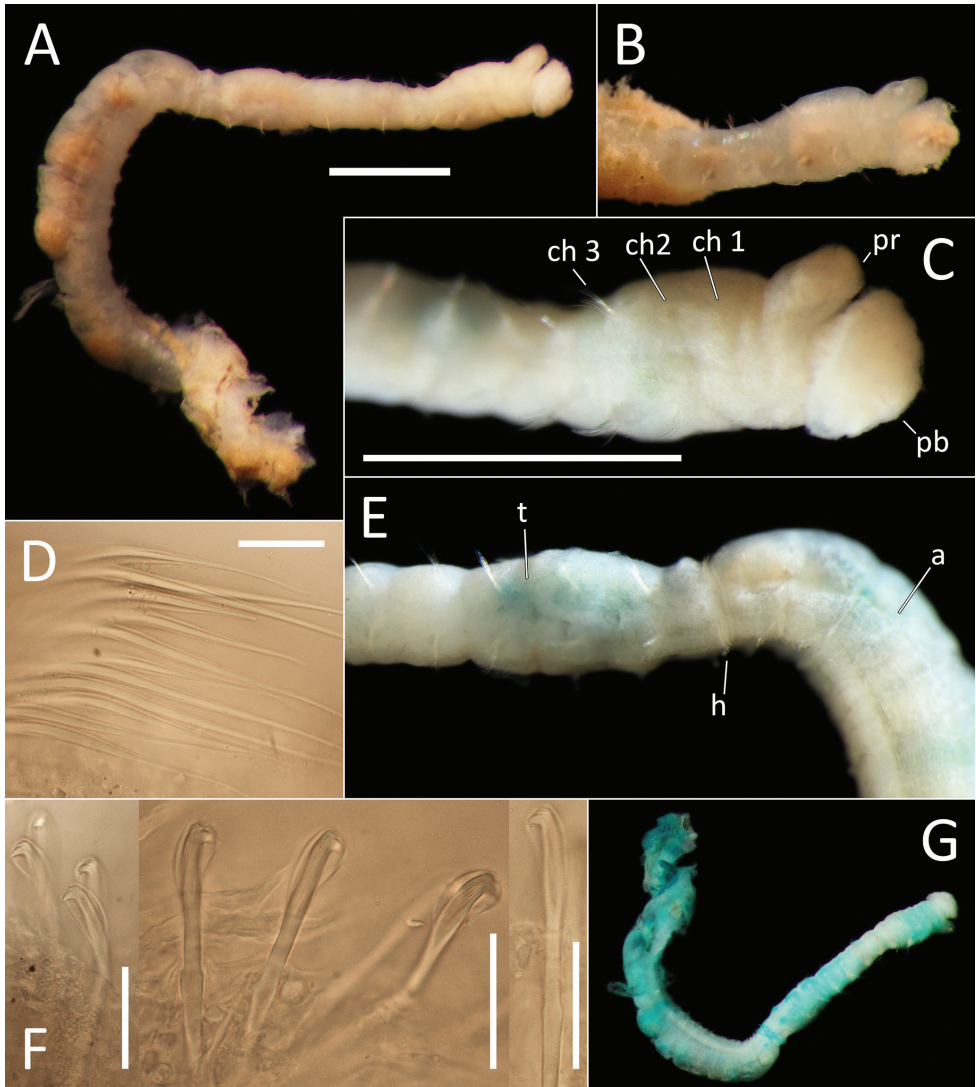


Figure 2. Capitellidae sp. NHM_1486 (specimen NHM_1486). **A** Lab image, whole specimen **B** Live image, anterior **C** Lab image, anterior, highlighting first three chaetigers (faded stain, pr = prostomium, pb = proboscis) **D** Lab image, thoracic capillary chaetae **E** Lab image, transitional chaetigers between thorax and abdomen (faded stain) (t = thorax, h = hooks, a = abdomen) **F** Lab image, hooks **G** Lab image, whole specimen (methyl green stain). Scale bars: 1 mm (**A**, **C**); 25 μ m (**D**, **F**).

morphological criteria supported also by genetic data, a new genus as well. Because the material is not complete (morphology for the posterior end is missing) the species is here not formally described.

Ecology. Found in the eastern polymetallic nodule province of the CCZ.

Notomastus* M. Sars, 1851**Notomastus* sp. (NHM_162)**

Fig. 3A–I

Material examined. NHM_162 NHMUK ANEA 2019.7100, coll. 13 Oct. 2013, 13°57.794N, 116°34.093W, 4084 m <http://data.nhm.ac.uk/object/f34e2921-7b6d-4c14-b217-690d9315f073>; NHM_915B NHMUK ANEA 2019.7101, coll. 23 Feb. 2015, 12°34.28N, 116°36.63W, 4198 m <http://data.nhm.ac.uk/object/98291a2a-c89a-4f62-bde5-91171368c749>; NHM_1025D NHMUK ANEA 2019.7102, coll. 24 Feb. 2015, 12°08.02N, 117°17.52W, 4122 m <http://data.nhm.ac.uk/object/3e34e783-a51b-4a84-bc2e-6a19bac82b4e>; NHM_1200 NHMUK ANEA 2019.7103 coll. 27 Feb. 2015, 12°00.567N, 117°10.687W, 4144 m <http://data.nhm.ac.uk/object/2612dd53-cce5-47b9-aeed-c321bda6c3d8>; NHM_1948J NHMUK ANEA 2019.7104, coll. 13 Mar. 2015, 12°02.49N, 117°13.03W, 4094 m <http://data.nhm.ac.uk/object/24374a21-17b6-4de5-8436-18c160aa5c8d>.

Description. All specimens short anterior fragments, posteriorly incomplete with thorax only or thorax and 2–5 abdominal segments only. Small species, 2–4 mm long and 0.3–0.8 mm wide for 11–16 chaetigers. Preserved specimens creamy white in ethanol; live specimens white to light brown semi-opaque/translucent. Epithelium of peristomium and first two chaetigers smooth or at best weakly annulated, on chaetigers 3–11 epithelium tessellated, distinctly bi-annulated (Fig. 3A–D).

Prostomium low, rounded mound (Fig. 3D). Eyespots not observed. Nuchal organs inconspicuous. Peristomium as a broad, non-tessellated, achateous ring.

Thorax with 11 chaetigers, first with notochaetae only. All thoracic chaetae long, slender, bilimbate capillaries (Fig. 3G). Genital pores and lateral organs not observed under light microscopy. Transition between thorax and abdomen marked abruptly by the segment size, neuropodia development and chaetal type.

Abdominal segments with hooded hooks only in both rami. Noto- and neuropodia free laterally, notopodia widely separated dorsally. Abdominal notopodia coalesce into lobe, which protrudes from dorsum (Fig. 3E). Superior edges of the neuropodia taper to broadly rounded lobes (Fig. 3F, G). All abdominal chaetae hooded hooks, about 45 per ramus (Fig. 3H). All hooded hooks similar in shape on noto- and neuropodia; hooks with long shaft, with swelling at mid-point; with a main fang and rows of small teeth. The rest of the body unknown.

Methyl green stain. Anterior fragment with 13 chaetigers staining more or less uniformly; more pronounced in chaetigers 6–11 (Fig. 3I).

Genetic data. GenBank MN217417–MN217421 for 16S, MN217497 for 18S. COI was unsuccessful for this species, no identical matches on GenBank for 16S or 18S. In our phylogenetic tree *Notomastus* sp. (NHM_162) is sister to *Notomastus latericeus* M. Sars, 1851, but the genus *Notomastus* is not monophyletic in our tree (Fig. 4).

Remarks. This species is consistent with the genus *Notomastus* in possessing 11 chaetigers with notochaetae only, followed by abdominal chaetigers with hooded hooks only. As the specimens are poorly preserved with the thorax only or with 2–5

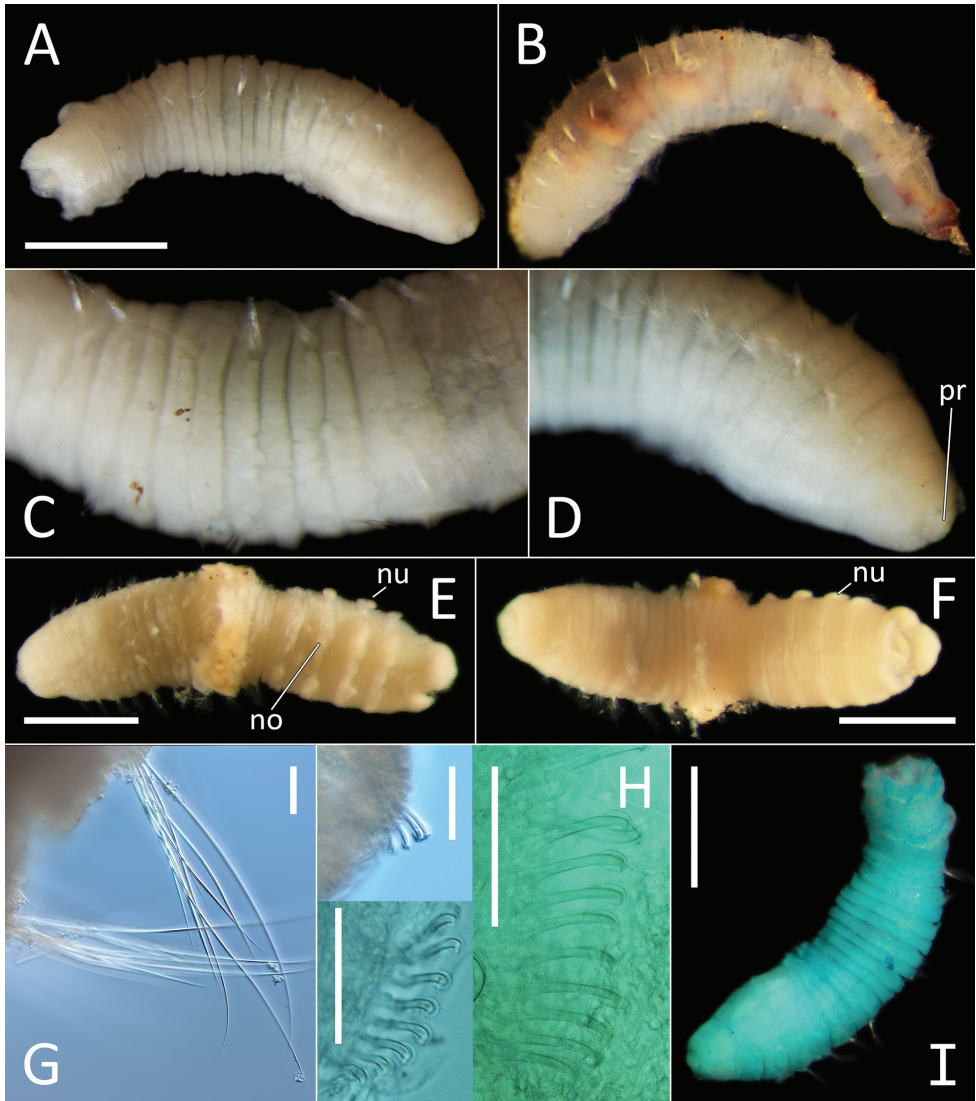


Figure 3. *Notomastus* sp. NHM_162. **A** Lab image, whole specimen (specimen NHM_162) **B** Live image, whole specimen (specimen NHM_162) **C** Lab image, biannulated chaetigers (specimen NHM_162) **D** Lab image, prostomium (specimen NHM_162, pr = prostomium) **E** Lab image, whole specimen, dorsal (specimen NHM_915B, no = notopodial lobe, nu = neuropodial lobe) **F** Lab image, whole specimen, ventral (specimen NHM_915B, nu = neuropodial lobe) **G** Lab image, thoracic chaetae, (specimen NHM_162) **H** Lab image, thoracic hooks (specimen NHM_162) **I** Lab image, whole specimen (specimen NHM_162, methyl green stain). Scale bars: 1 mm (**A, E, F, I**); 50 μ m (**G, H**).

abdominal segments observed, this species cannot be meaningfully compared with other known species in this genus and is therefore not formally described.

Ecology. Found in the eastern polymetallic nodule province of the CCZ.

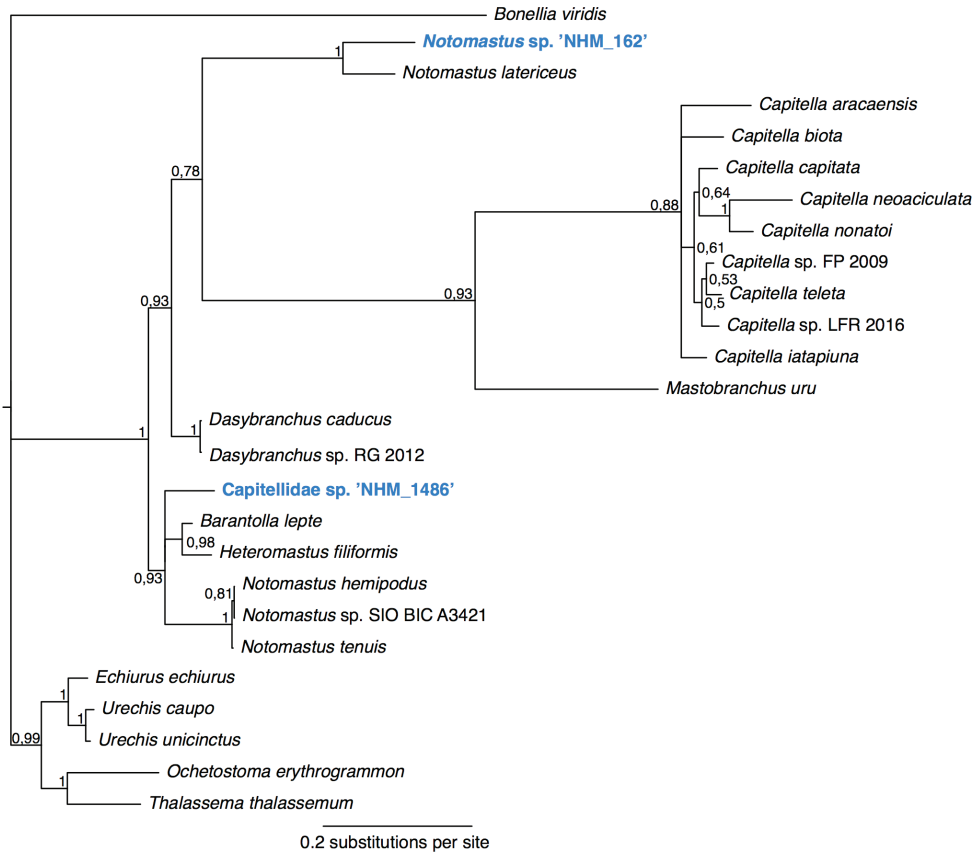


Figure 4. Phylogenetic analysis of Capitellidae. 50% majority rule tree from the Bayesian analyses using 18S and 16S, with posterior probability values on nodes. Twenty-four taxa from GenBank were included, and Echiura was chosen as outgroup following the annelid phylogeny of Weigert and Bleidorn (2016).

Opheliidae Malmgren, 1867

Notes. Due to their simple morphology, there is much confusion in the taxonomic literature dealing with Opheliidae, and many species and genera are currently considered invalid (Read and Fauchald 2018c). Useful recent studies clarifying some of the confusion are Kongsrud et al. (2011) and Parapar et al. (2011) based on material collected from North-East Atlantic. It would appear that several previous descriptions were based on what are in fact different, if morphologically very similar, species. Characters such as the shape of the prostomium and associated palpode are often reported in descriptions and used to distinguish species, but the UKSR material showed that the shape in preserved specimens may be variable and the shape and size of the associated palpode can also vary with preservation. Additionally, the shape of the prostomium in live specimens can be of different shape to that observed in preserved specimens (L. Neal pers. obs.) and thus this character might not be useful. Mouth structures in opheliids are rarely observed and re-

ported but considered important by some authors (Tzetlin and Zhadan 2009). The number of chaetigers in a specimen has been deemed as a useful character by e.g. Kongsrud et al. (2011) and Blake (2000b). The chaetae of the opheliids are relatively uniform smooth capillaries of limited taxonomical importance. However, Sarda et al. (2009) reported the presence of hirsute capillaries in *Ophelina margaleffi* Sarda et al., 2009 observed under SEM. Opheliid branchiae are very fragile structures which are easily lost and thus their distribution and number can be difficult to observe. Kongsrud et al. (2011) illustrated the importance of examining a relatively large number of specimens in order to correctly establish the characters of these structures. The anal tube is also a very fragile structure that is easily lost, and true absence is difficult to distinguish from loss due to damage. Kongsrud et al. (2011) again illustrated the importance of examining a relatively large number of specimens in order to correctly establish the presence and form of this structure.

Unfortunately, the ABYSSLINE material provides very few specimens (often just one) per species, which complicates the morphological interpretation. Nevertheless, in combination with DNA data, we believe it is important to provide the currently best possible morphology, which can be amended as more and better-preserved examples become available in the future. As a result, only 8 out of 15 opheliid species found in the ABYSSLINE material are here formally described. Morphologically, the ABYSSLINE material can be assigned to two known genera, *Ammotrypanella* McIntosh, 1878 and *Ophelina* Örsted, 1843.

***Ammotrypanella* McIntosh, 1878**

Fig. 5A–C

Notes. The confused taxonomic history of *Ammotrypanella* and its type species, *Ammotrypanella arctica* McIntosh, 1878 has been summarized by Parapar et al. (2011) and attributed to the short description and drawings provided by McIntosh (1878). Støp-Bowitz (1945) proposed that *Ammotrypanella* should be considered as synonymous with *Ophelina*, while Fauchald (1977) treated *Ammotrypanella* as a valid genus characterized by having the branchiae limited to the posterior part of body. Schüller (2008) provided a re-diagnosis of *Ammotrypanella*, following the examination of the type material of *A. arctica*, and while she pointed out that the holotype (BMNH.1921.1.2392) is in a poor state, she confirmed the presence of branchiae in the posterior part of the body only. Based on this observation Schüller (2008) then provided descriptions of three new species from abyssal Southern Ocean (*A. cirrosa*, *A. mcintoshi* and *A. princessa*), bringing the currently valid number of *Ammotrypanella* species to four. The holotype of *A. arctica* has also been examined as part of this study (Fig. 5A–C) but is in too poor condition (now in three fragments) to provide meaningful information.

As a taxonomic revision is beyond the scope of this study, we follow the definition of *Ammotrypanella* given by Schüller (2008), with one amendment. Schüller (2008) considered that anal tube may be absent, while here we suggest that it was likely missing due to damage.



Figure 5. *Ammotrypanella arctica* holotype (BMNH 1921.12392). **A** Whole specimen (fragmented) **B** Anterior-most fragment **C** Posterior-most fragment. Scale bars: 1 mm (**A, B, C**).

Diagnosis. Body long and thin, with ventral groove along whole length of body. Prostomium bluntly rounded to conical with small palpode, peristomium indistinct. Eyes absent. Parapodia embedded into lateral groove in median region, becoming more distinct in posterior region. Parapodia with branchiae in third quarter of body. All chaetae simple. Branchiae flat, wide at base, tapering to top. Anal tube present.

Several morphotypes with branchiae restricted to the posterior part of the body were encountered in the UKSR material, which is consistent with genus *Ammotrypanella* as discussed above. The UKSR-collected species can be distinguished from four known species assigned to this genus mainly by the form of anal tube:

Ammotrypanella arctica McIntosh, 1878 has an elongated anal tube about same length as posterior abranchiate region and provided with a deciduous anal cirrus and terminal anus (see Schüller et al. 2008; Parapar et al. 2011).

Ammotrypanella cirrosa Schüller, 2008 has an elongated anal tube, its length equals to length of last 5–8 chaetigers, posterior margin with numerous cirri.

Ammotrypanella mcintoshi Schüller, 2008 lacks an anal tube. Although the absence of an anal tube was considered real and a distinguishing feature of this species by Schüller (2008), it is not clear if the anal tube was in fact missing (fallen off) (see comment in Parapar et al. 2011).

Ammotrypanella princessa Schüller, 2008 has a prostomium which mimics the shape of a royal crown (Schüller 2008).

Additionally, *Ophelina opisthobranchiata* Wirén, 1901 described from the deep sea of Spitsbergen, also has a posterior distribution of branchiae. In his recent re-description Kongsrud et al. (2011) preferred not to recognize this species as *Ammotrypanella* due to lack of phylogenetic analysis and variation of morphology in *Ophelina*.

Our molecular analysis revealed the presence of four distinct CCZ species, forming a well-supported clade. Three of those species (*Ammotrypanella keenani* sp. nov., *Ammotrypanella kersteni* sp. nov. and *Ammotrypanella* sp. NHM_1653) are represented by reasonably well-preserved specimens. Unfortunately, species NHM_2114 is represented by a single specimen with all branchiae now lost and it is therefore assigned to this genus only based on molecular data.

***Ammotrypanella keenani* sp. nov.**

<http://zoobank.org/BF6FB02D-DF8E-4781-A76D-9B209FCC086B>

Fig. 6A–J

Material examined. NHM_1166C NHMUK ANEA 2019.7109, coll. 26 Feb. 2015, 12°06.93N, 117°09.87W, 4100 m <http://data.nhm.ac.uk/object/483c6faa-0338-4cf5-a21d-6f448c72f4aa>; NHM_1250 (**holotype**) NHMUK ANEA 2019.7110, coll. 01 Mar. 2015, 12°15.44N, 117°18.13W, 4302 m <http://data.nhm.ac.uk/object-1514d25d-b485-4b90-8981-3e84381bf250>; NHM_1871 (**paratype**) NHMUK ANEA 2019.7111, coll. 13 Mar. 2015, 12°02.49N, 117°13.03W, 4094 m <http://data.nhm.ac.uk/object/d93680b5-a3a3-4623-afc4-17062e1a1a58>; NHM_1949 NHMUK ANEA 2019.7112, coll. 14 Mar. 2015, 12°11.406N, 117°22.282W, 4182 m <http://data.nhm.ac.uk/object/cff2696d-06ab-42a1-843e-6ef894872f32>.

Type locality. Pacific Ocean, CCZ, 12°15.44N, 117°18.13W, depth 4302 m, in mud between polymetallic nodules.

Description. This is a small to medium-sized species (6–16 mm long), represented by four specimens. NHM_1250 and NHM_1871 are complete specimens in good condition 12 mm long and 0.8 mm wide for 38 chaetigers and 16 mm long and about 1 mm wide respectively for 38 chaetigers. NHM_1166C and NHM_1949 are complete, but much smaller specimens in poor condition, 6–7 mm long, with mid-body region twisted and damaged, therefore the exact number of chaetigers cannot be established, but at least 34 chaetigers observed in both specimens.

Body cylindrical, iridescent and smooth, no annulation detectable. Ventral groove along the entire body length. Preserved specimen pale yellow in ethanol (Fig. 6A). Live specimens translucent with orange gut (Fig. 6B). First 5–8 and posterior (branchial and 7 postbranchial) chaetigers crowded, chaetigers in midbody elongated.

Prostomium conical with distinct, slightly elongated palpode (NHM_1871, NHM_1166C) (Fig. 6C, H) or broad with short, button-like palpode (Fig. 6D, E). (NHM_1250, NHM_1949). Nuchal organs everted in NHM_1871, not pigmented (Fig. 6C, H).

Branchiae present, but limited to posterior region only, where at least 10 or 11 pairs present in chaetigers 22(23)–32, but only seven pairs were observed in smaller specimens (NHM_1166C and NHM_1949). All branchiae cirriform; first two pairs observed in NHM_1781 reduced in size, with the first pair (ch. 22) smallest (Fig. 6F); first (ch. 23) and last pair observed in NHM_1250 reduced in size (Fig. 6G); all branchiae of similar size in NHM_1166C and NHM_1949.

Parapodia distinct, biramous; observed as broad lobes in chaetigers 1–5 (Fig. 6H), becoming smaller in subsequent chaetigers; parapodia embedded in distinct lateral grooves. Chaetae are capillaries (Fig. 6I), anterior 5–8 crowded chaetigers with numerous chaetae in bundles, fewer chaetae in following chaetigers; chaetae longest in the anterior crowded chaetigers.

Anal tube the length of about half of the length of abranchiate posterior region, elongated, cylindrical; distal end with cirlet of about four tightly packed cushion-like pads and thickened ventral pad observed in specimen NHM_1250 (damaged in other specimens) (Fig. 6J), ventral cirrus not observed.

Genetic data. GenBank MN217408–MN217411 for 16S, MN217491 for 18S and MN217513–MN217514 for COI. This species is genetically identical or very similar to COI sequences attributed to “Opheliidae sp. 2” in Janssen et al. (2015) collected in the German and French exploration contract areas, with K2P values ranging from 0.0–0.008 between *A. keenani* sp. nov. and specimens with accession numbers KJ736399–KJ736403. In our phylogenetic analyses *A. keenani* sp. nov. is basal in a well-supported clade containing the three other *Ammotrypanella* species from this study.

Remarks. Posterior distribution of branchiae and variously preserved cylindrical tube was observed in all specimens examined, irrespective of their size. These specimens represent one of several species consistent with genus *Ammotrypanella* recognized from the UKSR material. This species is most similar to *Ammotrypanella* sp. NHM_1653 in the relatively small body size and possession of an elongated (cylindrical) anal tube. This species can be distinguished from other *Ammotrypanella* material in this study and known *Ammotrypanella* species in having an anal tube distally with 4 or 5 cushion-like pads rather than distinct cirri, although this observation is based on only single specimen.

Ecology. Found in the eastern part of polymetallic nodule province in the CCZ.

Etymology. Named in honor of Edward Keenan, boatswain onboard RV Melville on the AB01 ABYSSLINE cruise in 2013.

***Ammotrypanella kersteni* sp. nov.**

<http://zoobank.org/79227777-2043-4206-AF84-B51FF7293231>

Figs 7A, B, 8A–F

Material examined. NHM_254 (**holotype**) NHMUKANEA 2019.7107, coll. 17 Oct. 2013, 13°45.21N, 116°29.12W, 4128 m <http://data.nhm.ac.uk/object/3441cd68-7432-4dec-8415-966b104c3077>.

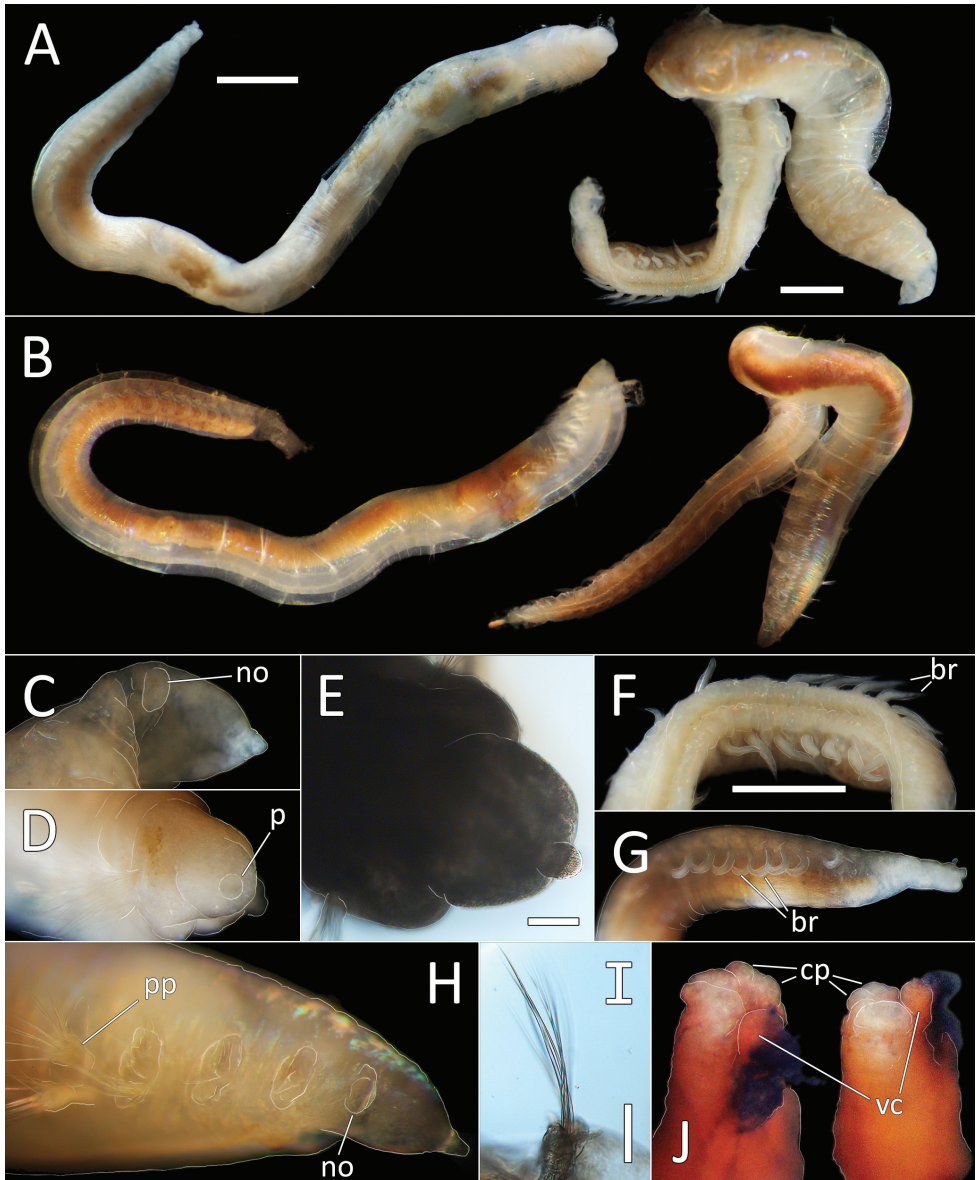


Figure 6. *Ammotrypanella keenani* sp. nov. **A** Lab images, whole specimens (holotype [specimen NHM_1250], post-staining, faded stain [left], paratype NHM_1871, unstained [right]) **B** Live images, whole specimens (holotype [left], paratype NHM_1871 [right]) **C** Lab image, prostomium (paratype NHM_1871, damaged, no = everted nuchal organ) **D** Lab image, prostomium (holotype, p = palpode) **E** Lab image, detail of palpoae (holotype) **F** Lab image, posterior branchiae (paratype NHM_1871, br = branchiae) **G** Lab image, posterior branchiae (holotype, br = branchiae) **H** Live image, anterior (paratype NHM_1871, pp = parapodia, no = nuchal organ) **I** Lab image, detail of capillary chaetae (holotype) **J** Lab image, detail of anal funnel, ventro-distal (left) and latero-distal (right) views (holotype, stained, cp = cushioned pad, vc = ventral cirrus). Morphological features in plates **C–H, J** have been outlined with a fine white line to improve clarity of those features. Scale bars: 1 mm (**A, F, G**); 100 μ m (**E, I**).

Type locality. Pacific Ocean, CCZ, 13°45.21N, 116°29.12W, depth 4128 m, in mud between polymetallic nodules.

Description. This species is represented by a single specimen in very good condition, although now split into two fragments, following tissues sampling for molecular analysis. Specimen (when complete) 31 mm long and 1.5 mm wide for 36 chaetigers. Body cylindrical, iridescent and smooth, no annulation detectable (Fig. 7). Ventral groove along the entire body length. Preserved specimen pale yellow in ethanol (Fig. 8). First seven and posterior (branchial and last six post branchial) chaetigers crowded, chaetigers in midbody elongated.

Prostomium of preserved specimen oval and broad (about as long as wide) and anteriorly blunt, somewhat truncated and bearing very distinct short, button-like palpode (Fig. 8C). Nuchal organs observed as narrow slits laterally on posterior part of prostomium.

Branchiae present, but limited to posterior region only, where present in chaetigers 22–28, seven pairs. All branchiae cirriform, of similar length, with red pigment in live specimen (Fig. 7B).

Parapodia distinct, biramous; observed as a broad lobe in chaetigers 1–7 (Fig. 8B), becoming smaller in subsequent chaetigers; parapodia embedded in distinct lateral grooves. Chaetae are capillaries (Fig. 8E), first seven chaetigers with numerous chaetae in bundles, fewer chaetae in following chaetigers; chaetae long, becoming progressively longer over the first seven chaetigers and then getting progressively shorter towards posterior part of the body.

Posterior achateous end (it is unclear if it represents anal tube) the length of two posterior chaetigers, a funnel-shaped structure with broad distal opening, distal margin smooth (Fig. 8F).

Reproductive information. Ovigerous specimen with eggs of 200–250 µm in size clearly observed in mid through to posterior part of the body (Fig. 7B).

Genetic data. GenBank MN217412 for 16S, MN217492 for 18S and MN217515 for COI. No identical matches on GenBank for COI, 16S or 18S. This taxon does not match any previous COI sequences, and we only have one specimen from the current study, which may indicate that this represents a rare species. In our phylogenetic analyses it forms a monophyletic clade with *Ammotrypanella keenani* sp. nov., *Ammotrypanella* sp. (NHM_2114) and *Ammotrypanella* sp. (NHM_1653) (Fig. 23).

Remarks. *Ammotrypanella princessa* Schüller, 2008 is most similar to our species because of the shape of prostomium; however, this may be a preservation artefact (see earlier comments), which mimics the shape of a royal crown (Schüller 2008). However, *A. princessa* is a much smaller species (5–11 mm long) with fewer body segments (33–35).

The anal tube commonly becomes detached in opheliids and when short anal tubes have been described in the past, it is important to be mindful that the anal tube may in fact be missing. The posterior achateous end in UKSR species is rather short, but it appears to have a distinct form, and therefore we suggest it may possibly represent anal tube rather than damaged posterior end. However, other *Ammotrypanella* species possess an elongated cylindrical anal tube, which could suggest that the anal tube in *A. kersteni* sp. nov. is in fact missing. At the same time, the anal tubes of Opheliidae



Figure 7. *Ammotrypanella kersteni* sp. nov. holotype (specimen NHM_254) live images. **A** Live image, whole specimen **B** Live image, detail of anterior (upper) and posterior (lower), with branchiae outlined in a fine black line (e = eggs, br = branchiae).

species show a variety of forms, and it is not impossible to speculate that similar variability can be found in *Ammotrypanella* as more species are discovered. With the current evidence based on single specimen we cannot clarify if the funnel-shaped posterior end represents the anal tube.

Ecology. Found in the eastern polymetallic nodule province of the CCZ.

Etymology. Named in honor of Oliver Kersten, member of the science party of both ABYSSLINE cruises.

Ammotrypanella sp. (NHM_1653)

Fig. 9A–H

Material examined. NHM_1653 NHMUK ANEA 2019.7108, coll. 10 Mar. 2015, 12°21.81N, 116°40.86W, 4233 m <http://data.nhm.ac.uk/object/a2f7ed04-7275-4a57-a058-bd750cacc715>.

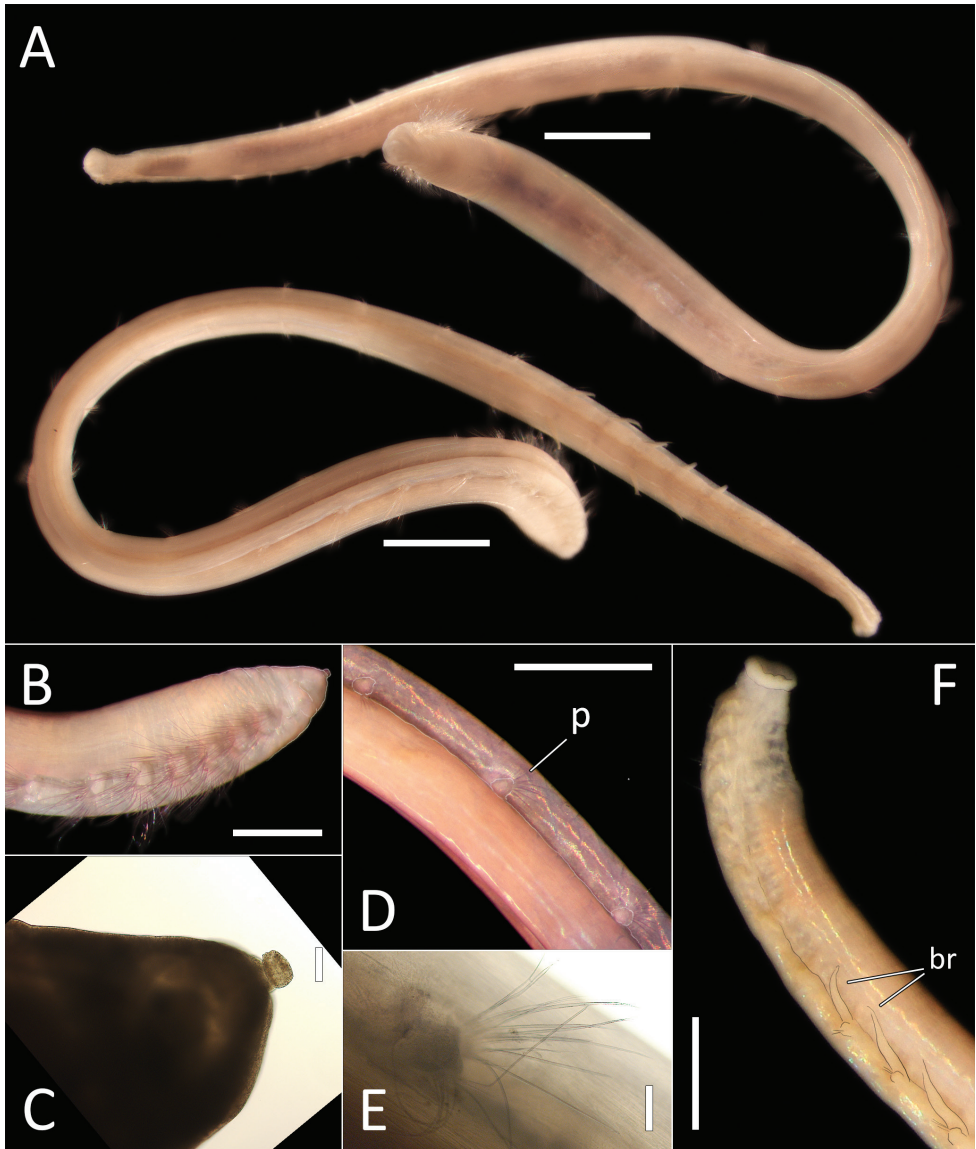


Figure 8. *Ammotrypanella kersteni* sp. nov. holotype (specimen NHM_254). **A** Lab images, whole specimens, dorsal (upper) and ventral (lower) **B** Lab image, anterior **C** Lab image, detail of palpod **D** Lab image, mid-body parapodia (p = parapodium) **E** Lab image, detail of parapodium **F** Lab image, posterior and anal funnel. Morphological features in plates **B**, **D**, **F** have been outlined with a fine white or black line to improve clarity of those features. Scale bars: 2 mm (**A**); 1 mm (**B**, **D**, **F**); 100 µm (**C**, **E**).

Description. This small species is represented by a single complete specimen in reasonable condition, except for some damage to anal tube (Fig. 9). Complete specimen 7.5 mm long and 0.5 mm wide for 34 chaetigers. Body cylindrical, with slight annulation detectable. Ventral groove along the entire body length. Preserved speci-

men pale pink in ethanol; live specimen semi-translucent with orange gut (Fig. 9B). First seven and posterior (branchial and last six postbranchial) chaetigers crowded, chaetigers in midbody elongated.

Prostomium conical (longer than wide) anteriorly tapering into blunt tip and bearing very distinct, round palpode (Fig. 9C, D). Nuchal organs observed as narrow, lightly pigmented slits, laterally on posterior part of prostomium.

Branchiae present, but limited to posterior region only, where present in chaetigers 22–28, seven pairs. All branchiae cirriform; large, of similar length except for the last branchial pair, which is reduced (Fig. 9E).

Parapodia distinct, biramous; observed as a small lobe in chaetigers 1–7, becoming smaller in subsequent chaetigers; parapodia embedded in distinct lateral grooves (Fig. 9F). Chaetae are capillaries (Fig. 9G), first seven chaetigers with numerous chaetae in bundles, fewer chaetae in following chaetigers; chaetae long in first seven and last six chaetigers, shorter in midbody.

Anal tube the length of three posterior chaetigers (Fig. 9H); cylindrical, distally slightly narrowing; due to some damage, the form of distal end cannot be established with certainty; short thick ventral cirrus attached near the distal end.

Genetic data. GenBank MN217413 for 16S, MN217493 for 18S and MN217516 for COI. This species is genetically identical or very similar to COI sequences collected in the German and French exploration contract areas and published in Jansen et al. (2015), with K2P values ranging from 0.0–0.002 between *Ammotrypanella* sp. (NHM_1653) and the already published sequences with accession numbers KJ736387–KJ736392. In our phylogenetic analyses it forms a monophyletic clade with *Ammotrypanella keenani* sp. nov., *A. kersteni* sp. nov. and *Ammotrypanella* sp. (NHM_2114) (Fig. 23).

Remarks. This is another species with branchiae limited to the posterior end consistent with the genus *Ammotrypanella*. While this species is similar to *Ammotrypanella kersteni* sp. nov., it can be clearly distinguished from it by a much smaller body size, shape of prostomium and bearing narrow, elongated, cylindrical anal tube. This form of tube is however similar to other known anal tube-bearing species of *Ammotrypanella* and due to some damage to this feature in the UKSR specimen, its form cannot be established with certainty.

Ecology. Found in polymetallic nodule province.

Ammotrypanella sp. (NHM_2114)

Fig. 10A–E

Material examined. NHM_2114 NHMUK ANEA 2019.7113, coll. 20 Mar. 2015, 19°27.874N, 120°01.525W, 4026 m, <http://data.nhm.ac.uk/object/f4492dd1-8088-47c6-97d9-32e43ae99552>.

Description. Single, minute, damaged specimen; now with posterior part of the body removed for molecular analysis. Anterior fragment 1.6 mm long 0.2 mm wide

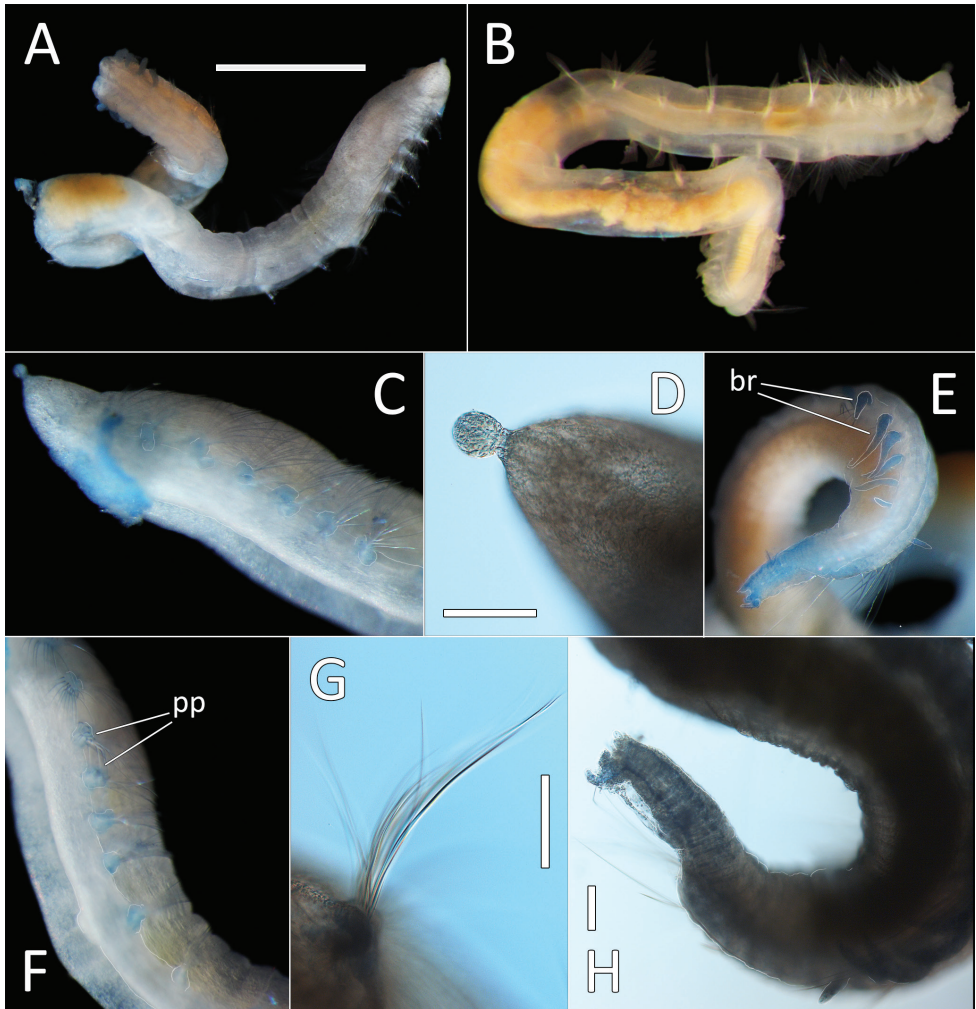


Figure 9. *Ammotrypanella* sp. NHM_1653 (specimen NHM_1653). **A** Lab image, whole specimen (faded stain **B** Live image, whole specimen **C** Lab image, anterior (faded stain) **D** Lab image, detail of palpode **E** Lab image, posterior (faded stain, br = branchiae) **F** Lab image, anterior-midbody (faded stain, pp = parapodia) **G** Lab image, detail of capillary chaetae **H** Lab image, detail of posterior and anal tube. Morphological features in plates **C**, **E**, **F**, **G** have been outlined with a very fine white to improve clarity of those features. Scale bars: 1 mm (**A**); 100 µm (**D**, **G**, **H**).

for about 16 chaetigers (chaetae observed on only 11 of these, the rest of the fragment damaged with chaetae missing). Ventral groove along the entire length of the fragment. First six chaetigers crowded. Preserved specimens pale yellow in ethanol; live specimen translucent with orange gut (Fig. 10A). Prostomium broad (slightly longer than wide) and anteriorly bluntly rounded, bearing distinct bi-articulated palpode, with globular distal articulation (Fig. 10B–D). Parapodia distinct, biramous; as a small lobe in chaetigers 1–9, becoming indistinct in the rest of the fragment. All chaetae observed simple capillaries (Fig. 10E).

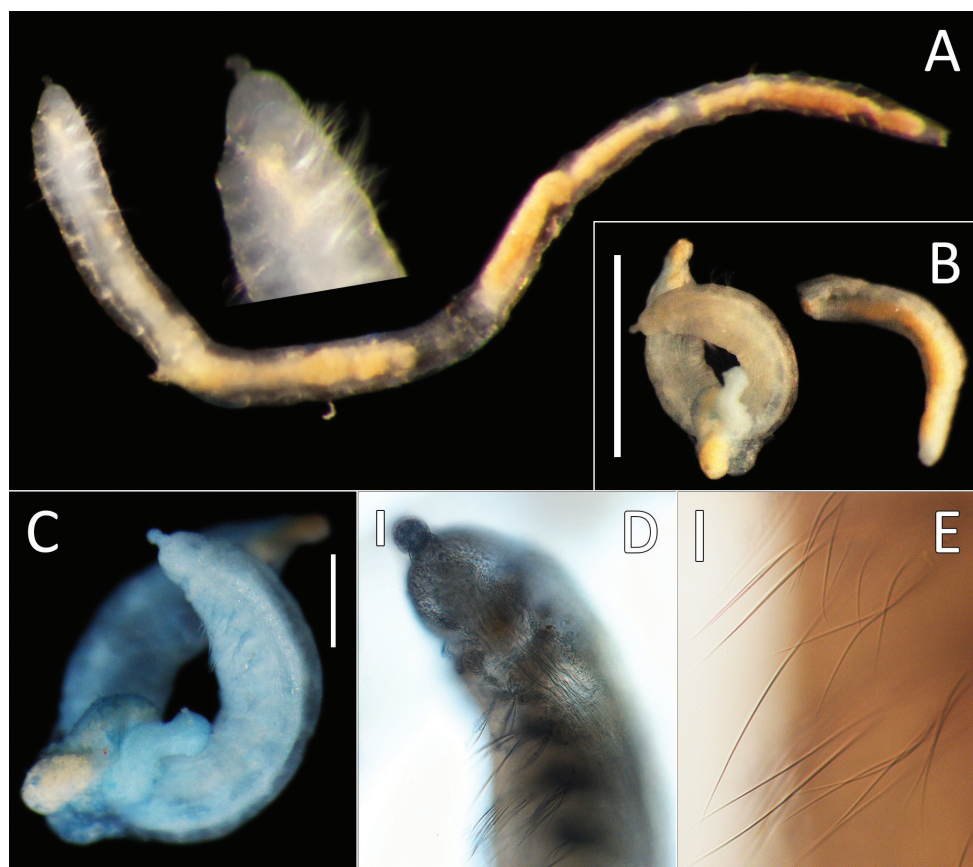


Figure 10. *Ammotrypanella* sp. NHM_2114 (specimen NHM_2114). **A** Live images, whole specimen with detail of anterior **B** Lab images, fragmented whole specimen, post-staining, (faded stain, anterior fragment [left], posterior fragment [right],) **C** Lab image, anterior fragment, post-staining, faded stain **D** Lab image, detail of anterior and palpode **E** Lab image, detail of capillary chaetae. Scale bars: 1 mm (**B**); 250 μ m (**C**) 50 μ m (**D**); 25 μ m (**E**).

Additional morphological observations from live specimen. Upon collection the live specimen was imaged and appears to be complete. Presence and distribution of branchiae cannot be established from the image. The anal tube was probably missing upon collection of the specimen.

Genetic data. GenBank MN217414 for 16S and MN217494 for 18S. COI was unsuccessful for this specimen, no identical GenBank matches for 16S or 18S. *Ammotrypanella* sp. (NHM_2114) cluster with the *Ammotrypanella keenani* sp. nov., *Ammotrypanella* sp. (NHM_1653) and *Ammotrypanella kersteni* sp. nov. in our phylogenetic analyses (Fig. 23).

Remarks. Although important diagnostic features cannot be fully confirmed in this specimen, in the phylogenetic tree it falls into a well-supported clade containing *Ammotrypanella* species and likely represents another species in this genus reported from UKSR material. At present, morphological information obtained from this single representative is limited which prevent us from providing a formal description.

Ophelina Ørsted, 1843

Notes. Ørsted (1843) erected *Ophelina* for *O. acuminata* from Danish coasts. It is now represented by around 60 species (Read and Fauchald 2019), although the numbers vary according to different workers due to its confused taxonomic history (Maciolek and Blake 2006; Parapar et al. 2011). *Ophelina* is the most diverse genus of the family Opheliidae, although it likely represents a paraphyletic grouping (Law et al. 2014). This genus is represented in UKSR-collected material by 11 species as revealed by molecular analysis.

The diagnosis of *Ophelina* presented here follows that given by Maciolek and Blake (2006).

Diagnosis. Body elongate, with deep ventral groove and two lateral grooves along entire length of body. Prostomium conical, sometimes with terminal palpode; eyes present or absent. Branchiae present or absent; if present, beginning on chaetiger 2, continuing to posterior end, sometimes absent from middle or far posterior chaetigers; branchiae single, cirriform. Segmental lateral eyes absent. Noto- and neuropodia with small fascicles of capillary chaetae; small ventral cirrus present. Pygidium with anal funnel sometimes bearing long unpaired cirrus and additional lateral cirri.

Ophelina curli sp. nov.

<http://zoobank.org/0929D0E7-E391-42F9-B7CE-D3034C7F70FB>

Fig. 11A–H

Material examined. NHM_2112 (**holotype**) NHMUK ANEA 2019.7131, coll. 20 Mar. 2015, 19°27.874N, 120°01.525W, 4026 m, <http://data.nhm.ac.uk/object/c1554f01-2324-4d8d-b775-dca42f5918e7>.

Type locality. Pacific Ocean, CCZ, 19°27.874N, 120°01.525W, depth 4026 m, in mud between polymetallic nodules.

Description. This species is represented by a single specimen 30 mm long and 1 mm wide for 28 chaetigers.

Ventral and lateral grooves distinct along whole length of body. Colour in alcohol yellow to light tan (Fig. 11A); live specimen semi-translucent, with red gut (Fig. 11B). Body very smooth, iridescent, segmental furrows and annulations indistinct (best observed in the anterior-most chaetigers). First five chaetigers slightly crowded, the subsequent chaetigers elongated.

Prostomium conical (longer than wide), with distinct, tear-shaped terminal palpode (Fig. 11C, D). Eyes not observed. Nuchal organs observed as slits, laterally on posterior part of prostomium; without pigmentation. Proboscis fully everted; dorsoventrally flattened multilobed structure with ventral groove (Fig. 11E).

Branchiae absent. Parapodia biramous, embedded in lateral grooves; parapodia small conical lobes, best observed on anterior seven chaetigers; no distinct pre- or postchaetal lobes observed (Fig. 11F).

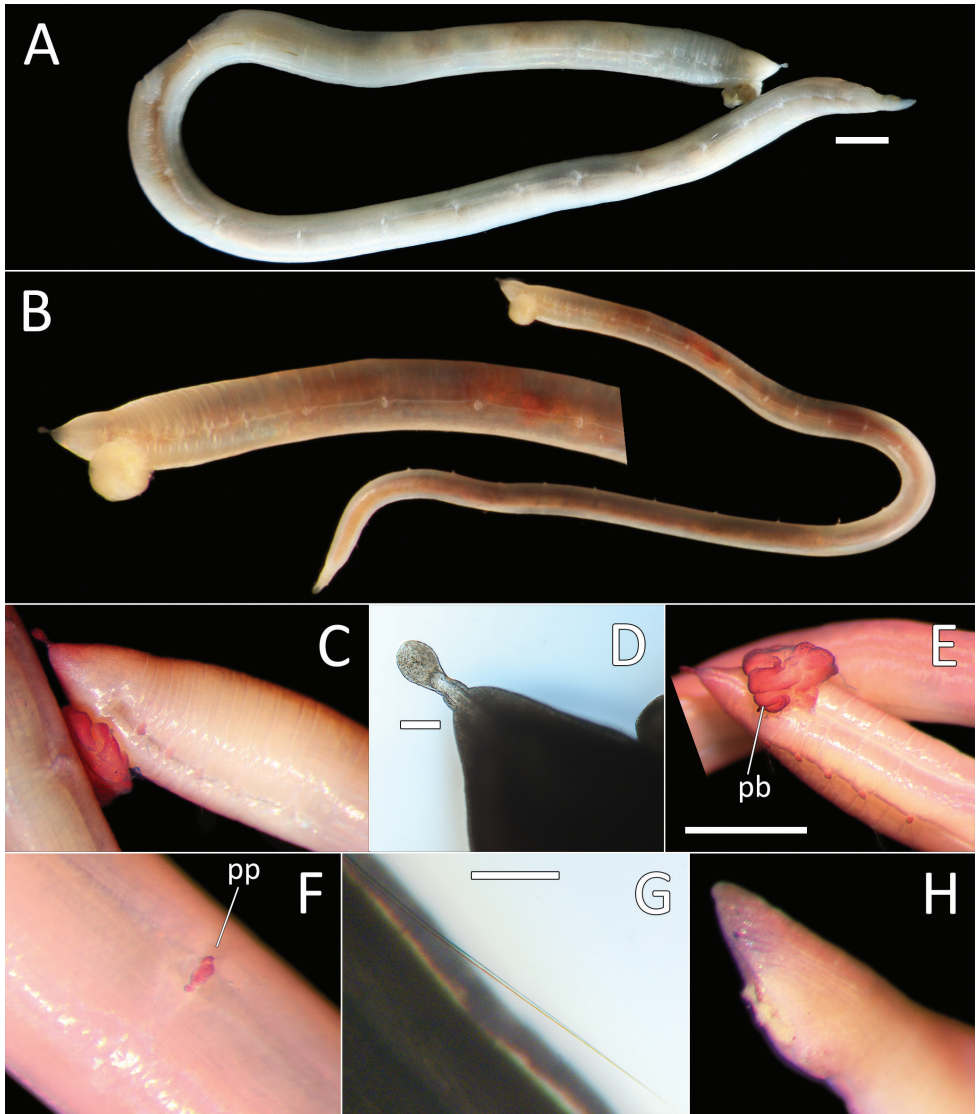


Figure 11. *Ophelina curli* sp. nov. holotype (specimen NHM_2112). **A** Lab image, whole specimen (post-staining, very faded stain) **B** Live image, with detail of anterior **C** Lab image, anterior and proboscis, lateral view, stained **D** Lab image, detail of palpode **E** Lab image, anterior and proboscis, ventral view (stained, pb = proboscis) **F** Lab image, mid-body parapodium (stained, pp = parapodia) **G** Lab image, detail of capillary chaeta **H** Lab image, anal funnel. Scale bars: 1 mm (**A**, **E**); 100 μ m (**D**, **G**)

Chaetae all slender, smooth capillaries (Fig. 11G), very few in both rami. Notochaetae mostly longer than neurochaetae.

Anal tube attached; narrow and smooth; no cirri observed (Fig. 11H). The proximal half cylindrical; distal half (in ventral view) as flattened sheath (if opened up),

but observed with lateral margins curled up, ventrally slit; distal half (in lateral view) distinctly asymmetrical with dorsal margin longer than ventral one.

Genetic data. GenBank MN217435 for 16S and MN217502 for 18S. COI was unsuccessful for this specimen, no identical GenBank matches for 16S or 18S. *Ophelina curli* sp. nov. is sister to *Ophelina juhazi* sp. nov. in our phylogenetic analyses (Fig. 23).

Remarks. Morphologically this species is very similar to *Ophelina nematoides* (Ehlers, 1913) and to UKSR *Ophelina juhazi* sp. nov. in being abbranchiate and having 28–30 chaetigers. Two other abbranchiate species that are morphologically similar to *Ophelina abbranchiata* Støp-Bowitz, 1948 are also reported in this material, but these differ in having much smaller body size (4.5–8 mm) and having only 17 or 18 chaetigers.

Ehlers (1913) provided description (but no drawings) of *O. nematoides* (as *Ammotrypane nematoides*) based on specimens from 2725 m depth in the Indian Ocean sector of the Southern Ocean (65°32'0"S, 85°30'0"E). Other reports from the Southern Ocean have been shallower (Read and Fauchald 2019). Brief diagnosis based on translation of Ehlers (1913): “Specimen 30 mm long and 1 mm wide, with 30 chaetigers. Conical prostomium with palpode. No branchiae. Basal segment (= anal tube?) appears segmented in a brightened condition is a thick sheet, when stretched, of the length of the last two segments, the margins of which are curled against each other to form on the ventral surface the narrow entrance to a gutter emanating at the back. I did not see any attachments or papillae.”

The main difference between *O. nematoides* and *Ophelina curli* sp. nov. is the number of chaetigers, 30 in the former versus 28 in the latter. The shape of anal tube appears to be similar, but without drawing or access to Ehlers’ type specimen, this structure cannot be meaningfully compared using Ehlers’ description alone.

The morphologically similar species *Ophelina juhazi* sp. nov. also found in the UKSR material can be distinguished by its smaller size, 17 mm compared to the 30 mm *O. curli* sp. nov., and the shape of anal tube, which in *O. juhazi* sp. nov. is cylindrical throughout, entire (no ventral slit), distally slightly narrowing and symmetrical.

Ecology. Found in polymetallic nodule province of the eastern CCZ.

Etymology. Named in honor of Cassidy Curl, Ordinary Seaman onboard RV Melville on the AB01 ABYSSLINE cruise in 2013.

***Ophelina ganae* sp. nov.**

<http://zoobank.org/4B05DE1F-CD07-40CF-A87D-9BC1B45F5477>

Fig. 12A–I

Material examined. NHM_245 NHMUK ANEA 2019.7140, coll. 16 Oct. 2013, 13°48.70N, 116°42.60W, 4076 m <http://data.nhm.ac.uk/object/3a34b9cb-504b-48a3-a8e9-93077ec69520>; NHM_248 NHMUK ANEA 2019.7141, coll. 16 Oct. 2013, 13°48.70N, 116°42.60W, 4076 m <http://data.nhm.ac.uk/object/e67f7724-8c9f->

4463-943e-7cda20441728; NHM_473 NHMUK ANEA 2019.7142, coll. 22 Oct. 2013, 13°43.597N, 116°40.20W, 4160 m <http://data.nhm.ac.uk/object/79dcab18-936b-430e-b770-6aab60d285c5>; NHM_598 (SEM) (**paratype**) NHMUK ANEA 2019.7143, coll. 17 Feb. 2015, 12°23.174N, 116°32.92W, 4202 m <http://data.nhm.ac.uk/object/2fa20a59-8bb3-4ef8-b2e9-efcbe2c9414>; NHM_708 NHMUK ANEA 2019.7144, coll. 20 Feb. 2015, 12°32.23N, 116°36.25W, 4425 m <http://data.nhm.ac.uk/object/2077c6c6-0e3e-4dfa-97a0-16d6c386ff07>; NHM_1098 NHMUK ANEA 2019.7145, coll. 26 Feb. 2015, 12°06.93N, 117°09.87W, 4100 m <http://data.nhm.ac.uk/object/5661fb64-83a2-4e9a-b3c3-a8405705ed1a>; NHM_1137 (**holotype**) NHMUK ANEA 2019.7146, coll. 26 Feb. 2015, 12°06.93N, 117°09.87W, 4100 m <http://data.nhm.ac.uk/object/11616c16-bdb5-4813-9d17-7170bb62702b>; NHM_1309 (**paratype**) (SEM) NHMUK ANEA 2019.7147, coll. 01 Mar. 2015, 12°15.44N, 117°18.13W, 4302 m <http://data.nhm.ac.uk/object/1ff41b52-9801-4b2e-8e01-ea34597b708d>.

Type locality. Pacific Ocean, CCZ, 12°06.93N, 117°09.87W, depth 4100 m, in mud between polymetallic nodules.

Description. Small species (4.5–8 mm long without anal tube), represented by eight specimens; all preserved specimens without anal tube (likely missing due to damage). Holotype is 7 mm long and 0.3 mm wide for 17 chaetigers. Paratypes 7–8 mm long and 0.33–0.35 mm wide for 17 chaetigers. Body cylindrical and smooth without distinct annulation. Preserved specimen yellow in ethanol (Fig. 12A); live specimens translucent (Fig. 12B, G). Ventral and lateral grooves distinct along whole length of body. Anterior and posterior-most chaetigers slightly shorter than mid-body chaetigers.

Prostomium elongate, conical with small acute terminal palpode (Fig. 12C). Eyes not observed. Nuchal organs rounded, laterally on posterior part of prostomium. Peristomium indistinct. Anterior prechaetigerous region of body with three elongated achaetous segments, detected upon observation of three lateral organs under SEM; lateral organs detected in all chaetigers under SEM (Fig. 12D, E). Parapodia rudimentary, biramous, embedded in lateral grooves; no distinct pre- or postschaetal lobes.

Chaetae all slender, smooth capillaries (Fig. 12F), appear in small numbers in both rami, often broken off entirely. Notochaetae mostly longer than neurochaetae, extremely short chaetae observed in most fascicles under SEM.

Branchiae absent. Anal tube not observed in preserved specimens (e.g. Fig. 12H), but possibly captured in image of “live” specimen NHM_473 (Fig. 12G). Observed anal tube cylindrical, relatively short (only slightly longer than wide); with very long thin ventral cirrus attached subdistally on ventral side of anal funnel. Stained specimens without distinct pattern (Fig. 12I).

Genetic data. GenBank MN217436-MN217442 for 16S, MN217503 for 18S and MN217521-MN217523 for COI. In our phylogenetic analyses, *Ophelina ganae* sp. nov. is sister to *Ophelina* cf. *abbranchiata* (NHM_1769) and form a well-supported clade with this species and *Ophelina* cf. *abbranchiata* (NHM_2017) together with at least two other abbranchiate species (Fig. 23).

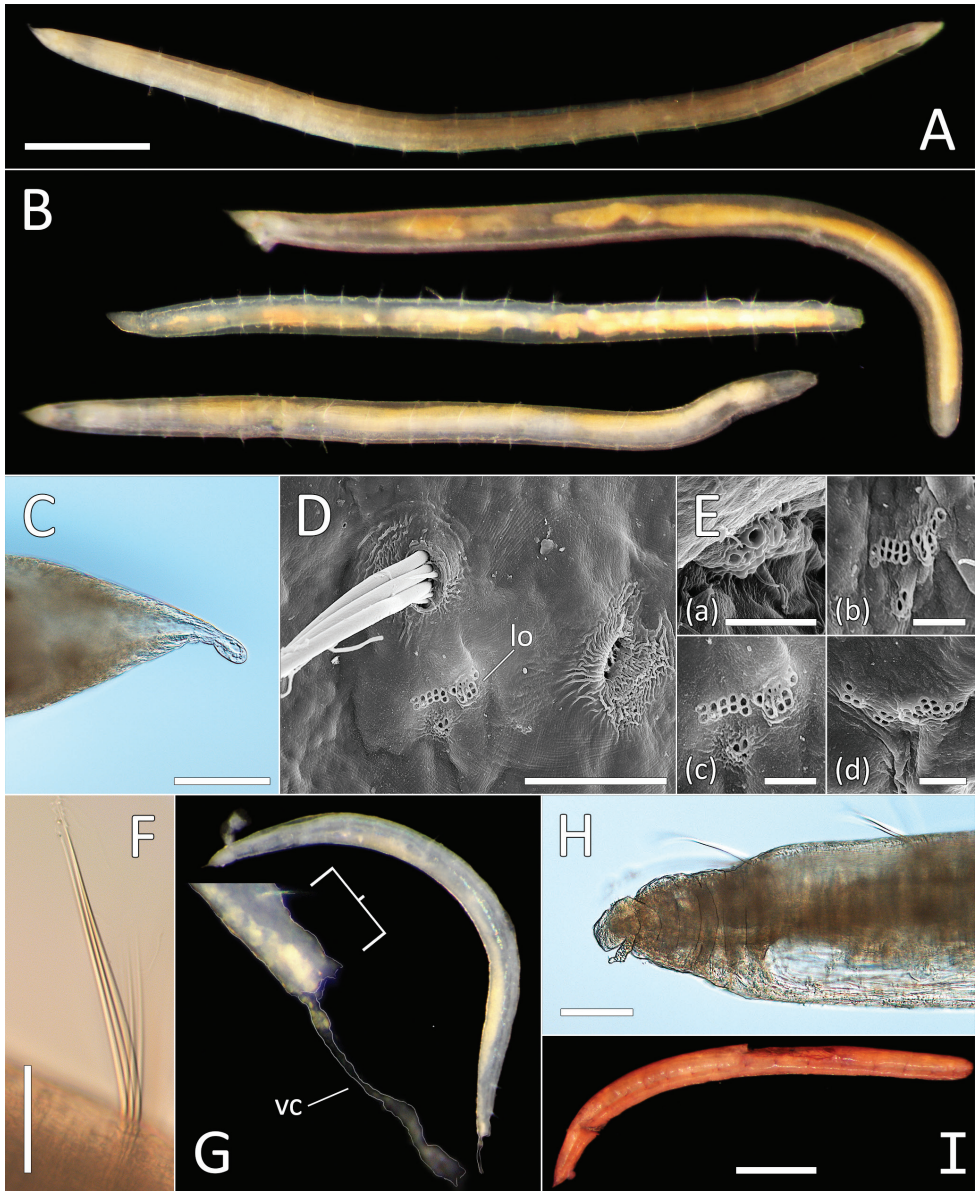


Figure 12. *Ophelina ganae* sp. nov. **A** Lab image, whole specimen (holotype [specimen NHM_1137]) **B** Live images, whole specimens (holotype [bottom], paratype NHM_598 [middle], paratype NHM_1309 [top]) **C** Lab image, detail of palpod (holotype) **D** SEM image, second chaetiger with lateral organ (paratype NHM_1309, lo = lateral organ) **E** SEM images, lateral organs, (a) pre-chaetigerous segment, (b) chaetiger 1, (c) chaetiger 2, (d) chaetiger 17 (last chaetiger) (paratype NHM_1309) **F** Lab image, detail of capillary chaetae (holotype) **G** Live image, with detail of potential anal funnel (specimen NHM_473, vc = potential ventral cirrus). **H** Lab image, detail of posterior (holotype) **I** Lab image, whole specimen (paratype NHM_598, stained). Morphological features in plates **G**, **H** have been outlined with a fine white or black line to improve clarity of those features. Scale bars: 1 mm (**A**); 100 μ m (**C**); 20 μ m (**D**); 5 μ m (**E**); 50 μ m (**F**); 100 μ m (**H**); 1 mm (**I**).

Remarks. Molecular analysis of the UKSR-collected material revealed presence of three distinct small abbranchiate species that morphologically resemble *Ophelina abbranchiata*. Given the taxonomic problems of this species, the challenge is not only to morphologically distinguish these species from each other, but also from *O. abbranchiata*. Here, we restrict the definition of *O. abbranchiata* to that provided by Kongsrud et al. (2011) based on re-description of holotype and material from the North Sea as consistently possessing 18 chaetigers only. Therefore, the new species is differentiated from *O. abbranchiata* by possessing 17 chaetigers only in all observed specimens. Furthermore, the photograph of live specimen (Fig. 12G) suggests possible presence of much shorter anal tube compared to elongated anal tubes observed in *O. abbranchiata*. This would represent another distinguishing character from the known species. We believe this structure to represent anal tube as it follows the chaetigerous regions of the body (i.e. the body is not interrupted immediately after the last chaetiger as it is common in *O. abbranchiata* when the anal funnels are missing). There also appear to be very long thin cirrus attached subdistally on ventral side and such structure is present in anal tubes of *Ophelina abbranchiata*. However, this conclusion is only tentative given the lack of anal tube in all preserved specimens of the newly described species and it is based on observation from the photograph only. See further discussion on specimens identified as *Ophelina* cf. *abbranchiata* later in this text.

Ecology. Found in polymetallic nodule province of the eastern CCZ.

Etymology. Named in honor of Bin Qi Gan, member of the science party of the ABYSSLINE AB02 cruise onboard the RV *Thomas G. Thompson*.

***Ophelina jubazi* sp. nov.**

<http://zoobank.org/24EFA36C-06BA-443D-8388-02981BE73D71>

Fig. 13A–G

Material examined. NHM_1073 (**holotype**) NHMUK ANEA 2019.7132, coll. 26 Feb. 2015, 12°06.93N, 117°09.87W, 4100 m <http://data.nhm.ac.uk/object/f7330230-224b-49e7-aa80-41e8654ea087>.

Type locality. Pacific Ocean, CCZ, 12°06.93N, 117°09.87W, depth 4100 m, in mud between polymetallic nodules.

Description. This species is represented by a single specimen 17 mm long and 0.5 mm wide for 29 chaetigers. Ventral and lateral grooves distinct along whole length of body. Live specimens translucent, with orange-red gut (Fig. 13A); colour in alcohol yellow to light tan (Fig. 13B). Body very smooth, iridescent, annulations indistinct (best observed in first five to seven anterior chaetigers). All chaetigers elongated, first five chaetigers only slightly crowded.

Prostomium conical (longer than wide), with distinct, tear-shaped terminal palpode (Fig. 13C, D). Eyes not observed. Nuchal organs observed as slits, laterally on posterior part of prostomium, without pigmentation.

Branchiae absent. Parapodia biramous, embedded in lateral grooves; parapodia small conical lobes, best observed on anterior seven chaetigers (Fig. 13E); no distinct

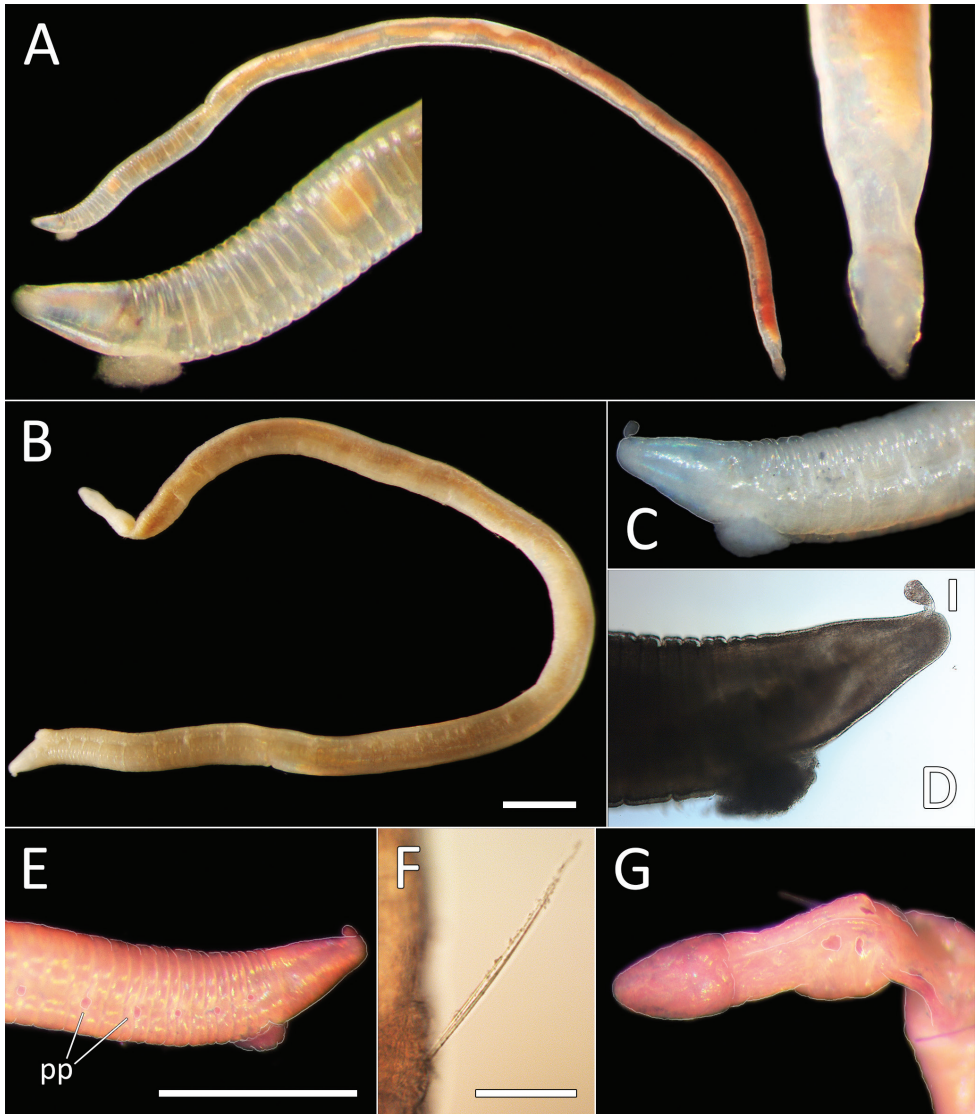


Figure 13. *Ophelina jubazi* sp. nov. holotype (specimen NHM_1073). **A** Live images, whole specimen (center) with detail of anterior (left) and posterior (right) **B** Lab image, whole specimen **C** Lab image, anterior and prostomium **D** Lab image, detail of palpod **E** Lab image, anterior and parapodia (stained, pp = parapodia) **F** Lab image, detail of capillary chaetae **G** Lab image, posterior and anal tube (stained). Morphological features in plates **C**, **E**, **G** have been outlined with a very fine white line to improve clarity of those features. Scale bars: 1 mm (**B**); 100 μ m (**D**); 50 μ m (**F**); 1 mm (**E**).

pre- or postchaetal lobes observed. Chaetae all slender, smooth capillaries (Fig. 13F), very few in both rami. Notochaetae mostly longer than neurochaetae.

Anal tube attached; narrow, cylindrical structure, symmetrical, smooth (no cirri observed) and distally slightly narrowing (Fig. 13G).

Genetic data. GenBank MN217443 for 16S and MN217504 for 18S. COI was unsuccessful for this specimen, no identical GenBank matches for 16S or 18S. In our phylogenetic analyses, *Ophelina juhazi* sp. nov. is sister to *O. curli* sp. nov. (Fig. 23).

Remarks. Morphologically similar to *Ophelina curli* sp. nov. and to *Ophelina nematoides*; see Remarks under *Ophelina curli* sp. nov. for details.

Ecology. Found in polymetallic nodule province of the eastern CCZ.

Etymology. Named in honor of Bob Juhazi, Oiler onboard RV *Melville* on the AB01 ABYSSLINE cruise in 2013.

***Ophelina martinezarbizui* sp. nov.**

<http://zoobank.org/9D6E1A60-B5BB-48BC-A756-81845EFABFBC>

Figs 14A–H, 15A–E

Material examined. NHM_681 (**holotype**) NHMUK ANEA 2019.7116, coll. 20 Feb. 2015, 12°32.23N, 116°36.25W, 4425 m <http://data.nhm.ac.uk/object/0de17415-a8bf-4461-a663-dea9a3e6a2b9>; NHM_718 NHMUK ANEA 2019.7117, coll. 20 Feb. 2015, 12°32.23N, 116°36.25W, 4425 m <http://data.nhm.ac.uk/object/f6e2fa9b-a479-4e0d-aec6-57efff6987b2>; NHM_883 NHMUK ANEA 2019.7118, coll. 20 Feb. 2015, 12°34.28N, 116°36.63W, 4198 m <http://data.nhm.ac.uk/object/d9a3a3b3-c16e-4359-8eb0-f09deed98401>; NHM_994 NHMUK ANEA 2019.7119, coll. 24 Feb. 2015, 12°08.02N, 117°17.52W, 4122 m <http://data.nhm.ac.uk/object/4f6d2b7a-169f-46a9-8b3b-5d91a021aa34>; NHM_1066 NHMUK ANEA 2019.7120, coll. 26 Feb. 2015, 12°06.93N, 117°09.87W, 4100 m <http://data.nhm.ac.uk/object/972f9cb1-79d7-4296-a6d6-e04543c9105c>; NHM_1766 (**paratype**) NHMUK ANEA 2019.7121, coll. 11 Mar. 2015, 12°10.43N, 117°11.57W, 4045 m <http://data.nhm.ac.uk/object/dc754b1c-e66b-4a58-a93e-796ebfd32f6a>; NHM_1870 NHMUK ANEA 2019.7122, coll. 13 Mar. 2015, 12°02.49N, 117°13.03W, 4094 m, <http://data.nhm.ac.uk/object/b6247e8d-d155-4646-87d7-e5358ada5352>; NHM_2088 (SEM specimen) NHMUK ANEA 2019.7123, coll. 20 Mar. 2015-03-20, 19°27.874N, 120°01.525W, 4026 m, <http://data.nhm.ac.uk/object/7dd04f2c-435b-44b1-a85f-3b05dd3014d7>; NHM_2092 NHMUK ANEA 2019.7124, coll. 20 Mar. 2015, 19°27.874N, 120°01.525W, 4026 m, <http://data.nhm.ac.uk/object/1a095836-fa97-48b8-ad4c-07ed28356ecb>; NHM_2102 NHMUK ANEA 2019.7125, coll. 20 Mar. 2015, 19°27.874N, 120°01.525W, 4026 m, <http://data.nhm.ac.uk/object/93e91313-61a3-4cd7-8221-66bf20232f14>; NHM_2116 (**paratype**) NHMUK ANEA 2019.7126, coll. 20 Mar. 2015, 19°27.874N, 120°01.525W, 4026 m, <http://data.nhm.ac.uk/object/d439156e-657d-4dd5-8bb5-3531e150961e>; NHM_2144 NHMUK ANEA 2019.7127, coll. 20 Mar. 2015, 19°27.874N, 120°01.525W, 4026 m, <http://data.nhm.ac.uk/object/79767cab-eb56-4ef1-acd0-5067ec3736de>; NHM_2149 NHMUK ANEA 2019.7128, coll. 20 Mar. 2015, 19°27.874N, 120°01.525W, 4026 m, <http://data.nhm.ac.uk/object/1caa9eb3-3281-4ed6-8424-dfaebcf1e20b>; NHM_2150 NHMUK ANEA 2019.7129, coll. 20 Mar.

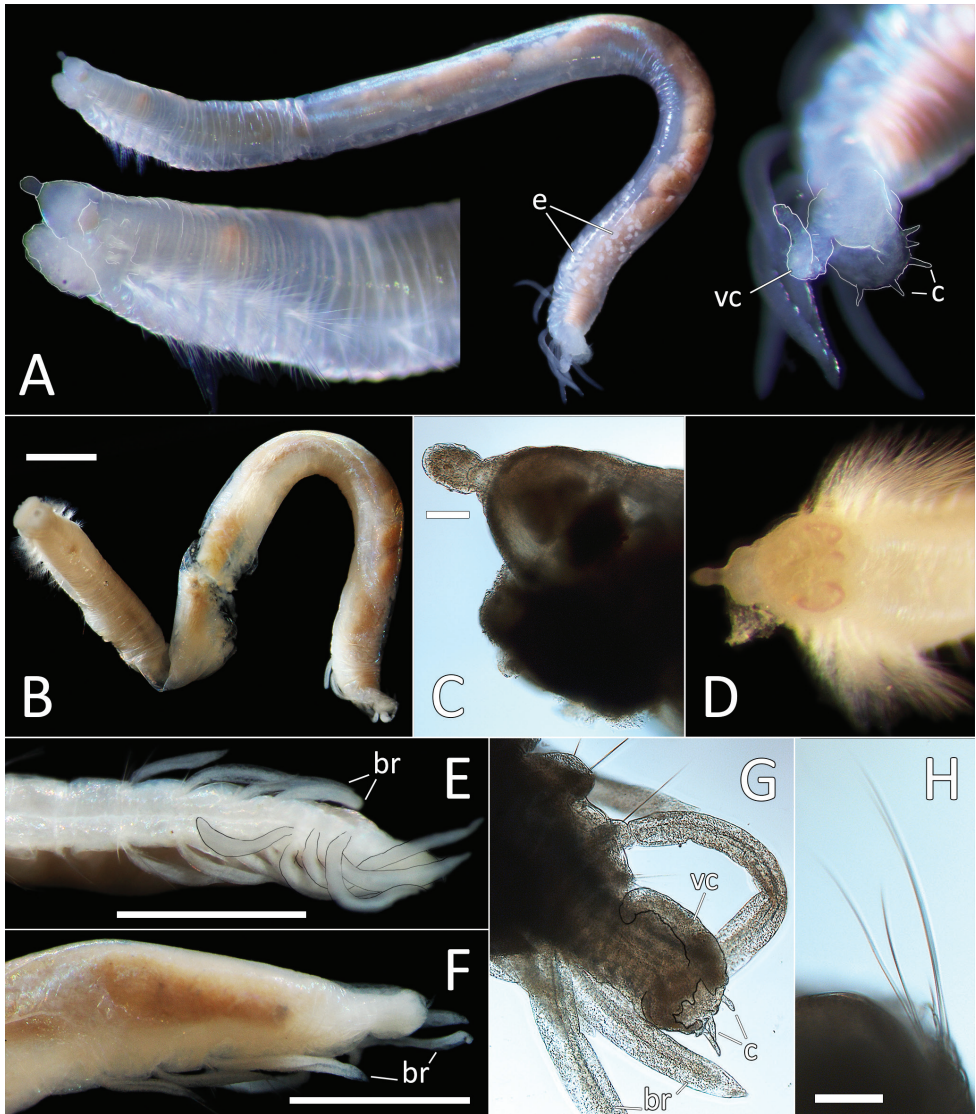


Figure 14. *Ophelina martinezarbizui* sp. nov. **A** Live images, whole specimen (center) with detail of anterior (left) and anal funnel (right) (holotype [specimen NHM_681], e = eggs, vc = enlarged ventral cirrus, c = cirri) **B** Lab image, whole specimen (holotype). **C** Lab image, detail of palpode (paratype NHM_2116) **D** Live image, prostomium, “royal crown” palpode (specimen NHM_2092) **E** Lab image, ventral posterior and branchiae (paratype NHM_1766, br = branchiae) **F** Lab image, lateral posterior and branchiae (paratype NHM_1766, br = branchiae) **G** Lab image, detail of anal funnel (paratype NHM_1766, vc = enlarged ventral cirri [folded over], c = cirri, br = branchiae) **H** Lab image, detail of capillary chaetae (holotype). Morphological features in plates **A**, **E**, **G** have been outlined with a fine white or black line to improve clarity of those features. Scale bars: 1 mm (**B**, **E**, **F**); 100 μ m (**C**, **H**).

2015, 19°27.874N, 120°01.525W, 4026 m, <http://data.nhm.ac.uk/object/993f577c-ee86-4660-b2d9-af0146606f92>.

Type locality. Pacific Ocean, CCZ, 12°32.23N, 116°36.25W, depth 4425 m, in mud between polymetallic nodules.

Description. This is a medium-sized species (8–14 mm long), represented by 14 specimens.

Body cylindrical, iridescent, some annulation detectable in first five to eight and last eight chaetigers, rest of body very smooth, no annulation detectable (Fig. 14A). Ventral and lateral grooves most distinct along the anterior half of the body, then less distinct. Preserved specimen yellow in ethanol (Fig. 14B); live specimens translucent, with orange gut (Figs 14A, 15A). Complete specimen with 31 chaetigers, first five to eight and last eight chaetigers crowded, chaetigers in between elongated, last six to eight chaetigers somewhat shifted ventrally.

Prostomium of all preserved specimens oval and broad (about as long as wide) and anteriorly bluntly rounded, somewhat truncated; bearing very distinct palpode, mostly short button-like sometimes distinctly bi-articulated with distal article oval in specimen NHM_2116 (Figs 14C, 15B, C). Similar form of prostomium (royal crown-shaped) can also be observed in live specimen NHM_2092 (Fig. 14D). Nuchal organs observed as slits laterally on posterior part of prostomium.

Branchiae present, with disjointed distribution in anterior and posterior chaetigers only, absent in mid-body chaetigers. Six very small (easily overlooked) branchial pairs observed consistently in chaetigers 2–7, with those on chaetigers 3–5 slightly longest. The number of attached posterior branchial pairs observed varied from one to eight pairs, with the most complete set observed in NHM_883 and NHM_1766, where eight pairs present in chaetigers 24–31 (the last chaetiger); first posterior pair small (1/2 the length of the subsequent pairs), others very long and robust in NHM_883, but all branchiae large in NHM_1766. All branchiae cirriform (Figs 14E–G, 15D).

Parapodia distinct, biramous; well developed in anterior part of the body, then becoming smaller in subsequent chaetigers. Parapodia with short rounded dorsal cirrus present; provided with a tongue-shaped lobe bearing lateral organs (observable under SEM) (Fig. 15E). Parapodia embedded in distinct lateral grooves in chaetiger 1–13, then grooves becoming less distinct. Chaetae are capillaries (Fig. 14H); first seven chaetigers with numerous chaetae in bundles, chaetae getting longer in chaetigers 2–4, being longest in chaetigers 3–5, then becoming shorter to chaetiger 13; in the posterior half of the body chaetae few and short, often missing (broken off) entirely.

Anal tube best preserved in specimen NHM_1766; anal tube relatively short (about the length of two posterior chaetigers) and thick distally asymmetrical with dorsal margin slightly longer than ventral one; distally with several short cirri, particularly on dorsal margin (Fig. 14A, G) and ventral margin with robust, short and thick ventral cirrus (Fig. 14A, G).

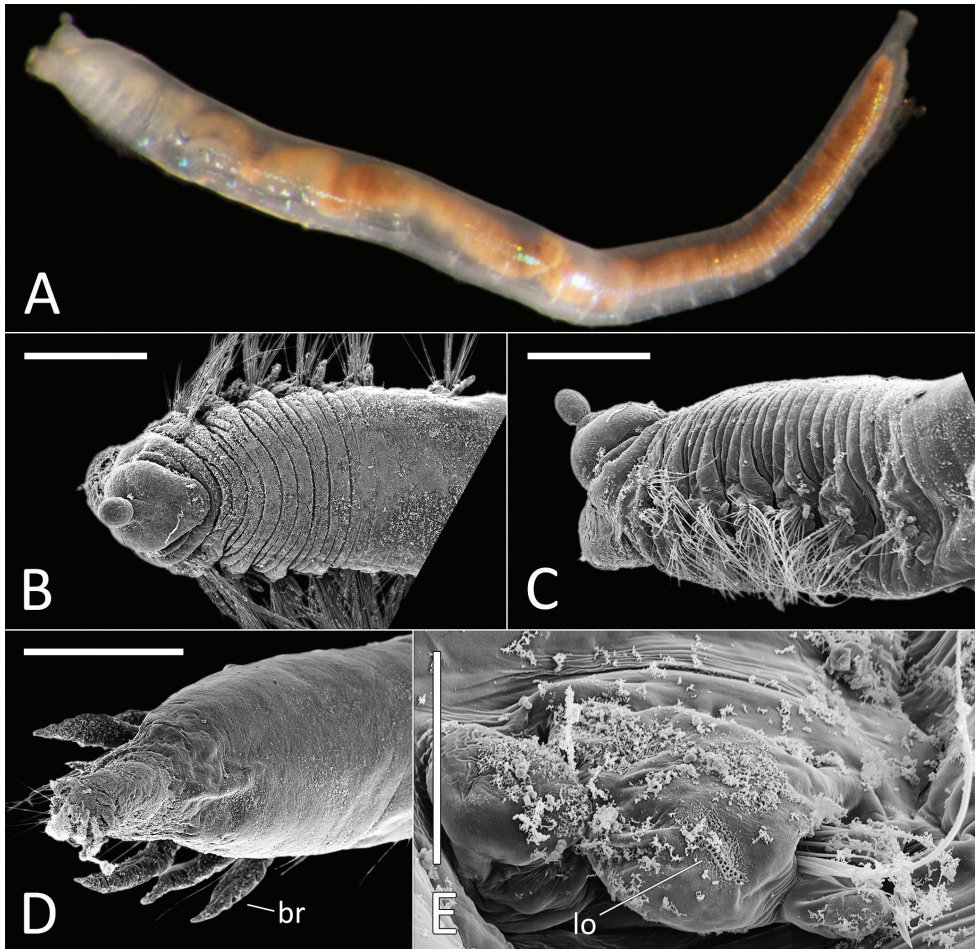


Figure 15. *Ophelina martinezarbizui* sp. nov. (specimen NHM_2088). **A** Live image, whole specimen **B** SEM image, dorsal anterior **C** SEM image, lateral anterior **D** SEM image, dorsal posterior, br = branchiae **E** SEM image, detail of mid-body lateral organ (lo = lateral organ). Scale bars: 300 μ m (**B, C, D**); 40 μ m (**E**).

Reproductive information. Holotype ovigerous, with eggs of roughly 100 μ m size clearly observed in mid through to posterior part of the body (Fig. 14A).

Morphological variation. This species is represented by the greatest number of specimens ($n = 13$) of Opheliidae species found in UKSR material. The features observed consistently are: the “royal crown”-like shape of prostomium (even in live specimens, Fig. 14D), 31 chaetigers, six pairs of tiny anterior branchiae in chaetigers 2–7. Number of attached posterior branchial pairs is variable as these are large and presumably more susceptible to damage, the exact number of posterior branchial pairs remains unknown, but the most complete observation was eight pairs in specimen NHM_883. The anal tube remains attached in all specimens, but the distal region is often damaged and ventral cirrus is often detached. The best-preserved anal tube has been observed in specimen NHM_1766 and can also be observed in the live image of the holotype.

Genetic data. GenBank MN217444–MN217456 for 16S, MN217505 for 18S and MN217524–MN217531 for COI. This species is genetically identical or very similar to “*Ophelina* sp. 2” (Janssen et al. 2015), with K2P values ranging from 0.0–0.006 between *O. martinezarbizui* sp. nov. and the already published sequences with accession numbers KJ736369–KJ736370 and KJ736372–KJ736377. In our phylogenetic analyses this species is sister to *Ophelina meyeræ* sp. nov. (Fig. 23).

Remarks. This species superficially resembles *Ammotrypanella* species due to the presence of large branchiae in the posterior part of the body, but very small and easily overlooked branchiae are present in anterior chaetigers 2–7 in *Ophelina martinezarbizui* sp. nov. The presence of these very small branchiae easily distinguish this species from other *Ophelina* species encountered in UKSR-collected material, which are either abbranchiate or branchiae are large (or at least easy to observe) in anterior chaetigers. *Ophelina martinezarbizui* sp. nov. represents a form with disjointed branchial distribution (see also comments under *Ophelina* sp. NHM_689 and NHM_1331), but it can be distinguished from these by the size of anterior branchiae, number of segments and form of anal funnel. *Ophelina martinezarbizui* sp. nov. also appears to have contrasting annulated and smooth body regions (Figs 14, 15).

Of the known *Ophelina* species, *O. ammotrypanella* Schüller, 2008 from the abyssal Southern Ocean shares the presence of small branchiae in anterior chaetigers and its “*Ammotrypanella*-like look” as the name suggests. However, in *O. ammotrypanella* the branchiae have a continuous distribution, being absent only in posterior quarter of the body.

Ecology. Found in polymetallic nodule province of the eastern CCZ. This species is represented by 13 sequenced specimens, with potentially another 28 specimens available in material that has not been sequenced yet, making it the most abundant opheliid species in the UKSR samples.

Etymology. Named in honor of Pedro Martinez Arbizu, member of the science party of the first ABYSSLINE cruise.

***Ophelina meyeræ* sp. nov.**

<http://zoobank.org/7F560FD4-73BF-4DEE-AD39-21FE5009FD90>

Fig. 16A–G

Material examined. NHM_1241(**holotype**) NHMUK ANEA 2019.7130, coll. 01 Mar. 2015, 12°15.44N, 117°18.13W, 4302 m <http://data.nhm.ac.uk/object/920d8670-507e-4126-a42b-6e208bbe66d3>.

Type locality. Pacific Ocean, CCZ, 12°15.44N, 117°18.13W, depth 4302 m, in mud between polymetallic nodules.

Description. This is a medium-sized species represented by a single specimen. Body cylindrical, iridescent, some annulation detectable in first five and few posterior chaetigers, the rest of body smooth, no annulation detectable (Fig. 16A, B). Ventral groove distinct throughout the body. Live specimen semi-translucent, with orange gut (Fig. 16A). Complete specimen 20 mm long and 1.5 mm wide, with 29 chaetigers;

anterior chaetigers not particularly crowded, degree of crowding observable in the posterior-most three to five chaetigers.

Prostomium of preserved specimen oval and broad (about as long as wide) and anteriorly bluntly rounded, somewhat truncated; bearing very distinct oval palpode (Fig. 16A). Nuchal organs observed as lightly pigmented slits laterally on posterior part of prostomium.

Branchiae present in all chaetigers, except for first chaetiger; branchiae remain attached in most chaetigers, including ch. 29, but are occasionally missing (lost) in some chaetigers. Branchiae easy to detect, although rather slender, best observed in anterior chaetigers (Fig. 16C), then getting progressively thinner and shorter and becoming more difficult to detect (Fig. 16D). All branchiae cirriform.

Parapodia distinct, biramous; with a broad lobe in chaetigers 2–10, becoming smaller in subsequent chaetigers; parapodia embedded in distinct lateral grooves (Fig. 16E). Chaetae are capillaries (Fig. 16F); not particularly numerous in any chaetigers, but most dense and longest in chaetigers 2–8, where of similar length, then becoming shorter, sometimes missing (broken off) entirely.

Anal tube well preserved; relatively short (about the length of two posterior chaetigers) and thick; distally symmetrical; distal opening with cirlet of about 20 short, slender cirri with the exception of ventral part of the margin, which is smooth; ventral cirrus not observed (Fig. 16G).

Genetic data. GenBank MN217457 for 16S and MN217506 for 18S. COI was unsuccessful for this specimen, no identical GenBank matches for 16S or 18S. In our phylogenetic analyses this species is sister to *Ophelina martinezarbizui* sp. nov. (Fig. 23).

Remarks. Similar to *Ophelina martinezarbizui* sp. nov. in overall look and form of anal tube, but slender branchiae are present in all chaetigers, midbody and posterior branchiae are smaller than those of the anterior region.

Ecology. Found in polymetallic nodule province of the eastern CCZ.

Etymology. Named in honor of Kirstin Meyer-Kaiser, member of the science party onboard RV *Thomas G. Thompson* on the AB02 ABYSSLINE cruise in 2015.

***Ophelina nunnallyi* sp. nov.**

<http://zoobank.org/3EE43467-76A5-4FFC-B19F-26C0063454CB>

Fig. 17A–I

Material examined. NHM_683 (**holotype**) NHMUK ANEA 2019.7133, coll. 20 Feb. 2015, 12°32.23N, 116°36.25W, 4425 m <http://data.nhm.ac.uk/object/220fa671-4576-45b7-930d-efde148f223f>; NHM_700 (**paratype**) NHMUK ANEA 2019.7134, coll. 20 Feb. 2015, 12°32.23N, 116°36.25W, 4425 m <http://data.nhm.ac.uk/object/63115f48-bcf1-4b3b-9c2e-c339b97845bd>; NHM_783F NHMUK ANEA 2019.7135, coll. 20 Feb. 2015, 12°32.23N, 116°36.25W, 4425 m <http://data.nhm.ac.uk/object/376a42db-0497-4b4a-851b-c1d5e07bd2b6>; NHM_1273 (**paratype**) NHMUK

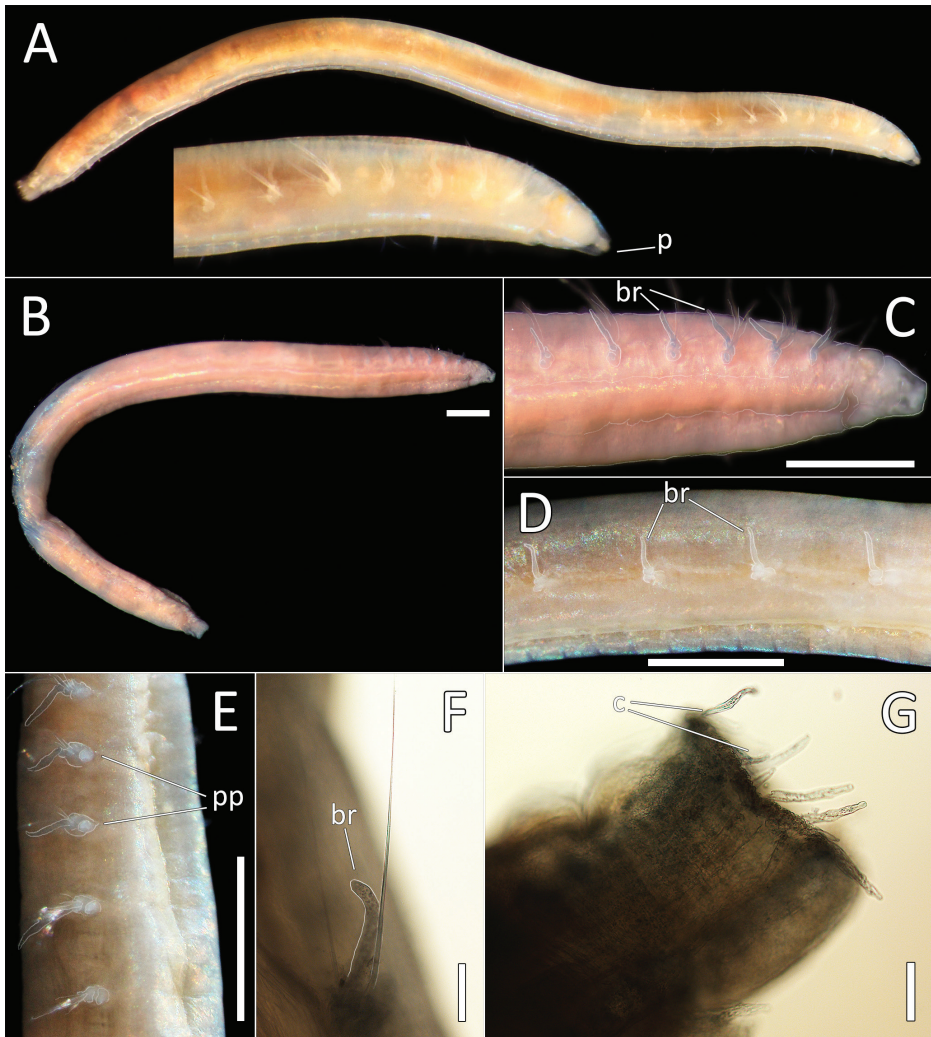


Figure 16. *Ophelina meyerae* sp. nov. holotype (specimen NHM_1241). **A** Live images, whole specimen with detail of anterior (p = palpode) **B** Lab image, whole specimen, lateral view (faded stain) **C** Lab image, anterior and branchiae (faded stain) (br = branchiae) **D** Lab image, mid-body branchiae (faded stain, br = branchiae) **E** Lab image, anterior parapodia (faded stain, pp = parapodia) **F** Lab image, detail of capillary chaetae (br = branchiae) **G** Lab image, detail of capillary chaetae (br = branchiae). Morphological features in plates **C–F** have been outlined with a fine white line to improve clarity of those features. Scale bars: 1 mm (**B–E**); 100 µm (**F, G**).

ANEA 2019.7136, coll. 01 Mar. 2015, 12°15.44N, 117°18.13W, 4302 m <http://data.nhm.ac.uk/object/a3540563-8a0c-475b-96b5-12969fb8c2ba>; NHM_1309A (SEM specimen) NHMUK ANEA 2019.7137, coll. 01 Mar. 2015, 12°15.44N, 117°18.13W, 4302 m <http://data.nhm.ac.uk/object/25066e63-ecc9-439a-9907-eaeab72e78c>.

Type locality. Pacific Ocean, CCZ, 12°32.23N, 116°36.25W, depth 4425 m, in mud between polymetallic nodules.

Description. This species is represented by five complete specimens, none in an excellent condition, anal tube damaged and not clearly observed. However, images of live specimens are available to observe some now missing or damaged features such as anal tube.

Small to medium-sized species 9–14 mm long and 0.25–0.8 mm wide, for 33 chaetigers. Body cylindrical and smooth without distinct annulation. Preserved specimen yellow semi-translucent, iridescent in ethanol (Fig. 17A); live specimens translucent (Fig. 17B). Ventral and lateral grooves distinct along whole length of the body. Chaetigers elongated, only slightly crowded in first eight anterior chaetigers and towards posterior end.

Prostomium of preserved specimen conical (longer than wide), anteriorly pointed and extending into very long, thick palpode (Fig. 17C, D). Rounded, slightly pigmented nuchal organs everted in specimen NHM_683.

Branchiae observed in anterior chaetigers only, some missing (broken off), present from chaetigers 4–9 (Fig. 17E). All branchiae cirriform, conspicuous but relatively short, straight, distally blunt.

Parapodia biramous, embedded in lateral grooves; observed as distinct conical lobes throughout the body (Fig. 17F). Chaetae are capillaries only (Fig. 17G); often missing (broken off), most abundant in anterior eight chaetigers.

Anal tube attached (in holotype, NHM_783F and NHM_1309A), but now poorly preserved and variably damaged, always separated from the rest of the body by a shallow constriction (Fig. 17H, I). Anal tube of live specimen well-imaged in Fig. 17H, where anal tube scoop-shaped, ventrally with wide depression; distally with two elongate, slender cirri; no other cirri observed, but may be missing.

Additional morphological observations. In addition to the material examined here, several more specimens consistent with this species have been found, but no DNA sequencing has been carried out on these and thus they are not included in this manuscript. Where the anal tube was observed, it is scoop-shaped, but the preservation of cirri is variable. In some specimens, short slender cirri can be detected on the lateral margins of the anal tube. Chaetiger counts consistent with 33 chaetigers. Branchiae were consistently observed on chaetigers 4–9. However, in the absence of DNA data we are reluctant to ascribe these specimens formally to *O. nunnallyi* sp. nov. until further analyses has been done.

Genetic data. GenBank MN217458–MN217462 for 16S, MN217507 for 18S and MN217532–MN217534 for COI. This species is genetically identical to or very similar to “*Ophelina* sp. 1” (Janssen et al. 2015), with K2P values ranging from 0.002–0.006 between *O. nunnallyi* sp. nov. and the already published sequences with accession numbers KJ736582–KJ736588. *Ophelina nunnallyi* sp. nov. is sister to *Ophelina* sp. (NHM_1068) in our phylogenetic analyses (Fig. 23).

Remarks. Other than sp. NHM_1068 (see Remarks under sp. NHM_1068), the DNA suggest similarity of *Ophelina nunnallyi* sp. nov. to *O. acuminata*, originally described from the shallow coast of Denmark, but frequently reported in all oceans (see references in Parapar et al. 2011). These frequent records likely constitute an

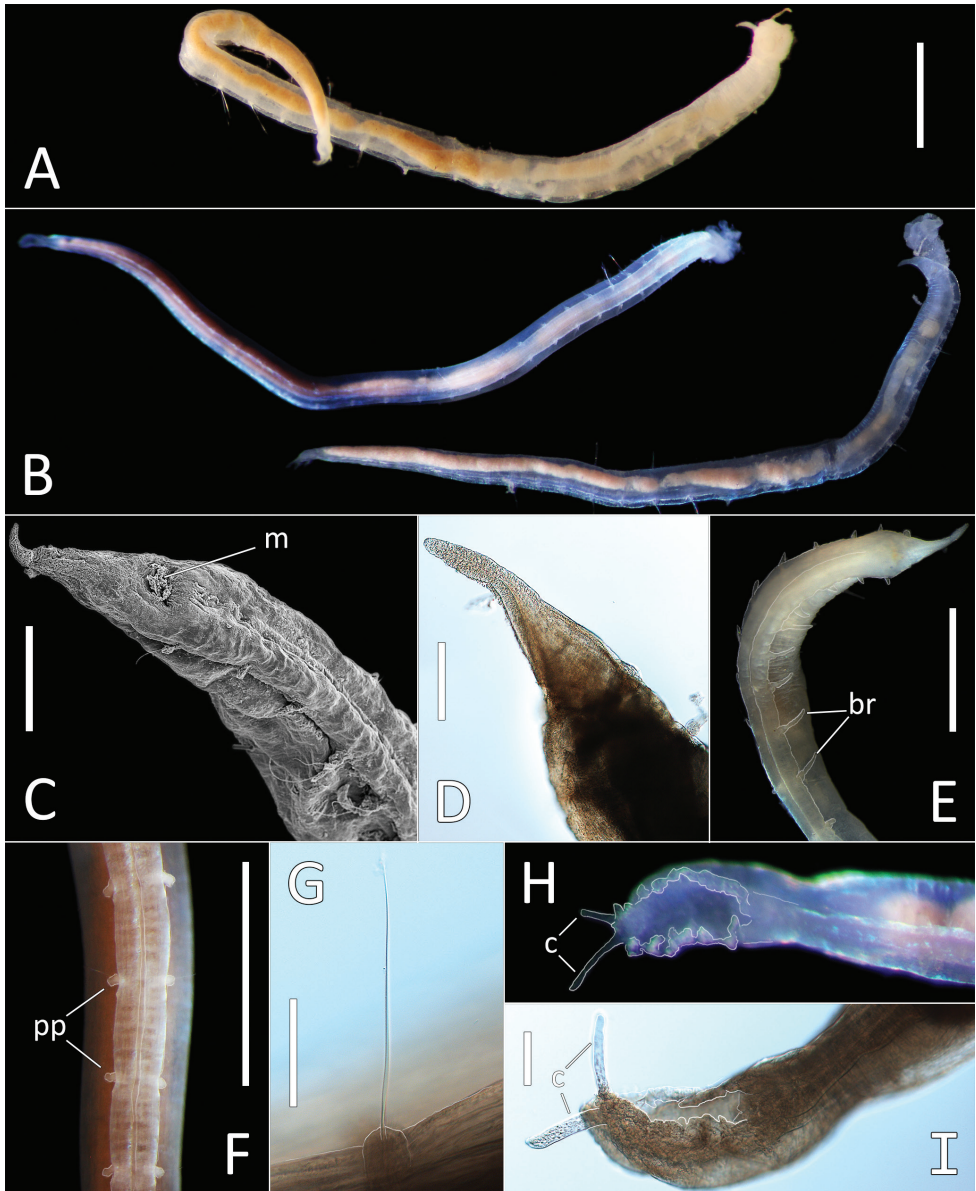


Figure 17. *Ophelina nunnallyi* sp. nov. **A** Lab image, whole specimen (paratype NHM_700) **B** Live images, whole specimens (holotype [specimen NHM_683] [left], paratype NHM_700 [right]) **C** SEM image, anterior and palpode (specimen NHM_1309A, m = mouth) **D** Lab image, detail of palpode, (paratype NHM_1273) **E** Lab image, anterior and branchiae (paratype NHM_1273, br = branchiae) **F** Lab image, parapodia (holotype, pp = parapodia) **G** Lab image, capillary chaeta (holotype) **H** Live image, anal funnel (holotype, c = cirri) **I** Lab image, detail of anal funnel (holotype, c = cirri). Morphological features in plates **E, F, H, I** have been outlined with a fine white line to improve clarity of those features. Scale bars: 1 mm (**A, E, F**); 200 μ m (**C, D**); 100 μ m (**G, I**).

error as similar, but unrecognized species were likely confused. Deep-sea records of *Ophelina aulogaster* (Rathke, 1843) by for example Hartman (1965), and Fauchald (1972, may refer to a similar, but unrecognized, species. Hartman (1965) recognized deep Atlantic specimens as a distinct species and later erected *Ophelina aulogastrella* (Hartman & Fauchald, 1971), which lacks branchiae in posterior region, with most of them present in chaetigers 4–10 (or 13) and anal tube is scoop-shaped with some (easily lost) cirri. Such morphology agrees well with UKSR specimens. However, Hartman (1965) reported variable number of segments (28–36) and wide bathyal distribution (196–5023 m) for *O. aulogastrella*, which may suggest that more than one species was in fact present in Hartman's material. The type locality of *O. aulogastrella* is North Atlantic.

The first occurrence of branchiae from chaetiger 4 is very unusual in *Ophelina*, where branchiae appear from chaetiger 2. Branchiae are fragile and easily lost structures; therefore, we cannot exclude a possibility that branchiae prior to chaetiger 4 are present but lost in our specimens. Nevertheless, this distribution has been observed in all material examined (including additional specimens, no DNA available) as well as in very similar species *Ophelina* sp. (NHM_1068).

Ecology. Found in polymetallic nodule province of the eastern CCZ.

Etymology. Named in honor of Clifton Nunnally, member of the science party of both the ABYSSLINE cruises.

***Ophelina* cf. *abranchiata* Støp-Bowitz, 1948**

General comments on *Ophelina abranchiata* and similar morphotypes. Three small, abranchiate morphospecies found in the UKSR material, *Ophelina ganae* sp. nov., *O. cf. abranchiata* NHM_1769 and *O. cf. abranchiata* NHM_2017, are very similar to *Ophelina abranchiata* Støp-Bowitz, 1948. This species has its type locality as East Greenland, 200 m depth, but has subsequently been reported worldwide, from predominantly deep waters [see references in Kongsrud et al. (2011), Parapar et al. (2011)]. Sene-Silva (2007) proposed *Polyophthalmus translucens* Hartman, 1960 and *Ophelina farallonensis* Blake, 2000, both described from deep waters off California, as junior synonyms of *O. abranchiata*. Blake (2000b) had separated *O. farallonensis* from *O. abranchiata* due to presence of long anal tube, but he most likely did not realize that the original description of *O. abranchiata* by Støp-Bowitz (1948) was based on an incomplete specimen without an anal tube as already suggested by Sene-Silva (2007), Kongsrud et al. (2011) and Parapar et al. (2011). The absence of branchiae also likely led to confusion of *O. abranchiata* with the much larger (30 mm long, 30 chaetigers) abranchiate species *Ophelina nematoides* by some workers (e.g. Maciolek and Blake 2006).

Such confused taxonomic history is further complicated by the fact that published (Neal et al. 2018) and unpublished (Kongsrud pers. comm.) molecular data suggest presence of several species within an *O. abranchiata* complex. Kongsrud et al. (2011)

provided a re-description of type material, together with report on material from North Sea and North Atlantic, but without providing genetic data. One possible, and previously overlooked, character may be the number of chaetigers as Kongsrud et al. (2011) reported an invariable number of 18 chaetigers for *O. abbranchiata*, and considered specimens bearing 17 chaetigers from Skagerrak in need of further evaluation, not ascribing these to *O. abbranchiata*. In other reports, variation of 17–19 chaetigers (4–10 mm long) was given by Barroso and Paiva (2013) and Parapar and Moreira (2008) referred to 16–22 segments with detectable annulation, rather than chaetigers. Hartman (1960) reported 18 chaetigers for *P. translucens* and Blake (2000b) reported 18 or 19 chaetigers (5–7 mm long) for *O. farallonensis*.

The anal tube, an important feature upon which opheliid species have been differentiated in the past is mostly missing in these morphotypes even where hundreds of specimens are available (Neal pers. obs.). Where the anal tube has been observed (Blake 2000b; Parapar and Moreira 2008; Kongsrud et al. (2011); Parapar et al. 2011; Barroso and Paiva 2013; Neal pers. obs.) its form appears to be very similar.

Parapar and Moreira (2008) provided the first SEM examination of *O. abbranchiata* morphotypes and reported presence of lateral organs between notopodia and neuropodia for Iberian specimens. Subsequently, examination of Icelandic morphotypes by Parapar et al. (2011) led to the report of presence of lateral organs in all chaetigerous segments as well as in the anterior segments of the body which are achaetigerous and devoid of parapodia, suggesting the presence of three such segments. However, this feature was not observed in SEM examination of bathyal material from Brazil by Barroso and Paiva (2013). Despite this variation, none of these authors suggested lateral organs as a useful taxonomic character and previously Purschke and Hausen (2007) only considered that they might be useful for higher level systematics of annelids. Although the presence and distribution of lateral organs was only investigated in non-type specimens (Parapar and Moreira 2008; Parapar et al. 2011; Barroso and Paiva 2013), their presence reported in some specimens and absence in others could possibly be result of interspecific variability. However, it is important to stress that these structures are extremely small (around 5 µm) and their observation depends on the quality of the specimens (i.e. in shriveled specimens, this feature may be impossible to observe). Two UKSR specimens were investigated under SEM for lateral organs. Lateral organs were confirmed in both specimens examined. Three lateral organs were associated with three prechaetigerous segments and then one observed between the noto- and neuropodium of each chaetiger. Such distribution is consistent with previous observations (Parapar and Moreira 2008; Parapar et al. 2011). The pattern which pore openings form in each morphotype appears to vary, but currently we cannot confirm consistency of such observation due to the low number of specimens examined so far.

Clearly, additional morphological characters are needed to distinguish small abbranchiate species currently lumped under *O. abbranchiata*, *P. translucens* and *O. farallonensis*.

***Ophelina* cf. *abranchiata* (NHM_1769)**

Fig. 18A–E

Material examined. NHM_1769 NHMUK ANEA 2019.7148, coll. 11 Mar. 2015, 12°10.43N, 117°11.57W, 4045 m <http://data.nhm.ac.uk/object/8a2cbe4f-277d-4355-a34f-0b53c797bef0>.

Description. This species is represented by a single specimen, in reasonable condition, but anal tube is missing. Small species, 5.3 mm long and 0.3 mm wide; the exact number of chaetigers is difficult to establish, but at least 16 counted, although 17 may be present.

Body cylindrical and smooth without distinct annulation (Fig. 18A, B). Preserved specimen yellow in ethanol; live specimen translucent, with yellow gut (Fig. 18A). Ventral and lateral grooves distinct along whole length of body. Anterior and posterior-most chaetigers slightly shorter than mid-body chaetigers.

Prostomium elongate, conical with small acute terminal palpode (Fig. 18C). Eyes not observed. Nuchal organs rounded, laterally on posterior part of prostomium. Peristomium indistinct. Anterior prechaetigerous region elongated, number of achaetous segments unknown (no SEM). Parapodia rudimentary, biramous, embedded in lateral grooves; no distinct pre- or postchaetal lobes.

Chaetae all slender, smooth capillaries (Fig. 18D), appear in small numbers in both rami, often broken off entirely. Notochaetae mostly longer than neurochaetae.

Branchiae absent. Anal tube not observed. Shirlastained specimens without distinct pattern (Fig. 18E).

Genetic data. GenBank MN217433 for 16S, MN217501 for 18S and MN217520 for COI. In our phylogenetic analyses it is part of a well-supported clade with *Ophelina ganae* sp. nov., *Ophelina* cf. *abranchiata* (NHM_2017) and at least two other abranchiate opheliids (Fig. 23).

Remarks. Please refer to section “General comments on *Ophelina abranchiata* and similar morphotypes” above and remarks for *Ophelina ganae* sp. nov.

***Ophelina* cf. *abranchiata* sp. (NHM_2017)**

Fig. 19A–F

Material examined. NHM_2017 NHMUK ANEA 2019.7149, coll. 16 Mar. 2015, 12°03.03N, 117°24.28W, 4235 m <http://data.nhm.ac.uk/object/9ebcd947-c53b-4616-81d4-da42afaeca03>.

Description. This species is represented by a single specimen, in reasonable condition, but anal tube is missing. Small species, 4 mm long and 0.35 mm wide; exact number of chaetigers difficult to establish, but at least 17 counted, although 18 may be present.

Body cylindrical and smooth without distinct annulation (Fig. 19A–C). Preserved specimen yellow in ethanol; live specimen translucent, with yellow gut (Fig. 19A).

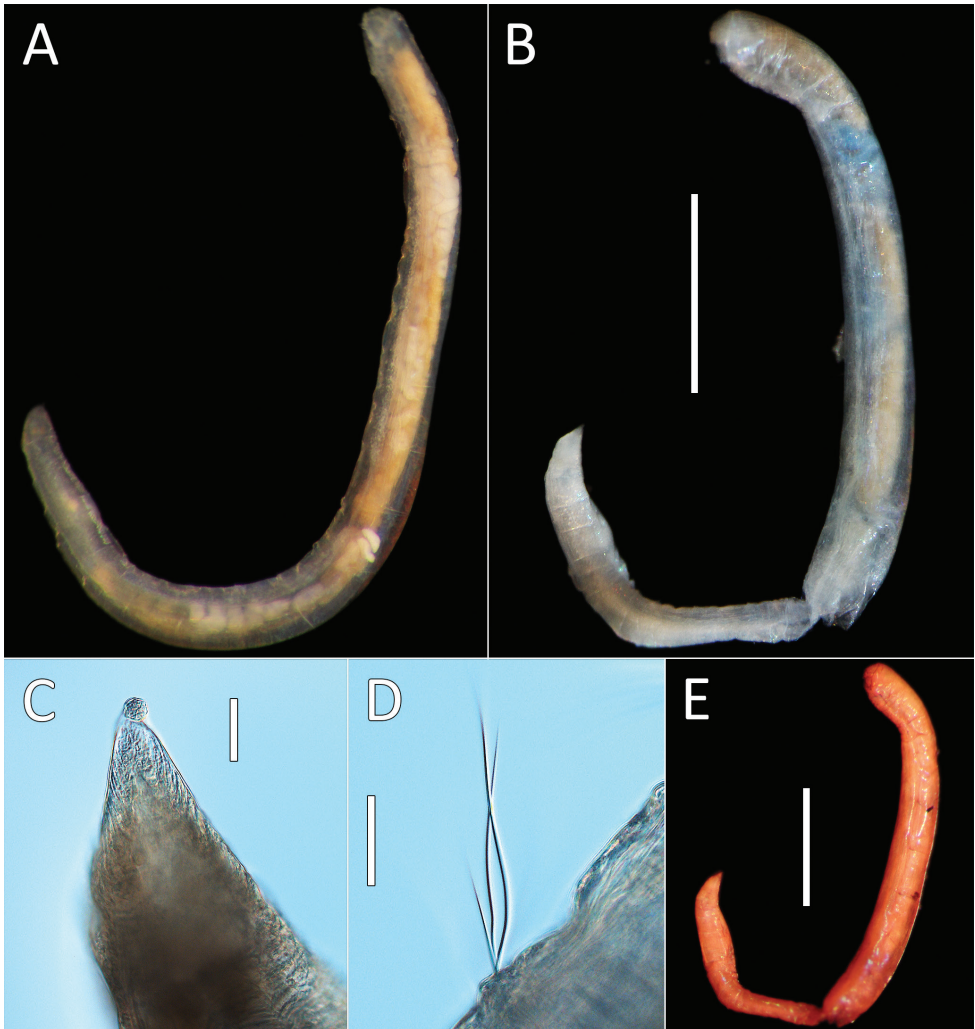


Figure 18. *Ophelina* cf. *abranchiata* sp. NHM_1769 (specimen NHM_1769). **A** Live image, whole specimen **B** Lab image, whole specimen (very faded post-stain,) **C** Lab image, detail of prostomium and palpode **D** Lab image, detail of chaetae **E** Lab image, whole specimen (stained). Scale bars: 1 mm (**B**, **E**); 50 μ m (**C**, **D**).

Ventral and lateral grooves distinct along whole length of body. Anterior and posterior-most chaetigers slightly shorter than mid-body chaetigers.

Prostomium elongate, conical with small acute terminal palpode (Fig. 19D, E). Eyes not observed. Nuchal organs rounded, laterally on posterior part of prostomium. Peristomium indistinct. Anterior prechaetigerous region elongated, number of achaetous segments unknown (no SEM). Parapodia rudimentary, biramous, embedded in lateral grooves; no distinct pre- or postschaetal lobes.

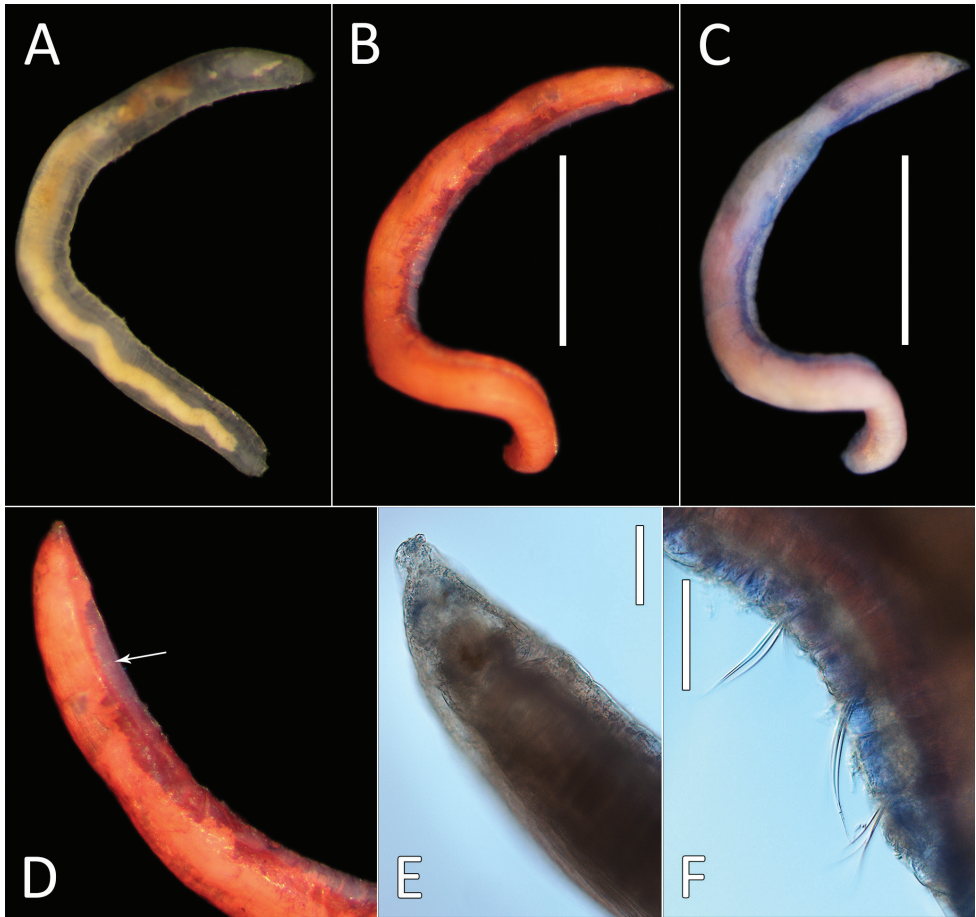


Figure 19. *Ophelina* cf. *abranchiata* sp. NHM_2017 (specimen NHM_2017). **A** Live image, whole specimen **B** Lab image, whole specimen (stained,) **C** Lab image, whole specimen (faded stain) **D** Lab image, anterior (stained, arrow highlighting dark banding) **E** Lab image, detail of anterior **F** Lab image, detail of capillary chaetae. Scale bars: 1 mm (**B, C**); 100 μ m (**E, F**).

Chaetae all slender, smooth capillaries (Fig. 19F), appear in small numbers in both rami, often broken off entirely. Notochaetae mostly longer than neurochaetae.

Branchiae absent. Anal tube not observed. Shirlastained specimens with wide, dark red, strongly stained stripe on the dorsum (Fig. 19B, D), not observed in species *Ophelina ganae* sp. nov. and *Ophelina* cf. *abranchiata* (NHM_1769).

Genetic data. GenBank MN217434 for 16S. In our phylogenetic analyses, *Ophelina* cf. *abranchiata* sp. (NHM_2017) is part of a well-supported clade including *Ophelina ganae* sp. nov., *Ophelina* cf. *abranchiata* (NHM_1769) and at least two other abranchiate opheliid species (Fig. 23).

Remarks. Please refer to section “General comments on *Ophelina abranchiata* and similar morphotypes” above and remarks for *Ophelina ganae* sp. nov.

***Ophelina* sp. (NHM_689)**

Fig. 20A–H

Material examined. NHM_689 NHMUK ANEA 2019.7114, coll. 20 Feb. 2015, 12°32.23N, 116°36.25W, 4425 m <http://data.nhm.ac.uk/object/6755d584-a20a-4ce5-a4f1-32ce0965128e>.

Description. This species is represented by a single specimen in poor condition, with anal tube and most of branchiae missing. Posteriorly incomplete specimen 4.7 mm long and 0.35 mm wide for at least 22 chaetigers (exact number of chaetigers is difficult to count in places). Body cylindrical and smooth without distinct annulation (Fig. 20A–C). Ventral and lateral grooves distinct throughout body. Preserved specimen yellow in ethanol (Fig. 20A); live specimen translucent, pale brown gut (Fig. 20C). Chaetigers crowded in anterior part of the body and posterior part of the body (the last four chaetigers), elongated in the mid-section of the body.

Prostomium of preserved specimen conical, broad (only slightly longer than wide), anteriorly bluntly rounded (but prostomium appears damaged) (Fig. 20D). Proboscis extended, damaged, soft inflated sack-like structure observed.

Branchiae present, but many are likely missing. Branchiae observed in chaetigers 2–4 (Fig. 20D, E) and then in posterior region, where only one branchia remains attached on the fourth before the last chaetiger (Fig. 20F); no branchiae observed in mid-body region.

Parapodia distinct, biramous; embedded in lateral grooves (Fig. 20G). Chaetae are capillaries only (Fig. 20H); all very long but longest on chaetiger 1 where they are nearly twice the length of chaetae of subsequent chaetigers. Anal tube likely missing (damaged).

Genetic data. GenBank MN217463 for 16S and MN217508 for 18S. COI was unsuccessful for this specimen, no identical GenBank matches for 16S or 18S. In our phylogenetic tree, *Ophelina* sp. (NHM_689) is sister to *Ophelina cylindricaudata* (Hansen, 1879) from the Atlantic (New England) (Fig. 23).

Remarks. Due to the condition of the single specimen representing this morphospecies, important diagnostic characters such as the structure of the anal tube and distribution of the branchiae cannot be determined. See Remarks under *Ophelina* sp. (NHM_1331) for more details.

***Ophelina* sp. (NHM_1068)**

Fig. 21A–H

Material examined. NHM_1068 NHMUK ANEA 2019.7138, coll. 26 Feb. 2015, 12°06.93N, 117°09.87W, 4100 m <http://data.nhm.ac.uk/object/b28fd52f-5717-45e3-b0cc-369172a690e5>; NHM_1874 NHMUK ANEA 2019.7139, coll. 13 Mar. 2015, 12°02.49N, 117°13.03W, 4094 m, <http://data.nhm.ac.uk/object/c3ffe5f4-6ca3-4816-966c-25ec98bbb003>.

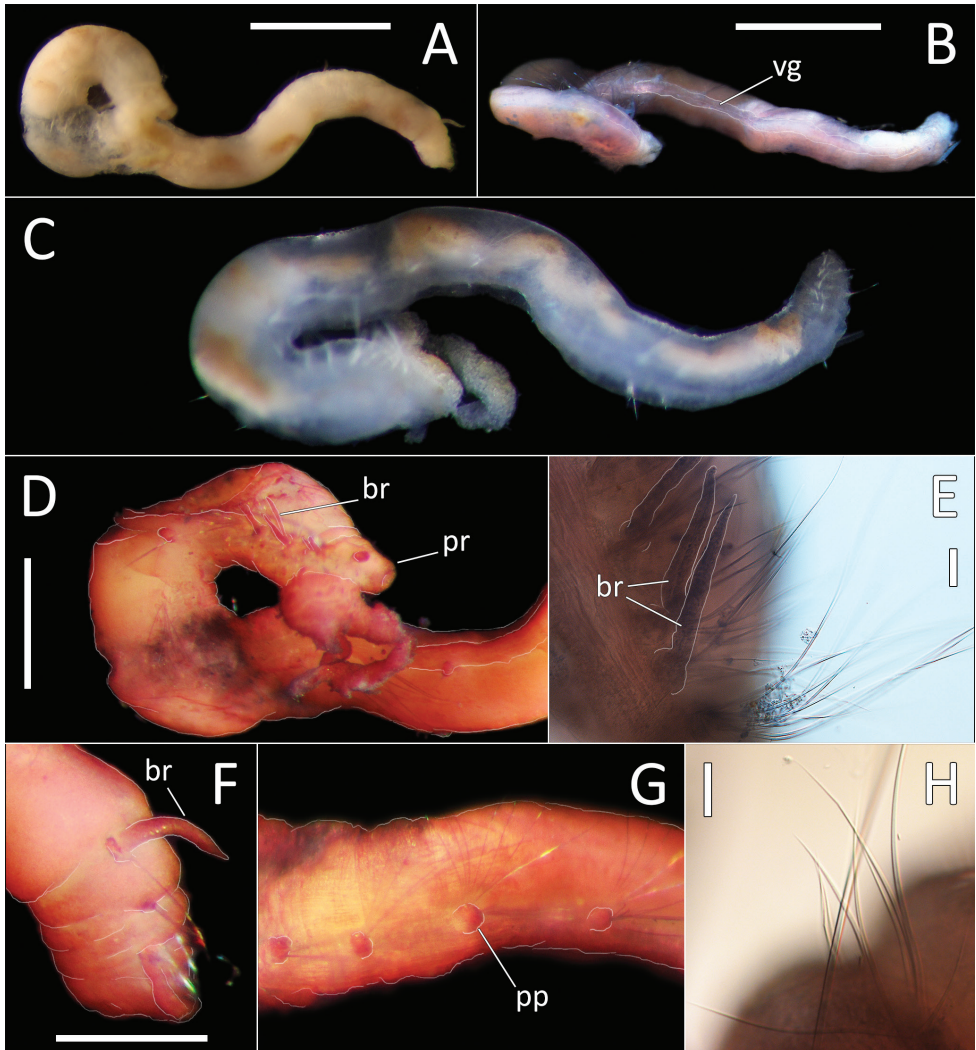


Figure 20. *Opbelina* sp. NHM_689 (specimen NHM_689). **A** Lab image, whole specimen, lateral view (pre-stain) **B** Lab image, whole specimen, ventral view (faded stain, vg = ventral groove) **C** Live image, whole specimen **D** Lab image, damaged anterior (stained, br = branchiae, pr = prostomium) **E** Lab image, detail of anterior branchiae (br = branchiae) **F** Lab image, posterior branchiae (stained, br = branchiae) **G** Lab image, mid-body parapodia (stained, pp = parapodia) **H** Lab image, detail of capillary chaetae. Morphological features in plates **B**, **D–G** have been outlined with a fine white line to improve clarity of those features. Scale bars: 1 mm (**A**, **B**); 0.5 mm (**D**); 50 μ m (**E**); 0.25 (**F**, **H**).

Description. This species is represented by two specimens, both in poor condition; specimen NHM_1874 posteriorly incomplete, specimen NHM_1068 mostly complete, but anal tube damaged. Large species 25–30 mm long and 0.8 mm wide, for minimum of 30 chaetigers (exact number of chaetigers cannot be established). Body cylindrical and smooth without distinct annulation (Fig. 21A–C). Preserved specimen

yellow in ethanol (Fig. 21A); live specimens translucent, yellowish (Fig. 21C, D). Ventral and lateral grooves distinct along whole length of the available fragments. Chaetigers somewhat crowded in anterior part of the body, then elongated in the rest of the body, posterior-most chaetigers not observed.

Prostomium of preserved specimen conical (longer than wide), anteriorly pointed and extending into very large and long thick palpode (Fig. 21D, E). Branchiae observed in anterior chaetigers only, but many missing (broken off) and the exact distribution cannot be confirmed; mainly observed in chaetigers 4–13; branchiae conspicuous but rather short, straight, distally blunt (Fig. 21D, F).

Parapodia biramous, embedded in lateral grooves; parapodia small conical lobes, no distinct pre- or postchaetal lobes observed (Fig. 21F). Chaetae are capillaries only; often missing (broken off).

Anal tube missing in specimen NHM_1874; damaged in NHM_1068, but probably scooped-shaped (Fig. 21G-H).

Genetic data. GenBank MN217464 and MN217466 for 16S and MN217509 for 18S. COI was unsuccessful for this specimen, no identical GenBank matches for 16S and 18S.

Remarks. According to our molecular results, this species forms a clade with *Ophelina nunnallyi* sp. nov., which is sister to *O. acuminata* (Fig. 23), but due to specimen damage, meaningful morphological comparison cannot be currently provided. *Ophelina* sp. (NHM_1068) and *O. nunnallyi* sp. nov. share a similar prostomium shape and its associated robust palpode, branchiae occurring from chaetiger 4 that are limited to anterior part of the body (ch. 4–9). However, *Ophelina* sp. (NHM_1068) has a larger body size. See also Remarks under *Ophelina nunnallyi* sp. nov. above.

***Ophelina* sp. (NHM_1331)**

Fig. 22A–G

Material examined. NHM_1331 NHMUK ANEA 2019.7115, coll. 01 Mar. 2015, 12°15.44N, 117°18.13W, 4302 m <http://data.nhm.ac.uk/object/06d48d7f-7339-4cc5-8445-b51a980e4e0f>.

Description. This species is represented by a single complete specimen in relatively good condition. Specimen about 4.5 mm long and 0.5 mm wide for about 28 chaetigers. Body cylindrical and smooth with some annulation detectable (Fig. 22A–C). Ventral and lateral grooves distinct throughout body. Preserved specimen yellow in ethanol; live specimen translucent, with yellow gut (Fig. 22C); everted nuchal organs with golden brown pigment (Fig. 22A–D). Chaetigers crowded in anterior part of the body and posterior part of the body (the last four chaetigers), elongated in the mid-section of the body.

Prostomium of preserved specimen conical, broad (only slightly longer than wide) and anteriorly bluntly rounded; palpode not observed (Fig. 22D, E). Nuchal organs laterally on posterior part of prostomium, everted, round with golden brown pigment observable even in preserved specimen.

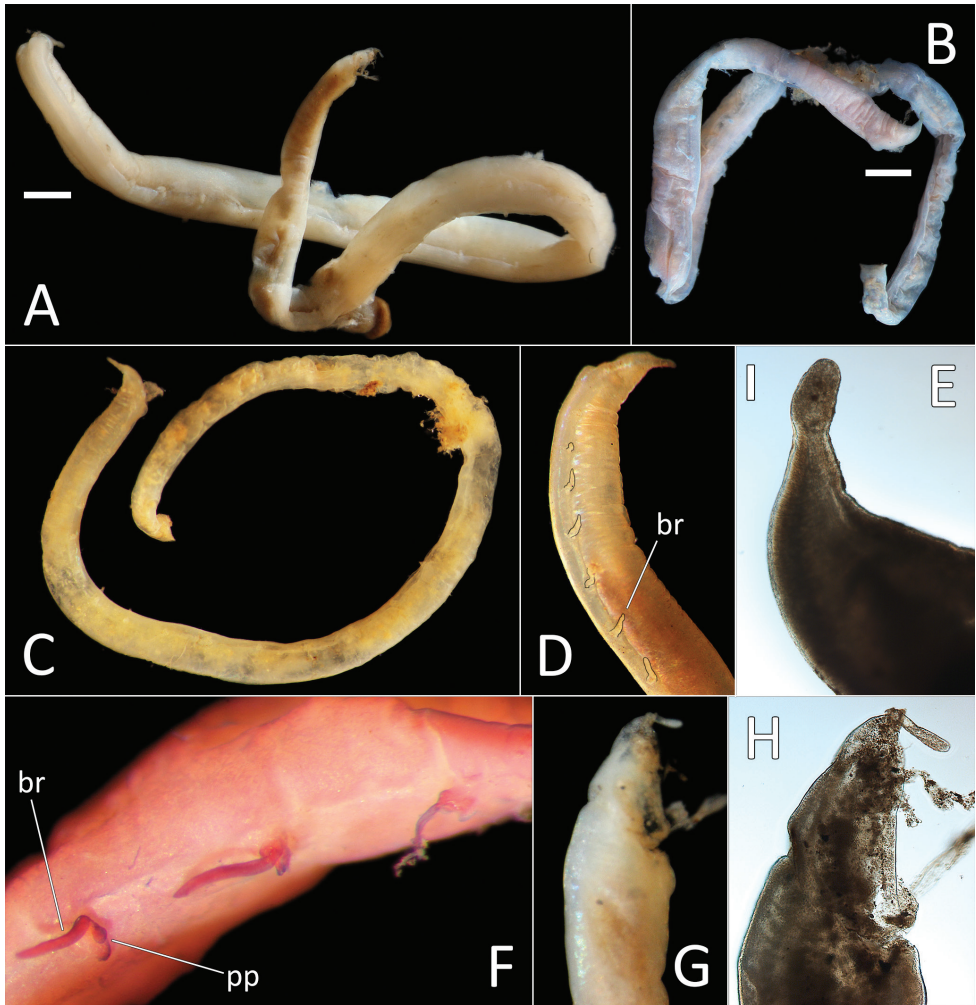


Figure 21. *Ophelina* sp. NHM_1068. **A** Lab image, whole specimen (specimen NHM_1068,) **B** Lab image, whole specimen (specimen NHM_1874, faded stain) **C** Live image, whole specimen (specimen NHM_1874) **D** Live image, anterior, with branchiae outlined in a fine black line (specimen NHM_1068, br = branchiae) **E** Lab image, detail of palpode (specimen NHM_1068) **F** Lab image, detail of anterior parapodia and branchiae (specimen NHM_1874, stained) **G** Lab image, posterior (specimen NHM_1068) **H** Lab image, detail of anal funnel (specimen NHM_1068). Scale bars: 1 mm (**A**, **B**); 100 µm (**E**).

Branchiae present; with disjointed distribution, with three pairs on chaetigers 2–4 (Fig. 22D, E) and three pairs in posterior region on chaetigers 21–24 (Fig. 22F, G); branchiae in other chaetigers not observed, branchiae considered absent in the last four crowded chaetigers. All branchiae cirriform, of similar length.

Parapodia distinct, biramous; embedded in lateral grooves on chaetigers 1–24; no distinct pre- or postchaetal lobes. Chaetae are capillaries only; all very long but

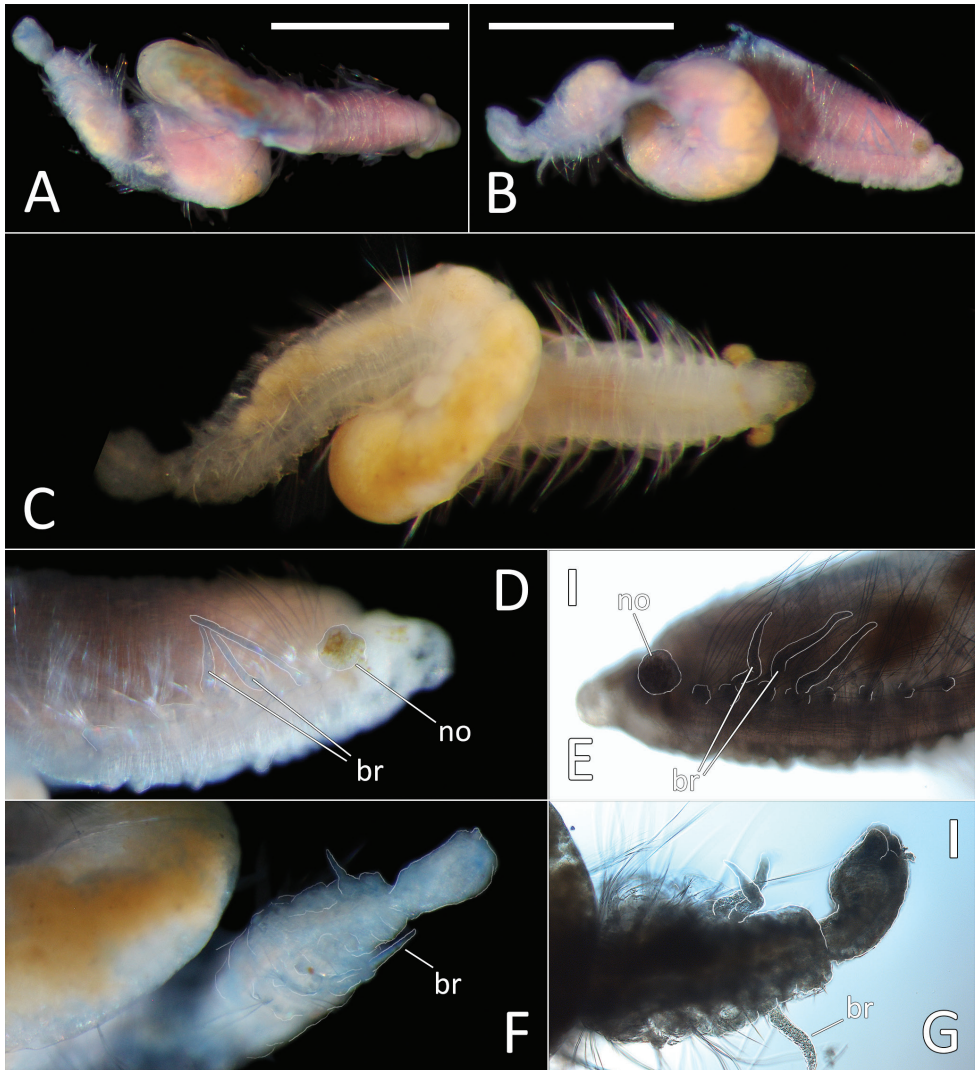


Figure 22. *Ophelina* sp. NHM_1331 (specimen NHM_1331). **A** Lab image, whole specimen, dorsal view (faded stain) **B** Lab image, whole specimen, lateral view (faded stain) **C** Live image, whole specimen **D** Lab image, anterior (faded stain, br = branchiae, no = nuchal organ) **E** Lab image, detail of anterior (br = branchiae, no = nuchal organ) **F** Lab image, posterior, anal funnel (br = branchiae) **G** Lab image, detail of posterior and anal funnel (br = branchiae). Morphological features in plates **B, D–G** have been outlined with a fine white line to improve clarity of those features. Scale bars: 1 mm (**A, B**); 100 μ m (**E, G**).

longest on chaetiger 1 where they are nearly twice the length of chaetae of subsequent chaetigers.

Anal tube attached, but not well preserved; cylindrical; appears distally asymmetrical with dorsal lobe overlapping the ventral lobe (but this may be an artefact of poor preservation) (Fig. 22F, G); cirrus not observed.

Genetic data. GenBank MN217465 for 16S and MN217510 for 18S. COI was unsuccessful for this specimen, no identical GenBank matches for 16S or 18S. In our phylogenetic tree, *Ophelina* sp. (NHM_1331) is sister to “*Ophelina* sp. F14588” forming a clade with the taxa *Ophelina cylindricaudata* from the Atlantic (New England) and *Ophelina* sp. (NHM_689) (Fig. 23).

Remarks. Morphologically, *Ophelina* sp. (NHM_1331) is similar to *Ophelina* sp. (NHM_689) in having a broad prostomium and very long chaetae on chaetiger 1. Their branchiae appear to be arranged in a similar pattern (three pairs are present in chaetigers 2–5 and then few pairs present in posterior chaetigers). Nuchal organs are

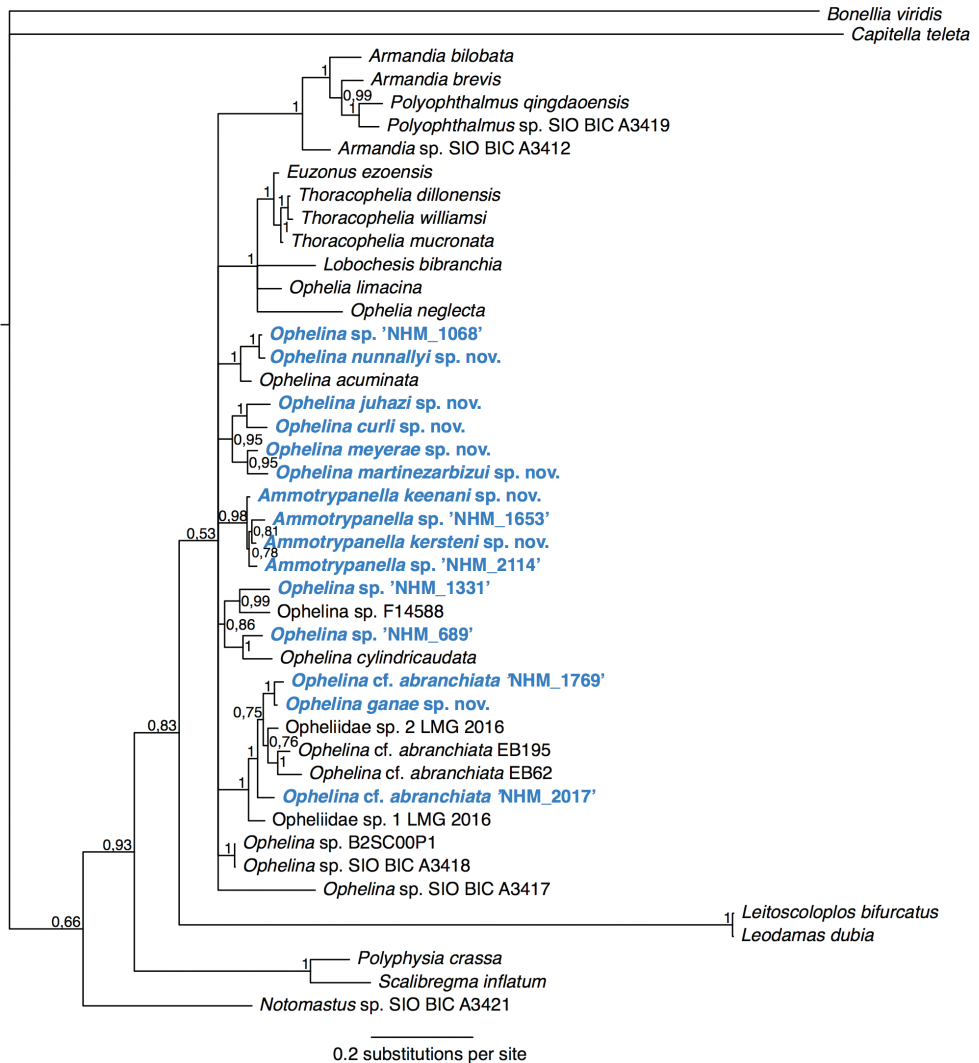


Figure 23. Phylogenetic analysis of Opheliidae. 50% majority rule tree from the Bayesian analyses using 18S and 16S, with posterior probability values on nodes. Twenty-nine taxa from GenBank were included, and Capitellidae and Echiura was chosen as outgroup following the annelid phylogeny of Weigert and Bleidorn (2016).

not everted in *O. sp.* (NHM_689). They may differ in number of chaetigers, although this is difficult to establish due to damage of *O. sp.* (NHM_689), anal tube has not been observed in *O. sp.* (NHM_689) (assumed missing) and cannot be compared.

Of known species of *Ophelina*, *O. sp.* (NHM_1331) is similar to a group with 28 chaetigers and four posterior parapodia crowded: *O. cylindricaudata*, *O. breviata* (Ehlers, 1913) and *O. brattegardi* Kongsrud et al., 2011.

The lack of branchiae in midbody has been described in some of these species, but for *O. cylindricaudata* this has been clarified as a mistake in the original description. Kongsrud et al. (2011) reported that branchiae in the mid-body region may be present in *O. cylindricaudata* but are often reduced in size and when they are lacking there is no consistent pattern. The absence of branchiae is considered “true” in *Ophelina chaetifera* (Hartman 1965), described from the deep Atlantic (1330–5007 m) and *O. brattegardi* described from Iceland Sea (off East Greenland) in 1600 m depth. The UKSR species differs from both in having broad, anteriorly blunt prostomium. *Ophelina chaetifera* further differs in having only 26 chaetigers. However, with only single specimen available for examination, we cannot establish “true” branchial distribution in UKSR samples.

Scalibregmatidae Malmgren, 1867

Notes. The family Scalibregmatidae was established by Malmgren (1867) to accommodate annelids with rugose appearance of the cuticle and either elongate (arenicoliform) or maggot-shaped body form, with often anteriorly inflated bodies such as *Scalibregma inflatum* Rathke, 1843 and *Polyphysia crassa* (Ørsted, 1843). Currently, there are over 50 valid scalibregmatid species (Read and Fauchald 2018a) but see also discussion about *Travisia*.

The characters used to differentiate genera are the prostomial shape, presence and development of branchiae, presence of spines in anterior notopodia (and sometimes also in neuropodia), presence and development of branchiae and development of dorsal and ventral cirri, particularly in posterior part of the body (e.g. Blake 1981, 2000c). However, these characters are considered problematic due to their overlap between genera (Blake 2000c). Additionally, characters such as the form of the prostomium and presence of branchiae depend on the stage of ontogeny (Blake 2015). Recently, Blake (2015) reported previously overlooked characters that he considers species specific such as development of ventral part of the peristomium into complex upper and lower lips surrounding the mouth; form of short, spinous chaetae anterior to capillaries in parapodia preceding lyrate chaetae and development of internal glands within parapodia. Blake (2015) also concluded that small specimens cannot be reliably referred to a species or genus without a growth sequence and previously described species should be re-examined for characters such as presence of spinous chaetae in anterior parapodia and development of internal glands.

Although Scalibregmatidae range from the intertidal to the deep sea, most species occur below 1000 m (Blake 2015). Four scalibregmatid species were encountered in the UKSR-collected material. Three of these are assigned to the genus *Oligobregma* Kudenov & Blake, 1978, while one species could not be assigned to a genus based on

morphology due to its poor condition. Generic assignment of ABYSSLINE species to *Oligobregma* is based on the presence of the following characters: elongate arenicoliform body, prostomium with prominent frontal horns, absence of branchiae, presence of spines in anterior chaetigers and presence of well-developed dorsal and ventral cirri in posterior chaetigers.

The diagnosis of *Oligobregma* presented here is amended from that given by Blake (2017), mainly to take into account a more posterior appearance of furcate chaetae, which Blake (2017) considered to appear prior to chaetigers 2–4.

Diagnosis. Body elongate and arenicoliform. Prostomium T-shaped with two prominent frontal horns. Eyes present or absent, nuchal organs present. Peristomium achaetous, surrounding prostomium dorsally and forming upper and lower lips of mouth ventrally. Branchiae absent. Parapodia well developed, with dorsal and ventral cirri on posterior chaetigers; interramal papillae present or absent. Large acicular spines present on anterior chaetigers. Capillaries present in all parapodia; lyrate chaeta present. Some species with short, slender, blunt or pointed spinous chaetae anterior to capillaries of chaetigers 1, 2 or 3, representing homologues of lyrate chaetae. Pygidium with anal cirri.

***Oligobregma brasierae* sp. nov.**

<http://zoobank.org/2FC2E16E-1463-4D6A-B3C1-90FEDFB222BC>

Figs 24A–J, 25A–C

Material examined. NHM_032 NHMUK ANEA 2019.7150, coll. 09 Oct. 2013, 13°50.232N, 116°33.506W, 4336 m <http://data.nhm.ac.uk/object/43545746-b8ad-43a8-92b7-53637dd131d6>; NHM_404 NHMUK ANEA 2019.7151, coll. 20 Oct. 2013, 13°51.797N, 116°32.931W, 4050 m <http://data.nhm.ac.uk/object/5fda0cac-0a77-4ec7-a2fa-5cd529548a19>; NHM_684 (**paratype**) NHMUK ANEA 2019.7152, coll. 20 Feb. 2015, 12°32.23N, 116°36.25W, 4425 m <http://data.nhm.ac.uk/object/d84c37ed-138e-4064-a11d-a11a2470dfdf>; NHM_823 (**holotype**) NHMUK ANEA 2019.7153, coll. 20 Feb. 2015, 12°32.23N, 116°36.25W, 4425 m <http://data.nhm.ac.uk/object/74781dbb-1f65-4839-a766-24d6cde63ed0>; NHM_1423 (**paratype**) NHMUK ANEA 2019.7154, coll. 03 Mar. 2015, 12°27.26N, 116°36.77W, 4137 m <http://data.nhm.ac.uk/object/d949e987-6e03-4092-8492-c51dd7fcf4d7>; NHM_1895 NHMUK ANEA 2019.7155, coll. 13 Mar. 2015, 12°02.49N, 117°13.03W, 4094 m, <http://data.nhm.ac.uk/object/02aaa9c0-837a-4836-8b34-5e68296c958e>.

Type locality. Pacific Ocean, CCZ, 12°32.23N, 116°36.25W, depth 4425 m, in mud between polymetallic nodules.

Description. Small species, represented by six specimens. Holotype posteriorly incomplete, but otherwise in good condition, 9 mm long and 1 mm wide at the widest point for 24 chaetigers; paratypes complete, 6.0–6.5 mm long and 0.5–0.7 mm wide for 26 chaetigers. Body most expanded (inflated) through chaetigers 5–9, thereafter

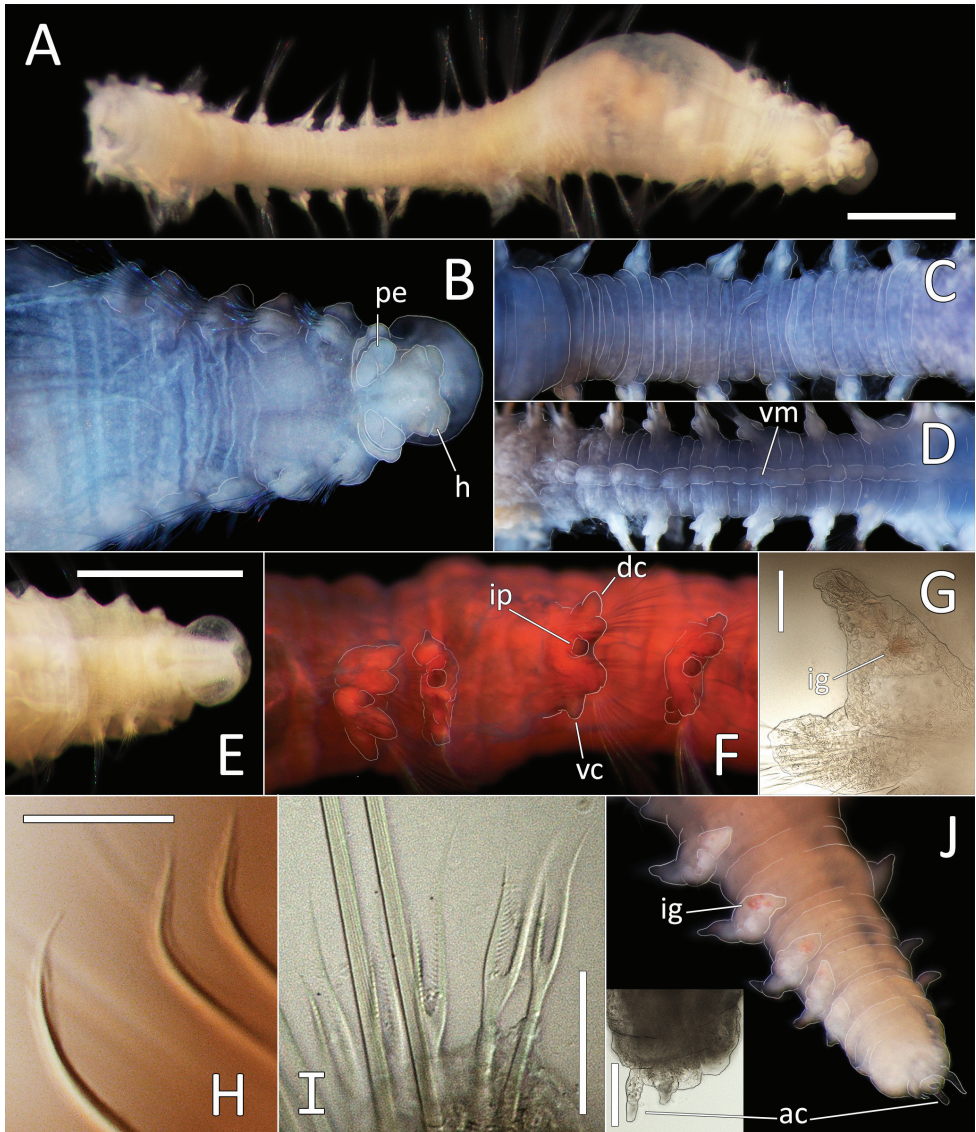


Figure 24. *Oligobregma brasierae* sp. nov. **A** Lab image, whole specimen (holotype [specimen NHM_823], pre-staining) **B** Lab image, dorsal anterior (holotype, faded stain, h = prostomial horns, pe = peristomial ring) **C** Lab image, dorsal segments, quadriannulate chaetigers (holotype, faded stain) **D** Lab image, ventral segments (holotype, faded stain, vm = ventral midline) **E** Lab image, ventral anterior, (holotype, pre-staining) **F** Lab image, mid-body parapodia (holotype, shirlastained, dc = dorsal cirrus, vc = ventral cirrus, ip = interramal papilla) **G** Lab image, detail of dorsal cirrus (paratype NHM_684, ig = internal gland) **H** Lab image, detail of hirsute notopodial spines on chaetiger 1 (paratype NHM_684, ig = internal gland) **I** Lab image, detail of capillary and lyrate chaetae (paratype NHM_684) **J** Lab images, posterior (paratype NHM_684, [bottom-left panel], ac = anal cirri, ig = internal gland). Morphological features in plates **B–D, F, G, H** have been outlined with a fine white or black line to improve clarity of those features. Scale bars: 1 mm (**A, E**); 50 µm (**G**); 25 µm (**H, I**); 100 µm (**J**).

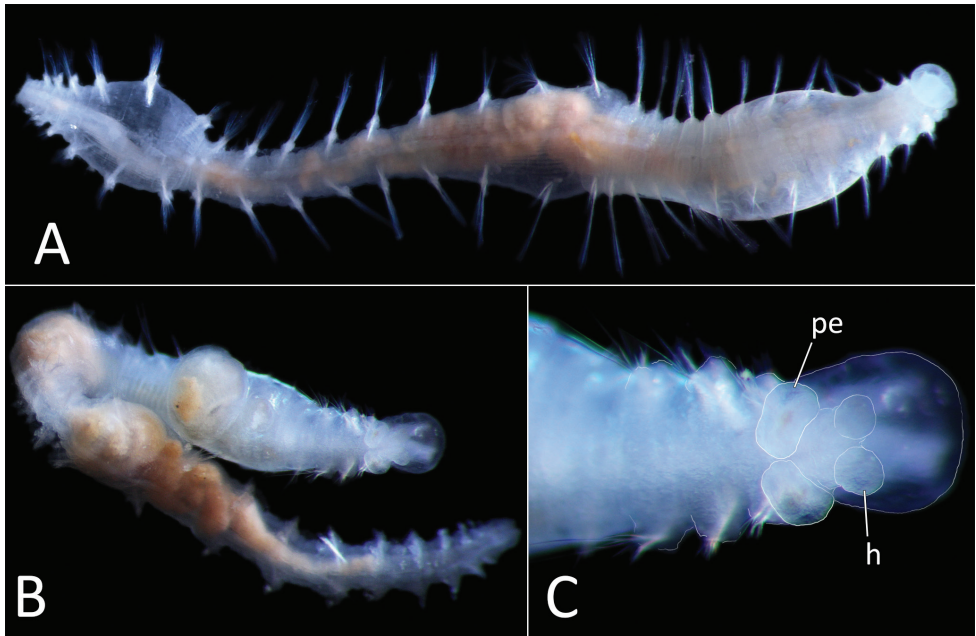


Figure 25. *Oligobregma brasierae* sp. nov. **A** Live image, whole specimen, ventral view (holotype [specimen NHM_823]) **B** Live image, whole specimen, dorsal view (paratype NHM_684) **C** Live image, dorsal anterior, with prostomial features outlined in a fine white line (paratype NHM_684, h = prostomial horns, pe = peristomial ring).

narrowing to posterior end. Colour in alcohol creamy white, without body pigment (Fig. 24A); live specimens translucent (Fig. 25)

Anterior body segments smooth, no obvious annulation of raised pads detected (even after staining) (Fig. 24B); annulation becomes most distinct in narrow, posterior part of the body, where segments quadriannulate (Fig. 24C). Venter with prominent ventral midline from chaetiger 2 composed of a row of large pads within a groove (Fig. 24D). Branchiae absent.

Prostomium broadly rounded anteriorly, weakly expanded laterally, narrowing posteriorly; with two short, rounded lobes (horns) emerging anterolaterally from anterior prostomial margin (Figs 24B, 25C). Eyes absent. Proboscis observed as a soft, smooth sac-like structure (Fig. 24E). Peristomium forming a smooth large ring around prostomium dorso-laterally, interrupted middorsally (Figs 24B, 25C), ventrally obscured by extended proboscis in holotype.

Parapodia biramous; inconspicuous in chaetigers 1–7, becoming longer posteriorly and prominent from around chaetiger 14. Tiny dorsal cirri detectable from chaetigers 14 in holotype, whereas ventral cirri occur from chaetiger 15 where well developed; both cirri large on subsequent segments; conical with broad base (Fig. 24F); without pigmentation; both dorsal and ventral cirri with detectable gold-pigmented internal glands (Fig. 24G). Interramal papilla present, inconspicuous in anterior parapodia (only observed upon staining), well developed in posterior parapodia Fig. 24F).

Curved acicular spines present in notopodia and neuropodia on chaetigers 1–4 (Fig. 24H). Notopodia with about 20 spines arranged in two rows in chaetigers 1 and 2, and with about 10 spines arranged in one row in chaetigers 3 and 4, spines accompanied posteriorly by single row of capillaries; neuropodial spines fewer in numbers arranged irregularly. Spines slightly curved, narrowing to slender elongated tip (Fig. 24H). Short spinous chaetae anterior to spines not observed. Subsequent chaetigers with long thin capillaries in both rami. Lyrate chaetae from chaetiger 5, in both rami, positioned anteriorly to capillaries. Lyrate chaetae short, with unequal tynes bearing short bristles (Fig. 24I), numbering two or three per noto- and neuropodium in anterior segments and up to six in posterior segments.

Single achaetigerous ring subsequent to the last chaetiger. Pygidium missing in holotype, but observed in paratypes; broad, triannulated, distally broadly rounded lobe; with few terminal, short anal cirri still attached in paratype NHM_684 (Fig. 24J).

Morphological variation: Some variability was noticed between different sized specimens. In the slightly bigger holotype (NHM_823) the spines can be observed on chaetigers 1–4 in both rami, and the dorsal cirri can be detected from chaetiger 14. In the smaller paratype (NHM_684), the spines cannot be unambiguously confirmed in ch. 4, particularly in neuropodia and dorsal cirrus can be detected from chaetiger 13.

Genetic data. GenBank MN217422–MN217427 for 16S, MN217498 for 18S and MN217517 for COI. This species is genetically identical or very similar to sequences published in Janssen et al. (2015), with K2P values ranging from 0.0–0.003 between *O. brasierae* and the already published sequences with accession numbers KJ736359–KJ736363. The three *Oligobregma* species in this study form a well-supported clade in our phylogenetic analyses, with *Oligobregma brasierae* sp. nov. as sister to *Oligobregma tani* sp. nov. (Fig. 32).

Remarks. Currently, there are nine valid species assigned to the genus *Oligobregma* (Read and Fauchald 2018b), with *O. blakei* Schüller & Hilbig, 2007 considered a nomen dubium. All three *Oligobregma* species from the ABYSSLINE material can be easily distinguished from those that have acicular spines in two (*O. pseudocollare* Schüller & Hilbig, 2007, *O. oculata* Kudenov & Blake, 1978) or three (*O. mucronata* Blake, 2015, *O. aciculata* (Hartman, 1965), *O. collare* (Levenstein, 1975), *O. notiale* Blake, 1981) anterior chaetigers only.

More specifically, *Oligobregma simplex* Kudenov & Blake, 1978, *O. lonchochaeta* Detinova, 1985 and *O. quadrispinosa* Schüller & Hilbig, 2007 share the presence of spines in chaetigers 1–4 with *O. brasieri* sp. nov., as well as having relatively large posterior dorsal and ventral cirri. *Oligobregma simplex* is a shallow water species (Western Port, Victoria, Australia, 11 m) and, while similar in size (5 mm long), it has a greater number of chaetigers (43 versus 26 in UKSR species) and more posterior appearance of dorsal and ventral cirri (on ch. 20–22 versus ch. 13–15). *Oligobregma lonchochaeta* has been described from a single, incomplete specimen from the abyssal North Atlantic, but its description is brief, not including the observation on the appearance of dorsal and ventral cirri, and there are no DNA data. Detinova (1985) differentiated her species from *O. simplex* by having first four chaetigers triannulate rather than uniannulate. However, there appears to be a typographical mistake in description of *O. simplex* by Kudenov and

Blake (1978), as the authors state: “Body segments are annulated as follows: chaetigers 1–12 are uniannulate; 3–4 biannulate; 5–12 (? or 15) quadriannulate.” It is likely that chaetigers 1 and 2 not 1 to 12 are uniannulate. *Oligobregma quadrispinosa* has been described from the lower bathyal and abyssal Southern Ocean (Scotia and Weddell Seas, in 2258–4069 m) and is most similar to UKSR species in possessing similar number of chaetigers ($n = 28$) and podial cirri can be also detected from around chaetiger 13 and 14 [(estimated from the drawing provided in the original description by Schüller and Hilbig (2007)]. However, the new species possess spines in both rami of chaetigers 1–4, while *O. quadrispinosa* has spines in notopodia only according to Schüller and Hilbig (2007).

Ecology. Found in polymetallic nodule province of the eastern CCZ.

Etymology. Named in honor of Madeleine Brasier, member of the science party of the ABYSSLINE AB02 cruise onboard the RV *Thomas G. Thompson*.

***Oligobregma tani* sp. nov.**

<http://zoobank.org/EB95F031-2A2D-449D-8F2A-114EC628C9D2>

Fig. 26A–J

Material examined. NHM_773A (**paratype**) NHMUK ANEA 2019.7156, coll. 20 Feb. 2015, 12°32.23N, 116°36.25W, 4425 m <http://data.nhm.ac.uk/object/4b673a6a-9090-4c24-a4eb-231190507b60>; NHM_1454 (**holotype**) NHMUK ANEA 2019.7157, coll. 03 Mar. 2015, 12°27.26N, 116°36.77W, 4137 m <http://data.nhm.ac.uk/object/67d3f58a-9c13-423e-93b7-3ddcf98a361e>; NHM_1480J NHMUK ANEA 2019.7158, coll. 03 Mar. 2015, 12°27.26N, 116°36.77W, 4137 m <http://data.nhm.ac.uk/object/d47f17aa-c0c1-44f0-a448-d3f3c395fc47>; NHM_1665 (**paratype**) NHMUK ANEA 2019.7159, coll. 10 Mar. 2015, 12°21.81N, 116°40.86W, 4233 m <http://data.nhm.ac.uk/object/eca166ae-3fe0-4367-860f-08c7410165dd>.

Type locality. Pacific Ocean, CCZ, 12°27.26N, 116°36.77W, depth 4137 m, in mud between polymetallic nodules.

Description. Small species, represented by four posteriorly incomplete specimens, 4–4.5 mm long and 0.4–0.7 mm wide. Holotype posteriorly incomplete, but otherwise in good condition, 4.5 mm long and 0.7 mm wide at the widest point for 18 chaetigers long fragment. Colour in alcohol creamy white, without body pigment (Fig. 26A); live specimens semi-translucent (Fig. 26B). Anterior body segments appears smooth, annulation of raised pads detected best upon staining (Fig. 26C–E) revealing chaetigers 1–4 with two transverse rows of relatively large lobes; subsequent chaetigers may be triannulate, but epithelium with mostly with wrinkled appearance till end of fragment (chaetiger 18) (Fig. 26B–E). Ventral midline on venter not too prominent, from chaetiger 2, composed of a row of large pads within a groove (Fig. 26E). Branchiae absent.

Prostomium broad (wider than long), nearly oval; with two very prominent, distinctly rounded lobes (horns) emerging from anterior prostomial margin (Fig. 26C,

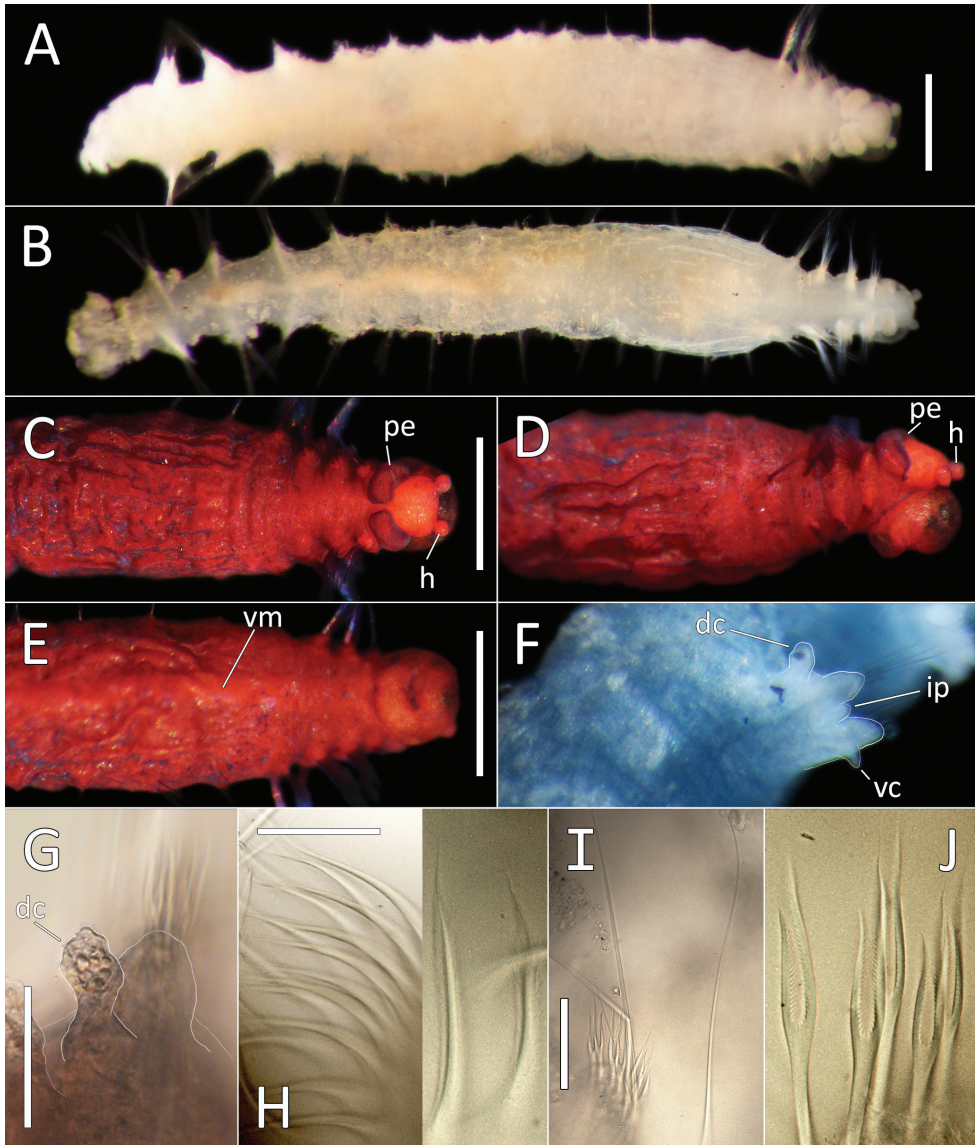


Figure 26. *Oligobregma tani* sp. nov. holotype (specimen NHM_1454). **A** Lab image, whole specimen (pre-stain,) **B** Live image, whole specimen **C** Lab image, dorsal anterior, (stained, h = prostomial horns, pe = peristomial ring) **D** Lab image, lateral anterior, (stained, h = prostomial horns, pe = peristomial ring) **E** Lab image, ventral anterior, (stained, vm = ventral midline) **F** Lab image, mid-body parapodia (faded stain, dc = dorsal cirrus, vc = ventral cirrus, ip = interramal papilla) **G** Lab image, detail of dorsal cirrus, with no internal gland visible (dc = dorsal cirrus) **H** Lab image, detail of hirsute spines on notopodia on chaetiger 1 ([left panel]) **I** Lab image, detail of capillary and lyrate chaetae on chaetiger 12 **J** Lab image, detail lyrate chaetae. Morphological features in plates **F**, **G** have been outlined with a fine white line to improve clarity of those features. Scale bars: 0.5 mm (**A**, **C**, **E**); 50 μ m (**G**–**I**).

D). Eyes absent. Peristomium forming a large smooth ring around prostomium dorso-laterally, with narrow interruption middorsally (Fig. 26C, D). Mouth obscured by everted proboscis in holotype, which is observed as soft inflated sac (Fig. 26E).

Parapodia biramous; inconspicuous in chaetigers 1–14, becoming conical and prominent from around chaetiger 15. Tiny dorsal cirri detectable from chaetiger 13 in holotype, whereas ventral cirri occur from chaetiger 15; both cirri best developed from chaetigers 16 and 17, remaining small and conical (less than 1/2 the size of corresponding podial lobes) (Fig. 26F); without pigmentation; internal glands not detected in few cirri present (Fig. 26G). Interramal papilla present, well developed from chaetiger 15 (Fig. 26).

Curved acicular spines present in notopodia only on chaetigers 1–4 (Fig. 26H); spines in chaetiger 4 transitional between distinct spines and capillaries. Notopodia with about 14 spines arranged in two rows in chaetigers 1 and 2 and with about five spines arranged in one row in chaetigers 3 and 4; spines accompanied posteriorly by single row of capillaries. Spines in chaetigers 1–3 curved, straw-coloured, with hirsute shaft, narrowing to slender, elongated and hirsute tip (Fig. 26H); spines in chaetiger 4 transitional, more slender and straighter than in chaetigers 1–3, but with hirsute shafts and shorter unlike accompanying capillaries. Short spinous chaetae anterior to spines not observed. Subsequent chaetigers with long thin capillaries in both rami, but very few present (Fig. 26I). Lyrate chaetae likely from chaetiger 5 in both rami, where very short and difficult to observe; best observed from chaetiger 8; accompanied by very few capillaries. Lyrate chaetae initially short but becoming longer and very prominent from around chaetiger 8; with unequal tynes bearing short bristles (Fig. 26I, J), numbering up to 5 or 6 in each ramus. The rest of the body and pygidium unknown.

Genetic data. GenBank MN217428–MN217431 for 16S, MN217499 for 18S and MN217518–MN217519 for COI. This species is genetically very similar to one sequence published in Janssen et al. (2015), with a K2P value of 0.008 between *O. tani* and the already published sequence with accession number KJ736365. The three *Oligobregma* species in this study form a well-supported clade, with *Oligobregma tani* sp. nov. as sister to *Oligobregma brasierae* sp. nov. in our phylogenetic analyses (Fig. 32).

Remarks. The UKSR-collected species is most similar to *Oligobregma quadrispinosa* described from abyssal Southern Ocean (Schüller and Hilbig 2007) in having the first four notopodia with acicular spines, lyrate chaetae from chaetiger 5 and podial cirri arising from around chaetiger 13–15. However, *O. quadrispinosa* differs in the following characters; spines in chaetiger 4 are prominent, stout and not hirsute, while the median and posterior chaetigers bear much larger ventral cirri. The UKSR species also has very prominent round “Mickey Mouse”-like anterior prostomial lobes (observed in all four specimens examined). For comparison with other *Oligobregma* species see Table 3.

Ecology. Found in polymetallic nodule province of the eastern CCZ.

Etymology. Named in honor of Koh Siang Tan, member of the science party of the ABYSSLINE AB02 cruise onboard the RV *Thomas G. Thompson*.

Table 3. Comparison of *Oligobregma* species with spines in chaetigers 1–4, including the new UKSR-collected species. Information collected from the literature.

	Distribution of spines in chaetigers 1–4	Annulation of chaetigers	Appearance of podial cirri	No. of chaetigers	Presence of furcate chaetae
<i>O. simplex</i>	In both rami	1–2 uni-; 3–4 bi-; 5–12 or 15 quadriannulate	Chaetigers 20–22	43 (complete)	From chaetiger 6
<i>O. lonchochaeta</i>	In both rami	1–4 triannulate	In posterior chaetigers, detail not given	22+ (incomplete)	In mid and posterior chaetigers
<i>O. quadrispinosa</i>	In notopodia only	Anterior quadriannulate; posterior with 5 annuli	Chaetigers 13–14	28 (complete)	From chaetiger 5
<i>O. brasierae</i> sp. nov.	In both rami, spines hirsute	Anterior smooth, posterior quadriannulate	Chaetigers 13–15	26 (complete)	From chaetiger 5
<i>O. tani</i> sp. nov.	In notopodia only, spines hirsute, transitional in ch. 4	Not observed	Chaetigers 13–15	18 (incomplete)	From chaetiger 5
<i>O. whaleyi</i> sp. nov.	In both rami	Anterior smooth, midbody quadriannulate	Chaetiger 14	26 (incomplete)	First observed from chaetiger 11

***Oligobregma whaleyi* sp. nov.**

<http://zoobank.org/6856E564-D7EC-42B0-8DED-9CCB95B8ABFE>

Fig. 27A–I

Material examined. NHM_822 (**holotype**) NHMUK ANEA 2019.7160, coll. 20 Feb. 2015, 12°32.23N, 116°36.25W, 4425 m <http://data.nhm.ac.uk/object/dde1c8f9-f87a-430b-be9d-5e34685772bb>.

Type locality. Pacific Ocean, CCZ, 12°32.23N, 116°36.25W, depth 4425 m, in mud between polymetallic nodules.

Description. Large species, represented by a single, posteriorly incomplete specimen, with 26 chaetigers, 16 mm long and about 2 mm wide at widest (inflated) region (first eight chaetigers, particularly chaetigers 3–8), with another widening of the body in chaetigers 23–26, likely due to sediment ingestion. Colour in alcohol creamy white, without body pigment, live specimens semi-translucent (Fig. 27A). Anterior body segments appear smooth, without distinct annulation, chaetigers 1–5 with three transverse rows of weakly developed lobes; subsequent segments quadriannulated until the end of the fragment (chaetiger 26) (Fig. 27B, C). Ventral midline on venter prominent, from chaetiger 2, composed of a row of large pads within a groove (Fig. 27C). Branchiae absent.

Prostomium broadly rounded anteriorly, weakly expanded laterally, narrowing posteriorly; with two well-developed, anterior rounded lobes (horns) emerging from anterior prostomial margin (Fig. 27D). Eyes absent. Proboscis observed as a soft, smooth sac-like structure. Peristomium forming smooth figure-of-8-like loops laterally to prostomium (Fig. 27D), dorsally interrupted, ventrally obscured by extended proboscis; with faint light-brown pigmentation.

Parapodia biramous; conspicuous even in anterior-most segments (Fig. 27E), becoming longer and prominent from around chaetiger 10. Dorsal and ventral cirri appear abruptly from chaetiger 14, where similar to those on subsequent segment;

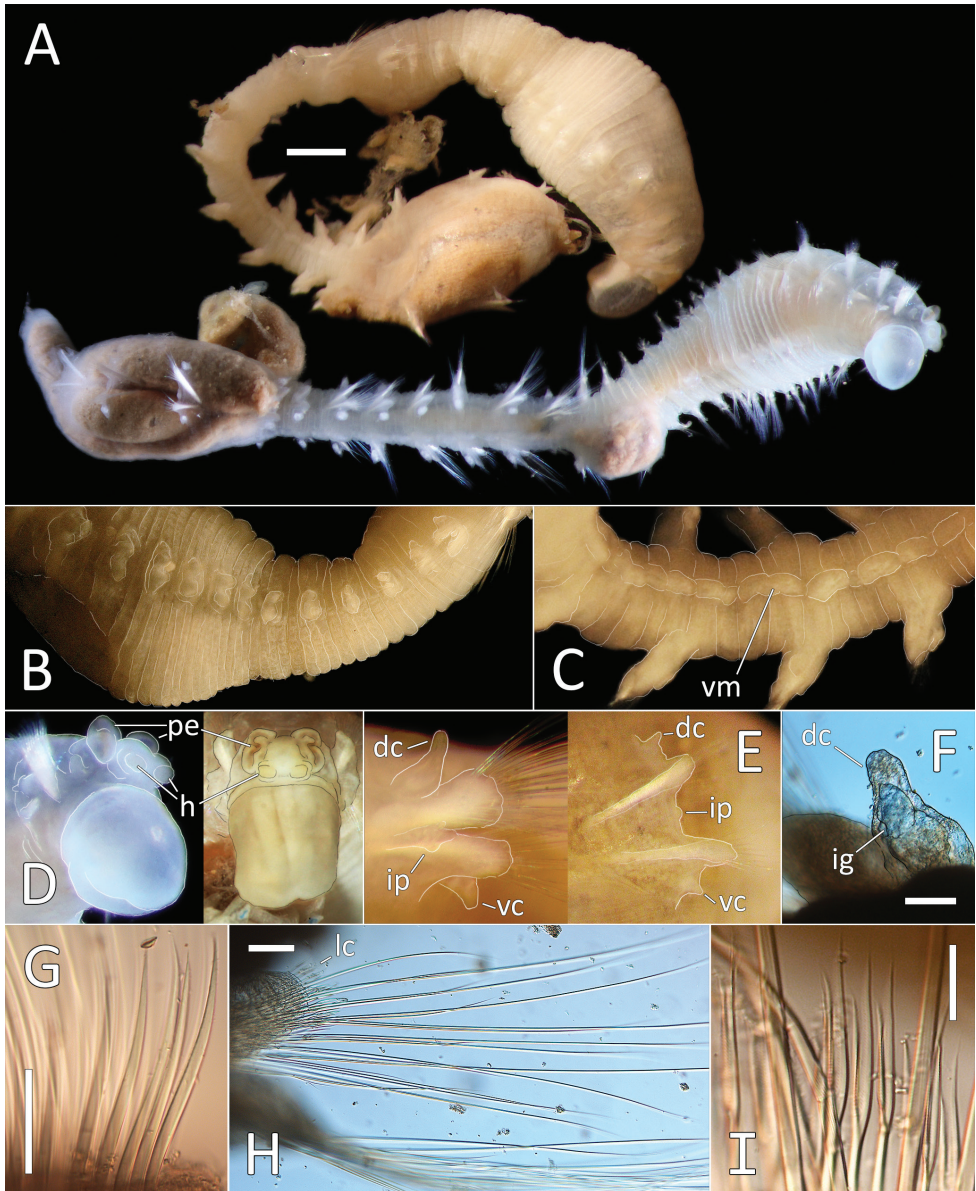


Figure 27. *Oligobregma whaleyi* sp. nov. holotype (specimen NHM_822). **A** Lab (upper) and live (lower) images, whole specimens [lab image] **B** Lab image, mid-body segments and annulation **C** Lab image, ventral midbody (vm = ventral midline) **D** Live (left) and lab (right) images of prostomium (pe = peristomial ring, h = prostomial horns) **E** Lab images, midbody and posterior parapodia, chaetigers 15 (left) and 24 (right) (dc = dorsal cirrus, vc = ventral cirrus, ip = interrampal papilla) **F** Lab image, detail of dorsal cirrus and internal gland (dc = dorsal cirrus, ig = internal gland) **G** Lab image, detail of notopodial spines on chaetiger 1 **H** Lab image, detail of capillary chaetae (lc = lyrate chaetae) **I** Lab image, detail of lyrate chaetae. Morphological features in plates **B–D, F, G, H** have been outlined with a fine white or black line to improve clarity of those features. Scale bars: 1 mm (**A**); 100 μ m (**F–H**); 50 μ m (**I**).

relatively small (about 1/2 the size of associated podial lobes) in posterior chaetiger; all conical with broad base (Fig. 27E), without pigmentation; some dorsal and ventral cirri with gold-pigmented internal glands, now bluish upon uptake of Shirlastain (Fig. 27F). Interramal papilla present, inconspicuous in anterior parapodia, well developed from chaetiger 10 (Fig. 27E).

Curved acicular spines present in notopodia and neuropodia on chaetigers 1–4. Notopodia with about 15 spines arranged in irregular row, accompanied posteriorly by single row of capillaries; neuropodial spines fewer in numbers arranged irregularly. Spines slightly curved, narrowing to slender elongated tip (Fig. 27G). Short spinous chaetae anterior to spines not observed. Subsequent chaetigers with long thin capillaries in both rami (Fig. 27H). Lyrate chaetae at least from chaetiger 11, in both rami, positioned anteriorly to capillaries. Lyrate chaetae short, with unequal tynes bearing short bristles (Fig. 27I), numbering 12–20 per noto- and neuropodium. The rest of the body and pygidium unknown.

Genetic data. GenBank MN217432 for 16S and MN217500 for 18S. The three *Oligobregma* species in this study form a well-supported clade. *Oligobregma whaleyi* sp. nov. is sister to a clade consisting of *Oligobregma tani* sp. nov. and *Oligobregma brasierae* sp. nov. in our phylogenetic analyses (Fig. 32).

Remarks. The UKSR-collected species *O. whaleyi* sp. nov. differs from other *Oligobregma* species bearing spines on the first four chaetigers in having a peristomial ring forming a figure-of-8 loops laterally to prostomium and in furcate chaetae appearing more posteriorly (first observed on chaetiger 11 although due to its large size the specimen was difficult to manipulate and removal of several parapodia would have damaged the single specimen significantly), while in other species the furcate chaetae are present from chaetiger 6. In *O. lonchochaeta* Detinova (1985) described the furcate chaetae as occurring only in mid- and posterior chaetigers but without specifically stating on which chaetiger they were first observed. Therefore, the newly described species can be distinguished from *O. lonchochaeta* by having the anterior chaetigers smooth, rather than triannulated. For further comparison see Table 3.

Ecology. Found in polymetallic nodule province of the eastern CCZ.

Etymology. Named in honor of Jeremy Whaley, Able Seaman onboard RV *Melville* on the ABYSSLINE cruise AB01 in 2013.

Scalibregmatidae sp. (NHM_2308)

Fig. 28A–F

Material examined. NHM_2308 NHMUK ANEA 2019.7161, coll. 01 Mar. 2015, 12°15.44N, 117°18.13W, 4302 m <http://data.nhm.ac.uk/object/7b9d4ab8-4b7b-45c4-9cf4-6fd6b1229f48>.

Description. This species is represented by a single, small, posteriorly incomplete specimen, 2.5 mm long and 0.4 mm wide for about 12 chaetigers, in poor condition. Colour of preserved specimen creamy yellow (Fig. 28A). Anterior part of the body

rugose, chaetigers 1–4 dorsally with two? (some damaged) transverse rows of tightly packed squarish lobes; subsequent chaetigers with three such row or damaged (Fig. 28B). Venter with prominent ventral midline from chaetiger 2 composed of a row of large pads within a groove (Fig. 28C).

Prostomium small, broadly rounded anteriorly, weakly expanded laterally, narrowing posteriorly; with two short, rounded lobes (horns) emerging anterolaterally from anterior prostomial margin (Fig. 28D). Eyes absent. Branchiae absent.

Heavily curved acicular spines present in notopodia only on chaetigers 1 and 2 (Fig. 28D). Notopodia of chaetigers 1, bearing 10 very prominent spines arranged in two rows, accompanied posteriorly by single row of capillaries; notopodia of chaetiger 2 with five spines arranged in a single row, accompanied posteriorly by single row of capillaries. Spines relatively straight, stout, straw-coloured, distally narrowing to slender, elongated and somewhat hairy tip (Fig. 28E). Short spinous chaetae anterior to heavy spines not observed. Neuropodia of chaetiger 1 and 2 with long slender capillaries; subsequent chaetigers with long thin capillaries in both rami. Lyrate chaetae from chaetiger 3 in both rami, positioned anteriorly to capillaries. Lyrate chaetae short, with unequal tyne bearing short bristles (Fig. 28F), around 4 or 5 per ramus.

Parapodia biramous, podial lobes not developed in 12 chaetigers long fragment. Dorsal and ventral cirri not observed in 12 chaetiger long fragment. Rest of the body unknown.

Genetic data. GenBank MN217467 for 16S. Scalibregmatidae (NHM_2308) does not cluster convincingly with any other Scalibregmatidae species available on GenBank (Fig. 32).

Remarks. Poor preservation of mid body and missing posterior part prevents reliable identification to genus level. Observations from the anterior part (the absence of branchiae and presence of acicular spines) suggest that this may be yet another representative of genus *Oligobregma* in the UKSR-collected material. It can be distinguished from other scalibregmatid species in this study by having spines in notopodia of chaetigers 1 and 2 only.

Travisiidae Hartmann-Schröder, 1971

Travisia Johnston, 1840

Notes. These distinctive, grub-like polychaetes with rugose epidermis were first described by Johnston (1840) with the discovery of *Travisia forbesii* Johnston, 1840. Later, Kinberg (1866) established the genus *Dindymenes* and Chamberlin (1919) established the genus *Kesun*, which he differentiated from *Travisia* by the complete absence of branchiae. Following a cladistic analysis of morphological characters, Dauvin and Bellan (1994) synonymized *Kesun* and *Dindymenides* with *Travisia* and recognized at least 27 species. Important species-level characters include the presence of lobes, the position and relative size of the nephridiopores, and the total

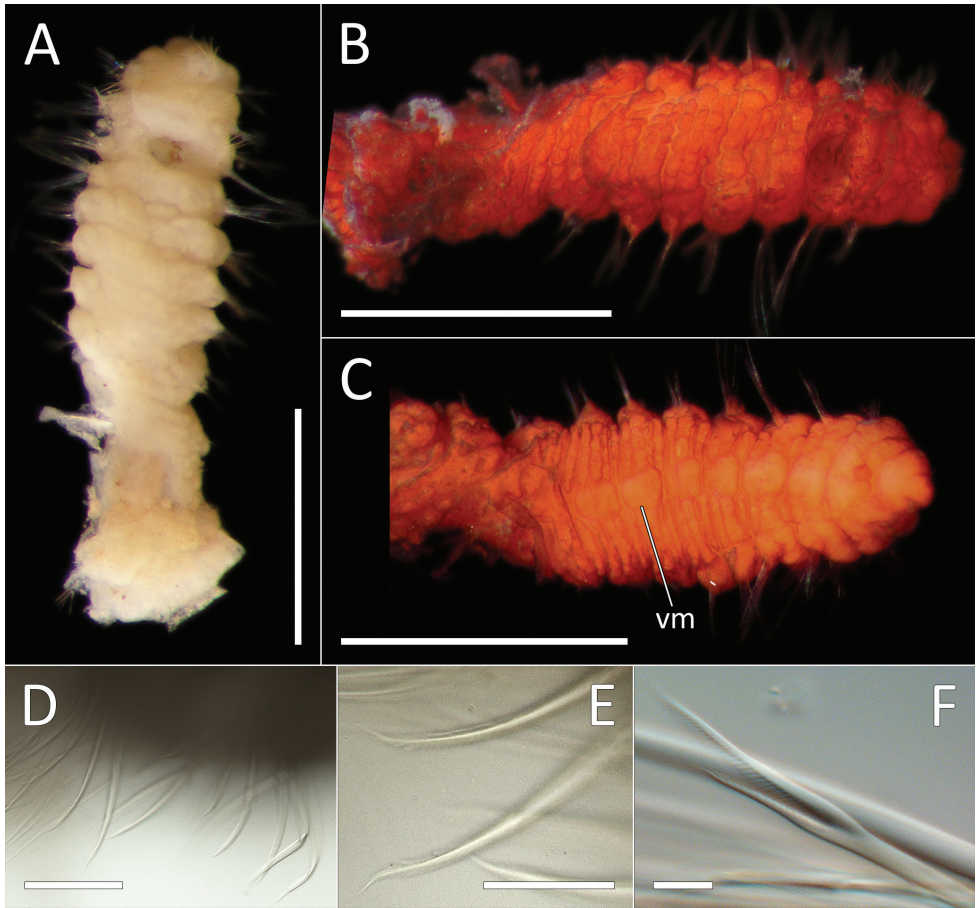


Figure 28. Scalibregmatidae sp. NHM_2308 (specimen NHM_2308). **A** Lab image, whole specimen, dorsal view (pre-stain) **B** Lab image, dorsal anterior (stained) **C** Lab image, ventral anterior, (shirla stained, vm = ventral midline) **D** Lab image, detail of hirsute spines on chaetigers 1 and 2 **E** Lab image, detail of hirsute spine tips **F** Lab image, detail of lyrate chaeta. Scale bars: 1 mm (**A–C**); 100 μm (**D**); 50 μm (**E**); 10 μm (**F**).

number of chaetigers, which appears to be stable in most, but not all, species (Dauvin and Bellan 1994).

The higher taxonomic position of *Travisia* has been in dispute for some time. While usually placed in Opheliidae, its relationship with Scalibregmatidae has also been long suggested (Ashworth 1902), mainly due to possession of rugose epidermis. Hartmann-Schröder (1971) created a subfamily, Traviisiinae, in Opheliidae to accommodate *Travisia*. More recently, phylogenetic analyses were employed to answer this question. Persson and Pleijel (2005) used molecular data to recover *Travisia* nested within the Scalibregmatidae, and molecular analysis of Paul et al. (2010) rejected affinity with Opheliidae and found strong support sister-group relationship of *Travisia* and Scalibregmatidae. Law et al. (2014) again placed *Travisia* within Scalibregmatidae

using molecular data. However, Blake and Maciolek (2016) proposed a new family, Traviisiidae, to accommodate *Travisia*.

Travisia species have predominantly deep-water distribution (Blake and Maciolek 2016) and two species, one of them very abundant, were found in UKSR material.

***Travisia zieglerae* sp. nov.**

<http://zoobank.org/74877AF0-D607-4C62-BD07-6844D90A2806>

Fig. 29A–G

Material examined. NHM_140 (**paratype**) NHMUK ANEA 2019.7162, coll. 11 Oct. 2013, 13°45.50N, 116°41.91W, 4080 m <http://data.nhm.ac.uk/object/ed10356b-32a0-4b45-9fe3-c56fbc696e87>; NHM_188 NHMUK ANEA 2019.7170, coll. 14 Oct. 2013, 13°57.43N, 116°30.10W, 4130 m <http://data.nhm.ac.uk/object/c8a0ef70-e7f7-4605-bf78-dc54ed9151eb>; NHM_241 NHMUK ANEA 2019.7163, coll. 16 Oct. 2013, 13°48.70N, 116°42.60W, 4076 m <http://data.nhm.ac.uk/object/5c0ac0b7-60cc-473e-a23b-2f49a40540f4>; NHM_356 NHMUK ANEA 2019.7164, coll. 17 Oct. 2013, 13°45.21N, 116°29.12W, 4128 m <http://data.nhm.ac.uk/object/8d2cbf0e-6522-403d-a58a-905fb13c70d6>; NHM_364 NHMUK ANEA 2019.7165, coll. 19 Oct. 2013, 13°55.98N, 116°42.977W, 4182 m <http://data.nhm.ac.uk/object/ef6e520f-7ef5-4ff9-87b5-985b8576271f>; NHM_748B (**paratype**) NHMUK ANEA 2019.7166, coll. 20 Feb. 2015, 12°32.23N, 116°36.25W, 4425 m <http://data.nhm.ac.uk/object/db527676-1030-4bf0-b28d-2382825bc6bf>; NHM_753 NHMUK ANEA 2019.7167, coll. 20 Feb. 2015, 12°32.23N, 116°36.25W, 4425 m <http://data.nhm.ac.uk/object/393203b1-cb80-4185-9e40-fca6e1b6fe34>; NHM_760 NHMUK ANEA 2019.7168, coll. 20 Feb. 2015, 12°32.23N, 116°36.25W, 4425 m <http://data.nhm.ac.uk/object/d3e8ec3c-d7f3-4908-b315-84f3758aacc1>; NHM_792 NHMUK ANEA 2019.7169, coll. 20 Feb. 2015, 12°32.23N, 116°36.25W, 4425 m <http://data.nhm.ac.uk/object/5d30a61b-5894-484f-b79a-df1cd4268ec1>; NHM_909 (**paratype**) NHMUK ANEA 2019.7171, coll. 23 Feb. 2015, 12°34.28N, 116°36.63W, 4198 m <http://data.nhm.ac.uk/object/5f570dab-4b56-4f74-b126-ed6ceab344e3>; NHM_970 NHMUK ANEA 2019.7172, coll. 23 Feb. 2015, 12°34.28N, 116°36.63W, 4198 m <http://data.nhm.ac.uk/object/4ccb364c-35f4-458c-9c71-6f77e71493ca>; NHM_1097 NHMUK ANEA 2019.7173, coll. 26 Feb. 2015, 12°06.93N, 117°09.87W, 4100 m, <http://data.nhm.ac.uk/object/939ba16d-b844-49ca-a740-bb42f039cc11>; NHM_1310 NHMUK ANEA 2019.71745, coll. 01 Mar. 2015, 12°15.44N, 117°18.13W, 4302 m <http://data.nhm.ac.uk/object/16844478-de27-448c-9acb-057835026447>; NHM_1311 NHMUK ANEA 2019.7175, coll. 01 Mar. 2015, 12°15.44N, 117°18.13W, 4302 m <http://data.nhm.ac.uk/object/192cbbb3-680b-4bcd-9cc4-a420f42af578>; NHM_1431 (**holotype**) NHMUK ANEA 2019.7176, coll. 03 Mar. 2015, 12°27.26N, 116°36.77W, 4137 m <http://data.nhm.ac.uk/object/fd6bab0e-0cda-4b42-808f-a6006d409535>; NHM_1543 (**paratype**) NHMUK ANEA 2019.7177, coll. 06 Mar. 2015, 12°30.38N, 116°29.07W, 4244 m

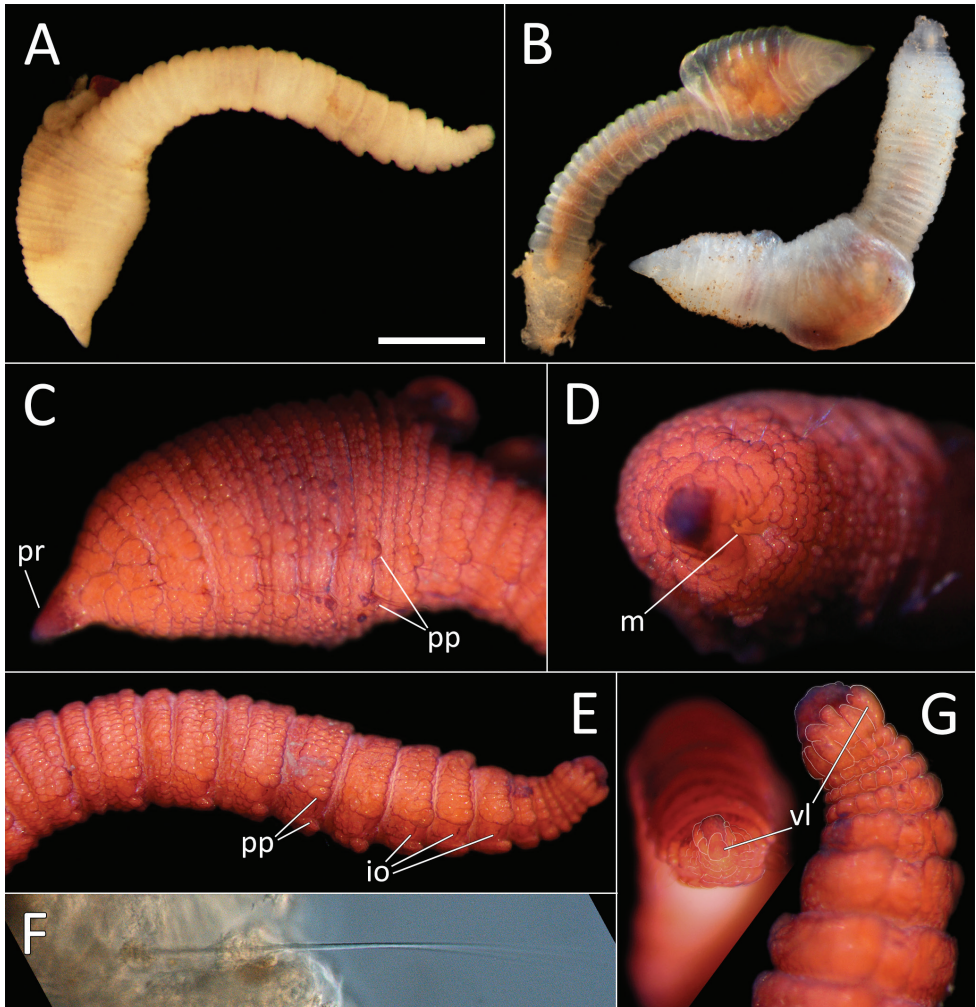


Figure 29. *Travisia zieglerae* sp. nov. **A** Lab image, whole specimen, pre-stain (holotype [specimen NHM_1431]) **B** Live images, whole specimens (specimen NHM_1911 [left], specimen NHM_188 [right]) **C** Lab image, lateral anterior, (holotype, stained, pr = prostomium, pp = parapodial lappets) **D** Lab image, distal anterior, (holotype, stained, m = mouth) **E** Lab image, lateral posterior, (holotype, stained, pp = parapodia, io = interramal organs) **F** Detail of capillary chaeta (paratype NHM_140) **G** Lab image, pygidium, distal view (left) and lateral view (right), with pygidial features outlined in a fine white line (holotype, stained, vl = ventral lobe). Scale bar: 1 mm (**A**).

<http://data.nhm.ac.uk/object/c78cc5fd-ca98-43b0-a0fb-8804fb606c71>; NHM_1873 NHMUK ANEA 2019.7178, coll. 13 Mar. 2015, 12°02.496N, 117°13.03W, 4094m, <http://data.nhm.ac.uk/object/24409a12-2a50-4689-80dc-902cdeb5af69>; NHM_1883 NHMUK ANEA 2019.7179, coll. 13 Mar. 2015, 12°02.49N, 117°13.03W, 4094 m, <http://data.nhm.ac.uk/object/9e8c22f7-a94b-45ed-a1d0-cae287a7ac2d>; NHM_1911 NHMUK ANEA 2019.7180, coll. 13 Mar. 2015

12°02.49N, 117°13.03W, 4094 m <http://data.nhm.ac.uk/object/489dd5a6-2c68-416b-9a06-ed773d4791d6>; NHM_2019 NHMUK ANEA 2019.7181, coll. 16 Mar. 2015, 12°03.03N, 117°24.28W, 4235 m <http://data.nhm.ac.uk/object/2684a5f8-b4d4-4bc8-b386-65775506cf87>; NHM_2024 NHMUK ANEA 2019.7182, coll. 16 Mar. 2015, 12°03.03N, 117°24.28W, 4235 m <http://data.nhm.ac.uk/object/cf54f81e-5836-4684-94dc-151f589ebab4>.

Type locality. Pacific Ocean, CCZ, 12°27.26'N 116°36.77'W, depth 4137 m, in mud between polymetallic nodules.

Additional material examined. *Travisia glandulosa* McIntosh, 1879, holotype BMNH 1921.5.1.2431 and specimen of Monro (1930), *Travisia gravierei* McIntosh, 1908, holotype BMNH 1921.5.1.2429.

Description. This species is represented by 21 specimens. It is a small species 1.2–7.5 mm long and 0.25–0.8 mm wide for 21–24 segments, 19 or 20 of which chaetigerous and 2–4 posterior-most achaetigerous. Preserved specimens pale yellow (Fig. 29A), live specimens translucent (Fig. 29B)

Holotype in good condition, 6 mm long and 0.8 mm wide (at the widest point). Body robust, compact, grub like, anteriorly (commonly on chaetigers 1–7) somewhat enlarged then tapering posteriorly and relatively slender. Body surface rugose, with transverse rows of small squarish lobes.

Prostomium short, smooth, conical (Fig. 29C). Peristomium trapezoidal, rugose, with squarish papillae larger and then in subsequent segments, two transverse rows observed using Shirlastain A (Fig. 29C). Mouth as a broad transverse slit extending to chaetiger 1 (Fig. 29D).

Branchiae absent. Parapodia biramous, located on row with largest lobes, both rami well separated (Fig. 29C, E). Parapodial lappets present, observable from chaetiger 2 and well developed from chaetiger 8. Chaetigers in anterior (inflated) half distinctly triannulate, with three transverse rows of small, squarish lobes, subsequent segments becoming less distinctly annulated, with the last four achaetigerous segments uniannulate; lobes always largest on the ventral most row. Interramal sense organs present, best observed on stained specimen (Fig. 29E). Chaetae all long, smooth, slender capillaries (Fig. 29F).

Pygidium short, thick (only slightly longer wide), ventrally with keel-like very thick lobe. In distal view (Fig. 29G) with cirlet of about 10 smaller, thinner lobes located dorsally to large ventral keel-like lobe.

Shirlastain pattern. Prostomium stains strongly and stain is retained even after one week. Interramal sense organs observed as darkly red stained spots (Fig. 29E).

Morphological variation. Number of segments is slightly variably and appears to be linked to size, with the smallest specimens possessing 21 segments (19 of which chaetigerous), while the largest specimen possessed 24 segments (20 of which chaetigerous). Body shape remains mainly consistent, although some specimens were slightly thinner or thicker. Thick, keel-like ventral lobe on pygidium observed consistently, but the detection of slenderer lobes differs (probably an artefact of preservation) and some occasionally appear inflated (Fig. 29G).

Remarks. Differences between the known *Travisia* species and the species delineated herein are discussed in the Remarks section for *Travisia* sp. (NHM_1244), see below.

Genetic data. GenBank MN217470–MN217490 for 16S and MN217512 for 18S. *Travisia zieglerae* sp. nov. fall within a clade consisting of the other *Travisia* species in this study as well as other *Travisia* species on GenBank and the taxon *Neolipobranchnus* sp., a result similar to Martinez et al. (2014), suggesting a paraphyletic genus *Travisia* (Fig. 32).

Ecology. Found in polymetallic nodule province of the eastern CCZ.

Etymology. Named in honor of Amanda Ziegler, member of the science party of the ABYSSLINE AB02 cruise onboard the RV *Thomas G. Thompson*.

Travisia sp. (NHM_1244)

Fig. 30A–G

Material examined. NHM_1244 NHMUK ANEA 2019.7183, coll. 01 Mar. 2015, 12°15.44N, 117°18.13W, 4302 m <http://data.nhm.ac.uk/object/f6906eae-67ec-4d37-83c6-590f3c53df76>; NHM_1863 NHMUK ANEA 2019.7184, coll. 13 Mar. 2015, 12°02.49N, 117°13.03W, 4094 m, <http://data.nhm.ac.uk/object/fa708aca-6dd1-4b53-8d54-c76a93f43363>.

Description. This species is represented by two specimens only. It is a small species 5.5–6 mm long and 0.7 mm wide for 24 segments, 20 of which chaetigerous and four posterior-most achaetigerous. Preserved specimens pale yellow (Fig. 30A), live specimens milky, semi-transparent (Fig. 30B). Body robust, compact, grub like, anteriorly half enlarged, particularly over chaetigers 11–13, tapering posteriorly, but remaining relatively thick. Body surface rugose, with transverse rows of small, tightly packed squarish lobes.

Prostomium short, smooth, conical (Fig. 30C, D). Peristomium trapezoidal, rugose, with small, tightly packed squarish papillae, appearing in two rows dorsally. Mouth as a transverse slit between chaetigers 1 and 2 (Fig. 30D).

Branchiae absent. Parapodia biramous, located on row with largest lobes, both rami well separated (Fig. 30E). Parapodial lappets present, observable from chaetiger 1 and well developed from chaetiger 6. Chaetigers in anterior half distinctly triannulate, with three transverse rows of small, squarish lobes, subsequent segments becoming less distinctly annulated, with the last four achaetigerous segments uniannulate; lobes always largest on the ventral most row. Interramal sense organs present, best observed on stained specimen (Fig. 30E). Chaetae all long, smooth, slender capillaries (Fig. 30F).

Pygidium very short, thick (slightly longer wide); in distal view with a tightly packed cirlet of around 11 lobes (Fig. 30G), of these five large, thick and tightly packed with the ventral most single lobe thickest, dorso-laterally bordered by about six much smaller lobes (Fig. 30G).

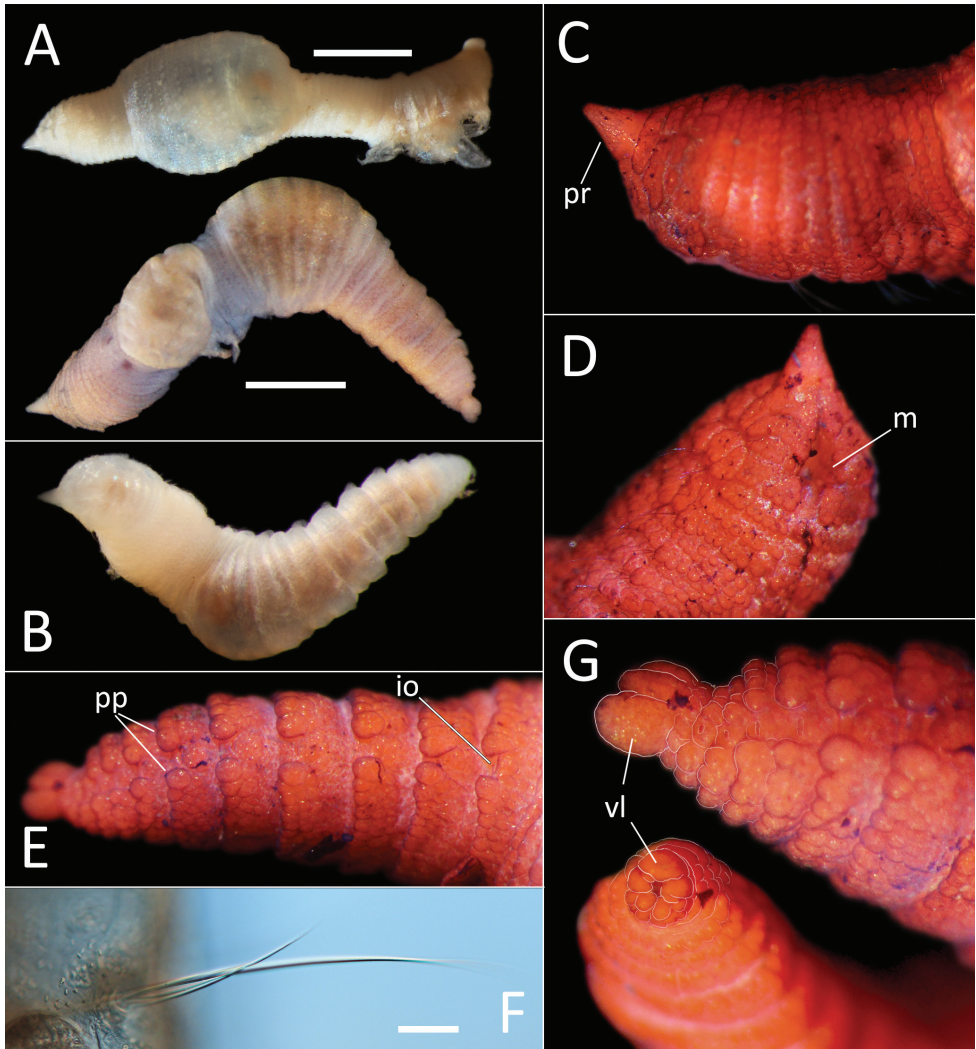


Figure 30. *Travisia* sp. NHM_1244. **A** Lab images, whole specimens (specimen NHM_1244, unstained [top], specimen NHM_1863, faded stain [bottom]) **B** Live image, whole specimen (specimen NHM_1863) **C** Lab image, dorsal anterior (specimen NHM_1863, stained, pr = prostomium) **D** Lab image, ventral anterior, (stained) (specimen NHM_1863, m = mouth) **E** Lab image, lateral posterior (specimen NHM_1863, stained, pp = parapodia, io = interramal organs) **F** Lab image, detail of capillary chaetae (specimen NHM_1244) **G** Lab image, pygidium, distal view (lower left) and lateral view (upper right), with pygidial features outlined in a fine white line (specimen NHM_1863, stained, vl = ventral lobe). Scale bars: 1 mm (**A**); 50 μ m (**F**).

Shirlastain pattern. Stain retained uniformly. Interramal sense organs observed as darkly red stained spots (Fig. 30E). Specimen stain within few (about 5) days.

Genetic data. GenBank MN217468–MN217469 for 16S and MN217511 for 18S. *Travisia* sp. (NHM_1244) is sister to *Neolipobranchus* sp. and fall within a clade consisting of *Travisia zieglerae* sp. nov. as well as other *Travisia* species from GenBank (Fig. 32).

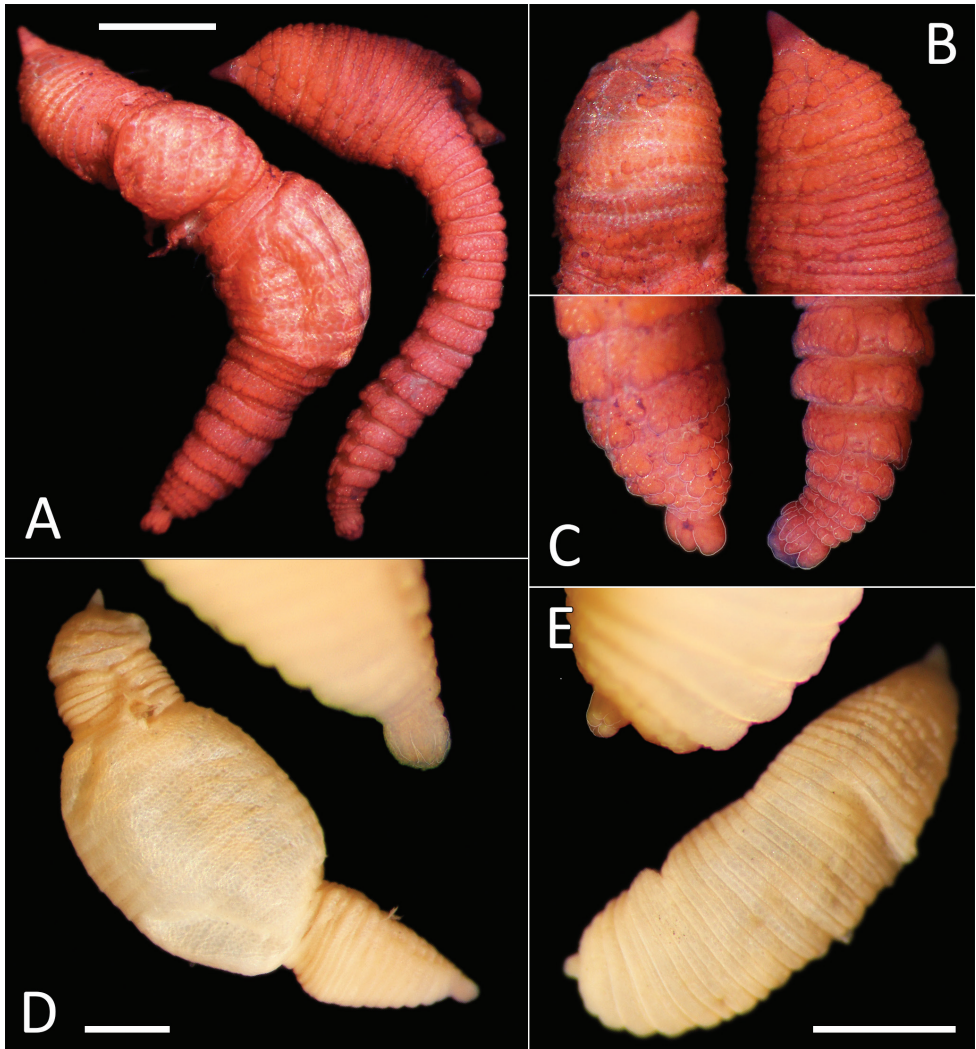


Figure 31. Comparison between *Travisia* sp. NHM_1244 and *Travisia zieglerae* sp. nov., and holotypes of *Travisia glandulosa* (BMNH 1921.5.1.2431) and *Travisia gravieri* (BMNH 1921.5.1.2429). **A** Lab images, whole specimens (*Travisia* sp. NHM_1244 specimen NHM_1863 [left], *Travisia zieglerae* sp. nov. holotype [specimen NHM_1431] [right], stained,) **B** Lab images, comparison of prostomia (*Travisia* sp. NHM_1244 specimen NHM_1863 [left], *Travisia zieglerae* sp. nov. holotype [right], stained) **C** Lab images, comparison of pygidia (*Travisia* sp. NHM_1244, specimen NHM_1863 [left], *Travisia zieglerae* sp. nov. holotype [right], stained) **D** *Travisia glandulosa* holotype, with detail of pygidium **E** *Travisia gravieri* holotype, with detail of pygidium. Morphological features in plates **C–E** have been outlined with a very fine white line to improve clarity of those features. Scale bars: 1 mm (**A, D, E**).

Remarks. Both UKSR-collected species are morphologically very similar, in having a similar number of segments and in being abbranchiate. They can be distinguished by a suite of subtle characters, which in case of *Travisia* sp. NHM_1224 is represented by only two specimens, so caution is needed. The two species differ somewhat in body

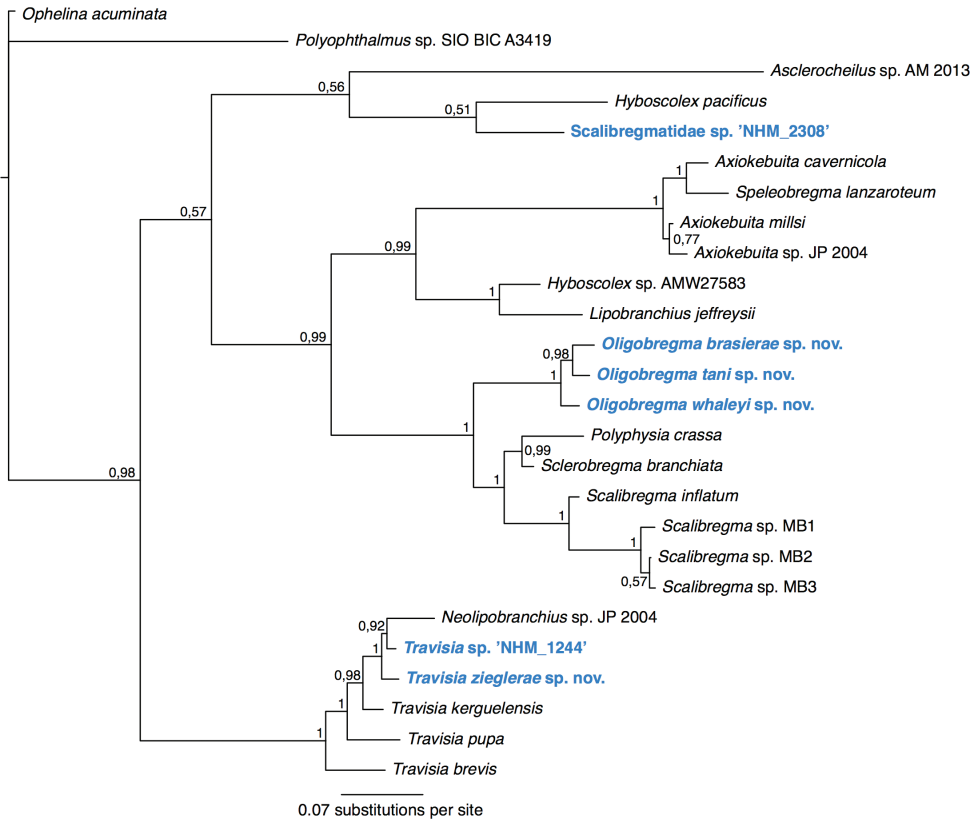


Figure 32. Phylogenetic analysis of Scalibregmatidae and Traviisiidae. 50% majority rule tree from the Bayesian analyses using 18S and 16S, with posterior probability values on nodes. Twenty taxa from GenBank were included, and Opheliidae was chosen as outgroup following the annelid phylogeny of Weigert and Bleidorn (2016).

shape as *Travisia zieglerae* sp. nov. is more slender in the posterior half, while *Travisia* sp. NHM_1224 is thicker (Fig. 31A). The rugosity of transverse rows differs, as the lobes are more tightly packed in *Travisia* sp. NHM_1244 and looser in *Travisia zieglerae* sp. nov., at least in the anterior region (Fig. 31B). Another difference is the arrangement of pygidial lobes (Fig. 31C). Finally, difference can be detected upon staining with Shirlastain, where prostomium of *Travisia zieglerae* sp. nov. stains darkly unlike that of *Travisia* sp. NHM_1244 (Fig. 31B) and the stain is retained after even 5 days since staining.

Of the known species of *Travisia*, only five were described as completely abranchiate, with four of these currently valid: *T. glandulosa* McIntosh, 1879; *T. gravieri* McIntosh, 1908; *T. nigrocincta* Ehlers, 1913 and *T. fusus* (Chamberlin, 1919) with *T. abyssorum* (Monro, 1930) considered a subjective synonym of *T. glandulosa*. Type specimens of McIntosh (1879; 1908) and the specimen of Monro (1930) were examined as part of this study. These can be distinguished from the UKSR species as follows:

T. fusus: has a larger body size of 14 mm and 28 chaetigers. Pygidium is divided into 12–14 inconspicuous lobes. Type locality: Pacific Ocean, towards the Marquesas Islands, 0°60'N, 137°54'W, 4504 m.

T. glandulosa (Fig. 31D): similar number of chaetiger to UKSR species (tentatively around 20 chaetigers counted), posteriorly thick, pygidium with circler of about 12 small lobes; of these inner 4 or 5 also small. Original description of not much help, and McIntosh (1879) expressed doubt about naming the species due to its poor condition. Type locality: Arctic Ocean, Davis Strait, Greenland, 3264 m.

T. gravieri (Fig. 31E): very compact, grub-like, not thinner in posterior half; tentatively about 16 or 17 chaetigers observed. Type locality: North Atlantic, 986 m.

T. nigrocincta: much larger species, up to 34 mm long and 6 mm wide for 25 segments (the smallest specimen reported by Ehlers was 6 mm long and about 2 mm wide for 17 chaetigers), with dark transverse bands; pygidium not described in detail. Type locality: Southern Ocean, Wilhelm II Coast, 2725 m.

Discussion

We have added 23 annelid species and 85 records to the total available knowledge of the benthic macrofauna of the CCZ. While this is certainly less than 10% of the estimated annelid diversity (based on the around 350 DNA-delineated species that are present in the UKSR collections), it represents a substantial increase in the published taxonomic knowledge linked to accessible voucher material, online genetic data and imagery of morphological features. Several of the taxa we report on are likely to be common and may have wide distributions across at least the eastern CCZ.

In terms of comparison to other studies, there are few sequences from just a few benthic faunal groups from the CCZ available on GenBank, for example echinoderms (Glover et al. 2016), cnidarians (Dahlgren et al. 2016), molluscs (Wiklund et al. 2017), polychaetes (Bonifácio and Menot 2018, Janssen et al. 2015), Porifera (Lim et al. 2017) and crustaceans (Janssen et al. 2015). With our study including both morphological and molecular data, we add to the knowledge of genetic information in the CCZ and aim to improve the taxonomic understanding of benthic fauna to provide a better picture of the distribution of taxa in the area, essential data for the establishment of conservation strategies in the light of potential future mineral extraction. These data are also the critical first step towards useful, practical identification guides to the fauna of this region.

Acknowledgements

The UKSR ABYSSLINE (ABYSSal baseLINE) environmental surveys were supported by a collaborative partnership between six non-profit global academic research institutes (University of Hawaii at Manoa, Natural History Museum, NORCE Norwegian Research Centre, National Oceanography Centre, Senckenberg Institute) and through an arrange-

ment with UKSRL. Additional support was provided by the Swedish research council FORMAS (TGD). We acknowledge Magdalena Georgieva and Madeleine Brasier from the Natural History Museum team and Swee Cheng Lim from National University of Singapore for support with sampling on board ship, and Chief Scientist Craig R. Smith for organizing. We also acknowledge the expert support from the Senckenberg Institute team in the deployment and recovery of successful Brenke Epibenthic Sledge samples. Comments from the editor and one reviewer greatly improved this manuscript. This study was made possible only by the dedicated help from the entire scientific party, the Masters and Crew of the RV *Melville* during the first cruise of the ABYSSLINE project in October 2013 and the Masters and Crew of the RV *Thomas G. Thompson* during the second ABYSSLINE cruise in February and March 2015. Thanks are also due to Emma Sherlock, Senior Curator of Annelida collection, Jackie Mackenzie-Dodds at the Molecular Collection Facility and Harry Rousham, Consultancy Manager, all at Natural History Museum.

References

- Amon DJ, Ziegler AF, Drazen JC, Grischenko AV, Leitner AB, Lindsay DJ, Voight, JR, Wicksten MK, Young CM, Smith CR (2017) Megafauna of the UKSRL exploration contract area and eastern Clarion-Clipperton Zone in the Pacific Ocean: Annelida, Arthropoda, Bryozoa, Chordata, Ctenophora, Mollusca. *Biodiversity Data Journal* (5): e14598. <https://doi.org/10.3897/BDJ.5.e14598>
- Ashworth JH (1902) The anatomy of *Scalibregma inflatum* Rathke. *Quarterly Journal of Microscopical Science*, London 45: 237–309.
- Baker E, Beaudoin Y (2013) Deep Sea Minerals: Manganese Nodules, a physical, biological, environmental, and technical review. Vol. 1B. Secretariat of the Pacific Community. ISBN: 978-82-7701-119-6
- Barroso R, Paiva PC (2013) Deep sea *Ophelina* (Polychaeta: Opheliidae) from southern Brazil. *Marine Biodiversity Records* 6: e51. <https://doi.org/10.1017/S1755267213000201>
- Bely AE, Wray GA (2004) Molecular phylogeny of naidid worms (Annelida: Clitellata) based on cytochrome oxidase I. *Molecular Phylogenetics and Evolution* 30(1): 50–63. [https://doi.org/10.1016/S1055-7903\(03\)00180-5](https://doi.org/10.1016/S1055-7903(03)00180-5)
- Blake JA (1981) The Scalibregmatidae (Annelida: Polychaeta) from South America and Antarctica collected chiefly during the cruises of the R/V Anton Bruun, R.V. Hero and USNS Eltanin. *Proceedings of the Biological Society of Washington* 94(4): 1131–1162.
- Blake JA (2000a) Family Capitellidae Grube, 1862. *Taxonomic Atlas of the Benthic Fauna of the Santa Maria Basin and the Western Santa Barbara Channel*. Santa Barbara Museum of Natural History, Santa Barbara, California 7: 47–96.
- Blake JA (2000b) Family Opheliidae Malmgren, 1867. *Taxonomic Atlas of the Benthic Fauna of the Santa Maria Basin and the Western Santa Barbara Channel*. Santa Barbara Museum of Natural History, Santa Barbara, California 7: 145–168.
- Blake JA (2000c) Family Scalibregmatidae Malmgren 1867. *Taxonomic Atlas of the Benthic Fauna of the Santa Maria Basin and the Western Santa Barbara Channel*. Santa Barbara Museum of Natural History, Santa Barbara, California 7: 129–144.

- Blake J (2009) Redescription of *Capitella capitata* (Fabricius) from West Greenland and designation of a neotype (Polychaeta, Capitellidae). *Zoosymposia* 2(1): 55–80.
- Blake JA (2015) New species of Scalibregmatidae (Annelida, Polychaeta) from the East Antarctic Peninsula including a description of the ecology and post-larval development of species of *Scalibregma* and *Oligobregma*. *Zootaxa* 4033: 57–93. <https://doi.org/10.11646/zootaxa.4033.1.3>
- Blake JA (2016) *Kirkegaardia* (Polychaeta, Cirratulidae), new name for *Monticellina* Laubier, preoccupied in the Rhabdocoela, together with new records and descriptions of eight previously known and sixteen new species from the Atlantic, Pacific, and Southern Oceans. *Zootaxa* 4166(1): 1–93. <http://doi.org/10.11646/zootaxa.4166.1.1>
- Blake JA, Maciolek NJ (2016) Traviisidae Hartmann-Schröder, 1971, new family status. In: Purschke G, Böggemann M, Westheide W (Eds) *Handbook of Zoology*. De Gruyter, Berlin.
- Bonifácio P, Menot L (2018) New genera and species from the Equatorial Pacific provide phylogenetic insights into deep-sea Polynoidae (Annelida). *Zoological Journal of the Linnean Society*. [Version of Record, published online 14 November 2018] <https://doi.org/10.1093/zoolinnean/zly063>
- Carr CM, Hardy SM, Brown TM, Macdonald TA, Hebert PD (2011) A tri-oceanic perspective: DNA barcoding reveals geographic structure and cryptic diversity in Canadian polychaetes. *PLoS ONE* 6: e22232. <https://doi.org/10.1371/journal.pone.0022232>
- Chamberlin R (1919) The Annelida Polychaeta. *Memories of the Museum of Comparative Zoology at Harvard College* 48: 1–514.
- Cohen BL, Gawthrop A, Cavalier-Smith T (1998) Molecular phylogeny of brachiopods and phoronids based on nuclear-encoded small subunit ribosomal RNA gene sequences. *Philosophical Transactions of the Royal Society of London B: Biological Sciences* 353: 2039–2061. <https://doi.org/10.1098/rstb.1998.0351>
- Dahlgren TG, Wiklund H, Rabone M, Amon DJ, Ikebe C, Watling L, Smith CR, Glover AG (2016) Abyssal fauna of the UK-1 polymetallic nodule exploration area, Clarion-Clipperton Zone, central Pacific Ocean: Cnidaria. *Biodiversity Data Journal*: e9277. <https://doi.org/10.3897/BDJ.4.e9277>
- Dauvin J-C, Bellan G (1994) Systematics, ecology and biogeographical relationships in the sub-family Traviisiinae (Polychaeta, Opheliidae). *Mémoires du Muséum national d'histoire naturelle* 162: 169–184.
- Detinova NN (1985) Многощетинковые черви хребта Рейкьянес (Северная Атлантика) [Polychaetous worms from the Reykjanes Ridge (the North Atlantic). *Bottom Fauna from Mid-Ocean Rises in the North Atlantic*. *Donnayafauna Otkryto. Okeanicheskikh. Podnyatij. Severnaya. Atlantika*]. *Trudy Instituta Okeanologii im. P.P. Shirshova* 120: 96–136. [in Russian]
- Donoghue MJ (1985) A critique of the biological species concept and recommendations for a phylogenetic alternative. *Bryologist* 88(3): 172–181. <https://doi.org/10.2307/3243026>
- Droege G, Barker K, Astrin JJ, Bartels P, Butler C, Cantrill D, Cottington J, Forest F, Gemeinholzer B, Hobern D, Mackenzie-Dodds J, Ó Tuama É, Petersen G, Sanjur O, Schindel D, Seberg O (2014) The Global Genome Biodiversity Network (GGBN) Data Portal. *Nucleic Acids Research* 42: D607–D612. <https://doi.org/10.1093/nar/gkt928>
- Edgar RC (2004) MUSCLE: multiple sequence alignment with high accuracy and high throughput. *Nucleic Acids Research* 32: 1792–1797. <https://doi.org/10.1093/nar/gkh340>

- Eisig H (1887) Monographie der Capitelliden des Golfes von Neapel und der angrenzenden meeres-abschnitte nebst untersuchungen zur vergleichenden anatomie und physiologie. Fauna und Flora des Golfes von Neapel und der angrenzenden Meeres-Abschnitte 16, 906 pp. [37 pls.] <https://doi.org/10.5962/bhl.title.11542>
- Ehlers E (1887) Florida-Anneliden No. 31. Memoirs of the Museum of Comparative Zoology (Harvard College) 15: 1–335.
- Ehlers E (1913) Die Polychaeten-Sammlungen der deutschen Südpolar-Expedition, 1901–1903. Deutsche Südpolar-Expedition 1901–1903 im Auftrage des Reichsamtes des innern herausgegeben von Erich von Drygalski Leiter Expedition 13(4): 397–598. [pls XXVI–XLVI]
- Ewing RM (1982) A partial revision of the genus *Notomastus* (Polychaeta: Capitellidae) with a description of a new species from the Gulf of Mexico. Proceedings of the Biological Society of Washington 95: 232–237.
- Ewing RM (1984) Capitellidae, Vol. 2. In: Uebelacker JM, Johnson PG (Eds) Taxonomic Guide to the Polychaetes of the Northern Gulf of Mexico. Final Report to the Minerals Management Service, contract. Barry A. Vinor and Associates Inc., Mobile, Alabama, 14.1–14.47
- Ewing RM (1991) Review of monospecific genera of the family Capitellidae (Polychaeta) (abstract). In: Petersen ME, Kirkegaard JB (Eds) Systematics, Biology, and Morphology of World Polychaeta. Proceedings of the 2nd International Polychaete Conference (Copenhagen), August 1986. Ophelia Supplement, Denmark, 692–693.
- Fauchald K (1972) Benthic polychaetous annelids from deep water off western Mexico and adjacent areas in the eastern Pacific Ocean. Allan Hancock Monographs in Marine Biology 7: 1–575.
- Fauchald K (1977) The polychaete worms. Definitions and keys to the orders, families and genera. Natural History Museum of Los Angeles County, Science Series 28: 1–190.
- Folmer O, Black M, Hoeh W, Lutz R, Vrijenhoek R (1994) DNA primers for amplification of mitochondrial cytochrome c oxidase subunit I from diverse metazoan invertebrates. Molecular Marine Biology and Biotechnology 3(5): 294–299.
- Gallardo VA (1968) Polychaeta from the Bay of Nha Trang, South Viet Nam. Naga Report 4(3): 35–279.
- Glover AG, Smith CR, Paterson GLJ, Wilson GDF, Hawkins L, Shearer M (2002) Polychaete species diversity in the central Pacific abyss: local and regional patterns, and relationships with productivity. Marine Ecology Progress Series 240:157–170. <https://doi.org/10.3354/meps240157>
- Glover AG, Dahlgren TG, Wiklund H, Mohrbeck I, Smith CR (2016a) An end-to-end DNA taxonomy methodology for benthic biodiversity survey in the Clarion-Clipperton Zone, Central Pacific Abyss. Journal of Marine Science and Engineering 4: 2. <https://doi.org/10.3390/jmse4010002>
- Glover AG, Wiklund H, Rabone M, Amon DJ, Smith CR, O'Hara T, Mah CL, Dahlgren TG (2016b) Abyssal fauna of the UK-1 polymetallic nodule exploration claim, Clarion-Clipperton Zone, central Pacific Ocean: Echinodermata. Biodiversity data journal: e7251. <https://doi.org/10.3897/BDJ.4.e7251>
- Glover AG, Wiklund H, Chen C, Dahlgren TG (2018) Managing a sustainable deep-sea 'blue economy' requires knowledge of what actually lives there. eLife 7: e41319. <https://doi.org/10.7554/eLife.41319>

- Gollner S, Kaiser S, Menzel L, Jones DO, Brown A, Mestre NC, Van Oevelen D, Menot L, Colaço A, Canals M, Cuvelier D (2017) Resilience of benthic deep-sea fauna to mining activities. *Marine Environmental Research* 129: 76–101. <https://doi.org/10.1016/j.marenvres.2017.04.010>
- Green KD (2002) Capitellidae (Polychaeta) from the Andaman Sea. *Phuket Marine Biological Center Special Publication* 24: 249–343.
- Grube AE (1862) Noch ein Wort über die Capitellen und ihre Stelle im Systeme der Anneliden. *Archiv für Naturgeschichte*, Berlin 28(1): 366–378.
- Hansen GA (1879) Annelider fra den norske Nordhavsexpedition i 1876. *Nyt Magazin for Naturvidenskaberne*, Christiania 24(1): 1–17.
- Hartman O (1960) Systematic account of some marine invertebrate animals from the deep basins off southern California. *Allan Hancock Pacific Expeditions* 22(2): 69–216.
- Hartman O (1965) Deep-water benthic polychaetous annelids off New England to Bermuda and other North Atlantic areas. *Occasional Papers of the Allan Hancock Foundation* 28: 1–384.
- Hartman O, Fauchald K (1971) Deep-water benthic polychaetous annelids off New England to Bermuda and other North Atlantic Areas. Part II. *Allan Hancock Monographs in Marine Biology* 6: 1–327.
- Hartmann-Schröder G (1971) Annelida, borstenwürmer, polychaeta. *Die Tierwelt Deutschlands und der angrenzenden Meeresteile nach ihren Merkmalen und nach ihrer Lebensweise* 58: 1–594. <https://doi.org/10.1086/407180>
- Hein JR, Mizell K, Koschinsky A, Conrad TA (2013) Deep-ocean mineral deposits as a source of critical metals for high- and green-technology applications: comparison with land-based resources. *Ore Geology Reviews* 51: 1–4. <https://doi.org/10.1016/j.oregeorev.2012.12.001>
- Hessler RR, Jumars PA (1974) Abyssal community analysis from replicate cores in the central North Pacific. *Deep Sea Research and Oceanographic Abstracts* 21: 185–209. [https://doi.org/10.1016/0011-7471\(74\)90058-8](https://doi.org/10.1016/0011-7471(74)90058-8)
- Hutchings PA (1974) Polychaeta of Wallis Lake, New South Wales. *Proceedings of the Linnean Society of New South Wales* 98(4): 175–195.
- Janssen A, Kaiser S, Meissner K, Brenke N, Menot L, Martínez Arbizu P (2015) A reverse taxonomic approach to assess macrofaunal distribution patterns in abyssal Pacific polymetallic nodule fields. *PLoS ONE* 10: e0117790. <https://doi.org/10.1371/journal.pone.0117790>
- Johnston G (1840) *Miscellanea Zoologica. British Annelids. Annals and Magazine for Natural History* London 1(4): 368–375. <https://doi.org/10.1080/00222934009512507>
- Katoh K, Misawa K, Kuma K, Miyata T (2002) MAFFT: a novel method for rapid multiple sequence alignment based on fast Fourier transform. *Nucleic Acids Research* 30: 3059–3066. <https://doi.org/10.1093/nar/gkf436>
- Kearse M, Moir R, Wilson A, Stones-Havas S, Cheung M, Sturrock S, Buxton S, Cooper A, Markowitz S, Duran C (2012) Geneious Basic: an integrated and extendable desktop software platform for the organization and analysis of sequence data. *Bioinformatics* 28: 1647–1649. <https://doi.org/10.1093/bioinformatics/bts199>
- Kinberg JGH (1867) *Annulata nova. Öfversigt af Kungliga Vetenskaps Akademiens Förhandlingar* 23: 97–103.

- Kongsrud JA, Bakken T, Oug E (2011) Deep-water species of the genus *Ophelina* (Annelida, Opheliidae) in the Nordic Seas, with the description of *Ophelina brattegardii* sp. nov. Italian Journal of Zoology 78: 95–111. <https://doi.org/10.1080/11250003.2011.606658>
- Kudenov JD, Blake JA (1978) A review of the genera and species of the Scalibregmidae (Polychaeta) with descriptions of one new genus and three new species from Australia. Journal of Natural History 12: 427–444. <https://doi.org/10.1080/00222937800770291>
- Law CJ, Dorgan KM, Rouse GW (2014) Relating divergence in polychaete musculature to different burrowing behaviors: A study using Opheliidae (Annelida). Journal of Morphology 42: 548–571. <https://doi.org/10.1002/jmor.20237>
- Levenstein RY (1975) The polychaetous annelids of the deep-sea trenches of the Atlantic sector of the Antarctic Ocean. Transactions of the P.P. Shirov Institute of Oceanology Academy. Trudy Instituta Okeanologia, Akademia nauk SSSR 103: 119–142. [in Russian]
- Lim SC, Wiklund H, Glover AG, Dahlgren TG, Tan KS (2017) A new genus and species of abyssal sponge commonly encrusting polymetallic nodules in the Clarion-Clipperton Zone, East Pacific Ocean. Systematics and Biodiversity 15(6): 507–519. <https://doi.org/10.1080/14772000.2017.1358218>
- McIntosh WC (1878) On the Annelida obtained during the Cruise of H.M.S. 'Valorous' to Davis Strait in 1875. Transactions of the Linnean Society of London. Second Series: Zoology 1(7): 499–511. [pl. LXV]
- McIntosh WC (1908) Notes from the Gatty Marine Laboratory, St. Andrews. Annals and Magazine of Natural History 1(8): 373–387. <https://doi.org/10.1080/00222930808692422>
- Maciolek NJ, Blake JA (2006) Opheliidae (Polychaeta) collected by the R/V Hero and the USNS Eltanin cruises from the Southern Ocean and South America. Scientia Marina 70: 101–113. <https://doi.org/10.3989/scimar.2006.70s3101>
- Malmgren AJ (1867) Annulata Polychaeta: Spetsbergiae, Groenlandiae, Islandiae et Scandinaviae. Hactenus cognita. Öfversigt af Kungliga Vetenskaps Akademiens Förhandlingar 24: 127–255. <https://doi.org/10.5962/bhl.title.13358>
- Martínez A, Di Domenico M, Worsaae K (2014) Gain of palps within a lineage of ancestrally burrowing annelids (Scalibregmatidae). Acta Zoologica 95: 421–429. <https://doi.org/10.1111/azo.12039>
- Medlin L, Elwood H, Stickel S, Sogin M (1988) The characterization of enzymatically amplified eukaryotic 16S-like rRNA-coding regions. Gene 71: 491–499. [https://doi.org/10.1016/0378-1119\(88\)90066-2](https://doi.org/10.1016/0378-1119(88)90066-2)
- Monro CCA (1930) Polychaete worms. Discovery Reports 2: 1–222.
- Neal L, Hardy SM, Smith CR, Glover AG (2011) Polychaete species diversity on the West Antarctic Peninsula deep continental shelf. Marine Ecology Progress Series 428: 119–134. <https://doi.org/10.3354/meps09012>
- Neal L, Taboada S, Woodall LC (2018) Slope-shelf faunal link and unreported diversity off Nova Scotia: evidence from polychaete data. Deep Sea Research Part I: Oceanographic Research Papers 138: 72–84. <https://doi.org/10.1016/j.dsr.2018.07.003>
- Nygren A, Sundberg P (2003) Phylogeny and evolution of reproductive modes in Autolytinae (Syllidae, Annelida). Molecular Phylogenetics and Evolution 29: 235–249. [https://doi.org/10.1016/s1055-7903\(03\)00095-2](https://doi.org/10.1016/s1055-7903(03)00095-2)

- OBIS (2018) Global biodiversity indices from the Ocean Biogeographic Information System. <http://www.iobis.org> [Accessed on: 2018-11-13]
- Ørsted AS (1843) *Annulatorum danicorum conspectus*. Volume Fasc. 1 Maricolae (Quaestio ab universitate Hafniensi ad solvendum proposita et proemio ornata). Librariae Wahlianae, Hafniae, 52 pp. <https://doi.org/10.5962/bhl.title.11849>
- Paul C, Halanych KM, Tiedemann R, Bleidorn C (2010) Molecules reject an opheliid affinity for *Travisia* (Annelida). *Systematics and Biodiversity* 8(4): 507–512. <https://doi.org/10.1080/14772000.2010.517810>
- Palumbi SR (1996) Nucleic acid. II. The polymerase chain reaction. In: Hillis DM, Moritz G, Mable BK (Eds) *Molecular Systematics*. Sinauer Associates, Sunderland, 205–247.
- Parapar J, Moreira J (2008) Sobre la presencia del género *Ophelina* Ørsted, 1843 (Polychaeta, Opheliidae) en el litoral de la península Ibérica. *NACC: Nova Acta Científica Compostelana. Biología* 117–134.
- Parapar J, Moreira J, Helgason GV (2011) Distribution and diversity of the Opheliidae (Annelida, Polychaeta) on the continental shelf and slope of Iceland, with a review of the genus *Ophelina* in northeast Atlantic waters and description of two new species. *Organisms Diversity and Evolution* 11: 83. <https://doi.org/10.1007/s13127-011-0046-2>
- Paterson GLJ, Glover AG, Froján CRSB, Whitaker A, Budaeva N, Chimonides J, Doner S (2009) A census of abyssal polychaetes. *Deep-Sea Research Part II* 56: 1739–1746. <https://doi.org/10.1016/j.dsr2.2009.05.018>
- Paterson GLJ, Neal L, Altamira I, Soto EH, Smith CR, Menot L, Billett DSM, Cunha MR, Marchais-Laguionie C, Glover AG (2016) New *Prionospio* and *Aurospio* species from the deep sea (Annelida: Polychaeta). *Zootaxa* 4092(1): 1–32. <http://doi.org/10.11646/zootaxa.4092.1.1>
- Persson J, Pleijel F (2005) On the phylogenetic relationships of *Axiokebuita*, *Travisia* and *Scalibregmatidae* (Polychaeta). *Zootaxa* 998: 1–14. <https://doi.org/10.11646/zootaxa.998.1.1>
- Purschke G, Hausen H (2007) Lateral organs in sedentary polychaetes (Annelida) – Ultrastructure and phylogenetic significance of an insufficiently known sense organ. *Acta Zoologica* 88: 23–39. <https://doi.org/10.1111/j.1463-6395.2007.00247.x>
- Rathke H (1843) Beiträge zur Fauna Norwegens. *Nova Acta Academiae Caesareae Leopoldino-Carolinae Naturae Curiosorum* 20: 1–264. <https://doi.org/10.5962/bhl.title.120119>
- Read G, Fauchald K (2018a) World Polychaeta database. *Scalibregmatidae* Malmgren, 1867. World Register of Marine Species. <http://www.marinespecies.org/aphia.php?p=taxdetails&id=925> [Accessed on: 2018-5-9]
- Read G, Fauchald K (2018b) World Polychaeta database. *Oligobregma* Kudenov & Blake, 1978. World Register of Marine Species. <http://www.marinespecies.org/aphia.php?p=taxdetails&id=324770> [Accessed on: 2018-5-10]
- Read G, Fauchald K (2018c) World Polychaeta database. Opheliidae Malmgren, 1867. World Register of Marine Species. <http://www.marinespecies.org/aphia.php?p=taxdetails&id=924> [Accessed on: 2018-5-10]
- Read G, Fauchald K (2019) World Polychaeta database. *Ophelina* Ørsted, 1843. World Register of Marine Species. <http://www.marinespecies.org/aphia.php?p=taxdetails&id=129414> [Accessed on: 2019-2-19]

- Ronquist F, Teslenko M, Van Der Mark P, Ayres DL, Darling A, Höhna S, Larget B, Liu L, Suchard MA, Huelsenbeck JP (2012) MrBayes 3.2: efficient Bayesian phylogenetic inference and model choice across a large model space. *Systematic Biology* 61: 539–542. <https://doi.org/10.1093/sysbio/sys029>
- Sardá R, Gil J, Taboada S, Gili JM (2009) Polychaete species captured in sediment traps moored in northwestern Mediterranean submarine canyons. *Zoological Journal of the Linnean Society* 155: 1–21. <https://doi.org/10.1111/j.1096-3642.2008.00442.x>
- Sars M (1851) Beretning om en i Sommeren 1849 foretagen zoologisk Reise i Lofoten og Finmarken. *Nyt Magazin for Naturvidenskaberne* 6: 121–211.
- Schüller M (2008) New polychaete species collected during the expeditions ANDEEP I, II, and III to the deep Atlantic sector of the Southern Ocean in the austral summers 2002 and 2005 – Ampharetidae, Opheliidae, and Scalibregmatidae. *Zootaxa* 1705: 51–68. <https://doi.org/10.11646/zootaxa.1705.1.4>
- Schüller M, Hilbig B (2007) Three new species of the genus *Oligobregma* (Polychaeta, Scalibregmatidae) from the Scotia and Weddell Seas (Antarctica). *Zootaxa* 1391: 35–45. <https://doi.org/10.11646/zootaxa.1391.1.2>
- Sene-Silva G (2007) Filogenia de Opheliidae (Annelida: Polychaeta). Unpublished Thesis presented for the degree, Doctor of Sciences, in Zoology, Universidade Federal do Paraná, Curitiba, Brazil, xii + 95 pp.
- Sjölin E, Erséus C, Källersjö M (2005) Phylogeny of Tubificidae (Annelida, Clitellata) based on mitochondrial and nuclear sequence data. *Molecular Phylogenetics and Evolution* 35: 431–441. <https://doi.org/10.1016/j.ympev.2004.12.018>
- Smith CR, Dahlgren TG, Drazen J, Gooday A, Glover AG, Kurras G, Martinez-Arbizu P, Shulze C, Spickermann R, Sweetman AK, Vetter E (2013) Abyssal Baseline Study (ABYSSLINE) Cruise Report. Seafloor Investigations Report 2013-1304-051J-SRDL-AB01.
- Smith CR, Church M, Chow J, Dahlgren TG, Drazen J, Glover AG, Gooday A, Kaylan B, Lui B, Kurras G, Martinez-Arbizu P, Sweetman AK, Tan KS, Vetter E (2015) Abyssal Baseline Study (ABYSSLINE) Cruise Report. Seafloor Investigations Report 2015-1408-061J-SRDL-AB02.
- Støp-Bowitz C (1945) Les ophéliens norvégiens. *Meddelelser fra det Zoologiske Museum, Oslo* 52: 21–61.
- Støp-Bowitz C (1948) Sur les polychètes arctiques des familles des glycériens des ophéliens, des scalibregmiens et des flabelligériens. *Tromsø Museums Årshefter* 66(2): 1–58.
- Tomassetti P, Porrello S (2005) Polychaetes as indicators of marine fish farm organic enrichment. *Aquaculture International* 13(1–2): 109–128. <https://doi.org/10.1007/s10499-004-9026-2>
- Tzetlin A, Zhadan A (2009) Morphological variation of axial non-muscular proboscis types in the Polychaeta. *Zoosymposia* 2: 415–427.
- Weigert A, Bleidorn C (2016) Current status of annelid phylogeny. *Organisms, Diversity and Evolution* 16(2) 345–362. <https://doi.org/10.1007/s13127-016-0265-7>
- Wiklund H, Taylor JD, Dahlgren TG, Todt C, Ikebe C, Rabone M, Glover AG (2017) Abyssal fauna of the UK-1 polymetallic nodule exploration area, Clarion-Clipperton Zone, central Pacific Ocean: Mollusca. *ZooKeys* 707: 1–46. <https://doi.org/10.3897/zookeys.707.13042>
- Wirén A (1901) Ueber die während der schwedischen arktischen Expedition von 1898 und 1900 eingesammelten Anneliden. *Zoologischer Anzeiger* 24: 253.

Citizen science yields first records of *Hippocampus japapigu* and *Hippocampus denise* (Syngnathidae) from Taiwan: A hotspot for pygmy seahorse diversity

Joseph Heard¹, Jeng-Ping Chen², Colin K.C. Wen^{1,3}

1 Department of Life Science, Tunghai University, Taichung, Taiwan **2** Taiwan Ocean Research Institute, National Applied Research Laboratories, Taiwan **3** Center for Ecology and Environment, Tunghai University, Taiwan

Corresponding author: Colin Wen (ckcwen@thu.edu.tw)

Academic editor: N. Bogutskaya | Received 3 September 2019 | Accepted 29 September 2019 | Published 28 October 2019

<http://zoobank.org/DF638AD-29CC-4217-A1FC-361097968234>

Citation: Heard J, Chen J-P, Wen CKC (2019) Citizen science yields first records of *Hippocampus japapigu* and *Hippocampus denise* (Syngnathidae) from Taiwan: A hotspot for pygmy seahorse diversity. ZooKeys 883: 83–90. <https://doi.org/10.3897/zookeys.883.39662>

Abstract

Relatively very little is known about pygmy seahorses, and even basic information regarding their distributions is largely inconsistent and often based on unofficial reports. However, monitoring marine diversity, particularly for small and cryptic species, such as pygmy seahorses, can be both costly and time consuming. In such cases, the use of citizen science can offer an effective tool for addressing knowledge gaps caused by a lack of biodiversity-related data. Scuba divers and underwater photographers were engaged through social media in order to investigate pygmy seahorse diversity in Taiwan. Using this approach five species of pygmy seahorses were identified, including two new records for Taiwan: *Hippocampus denise* and *Hippocampus japapigu*, the latter of which is the first record of the species from outside of Japan. These new records mark Taiwan as one of the world's pygmy seahorse diversity hotspots, matching that of Japan and Indonesia, as well as demonstrating the value of citizen science for marine biodiversity monitoring, particularly for small cryptic species.

Keywords

biodiversity monitoring, social media, web-based photographs

Introduction

There are currently seven species of pygmy seahorse contained within the syngnathid genus *Hippocampus* Rafinesque, 1810 (Lourie et al. 2016). Diminutive sizes are a key feature among this unofficial grouping, ranging from 13.6 mm SL in *H. satomi* Lourie & Kuitert, 2008 to 26.9 mm in *H. colemani* Kuitert, 2003 (Short et al. 2018). They can also be further differentiated from their congeners in possessing a single gill opening as opposed to a pair of openings, as well as trunk brooding rather than pouch brooding their young (Short et al. 2018).

The majority of pygmy seahorse species are known from a limited number of locations. For example, *H. waleananus* Gomon & Kuitert, 2008 is known only from Walea Island, Indonesia. As such, there is a severe paucity of information regarding various aspects of their ecology and biology. Basic occurrence data is also either lacking or inconsistent between online ichthyological database resources. Consequently, with the exceptions of *H. pontohi* Lourie & Kuitert, 2008 and *H. japapigu* Short et al., 2018, all other pygmy seahorse species are currently classified as “Data Deficient” on the IUCN Red List of Threatened Species. The latter, having only recently been described, has yet to be included.

Scientists are now increasingly and effectively utilising citizen science and other non-invasive methods to address knowledge gaps caused by constraints associated with the collection of biodiversity-related information (i.e., time and resources) (Miyazaki et al. 2014, 2015; Castilla et al. 2017; Campbell and Engelbrecht 2018; Pearson 2018). Social media (e.g., Facebook and Twitter), for example, has even been used to identify undescribed species (Skejo and Caballero 2016), as well as detecting illegal introductions of non-native species (Miyazaki et al. 2016). Such approaches are likely to prove particularly useful for small-sized, highly camouflaged cryptic taxa such as pygmy seahorses and sea slugs (Paz-Sedano et al. 2019). Recognising this, we engaged underwater photographers and dive guides through citizen science via social media in order to improve the current knowledge of pygmy seahorse diversity in Taiwan, where three species: *H. bargibanti* Whitely, 1970, *H. colemani*, and *H. pontohi* have so far been observed by scuba divers (Shao et al. 2008; Short et al. 2018).

Materials and methods

We performed searches of “Posts” and “Photos” between 2017 and 2019 containing pygmy seahorses using the keyword “豆丁海馬” (pygmy seahorse in Chinese) from Facebook and Instagram, the most popular forms of social media used in Taiwan. For Facebook, three different user accounts were used in order to broaden potential search results due to Facebook’s algorithm. Manual searches of a number of Taiwanese underwater photography and marine organism identification groups were also performed to generate additional sighting data. Individual users who frequently shared photographs of pygmy seahorses were also contacted directly to inquire about any additional sightings they may have made. The species, location, date, and depth (where available) were recorded for all photographs of pygmy seahorses taken within Taiwan.

Results and discussion

Our search results returned 259 social media items, 75 of which included in situ photographs of pygmy seahorses from five different locations in Taiwan (Fig. 1). From these we were able to identify 78 individuals belonging to five species (*H. bargibanti*, *H. colemani* and *H. pontohi*), including two new records for Taiwan (*H. denise* and *H. japapigu*). Firstly, we report the first record of *H. japapigu* from Taiwan based on four separate in situ observations, which also represent the first records of the species from outside of Japan. The earliest observation of what appears to be *H. japapigu* was photographed at Green Island in 2010 (Fig. 2A). This was mistakenly lauded on social media as Taiwan's first record of *H. pontohi*, the closest congener of *H. japapigu*, which had yet to be described at the time. A group of seven *H. japapigu* were later observed in association with *Halimeda* algae at 5 m during a night dive in Hejie, Kenting in southern Taiwan in 2017 (Fig. 2B). These were again mistaken by the photographer as *H. pontohi*; however, in hindsight we can now confirm these individuals were *H. japapigu* based on their distinctive reticulated white patterning, single pair of bilaterally paired wing-like protrusions, raised dorsal ridge, as well as a pronounced eighth lateral trunk ridge spine (Short et al. 2018). Further sightings have since been reported, with a single individual observed again in Hejie in 2017 (Fig. 2C), as well as a single individual in Longdong in northern Taiwan in 2019 (Fig. 2D).

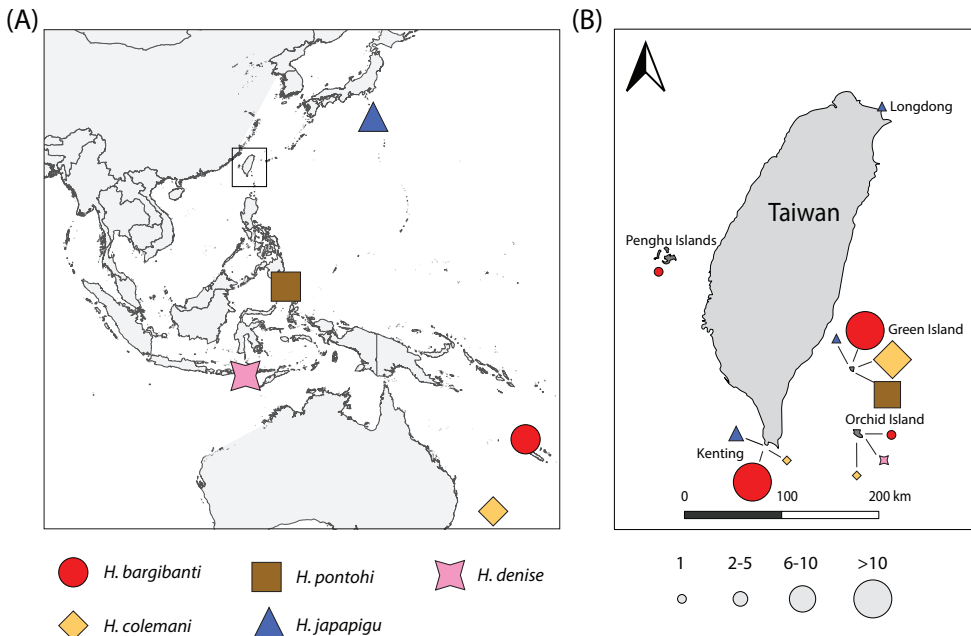


Figure 1. Map showing **A** the original collection locations of specimens for the five pygmy seahorse species recorded in Taiwan during this study, as well as **B** their distributions in Taiwan and surrounding islands (Penghu islands, Green Island, and Orchid Island). Symbols are scaled relatively according to the number of observations per species at each location obtained through social media.

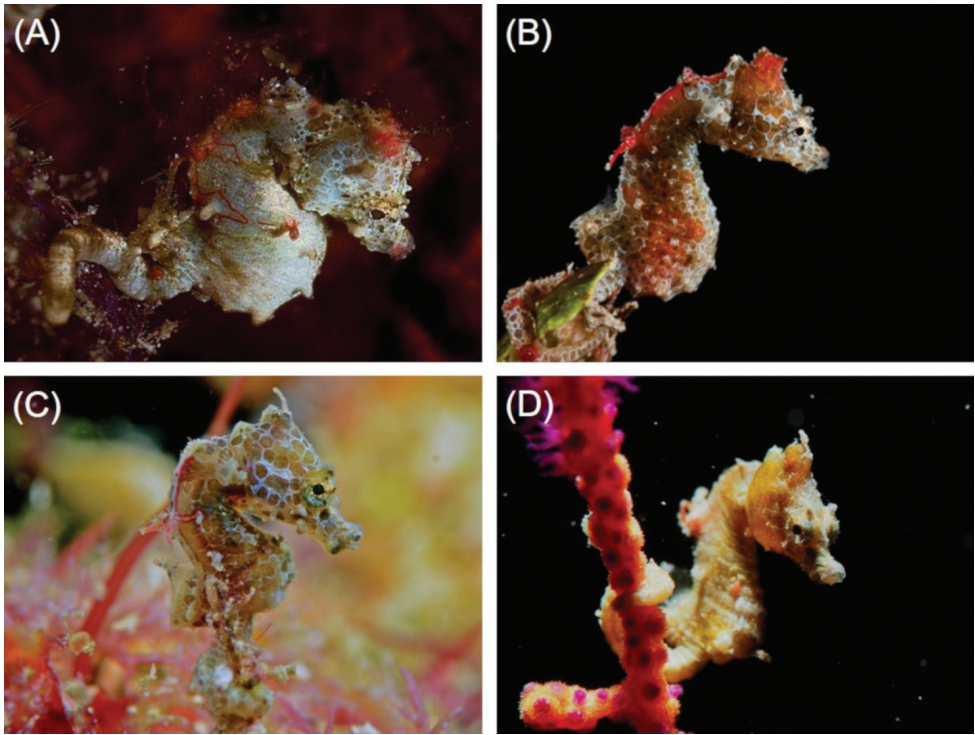


Figure 2. *Hippocampus japapigu* in situ **A** Green Island, Taiwan **B** Hejie, Kenting, Taiwan at 5 m depth **C** Hejie, Kenting, Taiwan **D** 82.5 k near Longdong, northern Taiwan (Photographs **A** Jolly Huang **B** Jay Chiu **C** Chao-Tsung Chen **D** Jung-Chao Yeh).

We also report the first finding of *H. denise* from Taiwan, which is one of the smallest and most widely distributed of the pygmy seahorses, occurring throughout much of the Indo-West Pacific (Lourie and Randall 2003; Foster et al. 2011). A single female was observed inhabiting the branches of an *Annella* gorgonian coral at a depth of 28 m at Orchid Island (Lanyu), off the southeast coast of Taiwan (Fig. 3A). This species can be easily distinguished from its nearest congener, *H. bargibanti* (Fig. 3B), based on its fewer and less developed tubercles, orange body colouration, non-bulbous snout and slender and elongated body shape, the latter of which was the most frequently recorded and widely distributed species in this study. This is unsurprising given their conspicuousness and larger size relative to the majority of other pygmy seahorses. Indeed, *H. bargibanti* was the first species to be recorded in Taiwan, having initially been observed in Kenting in 2004, and to date remains the only species to have been formally documented (Shao et al. 2008).

Lastly, we also confirm the presence of *H. colemani* and *H. pontohi* (*H. severnsi* is a junior synonym of the latter) from Taiwan based on numerous observations. With the

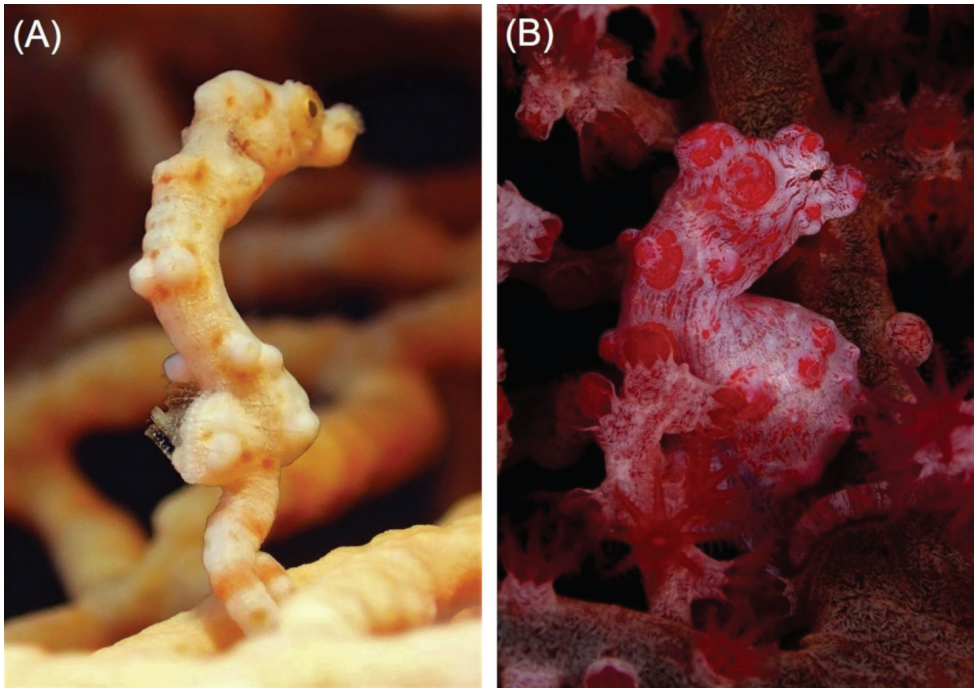


Figure 3. Comparison of **A** *Hippocampus denise* in situ, Orchid Island, Taiwan at 28 m depth, with its most similar congener **B** *Hippocampus bargibanti* in situ, Green Island, Taiwan. Note the differences in body colouration (orange in *H. denise* vs. purple in *H. bargibanti*), the number and size of tubercles (fewer and less pronounced in *H. denise*), snout length (bulbous tip in *H. bargibanti* vs. non-bulbous in *H. denise*) and overall shape (slender and elongate in *H. denise* vs. rotund in *H. bargibanti*) (Photographs **A** Yung-Kuang Ting **B** Ryan Ku).

exceptions of single sightings of *H. colemani* from both Orchid Island and Kenting, *H. colemani* was predominantly observed at Green Island, where it was the most commonly sighted species. Conversely, *H. pontohi* was only recorded from Green Island. The two species can be visually differentiated based on the low and rounded coronet of *H. colemani* (Fig. 3A–C), which is more distinct and angular in *H. pontohi* (Fig. 3D–F) (Short et al. 2018).

As five of the known seven species of pygmy seahorses have been observed in Taiwan, the country now ranks as one of the world's pygmy seahorse diversity hotspots. Of particular note, four species were found at Green Island alone, a small island measuring only 15.09 km². However, no voucher specimens of any pygmy seahorse species have so far been collected from Taiwan. This is unfortunate given the importance of scientific collections for studies of evolution, ecology, and conservation (Rocha et al. 2014). We therefore recommend the collection of specimens from Taiwan to facilitate further research into these poorly understood taxa.

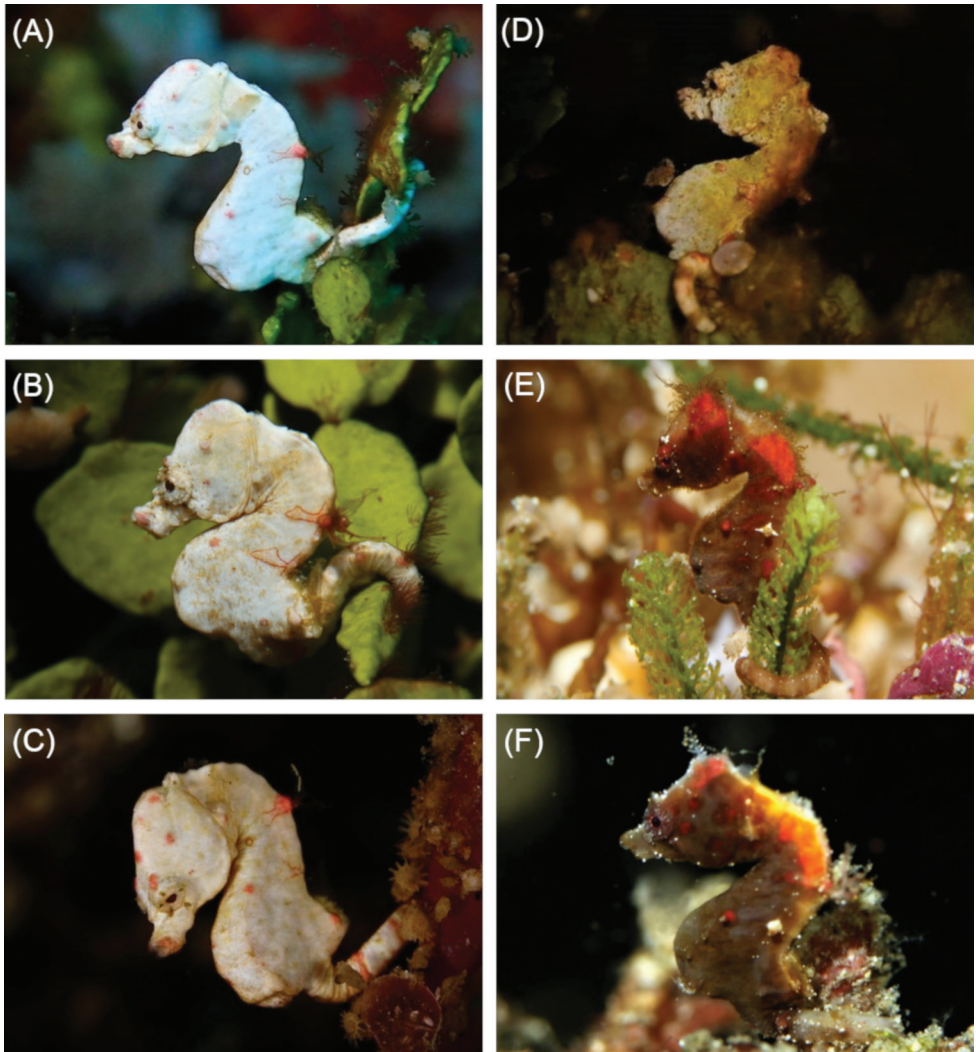


Figure 4. Comparison of **A–C** *Hippocampus colemani* in situ, Green Island, Taiwan with **D–F** *Hippocampus pontohi* in situ, Green Island, Taiwan. Note the differences in the shape and angle of the coronet (low and rounded in *H. colemani* vs. distinct and angular in *H. pontohi*), as well as differences in body colouration (*H. colemani* is known only to occur in shades of off-white, whereas *H. pontohi* is highly variable) (Photographs **A** Joe Chiu **B** Ryan Ku **C, E, F** Ming-Hung Yu **D** Ryan Ku).

Acknowledgements

The main project of this study was funded by MOST Taiwan (107-2611-M-029 -001 & 108-2611-M-029 -001) and the citizen science approach was initiated by Kah Leng Cherh. We foremost acknowledge the underwater photographers, dive guides, and naturalists whose efforts and passion for the underwater world made this work pos-

sible, and who kindly allowed us to use their photographs. In particular, Yung-Kuang Ting and Jolly Huang (although unknowingly at the time) deserve special mentions for being the first to photograph *H. denise* and *H. japapigu* in Taiwanese waters, respectively. We would also like to thank Richard Smith and Graham Short for their taxonomic advice, the latter of whom, as well as Harald Ahnelt, also provided a number of suggestions which helped to greatly improve the manuscript.

References

- Campbell H, Engelbrecht I (2018) The Baboon Spider Atlas—using citizen science and the ‘fear factor’ to map baboon spider (Araneae: Theraphosidae) diversity and distributions in Southern Africa. *Insect Conservation and Diversity* 11: 143–151. <https://doi.org/10.1111/icad.12278>
- Castilla AM, Riera R, Ali Humaid M, Garland T, Alkuwari A, Muzaffar S, Naser HA, Al-Mohannadi S, Al-Ajmi D, Chikhi A, Wessels J (2017) Contribution of citizen science to improve knowledge on marine biodiversity in the Gulf Region. *Journal of the Association of Arab Universities for Basic and Applied Sciences* 24: 126–35. <https://doi.org/10.1016/j.jaubas.2017.06.002>
- Gomon MF, Kuitert RH (2009) Two new pygmy seahorses (Teleostei: Syngnathidae: *Hippocampus*) from the Indo-West Pacific. *Aqua International Journal of Ichthyology* 15: 37–44.
- Foster R, Bridge TCL, Bongaerts P (2011) The first record of *Hippocampus denise* (Syngnathidae) from Australia. *aqua, International Journal of Ichthyology* 18: 55–57.
- Kuitert RH (2003) A new pygmy seahorse (Pisces: Syngnathidae: *Hippocampus*) from Lord Howe Island. *Records of the Australian Museum* 55: 113–116. <https://doi.org/10.3853/rj.0067-1975.55.2003.1382>
- Lourie SA, Randall JE (2003) A new pygmy seahorse, *Hippocampus denise* (Teleostei Syngnathidae) from the Indo-Pacific. *Zoological Studies* 42: 284–291.
- Lourie SA, Kuitert RH (2008) Three new pygmy seahorse species from Indonesia (Teleostei: Syngnathidae: *Hippocampus*). *Zootaxa* 1963: 54–68. <https://doi.org/10.11646/zootaxa.1963.1>
- Lourie SA, Pollom RA, Foster SJ (2016) A global revision of the Seahorses *Hippocampus Rafinesque* 1810 (Actinopterygii: Syngnathiformes): Taxonomy and biogeography with recommendations for further research. *Zootaxa* 4146: 1–66. <https://doi.org/10.11646/zootaxa.4146.1.1>
- Miyazaki Y, Murase A, Shiina M, Masui R, Senou H (2015) Integrating and utilizing citizen biodiversity data on the Web for science: An example of a rare triggerfish hybrid image provided by a sport fisherman. *Journal of Coastal Research* 31: 1035–1039. <https://doi.org/10.2112/JCOASTRES-D-14-00170.1>
- Miyazaki Y, Murase A, Shiina M, Naoe K, Nakashiro R, Honda J, Senou H (2014) Biological monitoring by citizens using Web-based photographic databases of fishes. *Biodiversity and Conservation* 23: 2383–2391. <https://doi.org/10.1007/s10531-014-0724-4>
- Miyazaki Y, Teramura A, Senou H (2016) Biodiversity data mining from Argus-eyed citizens: the first illegal introduction record of *Lepomis macrochirus macrochirus* Rafinesque, 1819 in Japan based on Twitter information. *ZooKeys* 569: 123. <https://doi.org/10.3897/zookeys.569.7577>

- Paz-Sedano S, Tanduo V, Yonow N, Yokeş MB, Kletou D, Crocetta F (2019) *Baeolidia moebii* Bergh, 1888 (Mollusca: Gastropoda: Nudibranchia) is spreading in the eastern Mediterranean Sea. *Regional Studies in Marine Science* 32: 100830. <https://doi.org/10.1016/j.risma.2019.100830>
- Pearson KD (2018) Rapid enhancement of biodiversity occurrence records using unconventional specimen data. *Biodiversity Conservation* 27: 3007–3018. <https://doi.org/10.1007/s10531-018-1584-0>
- Rocha LA, Aleixo A, Allen G, et al. (2014) Specimen collection: An essential tool. *Science* 344: 814–815. <https://doi.org/10.1126/science.344.6186.814>
- Shao KT, Ho HC, Lin PL, Lee PF, Lee MY, Tsai CY, Liao YC, Lin YC, Chen JP, Yeh HM (2008) A checklist of the fishes of southern Taiwan, northern South China Sea. *The Raffles Bulletin of Zoology* 19: 233–271.
- Short G, Smith R, Motomura H, Harasti D, Hamilton H (2018) *Hippocampus japapigu*, a new species of pygmy seahorse from Japan, with a redescription of *H. pontohi* (Teleostei, Syngnathidae). *ZooKeys* 779: 27. <https://doi.org/10.3897/zookeys.779.24799>
- Skejo JO, Caballero JH (2016) A hidden pygmy devil from the Philippines: *Arulenus miae* sp. nov. – a new species serendipitously discovered in an amateur Facebook post (Tetrigidae: Discotettiginae). *Zootaxa* 4067: 383. <https://doi.org/10.11646/zootaxa.4067.3.7>

A new species of the live-bearing fish genus *Poeciliopsis* from northern Mexico (Cyprinodontiformes, Poeciliidae)

Kevin W. Conway^{1,2}, Mariana Mateos¹, Robert C. Vrijenhoek³

1 Department of Wildlife and Fisheries Sciences, Texas A&M University, College Station, TX 77843, USA

2 Biodiversity Research and Teaching Collections, Texas A&M University, College Station, TX 77843, USA

3 Monterey Bay Aquarium Research Institute, 7700 Sandholdt Road, Moss Landing, CA 95039, USA

Corresponding author: Kevin W. Conway (kevin.conway@tamu.edu)

Academic editor: Kyle Piller | Received 30 June 2019 | Accepted 19 September 2019 | Published 28 October 2019

<http://zoobank.org/3008A803-7945-4D91-9D79-C90D357D32F3>

Citation: Conway KW, Mateos M, Vrijenhoek RC (2019) A new species of the live-bearing fish genus *Poeciliopsis* from northern Mexico (Cyprinodontiformes, Poeciliidae). ZooKeys 883: 91–118. <https://doi.org/10.3897/zookeys.883.37586>

Abstract

Poeciliopsis jackschultzi **sp. nov.**, is described based on seven specimens (17.9–26.7 mm SL) from the Río Concepción (also known as Río Magdalena), Sonora, Mexico. The new species belongs to the *Leptorhaphis* species group and can be distinguished from other members of this group by features of the skeleton and colouration. The new species is sympatric with *P. occidentalis*, a hybridogenetic all-female biotype *P. monacha-occidentalis*, and hybrids between *P. monacha-occidentalis* females and *P. jackschultzi* males. The distribution of *P. jackschultzi* is highly restricted, and the main habitat, spring-fed marshy streams and pools, is susceptible to loss and degradation in a desert environment with increasing human water demand.

Keywords

Taxonomy, Poeciliinae, Sonoran Desert, unisexual reproduction, gill rakers

Introduction

The live-bearing fish genus *Poeciliopsis* (subfamily Poeciliinae, tribe Girardinini Lucinda & Reis, 2005) is distributed from southern Arizona (USA) southwards through western Central America to Colombia (Rosen and Bailey 1963: map 17). *Poeciliopsis*

is among the few vertebrate taxa known to include all-female hybrid forms that reproduce asexually via gynogenesis or hybridogenesis, and has served as a model system for studying the evolution of unisexual reproduction (Schultz 1969; Vrijenhoek et al. 1989; Avise 2015). The genus was last revised by Rosen and Bailey (1963) who provided a rediagnosis based largely on osteological characters and divided the known species between two subgenera, *Poeciliopsis* and *Aulophallus*. The genus currently contains 24 valid species, 21 of which are classified in subgenus *Poeciliopsis* and three in subgenus *Aulophallus* (Mateos et al. 2002, 2019).

Prior to Rosen and Bailey (1963), Miller (1960) classified six species of *Poeciliopsis* into what he referred to as the *Leptorhaphis* species group (based on the generic name *Leptorhaphis* Regan, 1913; type species *Gambusia infans* Woolman, 1894), characterised by the presence of a jet black male colouration during courtship, the presence of a small, retrorse hook at the tip of the gonopodium, and the arrangement of the oral jaw teeth into an outer and inner row on the dentary and premaxilla. Miller (1960) originally classified *P. infans*, *P. porosus* (= *P. infans*), *P. lucida*, *P. occidentalis* s. s. and *P. sonoriensis* within this species group. *Poeciliopsis prolifica* was added subsequently to this species group by Mateos et al. (2002) based on the results of a molecular phylogenetic investigation of mitochondrial DNA sequences. A more recent molecular phylogenetic investigation of *Poeciliopsis* (Mateos et al. 2019) based on mitochondrial and nuclear DNA sequences recovered a monophyletic *Leptorhaphis* species group comprising four named species (*P. infans*, *P. lucida*, *P. occidentalis* s. l., and *P. prolifica*) and one undescribed species from the Río Concepción (Sonora, Mexico) (see below). Relationships among the members of the *Leptorhaphis* species group were largely unresolved in this multi-locus topology, but the grouping was firmly nested within the “predominantly Northern” clade of the subgenus *Poeciliopsis*, which also included *P. balsas*, *P. monacha* and *P. viriosa*.

In the early 1980s, one of us (RCV) collected individuals of *Poeciliopsis* at marshy localities in the Río Concepción drainage about 24 km south of Nogales (Sonora State). In addition to locally abundant *P. occidentalis* s. s. and the sperm-dependent, all-female, hybridogenetic biotype *P. monacha-occidentalis*, the samples included some unusual individuals that differed in colouration from other described members of the *Leptorhaphis* species group. Male and female specimens of this unrecognised taxon were reared in the laboratory and found to reproduce sexually. Subsequent multi-locus allozyme studies revealed that the unknown sexual species had several unique alleles, including a diagnostic “fast” allele at the *Pgd* locus. Except for some novel alleles, the new species was first interpreted to be a mosaic composed of genes derived from *P. occidentalis* and the hemiclinal *monacha* genome from hybridogenetic *P. monacha-occidentalis* (see Schenk 1992; Vrijenhoek 1993), but this initial inference was later shown to be incorrect. The new species is unique based on a recent analysis of nuclear and mitochondrial DNA sequences that place it near the root of the *Leptorhaphis* species group (Mateos et al. 2019). Retention of shared ancestral allozyme polymorphisms in this species likely explains the genomic mosaicism. Nonetheless, introgression from *P. monacha-occidentalis* hemiclones or *P. occidentalis* into the new species gene pool has

not been ruled out and awaits evaluation at a broader genomic level. The purpose of this study is to provide a formal description for this undescribed species of *Poeciliopsis* from the Río Concepción.

Materials and methods

Specimens of the new species were collected between 1999 and 2001. They were identified on the basis of one or both of the following traits: (a) homozygosity for the diagnostic “fast” *Pgd* allele (see Schenk 1992), following the methods described in Mateos and Vrijenhoek (2004); and (b) a mitochondrial gene sequence (e.g., Cytochrome b) that is distinct from all other *Poeciliopsis* (Mateos et al. 2019). The PGD protein (6-phosphogluconate dehydrogenase or 6Pgdh) is expressed in numerous tissues including fins, which enables “non-destructive” and rapid (~ 3 h) genotyping of specimens from a caudal fin clip that can regrow, or from a small clip of a pectoral fin from frozen specimens. Other specimens were obtained from museum collections with the following abbreviations:

CNP-IBUNAM	Colección Nacional de Peces, Instituto de Biología, Universidad Nacional Autónoma de México, Mexico City;
TCWC	Biodiversity Research and Teaching Collection, Texas A&M University, College Station;
UMMZ	University of Michigan Museum of Zoology, Ann Arbor.

Counts and measurements generally follow Bussing (2008). Measurements were taken point to point to the nearest 0.1 mm using digital callipers. The number in parentheses following a meristic value denotes the frequency of that value. An asterisk denotes the value obtained from the holotype (if available). Select specimens were cleared and double stained for bone and cartilage following the protocol of Taylor and Van Dyke (1985) or cleared and single stained for bone only by omitting the cartilage staining step in the protocol of Taylor and Van Dyke (1985). Values reported for teeth, gill rakers, fin rays and vertebrae were obtained from cleared and stained specimens only. Alcohol-preserved specimens, cleared and stained specimens, or parts thereof were observed and photographed using a Zeiss SteReo Discovery V20 Microscope equipped with a Zeiss AxioCam MRc5 digital camera. Computed tomography (CT) scans of select specimens were also obtained at the Karel F. Liem BioImaging Center (Friday Harbor Laboratories, University of Washington) using a Bruker (Billerica, MA) SkyScan 1173 scanner with a 1 mm aluminium filter at 60 kV and 110 μ A on a 2240 \times 2240 pixel CCD at a resolution of 8.8 μ m. Specimens were scanned simultaneously in a 50ml plastic Falcon tube (Corning, NY), in which they were wrapped with cheesecloth moistened with ethanol (70%) to prevent movement during scanning. The resulting CT data were visualised, segmented, and rendered in Horos (<http://www.horosproject.org>) and Amira (FEI).

General osteological terminology follows Rosen and Bailey (1963) and Parenti (1981). Gonopodial terminology follows Lucinda and Reis (2005). Canal neuromast terminology follows Tarby and Webb (2003) and Webb and Shirey (2003). The gill rakers of *Poeciliopsis* are morphologically heterogeneous. We refer to the different types using the following terminology: type 1a, an elongate, blade-like gill raker present only on the anterior edge of the first gill arch (typically in association with hypobranchial and ceratobranchial elements only); type 1b, as for type 1a but smaller, typically $\frac{1}{4}$ to $\frac{1}{2}$ length of type 1a, may be present on posterior edge of gill arches 1–3 and anterior edge of arches 2–4 (typically in association with hypobranchial and ceratobranchial elements only); type 2, dorso-ventrally compressed gill rakers with 4 or 5 comb-like projections dorsally, forming a series of low parallel ridges along posterior edge of gill arch 4 (ceratobranchial only) and anterior edge of gill arch 5 (ceratobranchial 5); and type 3, a trifid gill raker with a central shaft similar in size and shape to the type 1b gill raker combined with a pair of lateral processes that extend from the base of the central shaft and support multiple minute conical teeth, present on the anterior edge of arches 2–4 (ceratobranchial only). Names of subgroups and species of *Poeciliopsis* follow Mateos et al. (2019).

Genetic distances (uncorrected p) reported were obtained using Paup*4.0a (build 165) (Swofford 2002) and derived from sequences available from Mateos et al. (2019).

Taxonomy

Poeciliopsis jackschultzi sp. nov.

<http://zoobank.org/3949FE67-BD75-407B-8A23-2F41DD22F70E>

Figures 1–3, 4a, 5, 6, 7a, 8a, 9

Common name: Río Concepción topminnow (English); guatopote del Concepción (Spanish).

Holotype. CNP-IBUNAM 23406, male, 20.3 mm SL; Mexico, Sonora, La Atascosa, tributary of the Alisos-Bambuto branch of the Río Concepción at highway 15 road crossing close to Rancho Semarnap, small spring at right side bank, 30°58'47.86"N, 110°52'21.07"W, M. Mateos and R. C. Vrijenhoek, 17 January 2001.

Paratypes. TCWC 20082.01, 2 (C&S), 1 male/1 female, 19.0–23.0 mm SL; TCWC 20082.02, 2, 1 male/1 female, 17.9–26.7 mm SL; same data as holotype. – TCWC 20083.01, 1 (C&S), male, 20.2 mm SL; Mexico, Sonora, Rancho Las Playas, tributary of the Alisos-Bambuto branch of the Río Concepción, near town of La Providencia, 30°55'9.34"N, 110°51'38.25"W, M. Mateos, R. C. Vrijenhoek and L.A. Hurtado, 20 April 1999. – TCWC 20084.01, 1, male, 19.0 mm SL (DNA voucher); Mexico, Sonora, Cocospera-Babasac branch of the Río Concepción, at town of Imuris under Highway 15 bridge, 30°46'29.46"N, 110°51'28.80"W, M. Mateos, and R. C. Vrijenhoek, 11 May 2000.

Diagnosis. A member of the *Leptorhaphis* species group (Miller 1960) based on the presence of a small, retrorse hook at the tip of the gonopodium and arrangement of the oral jaw teeth into an outer and inner row on the dentary and premaxilla. The new



Figure 1. *Poeciliopsis jackschultzi*, CNP-IBUNAM 23406, holotype, male, 20.3 mm SL; Mexico, Sonora, Río Concepción.

species can be distinguished from all other members of the *Leptorhaphis* species group and all other members of *Poeciliopsis* (except *P. monacha*) by the presence of type 3 gill rakers on the anterior edge of ceratobranchials 2–4. It is further distinguished from members of the *Leptorhaphis* species group by the following combination of characters: inner row of dentary and premaxilla with 7–10 weakly tricuspid teeth; 6 or 7 pores in preopercular portion of preoperculo-mandibular lateral line canal; a single ossification (posterior sclerotic) in scleral cartilage; a broken horizontal line comprising 15–17 small, dark-brown spots extending along posterior two-thirds of body; and the absence of a black spot at base of the anterior part of the dorsal fin.

Description. Male and female body shapes as in Figures 1 and 2. Morphometric characters in Table 1. Predorsal and preanal profile convex; postdorsal profile slightly concave; postanal profile almost straight, from insertion of posteriormost anal-fin ray to caudal-fin base. Anterior half of body moderately compressed in male, round in female; posterior half of body compressed in both sexes. Body depth greatest at imaginary vertical line through origin of anal fin in male; at imaginary vertical line through vent in female.

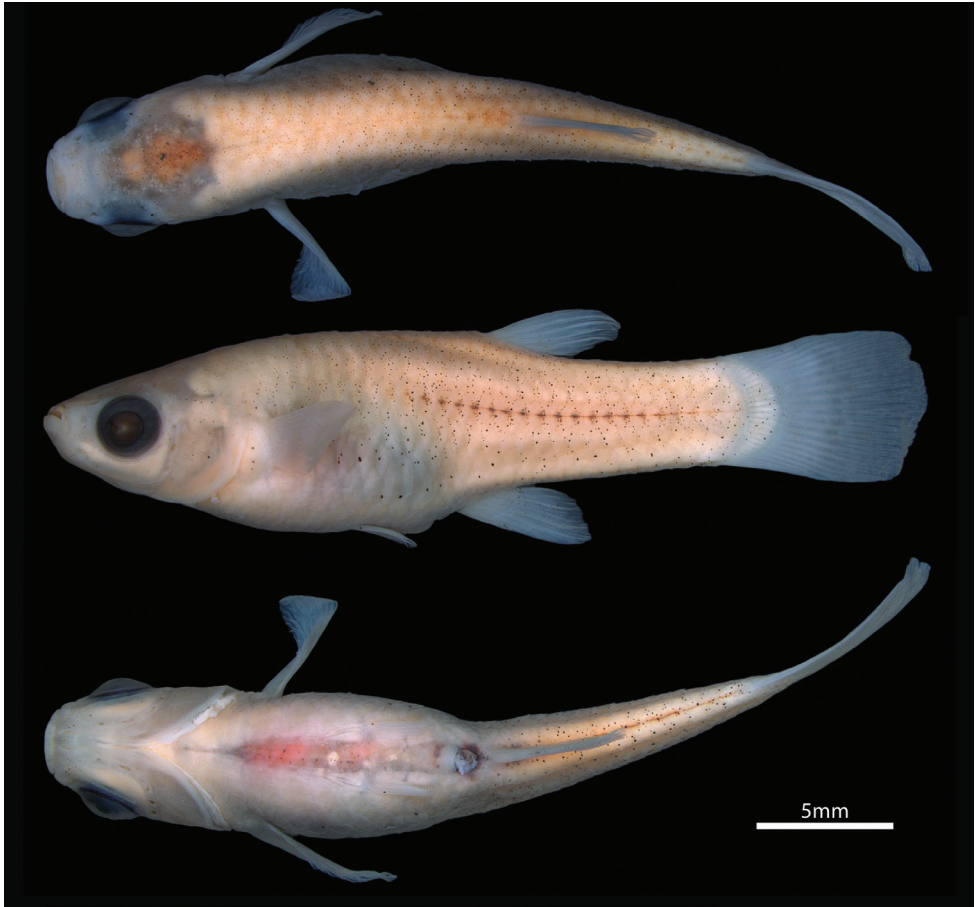


Figure 2. *Poeciliopsis jackschultzi*, TCWC 20082.01, paratype, female, 26.7 mm SL; Mexico, Sonora, Río Concepción.

Head and eye large. Anterior nostril a circular opening located at anterior tip of snout, lateral to upper lip (Fig. 3). Posterior nostril an oval opening, located medial to anterodorsal margin of orbit; a delicate fold of skin located lateral to posterior nostril. Single sclerotic bone (posterior) present in scleral cartilage (Fig. 4a). Mouth superior, almost aligned with upper margin of orbit. Two rows of teeth on premaxilla and dentary (Fig. 5). Teeth in outer row with spatula-shaped cusp, 2 or 3 times larger than teeth of inner row; teeth of inner row with weakly trifold cusp. Premaxilla with 10–12 teeth in outer row; 8–10 in inner row. Dentary with 9 or 10 teeth in outer row; 7–9 teeth in inner row. Upper pharyngeal jaw comprising teeth associated with ventral surface of pharyngobranchial 2, pharyngobranchial 3 and pharyngobranchial 4 toothplate (Fig. 6c, d). Teeth on pharyngobranchial 2 narrow, spatula-like, with small flattened cusp and elongate shaft; arranged randomly along ventral surface of bone. Teeth along anteromedial edge of ventral surface of pharyngobranchial 3 similar in size and shape to teeth on ventral surface of pharyngobranchial 2; arranged in three staggered rows

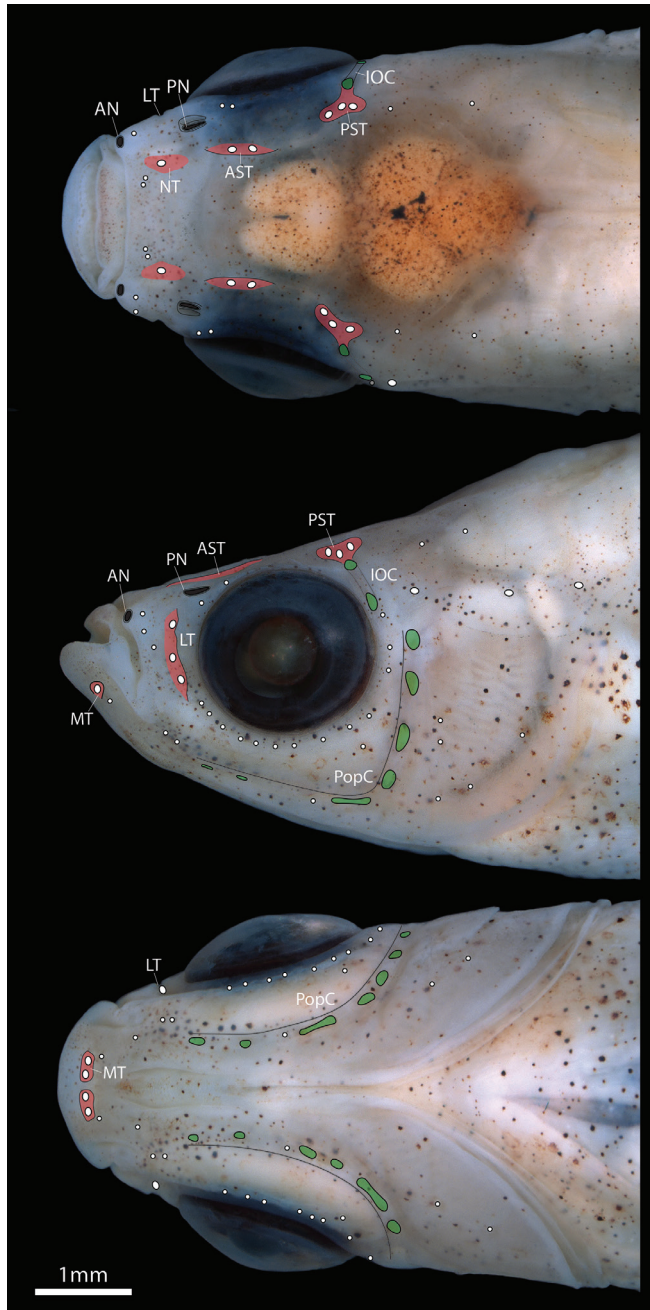


Figure 3. Head of *Poeciliopsis jackschultzi* in dorsal, lateral and ventral view (CNP-IBUNAM 23406, holotype, male, 20.3 mm SL). Sensory troughs containing presumptive canal neuromasts outlined in red. Pores in cephalic lateral line sensory canals in green. Small white circles represent superficial neuromasts. White ovals represent presumptive canal neuromasts. Abbreviations: AN, anterior nostril; AST, anterior supraorbital trough; IOC, infraorbital canal; LT, lachrymal trough; MT, mandibular trough; NT, nasal trough; PN, posterior nostril; PopC, preopercular canal; PST, posterior supraorbital trough.

Table 1. Select morphometric characters obtained from the holotype (male) and paratypes (2 males and 2 females) of *Poeciliopsis jackschultzi*. Ranges for males and females are separated (ranges reported for males include value obtained from holotype).

	Holotype	Males (N = 3)	Females (N = 2)
Standard length (SL)	20.3	17.9–20.3	23.0–26.7
Head length	27.1	24.5–29.0	25.6–29.6
Head width	16.3	16.2–16.8	17.8–18.3
Interorbital distance	10.8	10.0–10.9	9.6–11.9
Postorbital distance	12.8	10.7–12.9	10.9–12.7
Orbit length	7.9	7.9–9.2	7.8–9.5
Snout length	4.9	4.9–5.5	6.0–6.5
Body depth	22.2	21.4–22.7	19.6–21.3
Caudal peduncle depth	14.8	14.8–16.2	15.2–15.3
Predorsal distance	61.6	58.9–62.2	63.5–64.5
Preanal distance	49.3	45.8–50.0	58.4–60.0
Dorsal-fin origin to caudal-fin base	38.4	38.4–39.3	36.5–38.9
Anal-fin origin to caudal-fin base	54.7	47.0–55.6	40.8–42.7
Dorsal-fin length	18.7	17.8–21.8	16.9–19.8
Anal-fin length	36	35.9–38.8	16.9–17.9
Pectoral-fin length	19.7	19.4–19.8	16.9–19.8
Pelvic-fin length	8.4	5.4–8.4	8.2–8.7

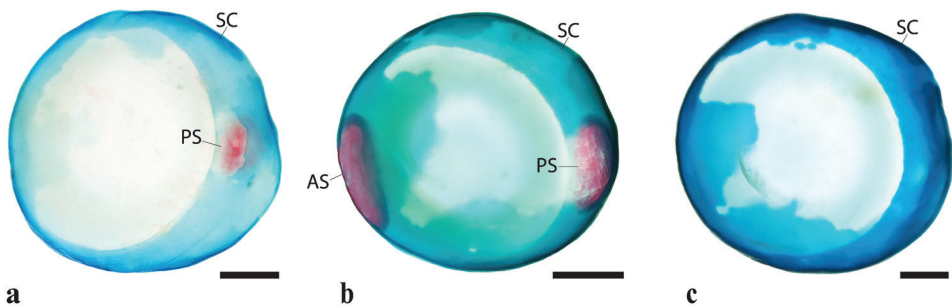


Figure 4. Sclerotic cartilage and sclerotic ossifications in members of *Poeciliopsis* (right side, image reversed) **a** *P. jackschultzi*, TCWC 20082.01, paratype, female, 23.0 mm SL **b** *P. lucida*, UMMZ 189041, female, 24.0 mm **c** *P. occidentalis*, UMMZ 202393, female, 35.0 mm SL. Abbreviations: AS, anterior sclerotic; PS, posterior sclerotic; SC, scleral cartilage; Scale bar: 0.4 mm.

(orientated along rostral-caudal body axis); each row comprising 8–9 or cohorts of 5–7 teeth arranged in a single row (orientated along medial-lateral body axis); each cohort located anterior to a deep crypt associated with development of replacement teeth. Teeth over remainder of ventral surface of pharyngobranchial 3 and pharyngobranchial 4 toothplate conical, with slightly recurved tip. Configuration of conical teeth similar to spatula-like teeth; arranged in multiple staggered rows each comprising multiple cohorts; each cohort comprising 4 or 5 teeth arranged in a single row (orientated along medial-lateral body axis) and located anterior to a deep replacement tooth crypt; size of tooth within each cohort increases gradually in a medial to lateral direction; largest conical teeth of upper pharyngeal jaw located along lateral edge of pharyngobranchial 3

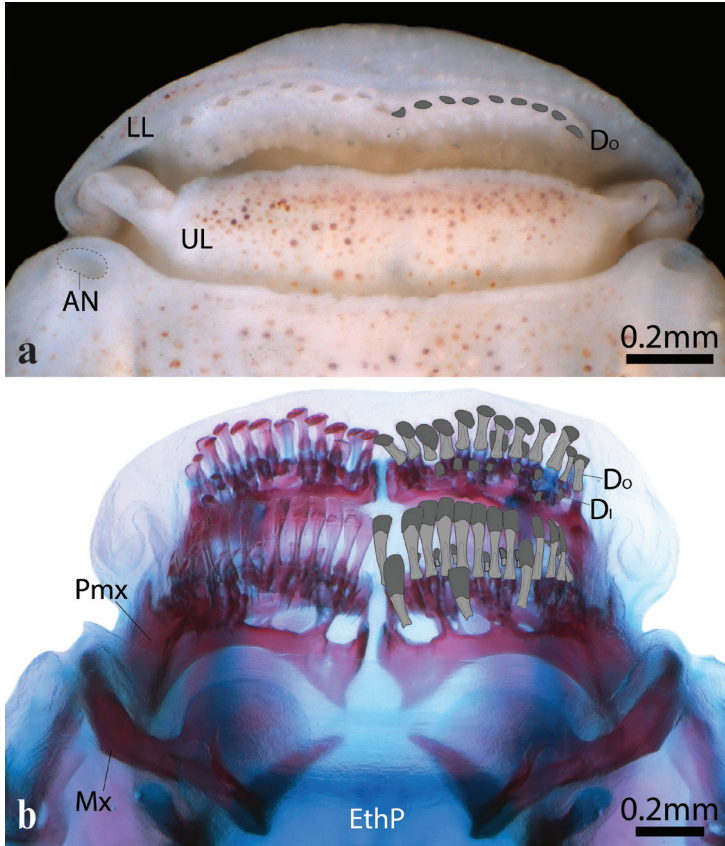


Figure 5. Mouth of *Poeciliopsis jackschultzi* in dorsal view (anterior to top of page) **a** CNP-IBUNAM 23406, holotype, male, 20.3 mm SL **b** TCWC 20082.01, paratype, female, 23.0 mm SL. Cusps of dentary teeth highlighted in dark grey on right side in a and b. Shaft of dentary teeth highlighted in light grey on right side in b. Abbreviations: AN, anterior nostril; D, dentary; DO, dentary teeth of outer row; DI, dentary teeth of inner row; EthP, ethmoid plate; Mx, maxilla; Pmx, premaxilla; LL, lower lip; UL, upper lip.

and pharyngobranchial 4 toothplate. Lower pharyngeal jaw comprising teeth associated with dorsal surface of ceratobranchial 5 (Fig. 6b). Medial edge of ceratobranchial 5 with 4 or 5 widely spaced conical teeth, arranged in a single row (orientated along the rostral-caudal body axis). Remainder of teeth spatula-like, similar in shape to teeth located on ventral surface of pharyngobranchial 2; size of teeth increases gradually from anterior to posterior, with largest teeth located along posterior edge of bone. Arrangement of spatula-like teeth becoming more regular towards posterior, culminating in two dense bands of teeth each comprising 2 or 3 rows of ca. 13–15 teeth; a deep crypt associated with development of replacement teeth located anterior to each band of teeth.

Gill rakers present on anterior and posterior margins of gill arches 1–4 and anterior margin of ceratobranchial 5 (Fig. 6b); number of gill rakers associated with each arch listed in Table 2. Anterior edge of gill arch 1 with 11 or 12 type 1a gill rakers as-

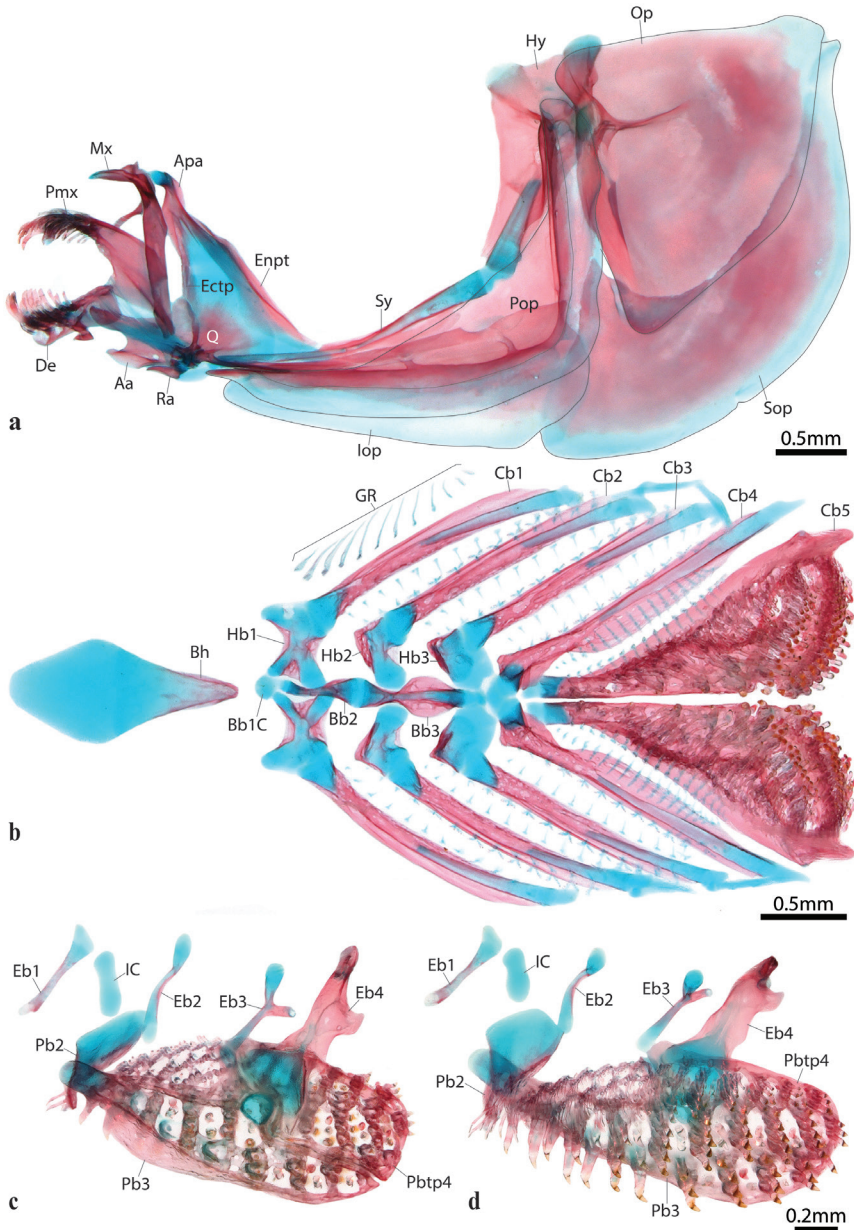


Figure 6. Viscerocranium of *Poeciliopsis jackschultzi* (TCWC 20082.01, paratype, female, 23.0 mm SL) **a** hypopalatine arch right side in lateral view (image reversed) **b** ventral gill arches in dorsal view **c** dorsal gill arches (right side) in dorsal view **d** dorsal gill arches (right side) in ventral view (image reversed). Opercular bones outlined in black in a. Scale bar shared between c and d. Abbreviations: Aa, anguloarticular; Apa, autopalatine; Bb1C, basibranchial 1 cartilage; Bb2-3, basibranchials 2–3; Bh, basihyal; Cb1-5, ceratobranchials 1–5; De, dentary; Eb1-4, epibranchial 1–4; Ectp, ectopterygoid; Enpt, endopterygoid; Hb1-3, hypobranchials 1–3; Hy, hyomandibular; IC, interarcular cartilage; Iop, interopercle; GR, gill raker; Mx, maxilla; Op, opercle; Pb2-3, pharyngobranchial 2–3; Pbtp4, pharyngobranchial toothplate 4; Pmx, premaxilla; Pop, preopercle; Q, quadrate; Ra, retroarticular; Sop, subopercle; Sy, symplectic.

sociated with hypobranchial and ceratobranchial; posterior edge of gill arch 1–3 with 12–13 type 1b gill rakers associated with ceratobranchial. Anterior edge of gill arch 2–3 with 12–14 gill rakers, including 2 or 3 type 1b gill rakers associated with hypobranchial and lower part of ceratobranchial and 10 or 11 type 3 gill rakers associated with ceratobranchial (Fig. 7a). Anterior edge of gill arch 4 with 12–14 gill rakers along ceratobranchial, including 2 or 3 type 1b gill rakers and 10 type 3 gill rakers. Posterior edge of ceratobranchial 4 and anterior edge of ceratobranchial 5 with 16 or 17 type 2 gill rakers (Fig. 7a). Posterior edge of ceratobranchial 4 expanded as a flat membranous shelf to which base of gill rakers articulate (Fig. 7a).

Cephalic lateral line canal system with following components (Fig. 3): single large canal neuromast (stage IIa canal neuromast of Tarby and Webb 2003) located in shallow nasal trough (equivalent to nasal portion of supraorbital lateral line canal); two large canal neuromasts (stage IIa) located in shallow anterior supraorbital trough (anterior portion of supraorbital lateral line canal) dorsomedial to anterodorsal margin of orbit; three large canal neuromasts (stage IIa) located in shallow boomerang-shaped posterior supraorbital trough (posterior portion of supraorbital lateral line canal) dorsomedial to posterodorsal margin of orbit; three large canal neuromasts (stage IIb) located in dorso-ventrally elongate lachrymal trough anterior to orbit (lachrymal portion of infraorbital lateral line canal), edges of trough supported by flanges of bone extending from surface of lachrymal; two pores on dorsolateral surface of head posterior to orbit associated with dermosphenotic portion of infraorbital canal; two large canal neuromasts (stage IIa) located in shallow mandibular trough (mandibular portion of preoperculo-mandibular lateral line canal on dentary) located on lower jaw posterolateral to jaw symphysis; 6 or 7 pores of variable size associated with preopercular portion of preoperculo-mandibular lateral line canal. Lateral line canal on dermosphenotic and preopercle (Fig. 6a) an open trough of bone roofed by skin only (canal neuromasts inside of each canal stage III of Tarby and Webb 2003). Multiple superficial neuromasts placed over surface of head, most obvious on surface of skin bordering ventral margin of orbit (Fig. 3).

Dorsal-fin rays 8 (ii,4,ii or i,5,ii); anal-fin rays 10 (iii,6,i); pectoral-fin rays 14 (ii,9,iii); pelvic-fin rays 6 (i,3,ii or i,4,i). Total number of caudal-fin rays 29, comprising 15 (2) or 17 (1) principal rays, 13 (2) or 15 (1) branched rays. Dorsal procurrent

Table 2. Counts of gill rakers in members of the *Leptorbaphis* species group and *P. monacha*. Gill raker type in parentheses (see materials and methods for details).

Species	N	Gill arch 1		Gill arch 2		Gill arch 3		Gill arch 4		Gill arch 5
		Anterior	Posterior	Anterior	Posterior	Anterior	Posterior	Anterior	Posterior	Anterior
<i>P. jackschultzi</i>	3	11–12 (1a)	12–13 (1b)	2–3 (1b)/10–11 (3)	13–14 (1b)	2–3 (1b)/10–11 (3)	14 (1b)	2–3 (1b)/10 (3)	17 (2)	16 (2)
<i>P. infans</i>	4	14–15 (1a)	18–20 (1b)	16–17 (1b)	18–19 (1b)	18–19 (1b)	18–20 (1b)	20–22 (1b)	18–19 (2)	18–19 (2)
<i>P. lucida</i>	4	14–15 (1a)	20–21 (1b)	20–21 (1b)	20–21(1b)	20–21 (1b)	19–21 (1b)	18–19 (1b)	20–21 (2)	19–21 (2)
<i>P. occidentalis</i>	4	11–12 (1a)	18–19 (1b)	19–20 (1b)	19–21 (1b)	18–20 (1b)	17–19 (1b)	18–19 (1b)	24–25 (2)	23–24 (2)
<i>P. prolifica</i>	4	10–11 (1a)	14–15 (1b)	14–16(1b)	14–16 (1b)	14–16 (1b)	14–16 (1b)	15–16 (1b)	18–20 (2)	15–16 (2)
<i>P. monacha</i>	4	12–13 (1a)	14–16 (1b)	13–14 (3)	15–16 (1b)	16–18 (3)	15 (1b)	15 (3)	17–18 (2)	16–17 (2)

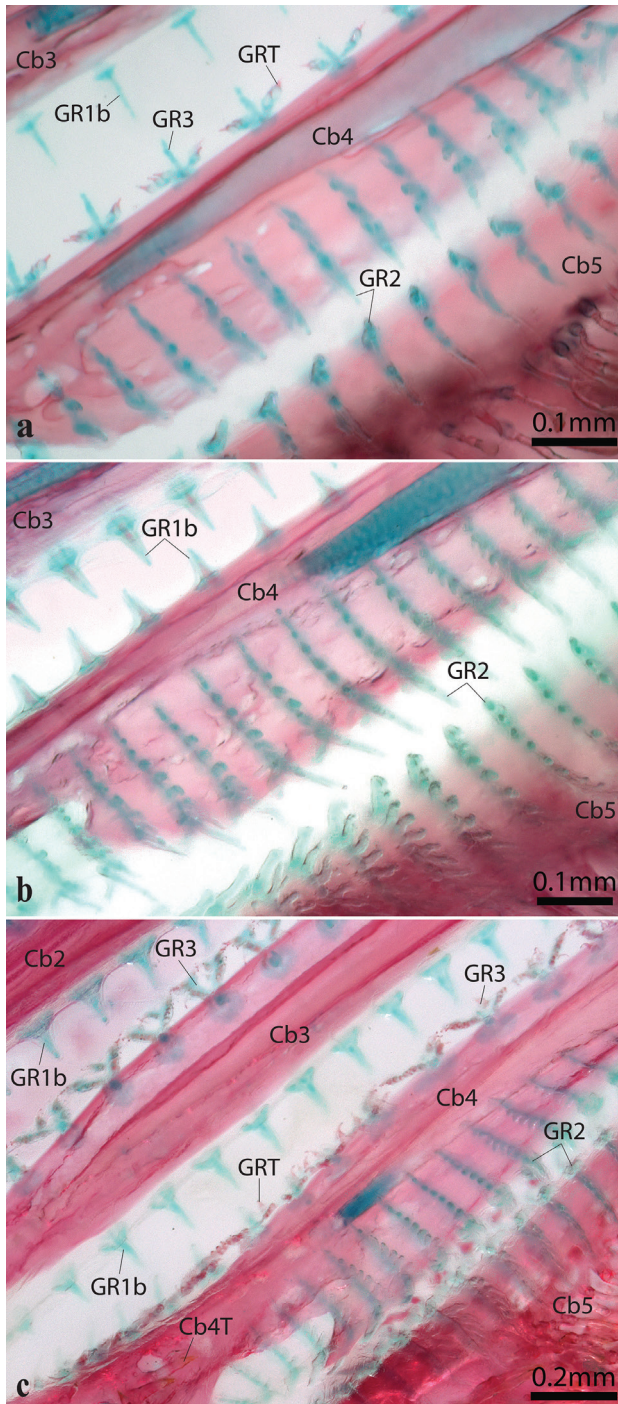


Figure 7. Gill rakers on ceratobranchials 2/3–5 in *Poeciliopsis* **a** *P. jackschultzi*, TCWC 20082.01, paratype, female, 23.0 mm SL **b** *P. lucida*, UMMZ 189041, female, 24.0 mm SL **c** *P. monacha*, UMMZ 178246, female, 22.0 mm SL. Gill filaments removed. Abbreviations: C2–5, ceratobranchials 2–5; Cb4T, teeth on ceratobranchial 4; GR1b, 2, 3, type 1b, 2, or 3 gill rakers; GRT, gill-raker tooth.

rays 6, ventral procurrent rays 6 (1) or 7 (2). Total number of vertebrae 31, comprising 13 abdominal+18 caudal vertebrae. Ribs 11 or 12; epicentrals 9. First dorsal-fin pterygiophore inserting into interneural space between vertebrae 13/14 in both sexes. First anal-fin pterygiophore inserting into interhemal space between vertebrae 13/14 in female (not obtainable in males). 28 (3*) or 29 (1) scales in lateral series plus 1(1) or 2 (3*) scales on base of caudal fin; 16 (2) or 17 (1) predorsal scales (count not obtained from holotype); 16 scales around caudal peduncle.

Gonopodial complex composed of three functional gonapophyses (modified hemal spines) and seven gonactinosts (modified proximal-middle pterygiophores). Second gonactinost a compound element; product of ontogenetic fusion of three proximal-middle pterygiophores. Ligostyle present. Gonopodium asymmetrical, sinistral (Fig. 8a). R3, unbranched with ~ 48 segments. Segments becoming progressively narrower distally; segment 1 largest element; distalmost segments tiny elements, approximately $\frac{1}{4}$ width of more proximal elements. Posterior margin of R3 with pronounced groove proximally (corresponding to segments 6–18), accommodating R4. R4, branched, branching point obscured by R3, segments of each branch difficult to count with precision. R4a without further division; extending to tip of gonopodium. R4p divided again at ca. midpoint along length; segments close to distal tip of sub-branches of R4p bearing a serra, forming a serration of ca. 14 paired serrae along dorsal edge of gonopodium (Fig. 8). R5 branched; branching point ca. 11 segments distal to ray base; sub-branches R5a and R5p remain in close contact towards distal tip, displaced to left side of gonopodium, terminating between R3 and sub-branches of R4p proximal to distal tip of gonopodium. Small retrorse hook present at distal tip of gonopodium; confluent with distalmost segment of R3 and R4A.

Colouration. In alcohol (Figs 1, 2), body background colour pale cream. A broken line comprising 15–17 small, dark-brown spots comprising diffuse clusters of melanophores extending along posterior two-thirds of body; spots located within pocket of scales 11–26 in lateral series. Horizontal septum along posterior two-thirds of body with dark brown pigment forming thin dark brown line deep to broken line. Vertical septum posterior to anal fin with dark brown pigment forming thin dark brown line along ventral midline. Side of body and base of caudal fin with irregular scatter of small dark brown melanophores. Posterior edge of scales, excluding those on predorsal surface, rimmed by small dark brown melanophores forming weak reticulate pattern over body surface. Fins hyaline. Dorsal, lateral, and ventral surface of head with irregular scatter of small dark brown melanophores. Upper lip with dense aggregation of small light brown melanophores forming faint brown line.

In life (Fig. 9), body translucent. Anterodorsal surface of body golden brown; remainder of body faint olive-yellow. Broken line along centre of body comprised of black spots, interspaced by small iridescent white-blue spots. Caudal-fin base with a faint golden-brown oval-shaped marking at centre. Majority of scales with light to dark brown pigment along posterior margin, forming obvious reticulate pattern. Fins of female (Fig. 9b) and paired fins of male hyaline. Dorsal and caudal fin of male with faint orange tint; fin membranes between central caudal-fin rays with faint dark brown or black markings.

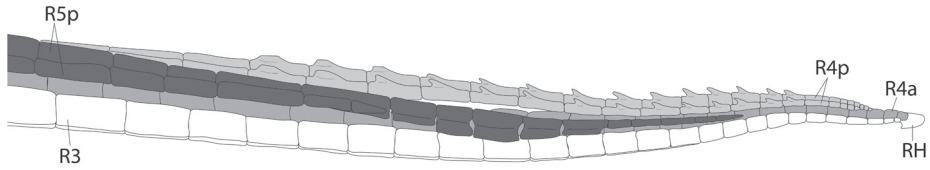


Figure 8. Schematic diagram of the distal tip of the gonopodium in *Poeciliopsis jackschultzi* (TCWC 20082.01, paratype, male, 19.0 mm SL). Abbreviations: R3, ray 3; R4a, ray 4 anterior branch (intermediate grey); R4p, ray 4 posterior branch (light grey); R5p, ray 5 posterior branch (dark grey).



Figure 9. *Poeciliopsis jackschultzi*, Mexico, Sonora, Río Concepción **a** male **b** female. Paratype specimens. Not measured, not identified in field.

Base of gonopodium bright orange (Fig. 9a). Dorsal surface of head golden brown. Upper part of opercle with small silver-white marking. Upper lip dark brown. Iris golden-white.

Distribution and habitat. Known currently from four sites in the Río Concepción, Sonora State, Mexico (Fig. 10). The type locality (Fig. 11a) is a small intermittent stream that passes under Hwy 15 and the railroad tracks; soon after, it merges into the Alisos-Bambuto branch of the Río Concepción. At the time of collection (January 2001), this site had a narrow ca. 1m wide stream with clear running water, as well as small and shallow pools. Parts of the stream were bordered by trees. The bottom was muddy. Approximately 250m north of the type locality, immediately west of Hwy 15, there is a warm spring (site B in Fig. 10), where *P. jackschultzi* was previously sampled (RCV, pers. obs.). Our 2001 collection, however, yielded only 18 female individuals of *Poeciliopsis*. Nine of these were genotyped for the *Cytb* gene; all shared the same *P. monacha*-derived haplotype (Table 4), and thus were not *P. jackschultzi* (i.e., pend-

ing analyses of nuclear markers, they are either *P. monacha-occidentalis* or *P. monacha-jackschultzi* hybrids; see Hybridisation section). Further south, near Rancho Las Playas (site F in Fig. 10), paratype TCWC 20083.01 was collected in an exposed pool of the Alisos-Bambuto branch mainstream. At the time of collection (April 1999), this site had clear running water and maximum depth ~ 60 cm. The nearby spring-fed area that had held water in a previous visit was dry (RCV, pers. obs.). *Poeciliopsis jackschultzi* has also been found in the Babasac-Cocospera branch of the Río Concepción (also intermittent, but larger than the Alisos-Bambuto branch), under the Hwy 15 bridge at the town of Imuris (site H in Figure 10; Fig. 11c). This is the locality of the voucher (MVH99-2a#5) used for molecular phylogenetic analysis by Mateos et al. (2019) and an additional paratype (TCWC 20084.01). This site has a muddy bottom and little aquatic vegetation, except for some floating vegetation. Based on all collections, *P. jackschultzi* seems to prefer marshy or pool sites, with still water or relatively slow current. Adjacent mainstream habitats with deeper water and faster currents favour the native cyprinids *Agosia* and *Gila*.

Sex ratios in wild caught specimens are typically not significantly different from 1:1 (Table 5).

Etymology. Named in honour of R. Jack Schultz, a pioneer of studies on hybridisation and all-female reproduction in *Poeciliopsis*. A noun in the genitive.

Genetic distances. Uncorrected P-distances between *P. jackschultzi* and other members of the *Leptorhaphis* species group (Table 3) range from 5.2–7.7% for a 2147 bp fragment of the mitochondrial genome (concatenated *Cytb* and *ND2*) and 0.5–0.9% for a 6173 bp fragment of the nuclear genome (concatenated *ENC*, *Glyt*, *SH3PX3*, *Myh6*, *Rag1*, *Rb*, *Xsrc*). Uncorrected P-distances for the same fragments of mitochondrial and nuclear DNA were much greater between *P. jackschultzi* and *P. monacha* (16.0% for mitochondrial DNA and 1.3% for nuclear DNA; Table 3).

Comparisons. *Poeciliopsis jackschultzi* differs from all other members of the *Leptorhaphis* species group (viz. *P. infans*, *P. lucida*, *P. occidentalis* s. l., and *P. prolifica*) and all other members of *Poeciliopsis* (excluding *P. monacha*) by having type 3 gill rakers along the anterior edge of ceratobranchials 2–4 (vs. type 1b gill rakers along the anterior edge of ceratobranchials 2–4; Fig. 7b). The number of sclerotic bones in the scleral cartilage also differs between the members of the *Leptorhaphis* species group (see Fig. 4) and *P. jackschultzi* can be distinguished from *P. infans*, *P. lucida*, and *P. prolifica*

Table 3. Uncorrected P-distances (%) among five members of the *Leptorhaphis* species group and *P. monacha* (outgroup). Nuclear genes (*ENC*, *Glyt*, *SH3PX3*, *Myh6*, *Rag1*, *Rb*, *Xsrc*) above diagonal, mitochondrial genes (*Cytb* and *ND2*) below diagonal.

	<i>P. jackschultzi</i>	<i>P. infans</i>	<i>P. lucida</i>	<i>P. occidentalis</i>	<i>P. prolifica</i>	<i>P. monacha</i>
<i>P. jackschultzi</i>	–	0.95	0.67	0.56	0.92	1.35
<i>P. infans</i>	7.73	–	0.93	0.95	0.96	1.60
<i>P. lucida</i>	5.44	8.70	–	0.54	0.69	1.51
<i>P. occidentalis</i>	5.21	8.38	4.02	–	0.78	1.39
<i>P. prolifica</i>	6.95	9.38	5.40	5.35	–	1.68
<i>P. monacha</i>	16.05	17.12	16.23	16.23	17.28	–

Table 4. Abundance of *P. jackschultzi* relative to other *Poeciliopsis* based on non-random sampling (mostly targeted at *P. jackschultzi*). Site letters correspond to labels shown in Figure 10. Type locality and collection (D) bold, underlined. Collections from which paratypes were obtained in bold. Most specimens were identified on the basis of at least the *Pgd* diagnostic allozyme (1981–1989; results from Schenk 1992). An asterisk indicates uncertainty regarding the precise location (i.e., up to ~ 3 km from the depicted coordinates). Similarly, a range of letters (e.g. B–D) implies uncertainty regarding the precise location. Geographic coordinates for the 1999–2001 collections were obtained at time of collection and verified in GoogleEarth. All other geographic coordinates were inferred from field notes, including kilometre marks along Mexico Highway 15.

Site	Latitude	Longitude	Collection ID	Locality Name (Year)	Total individuals genotyped	<i>P. jackschultzi</i> (relative abundance)	<i>P. monacha-jackschultzi</i> (relative abundance)	Other <i>Poeciliopsis</i>
B-D	–	–	VD81-1	La Atascosa Ciénega (1981)	130	21 (16.15%)	32 (24.62%)	77
F-G	30.881	-110.851	VM84-9	La Providencia Ciénega (1984)	128	5 (3.91%)	19 (14.84%)	104
G*	30.881	-110.851	VD86-6	La Providencia Ciénega (1986)	111	9 (8.11%)	14 (12.61%)	88
E*	30.956	-110.858	VD86-7	La Atascosa Ciénega (1986)	92	53 (57.61%)	23 (25.00%)	16
A	31.079	-110.909	VD86-8	La Cieneguita (1986)	134	14 (10.45%)	4 (2.99%)	116
H	30.775	-110.858	VD86-1	Imuris (1986)	145	24 (16.55%)	0 (0.00%)	121
F-G*	30.861	-110.850	VQH89-1	La Providencia mainstream (1989)	83	0 (0.00%)	55 (66.27%)	28
F-G*	–	–	VS94-1	La Providencia Ciénega (1994)	30	3 (10.00%)	2 (6.67%)	25
F	30.919	-110.861	MV00-1	Rancho Las Playas (2000)	48	0 (0.00%)	8 (16.67%)	40
H	30.775	-110.858	MV00-11	Imuris (2000)	150	1 (0.67%)	65 (43.33%) ^d	84
D	30.981	-110.872	MV01-2	La Atascosa, Rancho Semarnap (2001)	95	5 (5.26%)	12 (12.63%) ^d	78
F	30.919	-110.861	MVH99-1b	Rancho Las Playas (1999) ^{a,b}	–	1 (n/a)	–	–
B	30.982	-110.872	MV01-1	La Atascosa (2001) ^{a,b}	8	0 (n/a)	–	–
H	30.775	-110.858	MVH99-2a	Imuris (1999) ^a	–	1 ^c (n/a)	–	–

a fewer than 10 individuals genotyped; inadequate for meaningful frequency estimation

b based on mitochondrial gene sequence only

c individuals with a heterozygous (fast/slow) genotype at *Pgd*

d *Cytb* gene sequenced for three females from MV00-11 and three females from MV01-2. One female (from MV00-11) had identical sequence to *P. monacha-occidentalis* haplotype “d” (GenBank AF047343.1); the other five females had identical sequence to *P. monacha-occidentalis* haplotype “a” (GenBank AF047340.1).

e Specimen used in the molecular phylogeny of Mateos et al. (2019)

Table 5. Chi-squared test of equal sex-ratios in *Poeciliopsis jackschultzi* from the Río Concepción system (data from Schenk 1992). Sample IDs correspond to “Locality name (year)” in Table 4.

Sample	females	males	χ^2
Río Imuris (1986)	18	17	0.02
La Providencia Ciénega (1986)	6	4	2.0
La Providencia mainstream (1989)	0	0	na
La Atascosa (1986)	39	10	17.5*
La Cieneguita (1986)	9	10	0.05

* significant at p = 0.05.

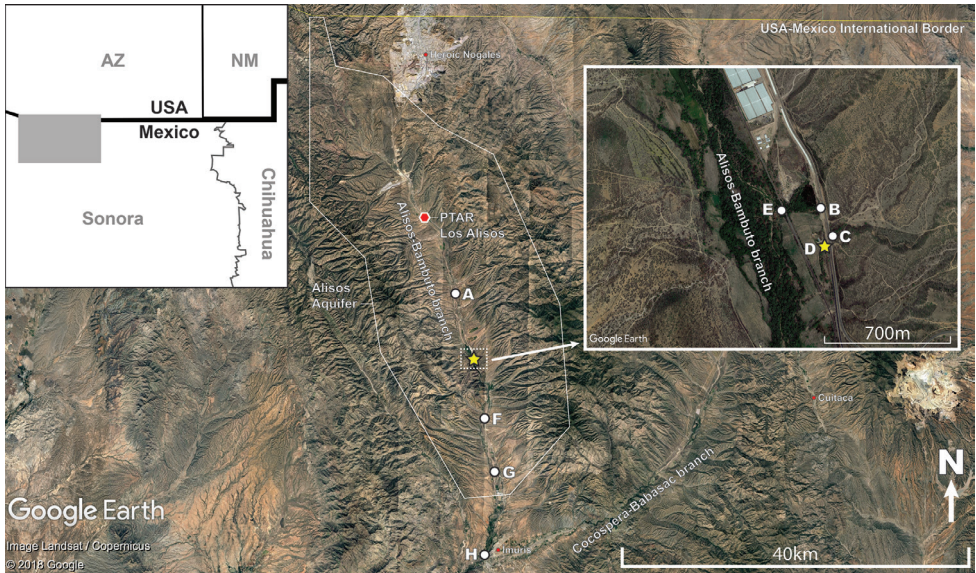


Figure 10. Distribution of sites (A-H) within the Río Concepción from which *Poeciliopsis jackschultzi* has been collected since 1981 (see Table 4). Type locality indicated by yellow star. Grey box in left inset figure indicates area presented in main figure. Right inset shows close up of area highlighted by white box. Extent of the Alisos Aquifer (also known as Rio Alisos Aquifer) is highlighted by a white line. The waste water treatment facility (PTAR Los Alisos) is indicated by a red polygon. The large commercial facility just north of the type locality is currently a Ganfer tomato greenhouse complex.

by the absence (*vs.* presence) of the anterior sclerotic, and from *P. occidentalis* s. l. by the presence (*vs.* absence) of the posterior sclerotic. *Poeciliopsis jackschultzi* can be further distinguished from *P. infans*, *P. occidentalis* s. l., and *P. prolifica* by having weakly trifid teeth in the inner row of the dentary and premaxilla (*vs.* conical teeth); from *P. occidentalis* s. l. by the absence (*vs.* presence) of a black spot at the base of the anterior part of the dorsal fin; and from *P. prolifica* by having 6 or 7 pores in the preopercular portion of the preoperculo-mandibular canal (*vs.* canal an open trough, without pores), posterior two-thirds of body with a broken (*vs.* solid) horizontal line along center, and by the absence (*vs.* presence) of two dark brown or black markings on the ventral surface of the head below the preorbit region.

Although distinct, *P. jackschultzi* shares some characteristics with *P. monacha*, a sexually reproducing species presently distributed > 400 km to the south in the Ríos Mayo, Fuerte and Sinaloa. The new species produces hybrids with hemiclinal *monacha* genomes derived from hybridogenetic *P. monacha-occidentalis* females (see Hybridisation section); therefore, introgression of *monacha* characteristics is possible. Nonetheless, *P. jackschultzi* clearly differs from *P. monacha* by having only 7–10 weakly tricuspid teeth arranged in a single row on the lingual surface of the premaxilla and dentary (*vs.* 50+ weakly tricuspid teeth arranged as a dense patch on lingual surface of premaxilla



Figure 11. Habitat of *Poeciliopsis jackschultzi* **a** La Atascosa, small spring tributary to Alisos-Bambuto branch of the Río Concepción at highway 15 road crossing close to Rancho Semarnap, type locality (site D in Fig. 10, Table 4) **b** pool at Rancho Las Playas, tributary to Alisos-Bambuto branch (site F in Fig. 10, Table 4) **c** Río Concepción at (Cocospera-Babasac branch) at town of Imuris (site H in Fig. 10, Table 4).

and dentary), the absence (*vs.* presence) of ceratobranchial 4 teeth, and the presence (*vs.* absence) of a retrorse hook at the tip of the gonopodium.

Poeciliopsis jackschultzi males do not appear to exhibit the black nuptial colouration exhibited by males of *P. monacha* and certain members of the *Lepitorhaphis* group (*viz.* *P. lucida* and *P. occidentalis* s. l.) (Miller 1960). However, *P. monacha*, *P. lucida* and *P. occidentalis* s. l. males rapidly “turn off” these nuptial displays when subjugated by behaviourally dominant males or if captured in nets (Vrijenhoek and Schultz 1974). The nuptial displays of these species are expressed clearly in aquaria, but we have not observed similar nuptial pigmentation in laboratory-reared *P. jackschultzi* males.

Poeciliopsis jackschultzi co-inhabits the Río Concepción basin with *P. occidentalis* s. l. and the hybrids *P. monacha-jackschultzi* and *P. monacha-occidentalis*. The presence of a black spot at base of the anterior part of the dorsal fin is the most reliable feature distinguishing *P. occidentalis* s. l. from *P. jackschultzi* in the field. We are currently unaware of reliable external morphological character(s) that could serve to distinguish *P. jackschultzi* from females of the two co-occurring hybrid forms of *Poeciliopsis* within the Río Concepción.

Remarks. The type series of *P. jackschultzi* comprises individuals collected from the Río Concepción and subsequently maintained in an aquarium for a short period of time. After death, specimens of the type series were maintained in formalin for several years prior to transfer to alcohol, which resulted in decalcification of the skeleton. Though we managed to successfully clear and double stain a female specimen of *P. jackschultzi* (TCWC 20082.01, 23.0 mm SL) for bone and cartilage investigation, our original attempt to clear and double stain a single male individual (TCWC 20082.01, 19.0 mm SL) was not successful: the bone did not stain with alizarin red S. Our attempts to CT scan the holotype and a single female paratype (TCWC 20082.02, 26.7 mm SL) were also unsuccessful, again likely due to decalcification.

Our description of the skeletal elements of the gonopodium reported herein is based solely on the examination of the poorly stained male paratype (TCWC 20082.01; Fig. 8), viewed with the aid of transmitted light. The retrorse hook is present in this individual and another paratype male (TCWC 20084.01, 19.0 mm SL), but not in another immature paratype male (TCWC 20083.01) that was single stained or the holotype, the tip of the gonopodium in which appears to have been damaged. Miller (1960) considered the retrorse hook to be diagnostic for his *Lepitorhaphis* species group and we can confirm, based on the material that we have examined, that this character is present in males of all five members of the group, including *P. prolifica*, a species in which the gonopodium has been reported to be “unmodified at the tip” (Miller 1960: 6).

The state of the available female specimens of *P. jackschultzi* precluded adequate assessment of their genital area pigmentation patterns. All other members of the *Lepitorhaphis* species group are characterised by a “pre-anal chevron”, and sparse pigmentation in the genital pit. In contrast, *P. monacha* and *P. viriosa* lack the pre-anal chevron and have much more pigmentation in the genital pit (see drawings in Lima et al. 1996; Vrijenhoek and Schultz 1974).

Discussion

Gill rakers

Our examination of cleared and double stained material of *Poeciliopsis* (listed below) has revealed an unexpected diversity in the morphology of the gill rakers. To facilitate discussion, we use numbers to refer to the different types (see materials and methods). The majority of the species of *Poeciliopsis* we have examined exhibit three different types of gill rakers, including type 1a (the largest of the different types, restricted to the anterior edge of the first gill arch; Fig. 6b), type 1b (similar in shape to type 1a but smaller, typically found from the posterior edge of the first gill arch to the anterior edge of the fourth; Fig. 6b, 7), and type 2 (a dorso-ventrally compressed gill raker with 4–5 comb-like projections dorsally; Fig. 6b, 7). In addition to type 1 and type 2 gill rakers, *P. jackschultzi* and *P. monacha* also exhibit type 3 gill rakers along the anterior edge of arches 2–4. Type 3 gill rakers not only exhibit a characteristic trifold shape (Fig. 7a, c), with a central shaft and a pair of lateral process, but also support a variable number of minute conical teeth, which are confined to the base of the central shaft and the lateral processes. In *P. jackschultzi*, the number of teeth associated with each type 3 gill raker is low (ranging from 4–6), whereas in *P. monacha* the number of teeth associated with each type 3 raker is higher (ranging from 10–14). Gill raker teeth were not observed in association with any of the other gill raker types (type 1a, 1b, and 2) present in the material of *Poeciliopsis* that we examined, but are typically found in association with gill rakers throughout the branchial arches of actinopterygian fishes (e.g., see Nelson 1969) and are present in all other members of the Poeciliinae that we examined, including members of *Alfaro*, *Brachyrhaphis*, *Gambusia*, *Heterandria*, *Neoheterandria*, *Phallichthys*, *Poecilia*, and *Priapichthys* (see comparative material). Interestingly, in these latter poeciliine taxa, gill raker teeth were only observed in association with those gill rakers (all type 1b) located along the anterior edge of arches 2–4, mirroring the distribution in *P. jackschultzi* and *P. monacha*. As gill raker teeth are typically found in association with gill rakers located throughout the entire branchial basket in non-poeciliid cyprinodontiforms (and other teleosts), the restricted distribution of gill raker teeth to those gill rakers located along the anterior edge of arches 2–4 in poeciliids is an interesting pattern and, if shown to be present in other members of this group, could represent an additional synapomorphy in support of Poeciliinae, or a more inclusive group. At the level of *Poeciliopsis*, the presence of gill raker teeth on type 3 gill rakers in *P. jackschultzi* and *P. monacha* is most logically interpreted as a symplesiomorphy but further investigation of the gill rakers in *Poeciliopsis*, including observations on other members of the “predominantly Northern” clade of the subgenus *Poeciliopsis* (viz. *P. balsas* and *P. viriosa*) will be needed to better understand the distribution of this character within the genus.

The majority of the other poeciliids that we examined exhibited only type 1a gill rakers (on the anterior edge of the first arch) and 1b (on the posterior edge of the first

gill arch to the anterior edge of the fifth). In addition to type 1a and 1b gill rakers, members of *Neoheterandria*, *Phallichthys* and *Poecilia* also exhibited type 2 gill rakers on the posterior edge of the fourth gill arch (ceratobranchial 4) and the anterior edge of the fifth (ceratobranchial 5), mirroring the condition in *Poeciliopsis*. As in *Poeciliopsis* (Fig. 7), in these aforementioned taxa the posterior edge of ceratobranchial 4 is expanded into a plate-like shelf to accommodate the comb-like type 2 gill rakers. Though comb-like gill rakers are known from other groups of teleosts (e.g., Cypriniformes; Conway 2011: fig. 31), to the best of our knowledge comb-like gill rakers (herein referred to as type 2 gill rakers) have not been reported in recent morphological investigations of poeciliids (e.g., Ghedotti 2000; Lucinda and Reis 2005) or cyprinodontiform fishes more generally (e.g., Parenti 1981; Costa 1998; although see Whitehead [1962] for description [p.119] and illustration [fig. 10] of “tooth-like” gill rakers in *Aplocheilichthys panchax* and description [p.119] of “tree-like and branched” gill rakers in *Aphanius dispar*). Based on our limited observations, the presence of type 2 gill rakers in poeciliids appears to be correlated with a widening of the bones supporting the pharyngeal jaws and also in the arrangement of the teeth into regular rows on these bones (e.g., Costa 1991, Ghedotti 2000, Lucinda and Reis 2005). These latter characters were interpreted as uniquely derived and unreversed synapomorphies of the supertribe Poeciliini by Lucinda and Reis (2005) and type 2 gill rakers may represent further evidence in support of this group or a more inclusive group. We note here that similar modifications of the bones supporting the pharyngeal jaws have been reported for *Pantanodon* by Whitehead (1962) and Bragança et al. (2018) but without associated modification of the gill rakers or expansion of ceratobranchial 4. A detailed survey of gill raker morphology across Poeciliinae was beyond the scope of this study but may be justified given the diversity that we have uncovered in this character complex based on the examination of only a relatively small number of taxa.

Hybridisation

Previous allozyme studies clearly revealed the occurrence of hybrids between *P. jackschultzi* and *P. monacha-occidentalis*, the locally occurring all-female hybridogenetic fish (Schenk 1992). The hybridogens are ‘hemiclinal’ transmitting only a maternally inherited, non-recombinant, *monacha* (M) genome to progeny (Schultz 1961, 1969; Vrijenhoek 1977). Their paternally derived *occidentalis* (O) genome is replaced in each generation by matings with *P. occidentalis* males. Consequently, fertilisation of *P. monacha-occidentalis* eggs by sperm from *P. jackschultzi* (J) males produces *P. monacha-jackschultzi* (MJ) hybrids. The MJ hybrids were identified by their heterozygous (fast and slow) genotype at the *Pgd* locus. All of the MJ hybrids identified in our 1999–2001 samples were females ($N = 85$; Table 4), but Schenk (1992) reported the occurrence of two MJ males among ~ 130 MJ females in the 1981–1989 samples. We maintained several MJ hybrid females in the laboratory, some of which produced offspring (also females).

Mitochondrial Cytochrome *b* sequences from six of the wild-caught MJ females (three from MV00-11 and three from MV01-2) were identical to the *P. monacha*-derived *Cytb* sequences previously identified by Sanjur (1998) as *P. monacha-occidentalis* haplotypes “a” and “d” from the Río Concepción (GenBank Acc. No. AF047343 and AF047344), verifying their hybrid status. The rare occurrence of males among hybridogenetic *Poeciliopsis* is not unprecedented (e.g., Schultz 1966, 1967 reported rare *P. monacha-latidens* males, which were sterile). Further work is needed to verify the reproduction mode of the MJ hybrids. Should such hybrids be sexual (i.e., have normal recombination and fertility), they could serve as a vehicle of introgression of the hemiclinal *monacha*-derived genome into the *P. jackschultzi* gene pool. Similarly, whether hybridisation (and introgression) occurs between *P. jackschultzi* and *P. occidentalis* has not been determined. Further studies involving a large number of nuclear gene markers are warranted.

Life history

The *Leptorhaphis* species group exhibits a broad range of placentation and maternal provisioning phenotypes, as measured by the matrotrophic index (MI; Reznick et al. 2002). At the lowest end of maternal provisioning is *P. infans* (MI = 0.86). *Poeciliopsis lucida* and *P. occidentalis* have intermediate levels of maternal provisioning (MI = 1.34 and 1.12, respectively). In contrast, *P. prolifica* has high maternal provisioning (MI = 5.4). Investigating the degree of maternal provisioning in *P. jackschultzi* will likely shed light on the evolution of this complex adaptation within the *Leptorhaphis* species group.

Conservation status

Several features of *P. jackschultzi* indicate that its conservation status is of concern. First, it has a highly restricted distribution. This is a microendemic species, known from only a handful of sites in the Río Concepción (Fig. 10). During the past 50 years, numerous specimens of *Poeciliopsis* have been collected at numerous other localities in the Río Concepción and neighbouring drainage systems in Arizona and Sonora (Moore et al. 1970; Vrijenhoek et al. 1985), but *P. jackschultzi* was not encountered at any of these localities (RCV pers. obs.). Based on Maderey-R and Torres-Ruata (1990), the Río Concepción is approximately 1000 km in length. Assuming that *P. jackschultzi* is found continuously between the northernmost locality (La Cieneguita; A in Figure 10) and the southernmost locality (at the town of Imuris; H in Figure 10) from which the holotype and members of the paratype series were collected, this species may occupy only an approximately 30km stretch (i.e. 3%) of the Río Concepción. Within this narrow stretch, *P. jackschultzi* has only been collected from marshy, shallow, and relatively still-water habitats, which

are patchily distributed throughout the basin (RCV, MM pers. obs.). Secondly, the local abundance of *P. jackschultzi* is low compared to *P. occidentalis* and the hybrids within each locality (below 17% at all sites except for La Atascosa in 1986; Table 4). Collections made after 1984 generally targeted individuals of *P. jackschultzi* and therefore their relative frequency in nature may be lower. Sadly, expansion of Federal Hwy 15 after 1986, nearly obliterated the primary habitat of *P. jackschultzi* at La Atascosa (RCV pers. obs.). The core distribution of *P. jackschultzi* appeared to be mostly spring-fed pools and marshy areas (cienegas) adjacent to the mainstream of Arroyo Alisos-Bambuto branch of the Río Concepción (Figs 10, 11). Although CONAGUA (2018) reports an overall positive recharge *vs.* extraction balance of the Alisos aquifer (Fig. 10), the human demand for water in this desert region continues to increase. From 1990 to 2012, water from the Alisos aquifer was extracted and exported to the city of Nogales. Residual water was transferred to the neighbouring drainage (Rio Santa Cruz) for treatment and release on the US side. Therefore, during this recent ca. 20-year period, recharge of the Alisos aquifer depended solely on precipitation. The Alisos Wastewater Treatment Plant (PTAR Los Alisos; Figure 10), which initiated operation in 2012, releases treated water into the Alisos-Bambuto branch, which is expected to increase water quantity in the mainstream and the aquifer. Nonetheless, pollutant loads of the discharge have been reported above the maximum permissible limits (Meranza-Castillón et al. 2017). An additional factor that may exert further pressure on *P. jackschultzi* is the presence of several exotic species of fishes throughout the Río Concepción, including the mosquitofish *Gambusia affinis* and green sunfish *Lepomis cyanellus* (MM pers. obs.; Hendrickson and Juárez-Romero 1990).

The present status of *P. jackschultzi* and its habitats are unknown, as surveys of this species and its known sites have not been undertaken since 2001. We recommend that future surveys include seining where feasible, as well as the use of minnow traps in the marshy areas where seining is not effective.

Comparative material

Alfaro

A. cultratus. TCWC 3870.16, 2 (C&S); Costa Rica, Heredia, Sarapiquí River drainage, 1 May 1984.

Brachyrhaphis

B. parismina. TCWC 3873.10, 2 (C&S); Costa Rica, Heredia, Sarapiquí River drainage, 4 May 1984.

Gambusia

G. affinis. TCWC 20085.01, 6 (C&S); USA, Texas, Washington Co., 15 May 2012.

Heterandria

H. formosa. TCWC 320.18, 4 (C&S); USA, Florida, Levy Co., 7 June 1975.

Neoheterandria

N. umbratilis. TCWC 6264.18, 2 (C&S); Costa Rica, Heredia, Sarapiquí River drainage, 28 April 1985.

Phallichthys

P. amates. TCWC 6264.17, 2 (C&S); Costa Rica, Heredia, Sarapiquí River drainage, 28 April 1985.

Poecilia

P. latipinna. TCWC 20086.01, 2 (C&S); USA, Texas, Galveston Island, December 2011.

Poeciliopsis (All Mexico unless otherwise noted).

P. catemaco. TCWC 775.07, 3 (C&S); Veracruz, Rio Papaloapan Drainage, Rio Grande (Lago Catemaco outlet), 21 August 1964.

P. gracilis. TCWC 1844.05, 5 (C&S); Chiapas, 2 miles south east of Huixtla, 12 June 1966. – TCWC 6233.05, 8 (C&S); Oaxaca, Los Minas near Zanatepec, 30 May 1983.

P. fasciata. TCWC 3197.08, 3 (C&S); Oaxaca, Las Mina, HWY 190, ca. 3 miles north of Tapanatepec, 31 December 1981.

Leptorhaphis species group. P. infans. UMMZ 172172, 30 of 280, 8.0–68.0 mm SL; Michoacan, Rio Lerma Drainage, Lago de Camecuaro, ca. 9 miles south east of Zamora, 9 March 1955. – UMMZ 173631, 36, 25.0–36.0 mm SL; Michoacan, Rio Lerma Drainage, canal at Tarecuato, south west of Zamora, 16 April 1939. – UMMZ 188806, 17 of 124, 17.0–46.0 mm SL; Guanajuato, roadside ditch, 7 miles east of Salamanca along highway between Salamanca and Celaya, 17.0–46.0 mm SL. – UMMZ 189041, 30 of 280 (4 C&S), 20.0–38.0 mm SL; Michoacan, Rio Lerma Drainage, Lago de Cuitzeo at highway 43, 28 March 1968. ***P. lucida***. UMMZ 178297, 22, 10.0–39.0 mm SL; Sinaloa, Rio de Mocerito just above El Alamo, ca. 24 miles east of Guamuchil, 21 February 1957. – UMMZ 184874, 30 of 76 (4 C&S), 14.0–34.0 mm SL; Sinaloa, tributary of the Rio Mocerito, at road crossing 0.9 miles north of San Benito, 24 March 1959. – UMMZ 184897, 13, 15.0–27.0 mm SL; Sinaloa, tributary of the Rio Mocerito, ca. 2.5 miles West of El Alamo, 22 February 1957. – UMMZ 188915, 30 of 142, 12.0–20.0 mm SL; Sinaloa, stream 1.1 miles south of El Rincon de Carrizalejo, 25 February 1969. ***P. occidentalis***. UMMZ 162670, 30 (of 115), 17.0–35.0 mm SL; Sonora, Gila River Drainage, Rio Santa Cruz, 4 miles south of US (Arizona) border, 19 April 1950. – UMMZ 202393, 41 (4 C&S), 15.0–42.0 mm SL; Sonora, stream at Rancho la Brisca, 16 km north east of Cucurpe, 5 June 1978. – UMMZ 211632, 29 (of 169), 9.0–31.0 mm SL; Sonora, Rio Yaqui drainage, Arroyo El Fresno, south west of Cabullonas, 18 July 1978. ***P. prolifica***. UMMZ 172267, 30 or 456 (4 C&S), 8.0–36.0 mm SL; Sonora, Rio

Culiacan Drainage, Arroyo Sonolona, 18.5 miles east of Culiacan, 2 April 1955. – UMMZ 173677, 17 of 114, 4.0–35 mm SL; Sinaloa, Rio Culiacan Drainage, Rio Tamazula, 6 km east of Culiacan.

P. monacha. UMMZ 178246, 30 of 379 (4 C&S), 12.0–27.0 mm SL; Sonora, Rio del Fuerte Drainage, Arroyo San Benito, ca. 1.5 miles east south east of Rancho Guirrocoba, 16 February 1957.

P. pleurospilus. TCWC 16342.04, 5 (C&S); El Salvador, Santa Ana, Laguna Metapan, 6 June 2011.

P. scarlii. UMMZ 178422, 30 of 127 (4 C&S), 10.0–40.0 mm SL; Guerrero/Michoacan, Rio Balsas at Zacatula, 18 March 1957. – UMMZ 178506, 18 (of 62), 18.0–49.0 mm SL; Guerrero, Laguna Tres Palos at northwest end near Acapulco Airport, 23 March 1957.

Priapichthys

P. annectens. TCWC 6268.10, 2 (C&S); Costa Rica, Heredia, Sarapiquí River drainage, 25 April 1985.

Acknowledgments

M. Schenk and O. Sanjur worked diligently on this project and reported their results in MS (1992) and PhD (1998) theses, respectively. The present results are completely original except for sex-ratio and 1981–1989 relative abundance data reproduced from Schenk (1992). We thank D. Nelson (UMMZ), H. Prestridge (TCWC), and H. Espinosa Pérez (CNP-IBUNAM) for providing access to material under their care and/or curatorial assistance, A. Summers for CT scanning specimens, A. Stankov for help with molecular work, and A. Pinion for making the base map used in Figure 10. A. Varela and L. A. Hurtado helped with field collections. A. Varela and D. Hendrickson helped with inferring the geographic locations of 1986 field collections based on field notes. We also thank M. Ghedotti, L. Parenti and one anonymous reviewer for comments and suggestions that helped improve the manuscript. This research was funded by Texas A&M Agrilife Research (TEX09452 to KWC) and NSF DEB 9902224 to RCV and MM. CT scanning was possible via funding from NSF (DBI 1702442 to KWC; DBI 1701665 to A. Summers at University of Washington). This is publication number 1610 of the Biodiversity Research and Teaching Collections publication number 257 the Center for Biosystematics and Biodiversity of Texas A&M University. SEMARNAP México issued collection permits nos. 020299-213-03 and 140200-213-03. The open access publishing fees for this article have been covered by the Texas A&M University Open Access to Knowledge Fund (OAKFund), supported by the University Libraries and the Office of the Vice President for Research.

References

- Awise JC (2015) Evolutionary perspectives on clonal reproduction in vertebrate animals. *Proceedings of the National Academy of Sciences USA* 112: 8867–8873. <https://doi.org/10.1073/pnas.1501820112>
- Bragança PH, Amorim PF, Costa WJEM (2018) Pantanodontidae (Teleostei, Cyprinodontiformes), the sister group to all other cyprinodontoid killifishes as inferred by molecular data. *Zoosystematics and Evolution* 94: 1–137. <https://doi.org/10.3897/zse.94.22173>
- Bussing WA (2008) A new species of poeciliid fish, *Poeciliopsis santealena*, from Peninsula Santa Elena, Area de Conservación Guanacaste, Costa Rica. *Revista de Biología Tropical* 56: 829–838. http://www.scielo.sa.cr/scielo.php?script=sci_arttext&pid=S0034-77442008000200031&lng=en&nrm=iso
- CONAGUA (2018) CONAGUA, Clave 2613. <http://sina.conagua.gob.mx/sina/tema.php?tema=acuiferos&n=regional> [Accessed 11 May 2019]
- Conway KW (2011) Osteology of the South Asian Genus *Psilorhynchus* McClelland, 1839 (Teleostei: Ostariophysa: Psilorhynchidae), with investigation of its phylogenetic relationships within the order Cypriniformes. *Zoological Journal of the Linnean Society* 163: 50–154. <https://doi.org/10.1111/j.1096-3642.2011.00698.x>
- Costa WJEM (1991) Description d'une nouvelle espèce du genre *Pamphorichthys* (Cyprinodontiformes: Poeciliidae) du bassin de l'Araguaia, Brésil. *Revue Française d'Aquariologie Herpétologie* 18: 39–42.
- Costa WJEM (1998) Phylogeny and classification of the Cyprinodontiformes (Euteleostei: Atherinomorpha): A reappraisal. In: Malabarba LR, Reis RE, Vari RP, Lucena ZM, Lucena CAS (Eds) *Phylogeny and Classification of Neotropical Fishes*. Edipucrs, Porto Alegre, 537–560.
- Ghedotti MJ (2000) Phylogenetic analysis and taxonomy of the poecilioid fishes (Teleostei, Cyprinodontiformes). *Zoological Journal of the Linnean Society* 130: 1–53. <https://doi.org/10.1111/j.1096-3642.2000.tb02194.x>
- Hendrickson DA, Juárez-Romero L (1990) Los peces de la cuenca del Río de la Concepción, Sonora, México, y el estatus del charalito sonoreño, *Gila ditaenia*, una especie en amenaza de extinción. *Southwestern Naturalist* 35: 177–187. <https://doi.org/10.2307/3671540>
- Lima, NRW, Koback CJ, Vrijenhoek RC (1996) Evolution of sexual mimicry in sperm-dependent clonal forms of *Poeciliopsis* (Pisces: Poeciliidae). *Journal of Evolutionary Biology* 9: 185–203. <https://doi.org/10.1046/j.1420-9101.1996.9020185.x>
- Lucinda PHE, Reis RE (2005) Systematics of the subfamily Poeciliinae Bonaparte (Cyprinodontiformes: Poeciliidae), with an emphasis on the tribe Cnesterodontini Hubbs. *Neotropical Ichthyology* 3: 1–60. <https://doi.org/10.1590/S1679-62252005000100001>
- Maderey-R, LE, Torres-Ruata C (1990) Hidrografía, escala 1:4000000. In: *Hidrografía e hidrometría*. Tomo II, Sección IV, 6.1. Atlas Nacional de México (1990–1992). Instituto de Geografía, UNAM, México.
- Mateos M, Vrijenhoek RC (2004) Independent origins of allotriploidy in the fish genus *Poeciliopsis*. *Journal of Heredity* 96: 32–39. <https://doi.org/10.1093/jhered/esi010>
- Mateos M, Sanjur OI, Vrijenhoek RC (2002) Historical biogeography of the livebearing fish genus *Poeciliopsis* (Poeciliidae: Cyprinodontiformes). *Evolution* 56: 972–984. <https://doi.org/10.1111/j.0014-3820.2002.tb01409.x>

- Mateos M, Domínguez-Domínguez O, Varela-Romero A (2019) A multilocus phylogeny of the fish genus *Poeciliopsis*: Solving taxonomic uncertainties and preliminary evidence of reticulation. *Ecology and Evolution* 9: 1845–1857. <https://doi.org/10.1002/ece3.4874>
- Meranza-Castillón, V, Ruiz-Hernandez S, Ortiz-Navar B, Gutiérrez-Gutiérrez R (2017) Impacto de la descarga de agua tratada en la cuenca los Alisos. *Revista de Ciencias Ambientales y Recursos Naturales* 3: 18–28. <https://www.itson.mx/publicaciones/rlnr/Documents/v3-n1-8-impacto-de-la-descarga-de-aguas-residuales.pdf>
- Miller RR (1960) Four new species of viviparous fishes, genus *Poeciliopsis*, from northwestern Mexico. *Occasional Papers of the Museum of Zoology University of Michigan* 619: 1–11. <http://hdl.handle.net/2027.42/57108>
- Miller RR (1975) Five new species of Mexican poeciliid fishes of the genera *Poecilia*, *Gambusia*, and *Poeciliopsis*. *Occasional Papers of the Museum of Zoology University of Michigan* 672: 1–44. <http://hdl.handle.net/2027.42/57108>
- Moore WS, Miller RR, Schultz RJ (1970) Distribution, adaptation and probable origin of an all-female form of *Poeciliopsis* (Pisces: Poeciliidae) in northwestern Mexico. *Evolution* 24: 789–795. <https://doi.org/10.1111/j.1558-5646.1970.tb01813.x>
- Nelson GJ (1969) Gill arches and the phylogeny of fishes, with notes on the classification of vertebrates. *Bulletin of the American Museum of Natural History* 141: 475–552. <http://hdl.handle.net/2246/1162>
- Parenti LR (1981) A phylogenetic and biogeographic analysis of cyprinodontiform fishes (Teleostei, Atherinomorpha). *Bulletin of the American Museum of Natural History* 168: 335–557. <http://hdl.handle.net/2246/438>
- Regan CT (1913) A revision of the cyprinodont fishes of the subfamily Poeciliinae. *Proceedings of the Zoological Society of London* 1913: 977–1018. <https://doi.org/10.1111/j.1096-3642.1913.tb02002.x>
- Reznick DN, Mateos M, Springer MS (2002) Independent origins and rapid evolution of the placenta in the fish genus *Poeciliopsis*. *Science* 298: 1018–1020. <https://doi.org/10.1126/science.1076018>
- Rosen DE, Bailey RM (1963) The poeciliid fishes (Cyprinodontiformes): their structure, zoogeography, and systematics. *Bulletin of the American Museum of Natural History* 126: 1–176. <http://hdl.handle.net/2246/1123>
- Sanjur OI (1998) *Molecular Systematics and Evolution of Fish in the Genus Poeciliopsis (Cyprinodontiformes: Poeciliidae)*. PhD Thesis, University of New Jersey, New Brunswick.
- Schenk M (1992) *A new sexual species of Poeciliopsis with clonal origins*. MSc Thesis, Rutgers University, New Brunswick.
- Schultz RJ (1966) Hybridization experiments with an all-female fish of the genus *Poeciliopsis*. *Biological Bulletin* 130: 415–429. <https://doi.org/10.2307/1539747>
- Schultz RJ (1967) Gynogenesis and triploidy in the viviparous fish *Poeciliopsis*. *Science* 157: 1564–1567. <https://doi.org/10.1126/science.157.3796.1564>
- Schultz RJ (1969) Hybridization, unisexuality, and polyploidy in the teleost *Poeciliopsis* (Poeciliidae) and other vertebrates. *American Naturalist* 103: 605–619. <https://doi.org/10.1086/282629>
- Swofford, DL (2002) PAUP*. *Phylogenetic Analysis Using Parsimony (*and Other Methods)*. Version 4. Sinauer Associates, Sunderland.

- Tarby ML, Webb JF (2003) Development of the supraorbital and mandibular lateral line canals in the cichlid, *Archocentrus nigrofasciatus*. *Journal of Morphology* 254: 44–57. <https://doi.org/10.1002/jmor.10045>
- Taylor WR, Van Dyke GG (1985) Revised procedure for staining and clearing small fishes and other vertebrates for bone and cartilage study. *Cybium* 9: 107–119. <http://sfi-cybium.fr/sites/default/files/pdfs-cybium/01-Taylor%5B92%5D107-119.pdf>
- Vrijenhoek RC, Douglas ME, Meffe GK (1985) Conservation genetics of endangered fish populations in Arizona. *Science* 229: 400–402. <https://doi.org/10.1126/science.229.4711.400>
- Vrijenhoek RC (1993) The origin and evolution of clones versus the maintenance of sex in *Poeciliopsis*. *Journal of Heredity* 84: 388–395. <https://doi.org/10.1093/oxfordjournals.jhered.a111359>
- Vrijenhoek RC (1994) Unisexual fish: Models for studying ecology and evolution. *Annual Review of Ecology and Systematics* 25: 71–96. <https://doi.org/10.1146/annurev.es.25.110194.000443>
- Vrijenhoek RC, Dawley RM, Cole CJ, Bogart JP (1989) A list of known unisexual vertebrates. In: Dawley R, Bogart J (Eds) *Evolution and Ecology of Unisexual Vertebrates*. Bulletin 466, New York State Museum, Albany, 19–23.
- Vrijenhoek RC, Schultz RJ (1974) Evolution of a trihybrid unisexual fish (*Poeciliopsis*, Poeciliidae). *Evolution* 28: 205–319. <https://doi.org/10.1111/j.1558-5646.1974.tb00750.x>
- Webb JF, Shirey JE (2003) Postembryonic development of the cranial lateral line canals and neuromasts in zebrafish. *Developmental Dynamics* 228: 370–385. <https://doi.org/10.1002/dvdy.10385>
- Whitehead PJP (1962) The Pantanodontinae, edentulous toothcarps from East Africa. *Bulletin of the British Museum of Natural History* 9: 105–137. <https://doi.org/10.5962/bhl.part.16339>
- Woolman AJ (1894) Report on a collection of fishes from the rivers of central and northern Mexico. *Bulletin of the U.S. Fish Commission* 14: 55–66. <https://www.biodiversitylibrary.org/bibliography/3971#/summary>

Species delimitation of crab-eating frogs (*Fejervarya cancrivora* complex) clarifies taxonomy and geographic distributions in mainland Southeast Asia

Siriporn Yodthong¹, Bryan L. Stuart², Anchalee Aowphol¹

1 Department of Zoology, Faculty of Science, Kasetsart University, Bangkok, Thailand **2** Section of Research & Collections, North Carolina Museum of Natural Sciences, Raleigh, NC, USA

Corresponding author: *Anchalee Aowphol* (fsciac@ku.ac.th)

Academic editor: *A. Crottini* | Received 21 June 2019 | Accepted 21 September 2019 | Published 28 October 2019

<http://zoobank.org/BB72DDFE-DD17-428E-AF0F-4EFACBDC8721>

Citation: Yodthong S, Stuart BL, Aowphol A (2019) Species delimitation of crab-eating frogs (*Fejervarya cancrivora* complex) clarifies taxonomy and geographic distributions in mainland Southeast Asia. ZooKeys 883: 119–153. <https://doi.org/10.3897/zookeys.883.37544>

Abstract

The taxonomy and geographic distributions of species of crab-eating frogs (*Fejervarya cancrivora* complex) in mainland Southeast Asia have been highly uncertain. Three taxonomic names are used in recent literature (*F. cancrivora*, *F. raja*, and *F. moodiei*) but the applications of these names to localities has been inconsistent, especially owing to the lack of available molecular data for *F. raja*. Morphometric and mitochondrial DNA variation was examined in these frogs, including name-bearing types and topotypes of all three species. Findings corroborate evidence for the existence of two species in coastal mainland Southeast Asia, with *F. moodiei* having a wide geographic distribution and *F. cancrivora* sensu stricto occurring only in extreme southern Thailand and peninsular Malaysia. *Fejervarya raja* is shown to be only a large-bodied population of *F. cancrivora* sensu stricto and is synonymized with that species. Revised descriptions of *F. moodiei* and *F. cancrivora* sensu stricto are provided.

Keywords

Amphibia, cryptic species, Dicroglossidae, systematics, taxonomy

Introduction

Southeast Asia harbors high levels of amphibian species diversity and endemism (Brown and Stuart 2012), and new species continue to be discovered and described (e.g., Geissler et al. 2014; Phimmachak et al. 2015; Sheridan and Stuart 2018). Moreover, recent evaluations of morphological and molecular diversity of Southeast Asian amphibians have routinely shown that long-recognized geographically widespread single species actually represent complexes of cryptic species (Stuart et al. 2006b; Aowphol et al. 2013; Phimmachak et al. 2015; Sheridan and Stuart 2018). The presence of cryptic species in Southeast Asian amphibians has hindered accurately assessing species boundaries and, ultimately, efforts to conserve them (Bickford et al. 2006; Sheridan and Stuart 2018). Even geographically widespread, human commensalist species may contain unrecognized diversity that alters their priority for conservation (Wogan et al. 2016).

Species of frogs in the genus *Fejervarya* Bolckay, 1915 have been subject to numerous investigations into cryptic diversity in efforts to resolve species boundaries and uncertain taxonomy in South, Southeast and East Asia (e.g., Vieth et al. 2001; Matsui et al. 2007; Islam et al. 2008; Kotaki et al. 2010; Sanchez et al. 2018). A notable challenge remains with the crab-eating frog, *F. cancrivora* (Gravenhorst, 1829), a species that is remarkable in its ability to thrive in brackish or salt water (e.g., Gordon et al. 1961; Balinsky et al. 1972; Wright et al. 2004; Hopkins and Brodie 2015). *Fejervarya cancrivora* occurs in coastal areas throughout much of Southeast Asia, and as expected owing to its large geographic range, recent molecular investigations have hypothesized the existence of cryptic species and discordance between taxonomy and species diversity within the taxon (Kurniawan et al. 2010, 2011). Historically, the name *F. cancrivora* had been erroneously applied to larger members of the *F. limnocharis* complex, but application of the name was stabilized following designation of a neotype specimen from Cianjur, West Java, Indonesia, by Dubois and Ohler (2000). Taylor (1920) described the Philippine populations of *F. cancrivora* as a distinct species, *F. moodiei* (originally *Rana moodiei* Taylor, 1920) based on an adult female collected at Manila, Luzon, Philippines. Smith (1930) described a population of *F. cancrivora* specimens having large body sizes from Pattani, Thailand, as *F. raja* (originally *R. cancrivora raja* Smith, 1930).

Two of these species, *F. cancrivora* and *F. raja*, have been reported from Thailand, where they occur in the vicinity of sea shores or river mouths (Smith 1930; Taylor 1962; Nutphud 2001; Chan-ard 2003; Chuaynkern and Chuaynkern 2012). However, these designations have been uncertain. Iskandar (1998) suggested that *F. raja* from Thailand might just be unusually large individuals of *F. cancrivora*. Other authors have questioned the distinctiveness of the Philippine *F. moodiei* from *F. cancrivora*, and have synonymized them (Smith 1927; Inger 1954) or considered *F. moodiei* to be invalid (Matsui et al. 2007). Analyses of morphological and molecular variation, as well as laboratory crossing experiments, revealed three distinct “types” (= forms) of *F. cancrivora* across its large geographic range: a large type considered to be true *F. cancrivora*, a mangrove type considered to be *F. moodiei*, and a Sulawesi type that might belong

to an undescribed species (Kurniawan et al. 2010, 2011). Their results also inferred that *F. raja* might be conspecific with *F. cancrivora*. A lack of molecular data from true *F. raja* and examination of type specimens in the *F. cancrivora* complex (Islam et al. 2008; Kurniawan et al. 2010, 2011) have hindered resolving species boundaries and taxonomy within the crab-eating frogs.

In this study, we examined morphology and mitochondrial DNA variation in historical and newly-collected museum specimens of the *F. cancrivora* complex from Thailand and adjacent Asian countries to evaluate and clarify the taxonomic status of *F. cancrivora*, *F. moodiei* and *F. raja*. Importantly, our analyses included molecular and morphological data of topotypes of *F. raja*, and morphological data from the name-bearing type specimens of *F. cancrivora* and *F. moodiei*.

Materials and methods

Sampling

During 2015–2017, specimens of *F. cancrivora* were collected at 12 localities and *F. raja* at two localities in Thailand (Fig. 1). Specimens were humanely euthanized using tricainemethanesulfonate (MS-222) solution. Liver or muscle tissue was removed from each individual, preserved in 95% ethyl alcohol, and stored at -20 °C for molecular analysis. Voucher specimens were initially fixed in 10% buffered formalin and later transferred to 70% ethyl alcohol for long-term preservation. Tissue samples and voucher specimens were deposited in the herpetological collection of the Zoological Museum, Kasetsart University, Bangkok, Thailand (ZMKU). Comparative material was also studied in the holdings of ZMKU, Carnegie Museum of Natural History (CM), Field Museum of Natural History [FMNH; formerly Chicago Natural History Museum (CNHM)], and Thailand Natural History Museum (THNHM; Table 1; Appendix 1).

DNA extraction, amplification and sequencing

Total genomic DNA was extracted from liver or muscle tissue using the GF-1 Tissue DNA Extraction Kit (Vivantis Inc.). A 961–962 bp fragment of mitochondrial (mt) DNA that encodes part of the 16S rRNA gene was amplified by the polymerase chain reaction (PCR; 94 °C 45s, 58 °C 30s, 72 °C 1 min) for 35 cycles using the primer pairs L-16SRanaIII (Stuart et al. 2006a) and 16Sbr-3' (Palumbi 1996). PCR products were purified using the NucleoSpin Gel and PCR Clean-up (Macherey-Nagel Inc.) and sequenced in both directions on an ABI 3730XL DNA analyzer by Bioneer Inc. (Daejeon, Korea) using Big Dye version 3 chemistry, the amplifying primers, and the internal primers H-16SRanaIII (Stuart et al. 2006a) and 16Sar-3' (Palumbi 1996). DNA sequences were edited and aligned using Geneious v7.0.6 (Biomatter, Ltd.), and deposited in GenBank under accession numbers MN453492–MN453527 (Table 1).

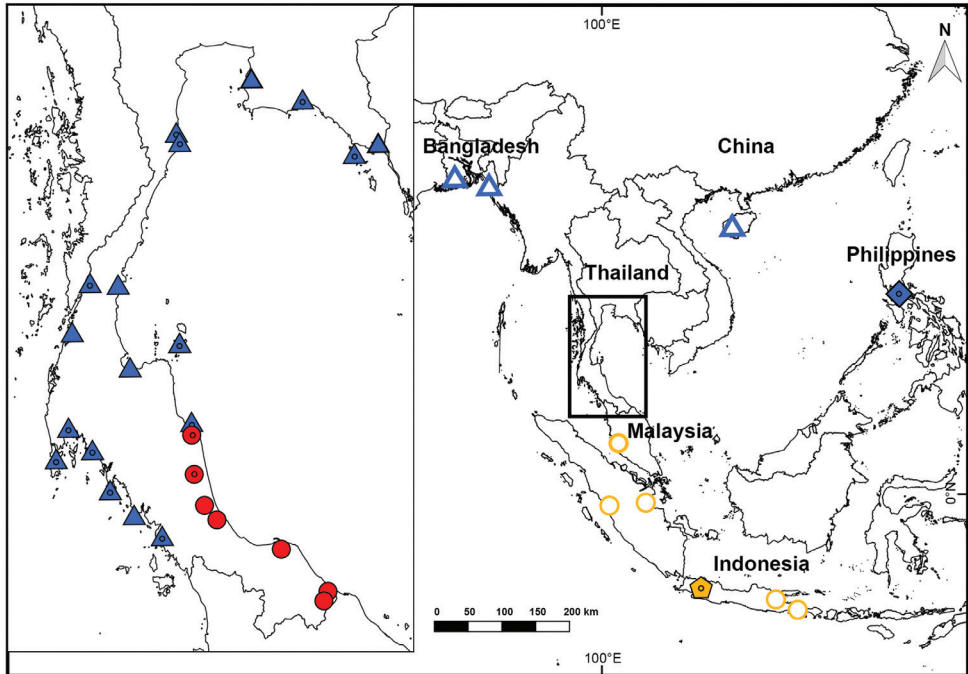


Figure 1. Map of sampling localities of the *Fejervarya cancrivora* complex, including *F. cancrivora* neotype (yellow pentagon), *F. cancrivora* sensu stricto (yellow circles), *F. moodiei* holotype (blue diamond), *F. moodiei* (blue triangles), and *F. cancrivora* samples that were referred to *F. raja* (red circles) prior to this study. Open symbols indicate molecular data only, shaded symbols indicate morphological data only, and shaded symbols with center dots indicate both molecular and morphological data were studied.

Phylogenetic analysis

Homologous sequences of *F. cancrivora* and *F. moodiei*, and the outgroup taxa *F. iskandari* Vieth, Kosuch, Ohler & Dubois, 2001, *F. limnocharis* (Gravenhorst, 1829), *F. multistriata* (Hallowell, 1861), *F. vittigera* (Wiegmann, 1834), *Euphlyctis cyanophlyctis* (Schneider, 1799), *Limnonectes jarujini* Matsui, Panha, Khonsue & Kuraishi, 2010, and *Occidozyga lima* (Gravenhorst, 1829) (following Islam et al. 2008; Kotaki et al. 2010; Kurniawan et al. 2010; Hasan et al. 2014), were downloaded from GenBank (Table 1). Downloaded sequences were trimmed to match the length of the 16S fragment obtained here and aligned to the newly-generated sequences using the MUSCLE plug-in as implemented in Geneious v 7.0.6. The best-fit nucleotide substitution model for the dataset was inferred to be GTR+I+G using the Akaike information criterion (AIC) as implemented in jModelTest v2.1.10 (Darriba et al. 2012). Phylogenetic analyses were performed using Bayesian inference with MrBayes 3.2.1 (Ronquist et al. 2012). Two independent runs, each with four Markov Chain Monte Carlo (MCMC) chains, were executed for 10 million generations using the default priors, trees were sampled every 1,000 generations, and the first 25% of trees were discarded as ‘burn-in.’ A 50% majority-rule consensus of the sampled trees was constructed to

calculate the posterior probabilities of the tree nodes. Run parameters, stationarity and convergence were assessed using the program Tracer v.1.7 (Rambaut et al. 2018). Uncorrected pairwise sequence divergences (p -distances) were calculated in MEGA X (Kumar et al. 2018).

Morphological study

Morphological analyses were performed on 108 sexually mature individuals (61 males, 47 females) of *F. cancrivora*, *F. moodiei*, and *F. raja* (Table 1; Appendix 2, 3). Importantly, these included the neotype (FMNH 256688) and topotypes of *F. cancrivora* from Java, Indonesia; the holotype of *F. moodiei* (CM 3724) from Luzon, Philippines; and topotypes of *F. raja* from Pattani, Thailand (Table 1). Sexual maturity was determined by presence of secondary characteristics, including nuptial pads or vocal sac folds in males, and convoluted oviducts or mature ova in females. Webbing formulae follow Savage and Heyer (1967).

Measurements were taken with digital Vernier calipers to the nearest 0.1 mm. Twenty-three morphological characters were measured following Djong et al. (2007) and Islam et al. (2008):

EL	eye length, greatest diameter of the eye including upper eyelids,
EN	distance from front of eye to nostril,
FAL	forelimb length, from elbow to base of outer palmar tubercle,
FOL	foot length, from base of inner metatarsal tubercle to tip of fourth toe,
HAL	hand length, from base of outer palmar tubercle to tip of third finger,
HL	head length, from back of mandible to tip of snout,
HLL	hindlimb length,
HW	head width, from left side back of mandible to right side back of mandible,
IMTL	length of inner metatarsal tubercle,
IN	internarial space, distance between the nostrils,
IOD	interorbital distance,
ITL	inner toe length,
NS	nostril-snout length, distance from nostril to tip of snout,
NTL	nostril-tympanum length, distance between nostril and front of tympanum,
SL	snout length, distance from front of eye to tip of snout,
STL	snout-tympanum length, tip of snout to front of tympanum,
SVL	snout-vent length,
TD	tympanum diameter, maximum diameter,
TEL	tympanum-eye length, distance between end of eye to front of tympanum,
TFOL	length of tarsus and foot, from base of tarsus to tip of fourth toe,
THIGHL	thigh length,
TL	tibia length,
UEW	maximum width of upper eyelids,
1FL	first finger length.

Table 1. Specimens of *Fejervarya* used in (A) molecular and/or (B) morphological analyses.

Species identification		Locality	Museum No.	GenBank Accession No.	Type of analyses	Reference
Previous study	This study					
<i>F. moodiei</i> (holotype)	<i>F. moodiei</i>	Manila, Luzon, Philippines	CM 3724	–	B	This study
<i>F. cancrivora</i>	<i>F. moodiei</i>	Malaysia	CNHM 161312	–	B	This study
<i>F. cancrivora</i>	<i>F. moodiei</i>	Northern Luzon	FMNH 161693	–	B	This study
<i>F. cancrivora</i>	<i>F. moodiei</i>	Northern Luzon	FMNH 161697	–	B	This study
<i>F. cancrivora</i>	<i>F. moodiei</i>	Chonburi, Thailand	FMNH 190532	–	B	This study
<i>F. cancrivora</i>	<i>F. moodiei</i>	Mueang Surat Thani, Surat Thani, Thailand	THNHM 05857	–	B	This study
<i>F. cancrivora</i>	<i>F. moodiei</i>	Moo Ko Chumphon National Park, Chumphon, Thailand	THNHM 01032	–	B	This study
<i>F. cancrivora</i>	<i>F. moodiei</i>	Moo Ko Chumphon National Park, Chumphon, Thailand	THNHM 01031	–	B	This study
<i>F. cancrivora</i>	<i>F. moodiei</i>	Moo Ko Chumphon National Park, Chumphon, Thailand	THNHM 01033	–	B	This study
<i>F. cancrivora</i>	<i>F. moodiei</i>	Ko Libong, Trang, Thailand	THNHM 02249	–	B	This study
<i>F. cancrivora</i>	<i>F. moodiei</i>	Songkhla lake, Songkhla, Thailand	THNHM 02405	–	B	This study
<i>F. cancrivora</i>	<i>F. moodiei</i>	Songkhla lake, Phatthalung, Thailand	THNHM 04332	–	B	This study
<i>F. cancrivora</i>	<i>F. moodiei</i>	Kleang, Rayong, Thailand	THNHM 14252	–	B	This study
<i>F. cancrivora</i>	<i>F. moodiei</i>	Kleang, Rayong, Thailand	THNHM 14254	–	B	This study
<i>F. cancrivora</i>	<i>F. moodiei</i>	Kleang, Rayong, Thailand	THNHM 14255	–	B	This study
<i>F. cancrivora</i>	<i>F. moodiei</i>	Kleang, Rayong, Thailand	THNHM 14256	–	B	This study
<i>F. cancrivora</i>	<i>F. moodiei</i>	Mueang Trat, Trat, Thailand	THNHM 16631	–	B	This study
<i>F. cancrivora</i>	<i>F. moodiei</i>	Tak Bai, Narathiwat, Thailand	THNHM 19720	–	B	This study
<i>F. cancrivora</i>	<i>F. moodiei</i>	Tak Bai, Narathiwat, Thailand	THNHM 19721	–	B	This study
<i>F. cancrivora</i>	<i>F. moodiei</i>	Tak Bai, Narathiwat, Thailand	THNHM 19724	–	B	This study
<i>F. cancrivora</i>	<i>F. moodiei</i>	Tak Bai, Narathiwat, Thailand	THNHM 19725	–	B	This study
<i>F. cancrivora</i>	<i>F. moodiei</i>	Suk Samran, Ranong, Thailand	THNHM 25736	–	B	This study
<i>F. cancrivora</i>	<i>F. moodiei</i>	Suk Samran, Ranong, Thailand	THNHM 26002	–	B	This study
<i>F. cancrivora</i>	<i>F. moodiei</i>	Suk Samran, Ranong, Thailand	THNHM 26016	–	B	This study
<i>F. cancrivora</i>	<i>F. moodiei</i>	Sam Roi Yot, Prachuap Khiri Khan, Thailand	ZMKU AM 01368	MN453492	A	This study
<i>F. cancrivora</i>	<i>F. moodiei</i>	Sam Roi Yot, Prachuap Khiri Khan, Thailand	ZMKU AM 01369	MN453493	A, B	This study
<i>F. cancrivora</i>	<i>F. moodiei</i>	Sam Roi Yot, Prachuap Khiri Khan, Thailand	ZMKU AM 01370	MN453494	A	This study
<i>F. cancrivora</i>	<i>F. moodiei</i>	Sam Roi Yot, Prachuap Khiri Khan, Thailand	ZMKU AM 01371	–	B	This study
<i>F. cancrivora</i>	<i>F. moodiei</i>	Kraburi, Ranong, Thailand	ZMKU AM 01373	MN453495	A, B	This study
<i>F. cancrivora</i>	<i>F. moodiei</i>	Kraburi, Ranong, Thailand	ZMKU AM 01375	MN453496	A, B	This study
<i>F. cancrivora</i>	<i>F. moodiei</i>	Mueang, Phuket, Thailand	ZMKU AM 01376	–	B	This study
<i>F. cancrivora</i>	<i>F. moodiei</i>	Mueang, Phuket, Thailand	ZMKU AM 01377	MN453497	A	This study
<i>F. cancrivora</i>	<i>F. moodiei</i>	Mueang, Phuket, Thailand	ZMKU AM 01381	MN453498	A, B	This study
<i>F. cancrivora</i>	<i>F. moodiei</i>	Ko Samui, Surat Thani, Thailand	ZMKU AM 01384	MN453499	A, B	This study
<i>F. cancrivora</i>	<i>F. moodiei</i>	Ko Samui, Surat Thani, Thailand	ZMKU AM 01386	–	B	This study
<i>F. cancrivora</i>	<i>F. moodiei</i>	Ko Samui, Surat Thani, Thailand	ZMKU AM 01387	MN453500	A, B	This study
<i>F. cancrivora</i>	<i>F. moodiei</i>	Mueang Phang-nga, Phang-nga, Thailand	ZMKU AM 01390	MN453501	A, B	This study
<i>F. cancrivora</i>	<i>F. moodiei</i>	Mueang Phang-nga, Phang-nga, Thailand	ZMKU AM 01394	MN453502	A, B	This study

Species identification		Locality	Museum No.	GenBank Accession No.	Type of analyses	Reference
Previous study	This study					
<i>F. cancrivora</i>	<i>F. moodiei</i>	Mueang Phang-nga, Phang-nga, Thailand	ZMKU AM 01397	MN453503	A, B	This study
<i>F. cancrivora</i>	<i>F. moodiei</i>	Mueang Phang-nga, Phang-nga, Thailand	ZMKU AM 01398	–	B	This study
<i>F. cancrivora</i>	<i>F. moodiei</i>	Mueang Phuket, Phuket, Thailand	ZMKU AM 01399	MN453504	A, B	This study
<i>F. cancrivora</i>	<i>F. moodiei</i>	Mueang Phuket, Phuket, Thailand	ZMKU AM 01400	–	B	This study
<i>F. cancrivora</i>	<i>F. moodiei</i>	Mueang Phuket, Phuket, Thailand	ZMKU AM 01404	–	B	This study
<i>F. cancrivora</i>	<i>F. moodiei</i>	Ko Lanta, Krabi, Thailand	ZMKU AM 01405	MN453505	A, B	This study
<i>F. cancrivora</i>	<i>F. moodiei</i>	Ko Lanta, Krabi, Thailand	ZMKU AM 01407	–	B	This study
<i>F. cancrivora</i>	<i>F. moodiei</i>	Ko Lanta, Krabi, Thailand	ZMKU AM 01409	MN453506	A	This study
<i>F. cancrivora</i>	<i>F. moodiei</i>	Ko Lanta, Krabi, Thailand	ZMKU AM 01413	MN453507	A	This study
<i>F. cancrivora</i>	<i>F. moodiei</i>	Khanom, Nakhon Si Thammarat, Thailand	ZMKU AM 01436	–	B	This study
<i>F. cancrivora</i>	<i>F. moodiei</i>	Ko Chang, Trat, Thailand	ZMKU AM 01442	MN453508	A, B	This study
<i>F. cancrivora</i>	<i>F. moodiei</i>	Ko Chang, Trat, Thailand	ZMKU AM 01446	MN453509	A, B	This study
<i>F. cancrivora</i>	<i>F. moodiei</i>	Ko Chang, Trat, Thailand	ZMKU AM 01451	MN453510	A, B	This study
<i>F. cancrivora</i>	<i>F. moodiei</i>	Ko Chang, Trat, Thailand	ZMKU AM 01453	–	B	This study
<i>F. cancrivora</i>	<i>F. moodiei</i>	Pak Phanang, Nakhon Si Thammarat, Thailand	ZMKU AM 01467	MN453511	A, B	This study
<i>F. cancrivora</i>	<i>F. moodiei</i>	Pak Phanang, Nakhon Si Thammarat, Thailand	ZMKU AM 01469	–	B	This study
<i>F. cancrivora</i>	<i>F. moodiei</i>	Pak Phanang, Nakhon Si Thammarat, Thailand	ZMKU AM 01470	–	B	This study
<i>F. cancrivora</i>	<i>F. moodiei</i>	Pak Phanang, Nakhon Si Thammarat, Thailand	ZMKU AM 01475	MN453512	A, B	This study
<i>F. cancrivora</i>	<i>F. moodiei</i>	Pak Phanang, Nakhon Si Thammarat, Thailand	ZMKU AM 01479	MN453513	A, B	This study
<i>F. cancrivora</i>	<i>F. moodiei</i>	Kraburi, Ranong, Thailand	ZMKU AM 01485	MN453514	A, B	This study
<i>F. cancrivora</i>	<i>F. moodiei</i>	Kraburi, Ranong, Thailand	ZMKU AM 01486	–	B	This study
<i>F. cancrivora</i>	<i>F. moodiei</i>	Mueang Krabi, Krabi, Thailand	ZMKU AM 01488	–	B	This study
<i>F. cancrivora</i>	<i>F. moodiei</i>	Mueang Krabi, Krabi, Thailand	ZMKU AM 01489	–	B	This study
<i>F. cancrivora</i>	<i>F. moodiei</i>	Kui Buri, Prachuap Khiri Khan, Thailand	ZMKU AM 01492	–	B	This study
<i>F. cancrivora</i>	<i>F. moodiei</i>	La-ngu, Satun, Thailand	ZMKU AM 01493	MN453515	A, B	This study
<i>F. cancrivora</i>	<i>F. moodiei</i>	La-ngu, Satun, Thailand	ZMKU AM 01494	–	B	This study
<i>F. cancrivora</i>	<i>F. moodiei</i>	La-ngu, Satun, Thailand	ZMKU AM 01498	MN453516	A, B	This study
<i>F. cancrivora</i>	<i>F. moodiei</i>	La-ngu, Satun, Thailand	ZMKU AM 01503	MN453517	A, B	This study
<i>F. cancrivora</i>	<i>F. moodiei</i>	Kleang, Rayong, Thailand	ZMKU AM 01516	MN453518	A, B	This study
<i>F. cancrivora</i>	<i>F. moodiei</i>	Kleang, Rayong, Thailand	ZMKU AM 01520	MN453519	A, B	This study
<i>F. cancrivora</i>	<i>F. moodiei</i>	Manila, Philippines	–	AB070738	A	Sumida et al. (2002)
<i>F. cancrivora</i>	<i>F. moodiei</i>	Negros Island, Philippines	–	AF206473	A	Chen et al. (2005)
<i>F. cancrivora</i>	<i>F. moodiei</i>	Hainan, China	–	DQ458252	A	Che et al. (2007)
<i>F. moodiei</i>	<i>F. moodiei</i>	Dacope, Khulna, Bangladesh	–	AB530508	A	Hasan et al. (2012)
<i>F. moodiei</i>	<i>F. moodiei</i>	Teknaf, Cox's Bazar, Bangladesh	–	AB543602	A	Hasan et al. (2012)
<i>F. cancrivora</i>	<i>F. cancrivora</i>	Cianjur, Java, Indonesia	–	AB444684	A	Kurniawan et al. (2010)

Species identification		Locality	Museum No.	GenBank Accession No.	Type of analyses	Reference
Previous study	This study					
<i>F. cancrivora</i>	<i>F. cancrivora</i>	Padang, Sumatra, Indonesia	–	AB444685	A	Kurniawan et al. (2010)
<i>F. cancrivora</i>	<i>F. cancrivora</i>	Selangor, Malaysia	–	AB444688	A	Kurniawan et al. (2010)
<i>F. cancrivora</i>	<i>F. cancrivora</i>	Bogor, Java, Indonesia	–	AB444689	A	Kurniawan et al. (2010)
<i>F. cancrivora</i>	<i>F. cancrivora</i>	Banyumas, Java, Indonesia	–	AB444690	A	Kurniawan et al. (2010)
<i>F. cancrivora</i>	<i>F. cancrivora</i>	Malang, East Java, Indonesia	–	AB570273	A	Kurniawan et al. (2014)
<i>F. cancrivora</i>	<i>F. cancrivora</i>	Denpasar, Bali, Indonesia	–	AB570277	A	Kurniawan et al. (2014)
<i>F. cancrivora</i> (neotype)	<i>F. cancrivora</i>	Cianjur, Java, Indonesia	FMNH 256688	–	B	This study
<i>F. cancrivora</i>	<i>F. cancrivora</i>	Java, Indonesia	CNHM 131093	–	B	This study
<i>F. cancrivora</i>	<i>F. cancrivora</i>	Java, Indonesia	CNHM 131100	–	B	This study
<i>F. cancrivora</i>	<i>F. cancrivora</i>	Java, Indonesia	CMNH 161102	–	B	This study
<i>F. cancrivora</i>	<i>F. cancrivora</i>	Java, Indonesia	CNHM 313095	–	B	This study
<i>F. cancrivora</i>	<i>F. cancrivora</i>	Java, Indonesia	FMNH 131108	–	B	This study
<i>F. cancrivora</i>	<i>F. cancrivora</i>	Java, Indonesia	FMNH 131111	–	B	This study
<i>F. raja</i>	<i>F. cancrivora</i>	Nakhon Si Thammarat, Thailand	FMNH 174052	–	B	This study
<i>F. raja</i>	<i>F. cancrivora</i>	Phatthalung, Thailand	FMNH 174053	–	B	This study
<i>F. raja</i>	<i>F. cancrivora</i>	Phatthalung, Thailand	FMNH 175923	–	B	This study
<i>F. raja</i>	<i>F. cancrivora</i>	Phatthalung, Thailand	FMNH 175924	–	B	This study
<i>F. raja</i>	<i>F. cancrivora</i>	Phatthalung, Thailand	FMNH 175925	–	B	This study
<i>F. raja</i>	<i>F. cancrivora</i>	Phatthalung, Thailand	FMNH 175926	–	B	This study
<i>F. raja</i>	<i>F. cancrivora</i>	Songkhla, Thailand	THNHM 04955	–	B	This study
<i>F. raja</i>	<i>F. cancrivora</i>	Songkhla, Thailand	THNHM 04956	–	B	This study
<i>F. raja</i>	<i>F. cancrivora</i>	Nong Chick, Pattani, Thailand	THNHM 15623	–	B	This study
<i>F. raja</i>	<i>F. cancrivora</i>	Su-Ngai Kolok, Narathiwat, Thailand	THNHM 19221	–	B	This study
<i>F. raja</i>	<i>F. cancrivora</i>	Tak Bai, Narathiwat, Thailand	THNHM 19771	–	B	This study
<i>F. raja</i>	<i>F. cancrivora</i>	Tak Bai, Narathiwat, Thailand	THNHM 19765	–	B	This study
<i>F. raja</i>	<i>F. cancrivora</i>	Tak Bai, Narathiwat, Thailand	THNHM 19766	–	B	This study
<i>F. raja</i>	<i>F. cancrivora</i>	Tak Bai, Narathiwat, Thailand	THNHM 19767	–	B	This study
<i>F. raja</i>	<i>F. cancrivora</i>	Tak Bai, Narathiwat, Thailand	THNHM 19768	–	B	This study
<i>F. raja</i>	<i>F. cancrivora</i>	Tak Bai, Narathiwat, Thailand	THNHM 19769	–	B	This study
<i>F. raja</i>	<i>F. cancrivora</i>	Tak Bai, Narathiwat, Thailand	THNHM 19770	–	B	This study
<i>F. raja</i>	<i>F. cancrivora</i>	Pak Phayun, Phatthalung, Thailand	THNHM 19852	–	B	This study
<i>F. raja</i>	<i>F. cancrivora</i>	Pak Phayun, Phatthalung, Thailand	THNHM 19853	–	B	This study
<i>F. raja</i>	<i>F. cancrivora</i>	Pak Phayun, Phatthalung, Thailand	THNHM 19854	–	B	This study
<i>F. raja</i>	<i>F. cancrivora</i>	Pak Phayun, Phatthalung, Thailand	THNHM 19855	–	B	This study
<i>F. raja</i>	<i>F. cancrivora</i>	Pak Phayun, Phatthalung, Thailand	THNHM 19857	–	B	This study
<i>F. raja</i>	<i>F. cancrivora</i>	Su-Ngai Kolok, Narathiwat, Thailand	THNHM 20754	–	B	This study
<i>F. raja</i>	<i>F. cancrivora</i>	Nong Chick, Pattani, Thailand	THNHM 21248	–	B	This study
<i>F. raja</i>	<i>F. cancrivora</i>	Pak Phanang, Nakhon Si Thammarat, Thailand	THNHM 25499	–	B	This study
<i>F. raja</i>	<i>F. cancrivora</i>	Khuan Khanun, Phatthalung, Thailand	ZMKU AM 01418	MN453520	A	This study
<i>F. raja</i>	<i>F. cancrivora</i>	Khuan Khanun, Phatthalung, Thailand	ZMKU AM 01423	MN453521	A, B	This study
<i>F. raja</i>	<i>F. cancrivora</i>	Khuan Khanun, Phatthalung, Thailand	ZMKU AM 01424	–	B	This study
<i>F. raja</i>	<i>F. cancrivora</i>	Khuan Khanun, Phatthalung, Thailand	ZMKU AM 01425	MN453522	A	This study
<i>F. raja</i>	<i>F. cancrivora</i>	Khuan Khanun, Phatthalung, Thailand	ZMKU AM 01426	MN453523	A, B	This study

Species identification		Locality	Museum No.	GenBank Accession No.	Type of analyses	Reference
Previous study	This study					
<i>F. raja</i>	<i>F. cancrivora</i>	Khuan Khanun, Phatthalung, Thailand	ZMKU AM 01429	–	B	This study
<i>F. raja</i>	<i>F. cancrivora</i>	Khuan Khanun, Phatthalung, Thailand	ZMKU AM 01430	MN453524	A, B	This study
<i>F. raja</i>	<i>F. cancrivora</i>	Khuan Khanun, Phatthalung, Thailand	ZMKU AM 01432	–	B	This study
<i>F. raja</i>	<i>F. cancrivora</i>	Pak Phanang, Nakhon Si Thammarat, Thailand	ZMKU AM 01507	MN453525	A, B	This study
<i>F. raja</i>	<i>F. cancrivora</i>	Pak Phanang, Nakhon Si Thammarat, Thailand	ZMKU AM 01508	–	B	This study
<i>F. raja</i>	<i>F. cancrivora</i>	Pak Phanang, Nakhon Si Thammarat, Thailand	ZMKU AM 01509	MN453526	A, B	This study
<i>F. raja</i>	<i>F. cancrivora</i>	Pak Phanang, Nakhon Si Thammarat, Thailand	ZMKU AM 01510	–	B	This study
<i>F. raja</i>	<i>F. cancrivora</i>	Pak Phanang, Nakhon Si Thammarat, Thailand	ZMKU AM 01511	MN453527	A, B	This study
<i>F. raja</i>	<i>F. cancrivora</i>	Pak Phanang, Nakhon Si Thammarat, Thailand	ZMKU AM 01512	–	B	This study
<i>F. raja</i>	<i>F. cancrivora</i>	Pak Phanang, Nakhon Si Thammarat, Thailand	ZMKU AM 01513	–	B	This study
<i>Fejervarya</i> sp.	<i>Fejervarya</i> sp.	Pelabuhan ratu, Java, Indonesia	–	AB444693	A	Kurniawan et al. (2010)
<i>Fejervarya</i> sp.	<i>Fejervarya</i> sp.	Makassar, Sulawesi, Indonesia	–	AB570278	A	Kurniawan et al. (2014)
<i>Fejervarya</i> sp.	<i>Fejervarya</i> sp.	Makassar, Sulawesi, Indonesia	–	AB570288	A	Kurniawan et al. (2014)
<i>F. cancrivora</i>	<i>Fejervarya</i> sp.	Selatan, Sulawesi, Indonesia	–	EU979849	A	Che et al. (2009)
<i>F. iskandari</i>	<i>F. iskandari</i>	Malang, Java, Indonesia	–	AB570268	A	Kurniawan et al. (2014)
<i>F. limnocharis</i>	<i>F. limnocharis</i>	Java, Indonesia	–	AB277292	A	Kotaki et al. (2008)
<i>F. multistriata</i>	<i>F. multistriata</i>	Yunan, China	–	AB354237	A	Djong et al. (2011)
<i>F. vittigera</i>	<i>F. vittigera</i>	Quezon, Luzon Island, Philippines	–	AY313683	A	Evans et al. (2003)
<i>Euphlyctis cyanophlyctis</i>	<i>E. cyanophlyctis</i>	Mangalore, India	–	AB488901	A	Kotaki et al. (2010)
<i>Limnonectes jarujini</i>	<i>L. jarujini</i>	Surat Thani, Thailand	–	AB558951	A	Matsui et al. (2010)
<i>Occidozyga lima</i>	<i>O. lima</i>	Kuala Lumpur, Malaysia	–	AB488903	A	Kotaki et al. (2010)

Qualitative characters were taken on the presence and condition of the vomerine ridge, skin on dorsum, coloration and pattern on dorsum, vocal sac pigmentation, fejervaryan lines (conspicuous ventrolateral lines on the ventral side of the body), tubercles on forelimbs and hindlimbs, dermal fringe on fingers II and III, inner tarsal ridge, dermal flap on outer side of Toe V, and foot webbing.

To correct for body size, each mensural character was divided by SVL to a ratio (r) and then converted to a percentage. Specimens were assigned to group (= species) based on their mtDNA assignment (below). Principal component analysis (PCA) was performed separately by sex using FactoMineR and factoextra R package (Lê et al. 2008;

Husson et al. 2017) in the R programs v.3.4.3 (R Core Team 2017) to assess morphometric differences between groups. All variables were tested for normality using Shapiro-Wilk's test. Statistical differences between species were tested by *t*-test for parametric data and Mann-Whitney U test for non-parametric data at a significance level of 95%.

Results

Phylogenetic analyses

The aligned dataset contained 61 individuals and 981 characters. The standard deviation of split frequencies was 0.003331 among the two Bayesian runs, and the Estimated Sample Sizes (ESS) of parameters were ≥ 200 . The Bayesian analysis recovered the *F. cancrivora* complex as monophyletic with strong support, and to contain two major clades referred to as Clades A and B (Fig. 2). Clade A contained subclade A1 consisting of *F. cf. cancrivora* from Indonesia (Pelabuhan Ratu and Sulawesi) and subclade A2 consisting of *F. cancrivora* from Indonesia (Sumatra, Java, Bali) and Malaysia (Selangor), as well as *F. raja* from Thailand (Phatthalung, Nakhon Si Thammarat). Clade B contained subclade B1 consisting of *F. cancrivora* from Thailand (Trat, Nakhon Si Thammarat, Surat Thani, Prachuap Khiri Khan, Rayong), Philippines and China, and subclade B2 consisting of *F. cancrivora* from Thailand (Phuket, Phang-nga, Ranong, Satun, Krabi) and *F. moodiei* from Bangladesh (Cox's Barza, Khulna).

Uncorrected pairwise sequence divergences (*p*-distances) were relatively low within subclades, with subclade A1 ranging from 0.6–6.0% (mean 3.6%), subclade A2 ranging from 0.0–1.4% (mean 0.3%), and subclades B1 and B2 each ranging from 0.0–1.6% (means 0.4%; Table 2). In contrast, genetic distances were relatively high between subclades (6.5–10.5%) except for subclades B1 and B2 (mean 1.7%; Table 2). As such, we refer to subclade A2 as "*F. cancrivora* Group A," and to the merged subclades B1 and B2 as "*F. cancrivora* Group B" (Fig. 3).

Morphological analyses

PCA analysis of males revealed morphometric differences between *F. cancrivora* Group A and *F. cancrivora* Group B, with no overlap on a plot of the first two axes (Fig. 3A). The first three principal components (PC) of males with Eigenvalues > 1.0 accounted for a cumulative 61.2% of the total variance (29.6% by PC1, 19.2% by PC2 and 12.4% by PC3; Table 3). PC1 was heavily and positively loaded on rTL, rHW, rFOL, rTHIGHL, rTFOL, and rSL. PC2 was heavily and positively loaded on rEL, rTD, rNTL, and negatively on SVL, suggesting a strong negative correlation between these characters. PC3 was heavily and positively loaded on rIFL. These results indicated that PC1 and PC2 were strongly influenced by body size. Males of *F. cancrivora* Group A had larger SVL, rTL, rHW, rFOL, rTHIGHL, rTFOL, and rSL, but smaller rEL, rTD, and rNTL than males of Group B based on scores of the first two axes (Fig. 3A).

Table 2. Uncorrected pairwise sequence divergences (p -distances) in the mitochondrial 16S rRNA gene of *Fejervarya cancrivora* and related species. Mitochondrial subclades A1, A2, B1, and B2 are defined in the text.

	<i>iskandari</i>	<i>multistriata</i>	<i>limnocharis</i>	<i>vittigera</i>	<i>cancrivora</i> B2	<i>cancrivora</i> B1	<i>cancrivora</i> A2	sp. A1
<i>iskandari</i>	–							
<i>multistriata</i>	(12.8)	–						
	12.8							
<i>limnocharis</i>	(12.1–12.7)	(0.2–0.4)	(0.9)					
	12.4	0.3	0.9					
<i>vittigera</i>	(16.2)	(12.2)	(11.7–13.5)	–				
	16.2	12.2	12.6					
<i>cancrivora</i> B2	(17.8–18.2)	(13.7–13.9)	(13.4–15.0)	(11.4–12.3)	(0.0–1.6)			
	18.0	13.8	13.9	11.5	0.4			
<i>cancrivora</i> B1	(14.3–18.6)	(13.9–14.2)	(13.4–14.8)	(9.5–12.9)	(0.9–3.4)	(0.0–1.6)		
	17.4	14.1	14.0	11.7	1.7	0.4		
<i>cancrivora</i> A2	(12.5–17.1)	(13.9–14.3)	(13.4–15.1)	(10.7–12.8)	(8.8–10.7)	(8.3–11.1)	(0.0–1.4)	
	15.5	13.7	14.1	11.9	9.7	9.3	0.3	
sp. A1	(10.9–12.5)	(12.8–13.7)	(12.3–13.5)	(9.5–10.2)	(9.8–11.0)	(8.9–11.0)	(4.5–7.9)	(0.6–6.0)
	11.7	13.4	13.2	9.8	10.5	9.3	6.5	3.6

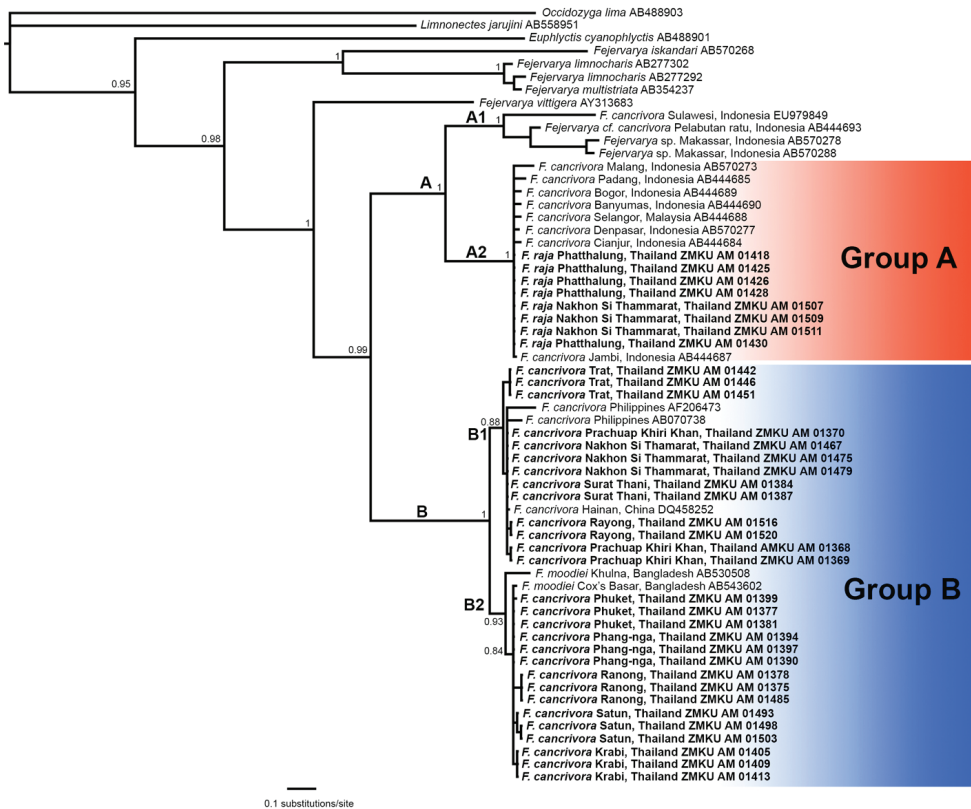
**Figure 2.** Bayesian consensus phylogram of the mitochondrial 16S rRNA gene of *Fejervarya cancrivora* and the closely related species, *F. moodiei* and *F. raja*. Numbers at nodes represent Bayesian posterior probability support values. Clade and subclade names are presented next to branches and group names are presented to the right of terminal taxa.

Table 3. Factor loading on the first three principal components of 23 morphological characters for male and female *Fejervarya cancrivora*, *F. moodiei*, and *F. raja*.

Character	Males			Females		
	PC 1	PC 2	PC 3	PC 1	PC 2	PC 3
SVL	0.395	-0.829	-0.211	0.136	-0.921	-0.008
rHL	0.614	0.462	-0.306	0.628	0.230	0.254
rHW	0.795	-0.093	-0.262	0.660	-0.445	0.297
rSTL	0.623	0.610	-0.222	0.762	0.201	0.353
rNS	0.272	0.574	-0.157	0.640	0.252	0.213
rSL	0.725	0.300	-0.343	0.829	-0.119	0.162
rNTL	0.511	0.703	-0.155	0.654	0.165	0.310
rEN	0.601	0.108	-0.347	0.715	0.016	0.240
rTEL	0.376	-0.236	-0.255	0.329	-0.589	-0.243
rTD	-0.211	0.744	-0.213	0.199	0.570	0.149
rIN	0.166	-0.041	-0.319	0.562	-0.185	0.136
rEL	-0.279	0.767	0.100	0.064	0.820	0.128
rIOD	-0.278	0.659	0.431	0.055	0.628	-0.356
rUEW	0.132	0.176	-0.556	0.104	0.286	0.575
rHAL	0.549	0.358	0.487	0.701	0.285	-0.447
rFAL	0.157	0.408	0.538	0.422	0.074	-0.325
rTHIGHL	0.768	-0.128	-0.138	0.675	-0.136	0.146
rTL	0.815	-0.384	-0.106	0.760	-0.281	0.208
rFOL	0.775	-0.011	0.421	0.800	0.055	-0.250
rTFOL	0.766	-0.249	0.382	0.766	-0.164	-0.135
rIFL	0.481	-0.163	0.664	0.657	0.110	-0.578
rIMTL	0.436	0.034	0.252	0.478	0.089	-0.383
rITL	0.674	-0.029	0.466	0.758	0.064	-0.373
Eigenvalue	6.807	4.420	2.860	8.112	3.337	2.146
Percentage of variance	29.595	19.218	12.435	35.268	14.508	9.331
Cumulative proportion	29.595	48.813	61.248	35.268	49.776	59.107

PCA analysis of females revealed morphometric differences between *F. cancrivora* Group A and *F. cancrivora* Group B, with only slight overlap on a plot of the first two axes (Fig. 3B). The first three PCs of females with Eigenvalues > 1.0 accounted for a cumulative 35.3% of the total variance (35.3% by PC1, 14.5% by PC2 and 9.3% by PC3; Table 3). PC1 was heavily and positively loaded on rSL, rFOL, rTFOL, rSTL, rTL, rITL, rEN, and rHAL, indicating that it was strongly influenced by body size. PC2 was heavily and positively loaded on rEL and negatively on SVL, implying a strong negative correlation between these characters. PC3 was moderately and positively loaded on rUEW and negatively on rIFL. Females of *F. cancrivora* Group A had larger SVL, rSL, rFOL, rTFOL, rSTL, rTL, rITL, rEN, and rHAL, but smaller rEL than females of Group B based on scores of the first two axes (Fig. 3B).

Summary statistics of morphological characters of adult males and females are shown in Table 4. The *t*-tests and Mann-Whitney U tests found significant differences ($p < 0.05$ – 0.0001). Males of *F. cancrivora* Groups A and B were significantly different in most morphometric characters (*t*-tests and Mann-Whitney U tests, $p < 0.05$ – 0.0001),

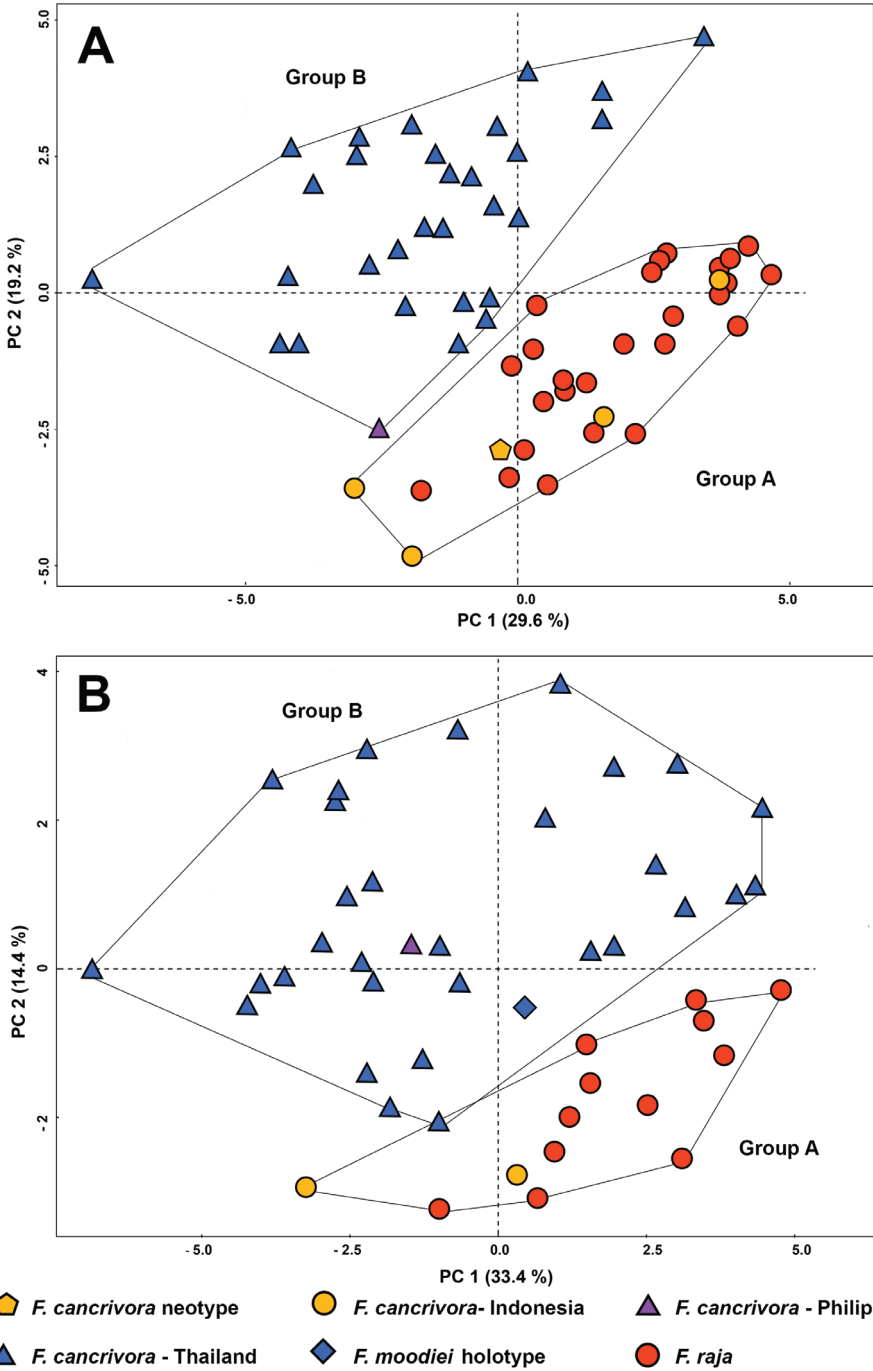


Figure 3. Principal component analysis of morphological measurements from males (A) and females (B) of *Fejervarya cancrivora*, *F. moodiei*, and *F. raja*.

Table 4. Comparisons of body sizes of *Fejervarya cancrivora* and *F. moodiei*. Data are given as mean and standard deviation, followed by range in parentheses. Key: ^atested by Mann-Whitney U test, *significance level at $p < 0.05$.

Characters	Males				Females			
	<i>F. cancrivora</i>	<i>F. moodiei</i>	<i>t</i> -test	<i>p</i>	<i>F. cancrivora</i>	<i>F. moodiei</i>	<i>t</i> -test	<i>p</i>
	<i>n</i> = 31	<i>n</i> = 30			<i>n</i> = 14	<i>n</i> = 33		
SVL	71.3 ± 5.6 (60.2–79.8)	51.4 ± 5.4 (42.7–62.7)	-13.826	< 0.0001*	94.2 ± 6.5 (85.1–107.1)	69.0 ± 10.1 (50.0–81.8)	0 ^a	< 0.0001*
rHL	40.8 ± 1.8 (36.7–43.5)	39.9 ± 1.7 (37.2–44.5)	340 ^a	0.0692	39.6 ± 2.4 (35.2–42.9)	39.4 ± 1.7 (35.9–42.2)	201.5 ^a	0.4953
rHW	37.1 ± 1.8 (32.5–40.6)	34.6 ± 1.1 (32.4–37.1)	-6.553	< 0.0001*	38.2 ± 1.6 (35.0–41.0)	35.6 ± 1.9 (32.5–38.7)	65.5 ^a	0.0001*
rSTL	30.3 ± 1.2 (27.5–32.1)	30.1 ± 1.0 (28.5–32.0)	414.500 ^a	0.4609	29.9 ± 1.1 (27.9–31.6)	29.3 ± 1.0 (27.6–31.3)	-1.867	0.0684
rNS	7.2 ± 0.6 (5.9–8.5)	7.4 ± 0.5 (6.1–8.8)	1.473	0.1460	7.3 ± 0.8 (5.4–8.2)	7.1 ± 0.6 (6.1–8.5)	177 ^a	0.2115
rSL	17.0 ± 1.0 (14.7–18.2)	16.4 ± 0.7 (15.2–17.9)	262.500 ^a	0.0033*	17.2 ± 0.9 (15.2–18.3)	16.1 ± 0.8 (14.6–17.9)	88 ^a	0.0008*
rNTL	23.28 ± 0.9 (21.6–25.3)	23.4 ± 1.1 (21.5–25.8)	0.402	0.6893	23.0 ± 0.7 (21.8–24.0)	22.7 ± 0.9 (21.2–24.4)	-0.783	0.4375
rEN	9.5 ± 0.5 (8.4–10.7)	8.8 ± 0.8 (7.4–11.3)	-3.759	0.0004*	9.5 ± 0.4 (8.5–10.1)	8.8 ± 0.7 (7.5–10.1)	95 ^a	0.0015*
rTEL	3.83 ± 0.64 (2.73–5.21)	3.23 ± 0.62 (2.40–5.05)	-3.840	0.0003*	4.83 ± 0.64 (4.06–6.32)	4.28 ± 0.83 (2.76–5.98)	-2.295	0.0265*
rTD	7.2 ± 0.5 (6.4–8.0)	7.9 ± 0.6 (6.8–9.3)	4.840	< 0.0001*	6.9 ± 0.4 (6.2–7.9)	7.1 ± 0.6 (5.7–8.0)	1.020	0.3131
rIN	4.9 ± 0.4 (4.17–5.62)	4.9 ± 0.6 (3.8–6.2)	371 ^a	0.1750	4.9 ± 0.4 (4.3–6.0)	4.6 ± 0.4 (3.8–5.5)	-2.270	0.0281*
rEL	9.8 ± 0.7 (8.1–11.2)	11.5 ± 1.1 (9.2–13.4)	7.026	< 0.0001*	8.9 ± 0.9 (7.5–10.3)	10.1 ± 1.0 (8.3–12.4)	3.850	0.0004*
rIOD	4.8 ± 0.6 (3.7–5.9)	6.2 ± 0.7 (4.6–8.2)	7.902	< 0.0001*	5.0 ± 0.4 (4.1–5.51)	5.6 ± 0.7 (4.1–7.5)	3.158	0.0028*
rUEW	8.3 ± 0.7 (6.8–9.6)	8.2 ± 0.6 (7.1–9.5)	-0.270	0.7882	8.0 ± 0.8 (6.4–9.4)	7.9 ± 0.7 (6.3–9.2)	-0.140	0.8895
rHAL	24.6 ± 0.9 (23.2–26.3)	24.7 ± 1.1 (21.3–26.8)	0.081	0.9359	23.9 ± 1.2 (21.2–25.6)	24.0 ± 1.5 (21.3–27.45)	218 ^a	0.7692
rFAL	19.3 ± 0.9 (17.6–21.4)	19.8 ± 1.2 (17.8–22.5)	1.609	0.1130	18.7 ± 0.8 (17.4–20.0)	18.8 ± 1.3 (16.7–21.4)	0.084	0.9335
rTHIGHL	47.8 ± 1.93 (42.1–51.1)	45.5 ± 1.9 (42.6–49.3)	178.5 ^a	< 0.0001*	46.0 ± 2.4 (40.0–48.5)	43.6 ± 2.1 (39.9–47.6)	92 ^a	0.0012
rTL	52.0 ± 1.4 (48.7–55.6)	47.6 ± 2.2 (41.0–53.0)	53 ^a	< 0.0001*	50.8 ± 3.0 (42.7–54.13)	46.4 ± 2.3 (43.4–50.7)	62.5 ^a	< 0.0001*
rFOL	54.1 ± 2.2 (49.8–57.8)	51.8 ± 3.0 (43.4–58.3)	261.5 ^a	0.0027*	52.1 ± 1.5 (50.0–55.0)	50.8 ± 3.1 (44.1–55.2)	174 ^a	0.1842
rTFOL	79.6 ± 3.3 (73.6–86.5)	75.1 ± 4.0 (63.6–81.6)	162 ^a	< 0.0001*	77.6 ± 4.0 (71.4–87.0)	72.9 ± 4.6 (66.3–81.2)	109.5 ^a	0.004616*
r1FL	18.9 ± 1.3 (17.2–21.2)	18.2 ± 1.3 (16.2–20.8)	-1.967	0.0539	19.0 ± 1.1 (16.6–20.6)	18.9 ± 1.1 (17.0–21.0)	-0.173	0.8637
rIMTL	6.0 ± 0.6 (4.0–6.9)	5.8 ± 0.6 (4.2–7.0)	342.5 ^a	0.0773	5.9 ± 0.5 (4.7–6.5)	6.0 ± 0.5 (4.8–6.7)	252 ^a	0.6317

Characters	Males				Females			
	<i>F. cancrivora</i>	<i>F. moodiei</i>	<i>t</i> -test	<i>p</i>	<i>F. cancrivora</i>	<i>F. moodiei</i>	<i>t</i> -test	<i>p</i>
	<i>n</i> = 31	<i>n</i> = 30			<i>n</i> = 14	<i>n</i> = 33		
rITL	18.6 ± 1.1 (15.1–20.1)	17.9 ± 1.8 (14.8–21.8)	327.5 ^a	0.0469*	18.4 ± 1.1 (15.9–19.8)	18.1 ± 1.4 (15.2–20.7)	-0.901	0.3724
HL/HW	1.1 ± 0.0 (1.0–1.2)	1.2 ± 0.0 (1.1–1.2)	4.913	< 0.0001*	1.0 ± 0.0 (1.0–1.1)	1.1 ± 0.1 (1.0–1.2)	4.462	< 0.0001*
IOD/HW	0.1 ± 0.0 (0.1–0.2)	0.2 ± 0.0 (0.1–0.2)	10.343	< 0.0001*	0.1 ± 0.0 (0.1–0.2)	0.2 ± 0.0 (0.1–0.2)	4.619	< 0.0001*
SL/HL	0.4 ± 0.0 (0.4–0.5)	0.4 ± 0.0 (0.4–0.5)	-1.448	0.1529	0.43 ± 0.0 (0.4–0.5)	0.4 ± 0.0 (0.4–0.5)	-4.426	< 0.0001*
EL/HL	0.2 ± 0.0 (0.2–0.3)	0.3 ± 0.0 (0.2–0.3)	8.662	< 0.0001*	0.2 ± 0.0 (0.2–0.3)	0.3 ± 0.0 (0.2–0.3)	375 ^a	0.0008*
NS/EN	0.8 ± 0.1 (0.6–0.9)	0.8 ± 0.1 (0.7–1.0)	4.505	< 0.0001*	0.8 ± 0.1 (0.6–0.9)	0.8 ± 0.1 (0.7–0.9)	2.278	0.0275*
EL/SL	0.6 ± 0.0 (0.5–0.7)	0.7 ± 0.1 (0.6–0.8)	8.775	< 0.0001*	0.5 ± 0.1 (0.5–0.6)	0.6 ± 0.1 (0.5–0.8)	5.664	< 0.0001*
EL/EN	1.0 ± 0.1 (0.9–1.2)	1.3 ± 0.2 (1.0–1.6)	9.196	< 0.0001*	0.9 ± 0.1 (0.8–1.1)	1.1 ± 0.1 (1.0–1.4)	6.303	< 0.0001*
IN/IOD	1.0 ± 0.2 (0.8–1.5)	0.8 ± 0.1 (0.5–1.2)	-6.372	< 0.0001*	1.0 ± 0.1 (0.8–1.1)	0.8 ± 0.1 (0.6–1.3)	-3.839	0.0004*
TD/EL	0.7 ± 0.1 (0.6–0.9)	0.7 ± 0.1 (0.6–0.8)	-3.201	0.0022*	0.8 ± 0.1 (0.6–0.9)	0.7 ± 0.1 (0.6–0.9)	-2.754	0.0085*
TEL/EL	0.4 ± 0.1 (0.3–0.6)	0.3 ± 0.1 (0.2–0.4)	-6.585	< 0.0001*	0.6 ± 0.1 (0.4–0.8)	0.4 ± 0.1 (0.2–0.6)	108 ^a	0.0044*
FAL/HAL	0.8 ± 0.0 (0.7–0.9)	0.8 ± 0.1 (0.7–0.9)	1.385	0.1712	0.8 ± 0.0 (0.7–0.8)	0.8 ± 0.1 (0.7–0.9)	0.031	0.9754
THIGHL/ TL	0.9 ± 0.0 (0.9–1.0)	1.0 ± 0.0 (0.9–1.1)	741 ^a	< 0.0001*	0.9 ± 0.1 (0.8–1.0)	0.9 ± 0.0 (0.9–1.0)	2.574	0.0134*
FOL/TL	1.0 ± 0.0 (1.0–1.1)	1.1 ± 0.1 (0.9–1.2)	755 ^a	< 0.0001*	1. ± 0.1 (1.0–1.2)	1.01 ± 0.1 (1.0–1.2)	405 ^a	< 0.0001*
IMTL/TL	0.1 ± 0.0 (0.1–0.1)	0.1 ± 0.0 (0.1–0.2)	615.5 ^a	0.0296	0.1 ± 0.0 (0.1–0.1)	0.1 ± 0.0 (0.1–0.2)	3.342	0.0017*

including body size (SVL), head (rHW), snout (rSL), eye (rEL, rEN, rTEL, rIOD), tympanum (rTD), and hindlimbs (rTHIGHL, rTL, rFOL, rTFOL; Table 4). Females of *F. cancrivora* Groups A and B were also significantly different ($p < 0.05$ – 0.0001) in most morphometric characters, including body size (SVL), head (rHW), snout (rSL), nostril (rIN), eye (rEN, rTEL, rEL, rIOD), and hindlimb (rTL, rTFOL; Table 4). Comparisons of morphometric measurements of adult males and females are given in Appendix 2, 3.

Species accounts

The genetic and morphometric data provide congruent, independent lines of evidence to support the hypothesis that *F. cancrivora* Groups A and B represent two separate species. Specifically, Group A consists of a composite of *F. cancrivora* from Indonesia and Malay-

sia, and *F. raja* from Thailand (Smith 1930; Taylor 1962; Chan-ard 2003; Chuaynkern and Chuaynkern 2012), while Group B consists of a composite of *F. cancrivora* and *F. moodiei* from Thailand, Philippines, China, and Bangladesh (Smith 1930; Taylor 1962; Chan-ard 2003; Kurniawan et al. 2010, 2011; Chuaynkern and Chuaynkern 2012; Table 1). We propose that Group A be referred to as *F. cancrivora* sensu stricto, with *F. raja* treated as a junior synonym of *F. cancrivora*. We propose that Group B be referred to as *F. moodiei*, with specimens of *F. "cancrivora"* in this clade reallocated to that species. The two species, *F. cancrivora* (Group A) and *F. moodiei* (Group B), can be recognized as follows.

***Fejervarya cancrivora* (Gravenhorst, 1829)**

Rana cancrivora Gravenhorst, 1829: 41; Dubois and Ohler 2000: 30; Sumida et al. 2002: 294

Rana cancrivora raja Smith, 1930: 96

Rana raja Taylor, 1962: 373; Stuart et al. 2006: 19

Fejervarya cancrivora: Dubois & Ohler, 2000: 35; Kurniawan et al. 2014: 1

Fejervarya cancrivora: Large type Kurniawan et al. 2010: 222; Kurniawan et al. 2011: 12

Fejervarya raja: Chan-ard 2003: 110; Chuaynkern and Chuaynkern 2012: 169

Diagnosis. *Fejervarya cancrivora* can be characterized by the following combination of characters: (1) large size, SVL 60.2–79.8 mm in males, 85.1–107.1 mm in females (Table 4; Appendix 2, 3); (2) head length slightly greater than head width; (3) skin on dorsum and flank with spinules and glandular warts, with irregular skin folds not arranged in series; (4) relative finger lengths $II < IV < I < III$; (5) dermal fringe on Finger II and III; (6) prepollax indistinct; (7) palmar tubercles indistinct; (8) foot moderately webbed with webbing formula $I1-11/2II1-2III1-2IV2-1V$; (9) dermal flap on postaxial side of Toe V; (10) Fejervaryan lines absent; (11) inner metatarsal tubercles prominent; (12) inner tarsal ridge prominent on distal half to two-thirds of tarsus, and (13) vocal sacs in adult males with wrinkled skin covered by triangular, very dark brown blotches on each side of throat.

Description of neotype. Dubois and Ohler (2000) designated and described the neotype adult male, FMNH 256688, from Java, Indonesia (Fig. 4A–B; Table 1). We supplement their description of the neotype, as follows: rather large size, body rather slender; head narrow, slightly longer than wide; snout oval in dorsal view, round in lateral view, projecting beyond lower jaw; nostril dorsolateral, pointed oval, with small lateral flap, closer to tip of snout than eye; canthus indistinct, rounded; loreal region concave and obtuse; eye diameter about 60% snout length; interorbital space flat, less than width of upper eyelid and internarial distance; pineal body visible; tympanum distinct, rounded [oval according to Dubois and Ohler (2000)], about 90% of eye diameter, not depressed relative to skin of temporal region, tympanic rim weakly elevated relative to tympanum, dorsoposterior margin obscured by supratympanic fold; two vomerine ridges bearing a few small teeth between choanae, obliquely oriented at an angle of 45° to body axis, closer to choanae than to each other; tongue large, cordate, emarginate

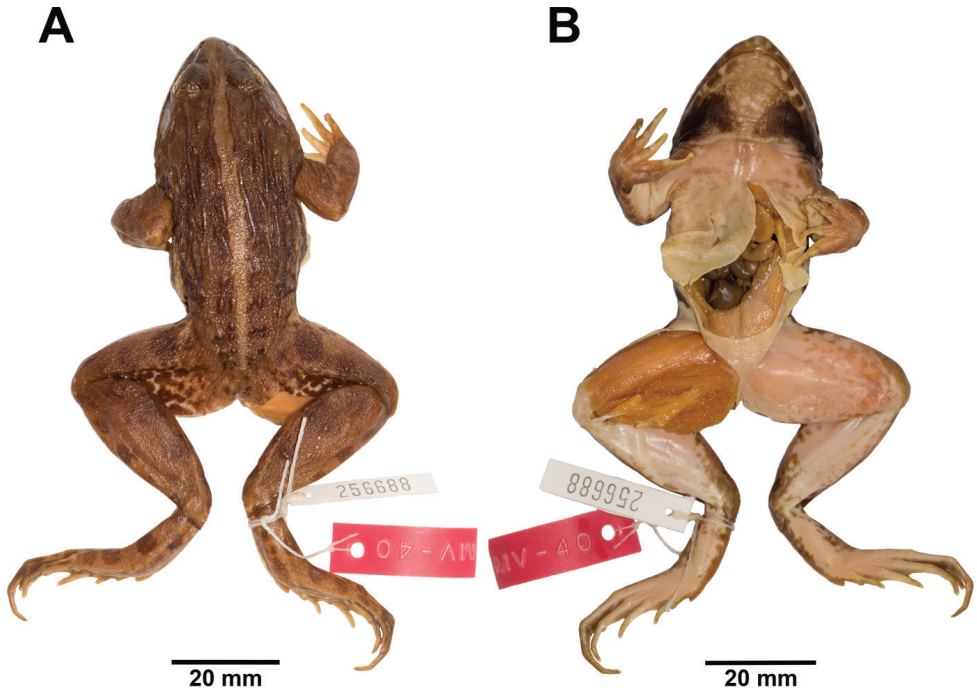


Figure 4. Adult male neotype of *Fejervarya cancrivora* (FMNH 256688) in preservative in **A** dorsal and **B** ventral views.

[based on Ohler and Dubois (2000), not examined by us]; distinct supratympanic fold extending from eye to axilla, not obscuring dorsoposterior margin of tympanum.

Forelimbs short, rather stout [rather thin according to Dubois and Ohler (2000)], slightly longer than hand; fingers rather long, thin; tip of fingers slightly rounded and swollen [pointed according to Dubois and Ohler (2000)], but not expanded into discs; relative length of fingers $II < IV < I < III$; fingers II and III with dermal fringe; webbing on fingers absent; subarticular tubercles prominent, rounded; supernumerary tubercles absent; prepollex indistinct, oval; palmar tubercles indistinct.

Hindlimbs moderately short, robust; tibia longer than thigh, but shorter than distance from base of inner metatarsal tubercle to tip of Toe IV; toes long, thin; tips of toes rounded [pointed according to Dubois and Ohler (2000)], not expanded into discs; relative length of toes $I < II < V < III < IV$; webbing moderate, deeply excised between toes, formula $I1-11/2 \ II1-1III1-2IV2-1V$, Toe I webbed to base of distal phalanx; preaxial side of Toe II webbed to point between distal subarticular tubercle and distal phalanx, continuing as narrow fringe to base of distal phalanx; postaxial side of Toe II webbed to base of distal phalanx; preaxial side of Toe III webbed to distal subarticular tubercle, continuing as narrow fringe to base of distal phalanx, postaxial side of Toe III webbed to base of distal phalanx; preaxial side of Toe IV webbed to distal subarticular tubercle, continuing as narrow fringe to base of distal phalanx, postaxial side of Toe IV webbed to distal subarticular tubercle, continuing as narrow fringe to base of distal phalanx; Toe V webbed to base of distal phalanx; dermal flap well developed, extending

along postaxial side of Toe V from level of inner metatarsal tubercles to distal phalanx; subarticular tubercles prominent; inner metatarsal tubercle prominent, oval, less than length of Toe I; distinct dermal ridge extending along inner metatarsal tubercle to distal phalanx of Toe I; distinct inner tarsal ridge on distal two-third of tarsus (Fig. 5A); outer metatarsal tubercles absent; supernumerary tubercles absent; tarsal tubercle absent.

Skin on snout and interorbital region shagreen; skin on eyelid with glandular warts and spinules; skin on dorsum with irregular skin folds, with intervening glandular warts and spinules; dorsolateral fold extending posteriorly to two-thirds length of dorsum; skin on side of head with small spinules; skin on flank with glandular warts; skin on cloacal region with dense glandular warts; skin on forelimbs, thigh, tibia and tarsus with glandular warts and spinules; skin on ventral surfaces smooth, except dense, fine spinules on chin. Nuptial pad with small translucent spinules on dorsal and medial surface of Finger I from base of distal phalanx to slightly over the base of prepollex; vocal sac present on both sides of throat, with wrinkled skin covered by triangular dark brown blotches. Fejervaryan lines absent.

Coloration of neotype in preservative. Dorsum and side of head medium brown with indistinct dark brown markings; dark brown band between outer margins of upper eyelids; tympanum brown with inferior half more translucent, lighter in coloration than head; flank creamy white with dark brown marbling; three wide dark brown vertical spots on upper lips; wide light brown mid-dorsal stripe continuous from tip of snout to vent; dorsal surfaces of forelimbs, thigh, tibia, and foot brown with dark brown transverse spots; posterior surface of thighs with irregular pattern of dark brown marbling on white background; chin mottled dark brown, throat with triangular dark brown blotches on each side; chest, belly and ventral surfaces of hindlimbs creamy white with indistinct dark brown mottling; ventral surfaces of forelimbs creamy white; ventral surfaces of hand and foot brown; lower lip creamy white with dark brown spots.

Coloration of referred Thai specimen in life. Adult male ZMKU AM 01426 (Fig. 6A–E) from Khuan Khanun District, Phatthalung Province, Thailand. SVL 60.3 mm. Dorsum dark brown with indistinct darker markings, side of head lighter brown; dark brown band between outer margins of upper eyelids; lower half of tympanum with brown blotches; dark brown streak on canthus rostralis from tip of snout to eye; dark brown streak from eye along supratympanic fold to posterior rim of tympanum; flank creamy white with dark brown marbling; three wide dark brown spots on upper lips; a wide beige mid-dorsal stripe continuous from tip of snout to vent; dorsal surfaces of forelimb, thigh, tibia, and foot dark brown with darker transverse spots; posterior part of thigh with irregular pattern of dark brown marbling on light brown background; chin and chest creamy white with dark brown mottling; throat with triangular dark brown blotches on each side; ventral surfaces of forelimbs and belly creamy white; ventral surfaces of hindlimbs creamy white with dark brown mottling; ventral surfaces of hand and foot brown; lower lip creamy white with dark brown spots.

Variations. Females are distinctly larger in size (Table 4; Appendix 3), lack nuptial pads and vocal sacs, and have fewer spinules and glandular warts on dorsum and flanks

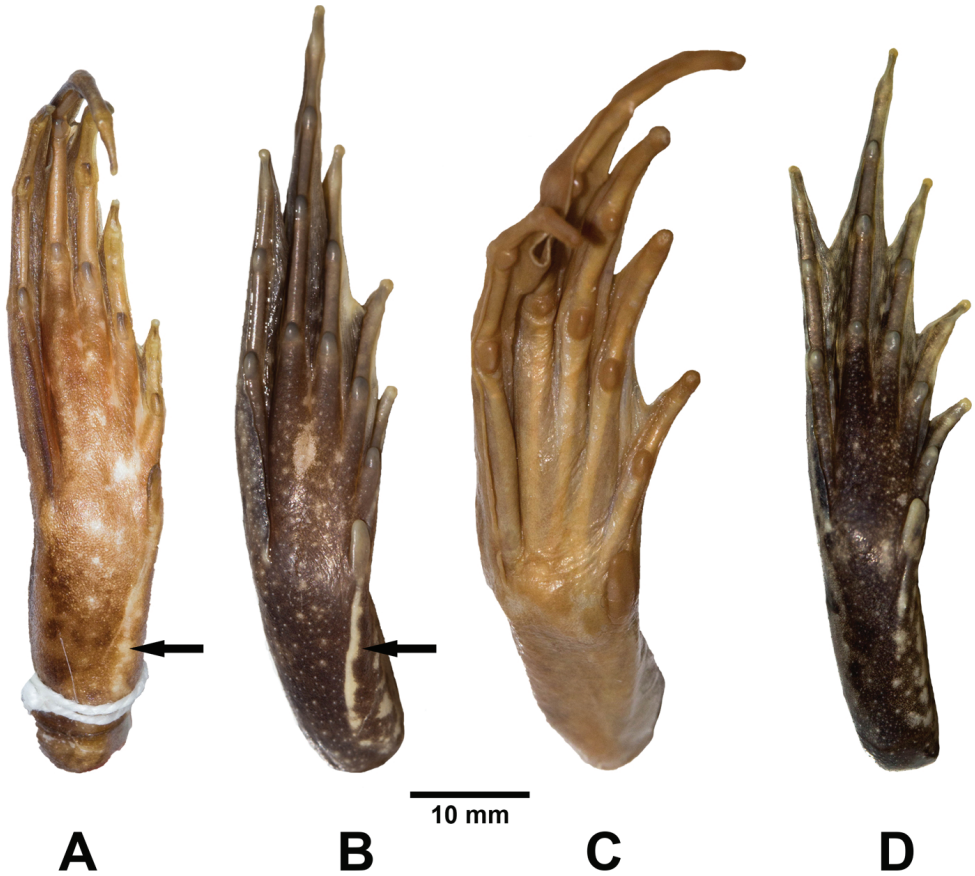


Figure 5. Plantar and metatarsal views of **A** adult male neotype of *Fejervarya cancrivora* (FMNH 256688) **B** adult male *F. cancrivora* (ZMKU AM 01426) from Khuan Khanun District, Phatthalung Province, Thailand **C** adult female holotype of *F. moodiei* holotype (CM 3724), and **D** adult male *F. moodiei* (ZMKU AM 10390) from Mueang Phang-nga District, Phang-nga Province, Thailand. The inner metatarsal ridge on the tarsus of *F. cancrivora* is indicated with an arrow.

than males. Two male specimens (ZMKU AM 01511 from Nakhon Si Thammarat Province, Thailand and CNHM 131100 from Java, Indonesia) have nuptial pads extending to the base of prepollax. Most male specimens have dense fine spinules over the entire surface of the chest, belly, and ventrolateral surface.

The examined male and female specimens closely resemble the neotype in morphology, with most observed variation pertaining to coloration. Dorsal coloration in preservative varied from medium to very dark brown with darker markings. Markings or spots on dorsum, and transverse spots on dorsal surface of forelimbs and hindlimbs fainter than neotype in some individuals. Flank pale brown with dark brown marbling in some individuals. Ventral coloration pale brown in some individuals, with dark mottling on chin and chest. Ventral surface of hand pale brown or creamy white in some individuals. Dorsal vertebral stripe present ($n = 18$, 41%) or absent ($n = 26$,

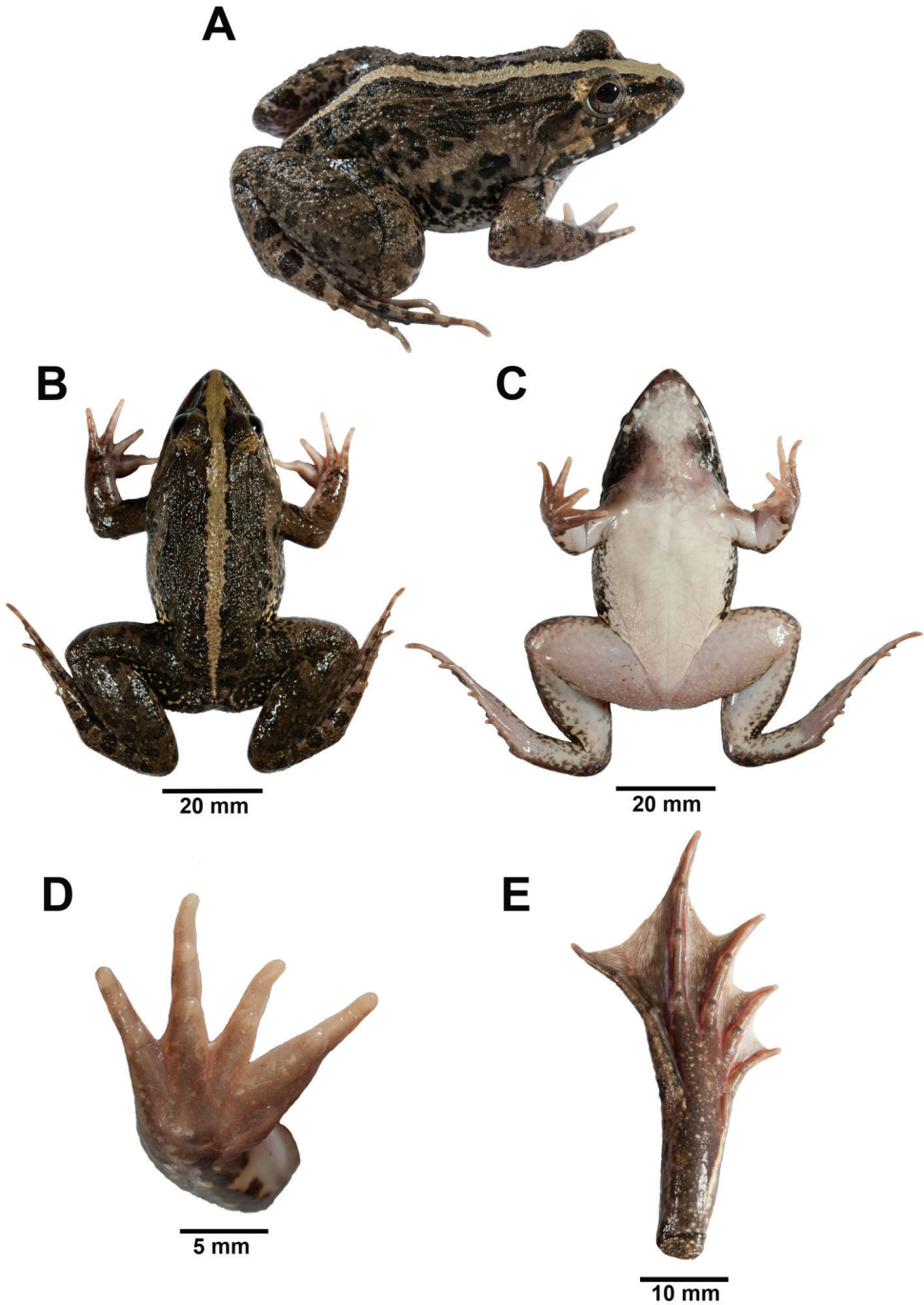


Figure 6. Adult male *Fejervarya cancrivora* (ZMKU AM 01426) from Khuan Khanun District, Phatthalung Province, Thailand (SVL = 66.9 mm) immediately prior to preservation in **A** right lateral **B** dorsal **C** ventral **D** right palmar, and **E** right plantar views. Photographs by Attapol Rujirawan.

59%). Two specimens from Nakhon Si Thammarat Province, Thailand (ZMKU AM 01509 and ZMKU AM 01513), have a narrow light brown stripe on tibia. Pineal body not visible in one male specimen from Pattani Province, Thailand (THNHM 21248).

Distribution. Based on a combination of the morphological and genetic studies of *F. cancrivora* large type (Kurniawan et al. 2010; 2011; 2014), the reported distribution of *F. raja* (Chan-ard 2013; Chuaynkern, and Chuaynkern 2012), and localities of specimens examined in this study, *F. cancrivora* is distributed from south of the Isthmus of Kra in Thailand, West Malaysia, Kalimantan (Borneo), Sumatra, West and Central Java, and Bali in Indonesia, with introduced populations in Papua New Guinea and Guam (Christy et al. 2007; Frost, 2019). In Thailand, *F. cancrivora* was confirmed to occur at Phatthalung, Nakhon Si Thammarat, Pattani, Songkhla, and Narathiwat Province (Fig. 1; Table 1).

Habitat, ecology and natural history. Specimens were collected in Thailand (Khuan Khanun District, Phatthalung Province and Pak Panang District, Nakhon Si Thammarat Province) at night (1900–2200 h) following light rain during May and October 2016. At Khuan Khanun, frogs were sampled in grasslands, rice paddy fields near standing or slow flowing ditches, and ponds at 1–24 m elevation (Fig. 7A). These were found sitting on the ground near water bodies, or hiding within grass or in mud cracks in the ground, and jumped to water bodies when disturbed. Other anuran species found in syntopy at this locality included *Duttaphrynus melanostictus* (Schneider, 1799), *F. limnocharis*, *Hoplobatrachus rugulosus* (Wiegmann, 1834), *Hylarana erythraea* (Schlegel, 1837), *Polypedates leucomystax* (Gravenhorst, 1829) and *Microhyla butleri* Boulenger, 1900. At Pak Phanang District, frogs were collected at night (1900–2100 h) after heavy rain in November 2017. These were found on the bank or in the water of brackish shrimp ponds near the Pak Phanang River at 0 m asl (Fig. 7B). No other anuran species were found in syntopy at this locality, although *F. moodiei* was sampled at a site approximately 4.5 air-km, or 5.2 km following the river course, upriver (below).

***Fejervarya moodiei* (Taylor, 1920)**

Rana moodiei Taylor, 1920: 234

Rana cancrivora: Taylor 1962: 377

Fejervarya moodiei: Dubois and Ohler 2000: 35; Brown et al. 2013: 17

Fejervarya cancrivora: Chan-ard 2003: 107; Chuaynkern and Chuaynkern 2012: 169; Kurniawan et al. 2010: 3

Fejervarya Bangladesh mangrove type Islam et al. 2008: 1084

Fejervarya cancrivora mangrove type Kurniawan et al. 2010: 222; Kurniawan et al. 2011: 12

Fejervarya cf. *cancrivora* Harikrishnan & Vasudevan, 2018: 241

Diagnosis. *Fejervarya moodiei* can be characterized by the following combination of characters: (1) medium to large size, SVL 42.7–62.7 mm in males, 50.0–81.8 mm in females (Table 4; Appendix 2, 3); (2) head length slightly greater than head width;

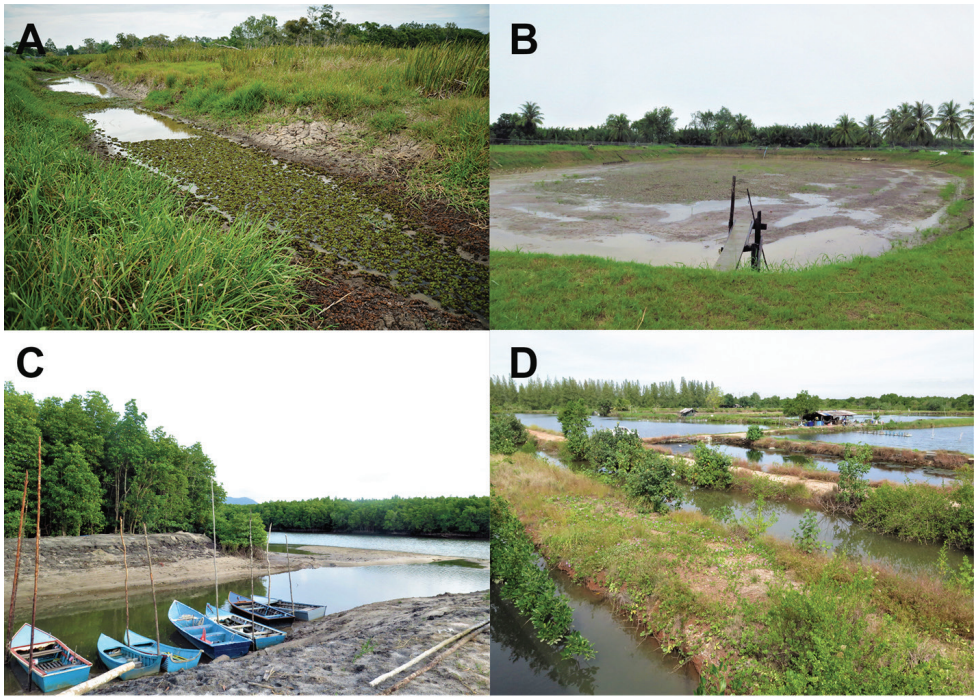


Figure 7. Exemplar habitats in Thailand of **A** *Fejervarya cancrivora* at a wetland in Khuan Khanun District, Patthalung Province **B** *F. cancrivora* at a brackish shrimp pond near Pak Phanang river, Pak Phanang District, Nakhon Si Thammarat Province **C** *F. moodiei* at mangrove forest in Thai Mueang District, Phang-nga Province, and **D** *F. moodiei* at brackish fish ponds near mangroves at the mouth of the Prasae River, Kleang District, Rayong Province. Photograph **A** by Attapol Rujirawan.

(3) skin on dorsum and flank with spinules, and glandular warts, with irregular skin folds not arranged in series, with darker marking on dorsal surface of forelimbs and hindlimbs; (4) relative finger lengths $II < IV < I < III$; (5) Most individual have dermal fringe on fingers II and III; (6) prepollax indistinct; (7) palmar tubercles indistinct; (8) foot moderately webbed, with webbing formula $I1-11/2III1-2III1-2IV2-1V$; (9) dermal flap on postaxial side of Toe V; (10) Fejervaryan lines absent; (11) inner metatarsal tubercles prominent; (12) indistinct inner tarsal ridge on distal half to two-thirds of tarsus (Fig. 6C–D) and (13) vocal sacs in adult males with wrinkled skin covered by triangular, very dark brown blotches on each side of throat.

Description of holotype. Taylor (1920) described the species based on an adult female, CM 3724, from Manila, Luzon, Philippines (Fig. 8A, B; Appendix 3). We supplement his description of the holotype, as follows: rather large body size; head narrow, slightly longer than wide; snout tip oval in dorsal view, round in lateral view, projecting beyond lower jaw; nostril dorsolateral, oval, with small lateral flap, closer to tip of snout than eye; canthus indistinct, rounded; loreal region slightly concave and oblique [loreal region broadly sloping, not concave according to Taylor (1920)]; eye diameter about 60% snout length [eye diameter equal to snout length according to Taylor (1920)]; interorbital region flat, about half width of upper eyelid and slightly

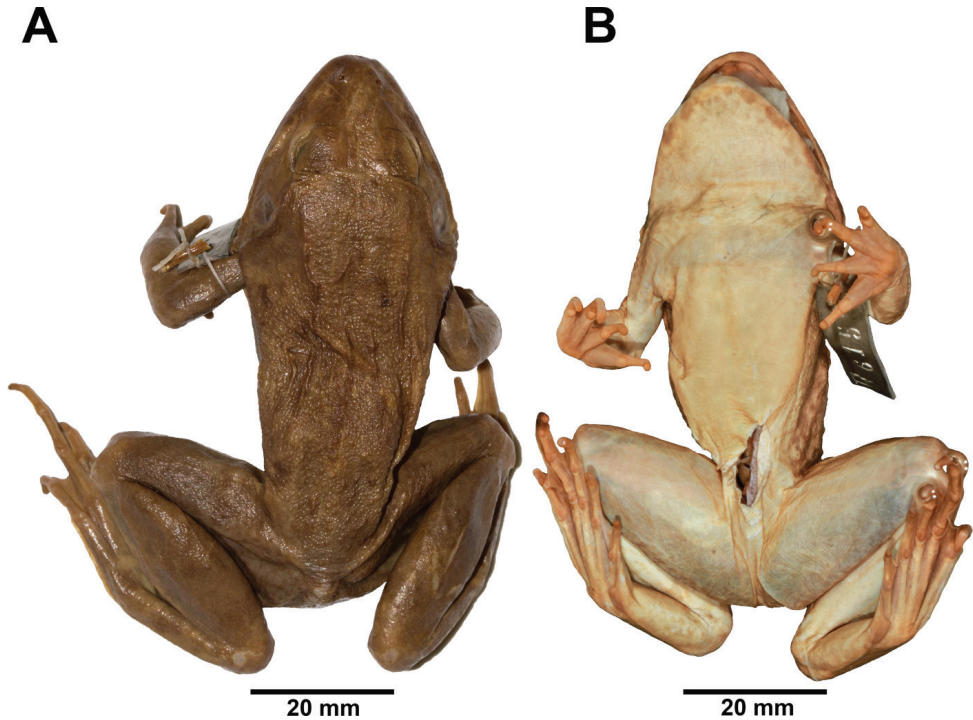


Figure 8. Adult female holotype of *Fejervarya moodiei* (CM 3724) in preservative in **A** dorsal and **B** ventral views. Photograph **B** by Carnegie Museum of Natural History.

less than internarial distance; pineal body present; tympanum distinct, rounded, about 90% of eye diameter, not depressed relative to skin of temporal region, tympanic rim weakly elevated relative to tympanum, dorsoposterior margin obscured by supratympanic fold; vomerine ridge present in two strongly oblique series, very slightly closer to each other than to choanae [based on Taylor (1920), not examined by us].

Forelimbs short, rather robust; fingers rather long, slightly swollen; tips of fingers slightly rounded, terminus slightly swollen but not expanded into discs; relative finger lengths $II < IV < I < III$ [first finger longer than second and fourth according to Taylor (1920)]; dermal fringe on fingers absent; webbing on fingers absent; subarticular tubercles distinct; supernumerary tubercles absent; prepollex indistinct, oval; palmar tubercles indistinct.

Hindlimbs moderately short, robust; tibia slightly longer than thigh, but shorter than distance from base of inner metatarsal tubercle to tip of Toe IV; toe long, stout; tips of toes rounded, not expanded into discs; relatively toe lengths $I < II < III < IV$, webbing moderate, deeply excised between toes, formula $I1-11/2II1-1III1-2IV2-1V$, Toe I webbed to base of distal phalanx; preaxial side of Toe II webbed to point between distal subarticular tubercle and distal phalanx, continuing as narrow fringe to base of distal phalanx; postaxial side of Toe II webbed to base of distal phalanx; preaxial side of Toe III webbed to distal subarticular tubercle, continuing as narrow fringe to base of distal phalanx, postaxial side of Toe III webbed to base of distal phalanx; preaxial side of

Toe IV wedged to webbed to proximal distal subarticular tubercle, continuing as narrow fringe to base of distal phalanx, postaxial side of Toe IV wedged to webbed to proximal distal subarticular tubercle, continuing as narrow fringe to base of distal phalanx, Toe V webbed to base of distal phalanx; dermal flap well developed, extending along postaxial side of Toe V from level of inner metatarsal tubercles to distal phalanx; subarticular tubercles prominent, inner metatarsal tubercle prominent, oval, length about 30% that of Toe I; distinct dermal ridge extending along inner metatarsal tubercle to distal phalanx of Toe I; indistinct inner tarsal ridge on distal two-third of tarsus (Fig. 7C); outer metatarsal tubercles absent; supernumerary tubercles absent; tarsal tubercle absent.

Skin on snout and between the eyes shagreened; skin on eyelid shagreened with glandular warts; skin on dorsum shagreened with glandular warts and irregular skin folds; dorsolateral fold extending posteriorly to two-thirds length of dorsum; skin on side of head smooth; skin on flank with glandular warts; skin on cloacal region with glandular warts; forelimbs shagreened; thigh with indistinct glandular warts; tibia, tarsus, throat, chest and belly smooth.

Coloration of holotype in preservative. Coloration mostly lost in preservative. Dorsum and side of head medium brown with a few dark brown markings; tympanum translucent brown with pale brown spot in center; flank pale brown with faint brown marbling; three wide brown vertical spots on upper lips; dorsal surfaces of forelimbs, thigh, tibia, and foot medium brown with a few dark brown spots, posterior surface of thigh with irregular pattern of indistinct dark brown marbling on light background; chin, chest, belly, and ventral surfaces of forelimb and hindlimb pale brown; ventral surfaces of hand and foot pale brown; lower lip pale brown with a few dark brown spots; vertebral and tibial stripes absent; Fejervaryan lines absent.

Coloration of referred Thai specimen in life. Adult male ZMKU AM 01390 (Fig. 9A–E) from Mueang Phang-nga District, Phang-nga Province, Thailand. SVL 44.7 mm. Dorsum and side of head light brown with indistinct olive brown marking; olive-brown band between outer margin of upper eyelids; tympanum with orange-brown blotches in center; olive-brown streak on canthus rostralis from tip of snout to eye; dark brown streak from eye along supratympanic fold to posterior rim of tympanum; flank creamy white with dark brown marbling; three wide dark brown spots on upper lips; dorsal part of limbs: forelimbs, thigh, tibia, and foot light brown with olive-brown transverse spots, posterior part of thigh with irregular pattern of dark brown marbling on creamy yellow background; ventral part of body: chin creamy white with indistinct mottled dark brown, triangular dark brown blotches and mottling on each side of throat; forelimbs, chest, belly creamy white and hindlimbs with indistinct dark brown mottling, hand brown and foot dark brown; lower lip creamy white with dark brown spots; Fejervaryan lines absent.

Variations. Vomerine ridges slightly closer to choanae than to each other in some individuals. Most adult males have nuptial pads with small translucent spinules on dorsal and medial surface of Finger I from base of distal phalanx to base of prepollex, but some individuals have the nuptial pad extending to slightly over the base of prepollex. Most adult males have dense, fine spinules covering only the chin, but some

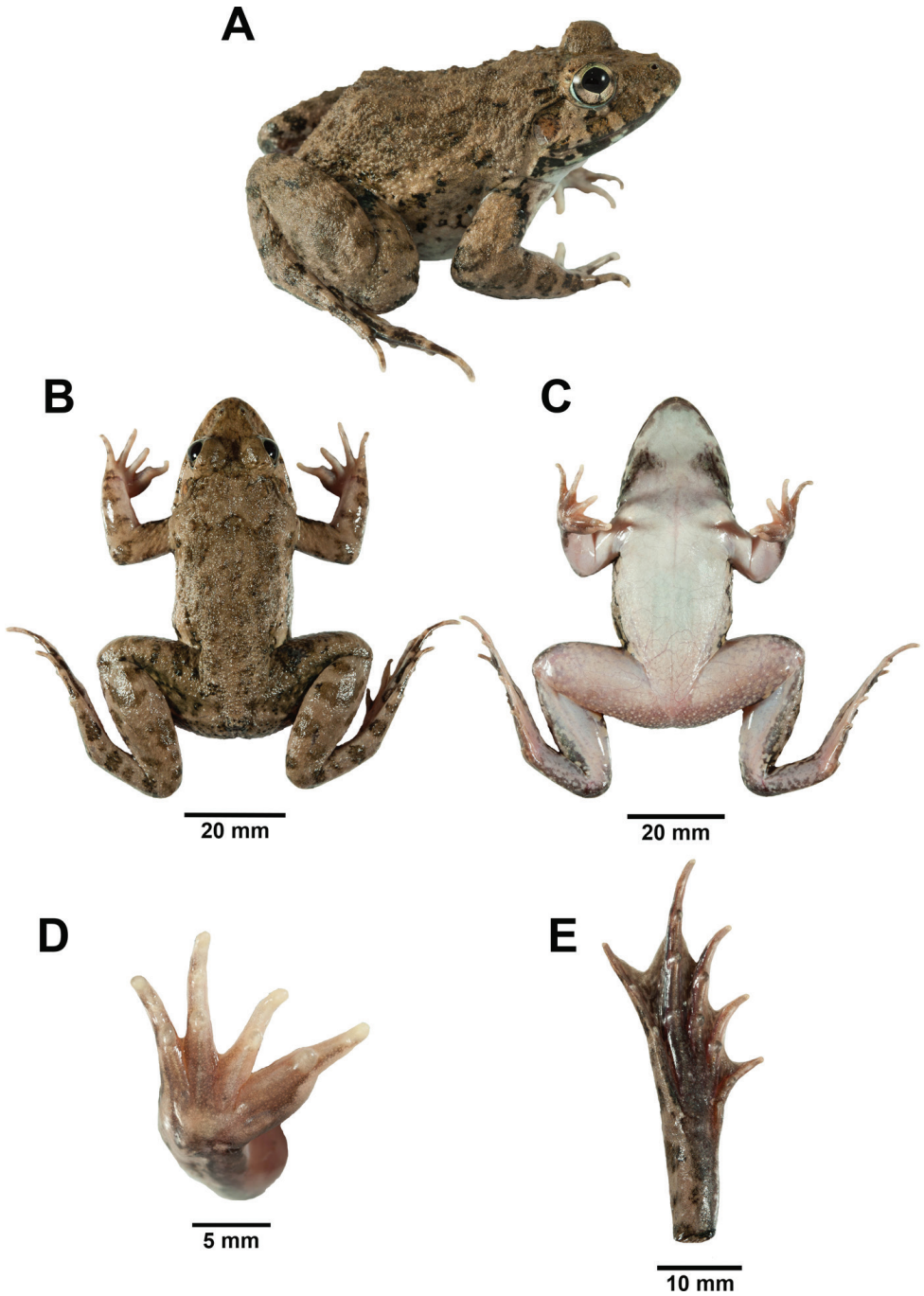


Figure 9. Adult male *Fejervarya moodiei* (ZMKU AM 01390) from Mueang Phang-nga District, Phang-nga Province, Thailand (SVL = 60.6 mm) immediately prior to preservation in **A** right lateral **B** dorsal **C** ventral **D** right palmar, and **E** right plantar views. Photographs by Attapol Rujirawan.

individuals have dense, fine spinules on the chin and chest. Adult males have vocal sac present on each side of throat with wrinkled skin covered by triangular, very dark brown blotches. Adult males with larger spinules and glandular warts on dorsum, dorsal surfaces of forelimbs, flank, hindlimbs and vent region. Females are distinctly larger in size (Table 4, Appendix 3), lack nuptial pads and vocal sacs, having fewer spinules and glandular warts on dorsal surface of body and flank than males.

Dorsal coloration in preservative varies in males and females from brown to dark brown with darker markings. Two female specimens from Trat Province, Thailand (ZMKU AM 01444 and 01451) have dark orange markings on anterior part of dorsum. Markings or transverse spots on dorsum and dorsal surfaces of forelimbs and hindlimbs usually distinct, but faint in a few individuals. Coloration on flank usually creamy white, but pale brown, with dark brown marbling, in some individuals. Ventral coloration usually creamy white, but pale brown with indistinct dark mottling on chin and chest in some individuals. Hand usually creamy white, but light brown in some individuals. Most specimens have dermal fringe on fingers II and III (males $N = 21$, 70%; females $N = 23$, 69.7%), but some individuals lack this fringe (males $N = 9$, 30%; females $N = 10$, 30.3%). One specimen from Narathiwat Province, Thailand (THNHM 19720) has a vertebral stripe.

Distribution. Based on a combination of morphological and genetic studies of *F. cancrivora* mangrove type (Kurniawan et al. 2010, 2011, 2014) and *Fejervarya* Bangladesh mangrove type (Islam et al. 2008), the reported distribution of *F. cancrivora* (Chan-ard 2003; Chuaynkern and Chuaynkern 2012), *F. moodiei* (Brown et al. 2013), and *F. cf. cancrivora* (Harikrishnan and Vasudevan 2018), and specimens studied here, *F. moodiei* occurs in coastal areas from eastern India, the Andaman and Nicobar Islands, and southern China, southward through Vietnam, Thailand, Myanmar, Malaysia and Luzon Island in the Philippines. In Thailand, *F. moodiei* was documented in all coastal regions except the extreme southeastern Gulf of Thailand coast, where it is replaced by *F. cancrivora* (Fig. 1).

Habitat, ecology, and natural history. In Thailand, specimens were collected at night (1900–2200 h) in a variety of coastal habitats at elevations ranging from 0–16 m asl. Most specimens were observed in marshes near slow flowing ditches, ponds, or canals in mangrove forest (Fig. 7C). The species was also found in man-made environments such as agricultural fields adjacent to mangroves. In Kleang District, Rayong Province, most specimens were collected in and around brackish fish ponds and ditches in mangrove areas near the mouth of the Prasae River (Fig. 7D). Specimens from Pak Phanang District, Nakhon Si Thammarat Province were found around brackish shrimp ponds and ditches near the mouth of the Pak Phanang River. Frogs were observed sitting on the ground, under tree roots, or in or on the bank of water bodies. When disturbed, they usually escaped into holes in the ground or jumped into brackish water. No other anuran species were found in syntopy at this locality, although *F. cancrivora* was sampled at a site approximately 4.5 air-km, or 5.2 km following the river course, downriver (above).

Comparisons. Twelve species of *Fejervarya* are known (Frost 2019), with nine species occurring in East and Southeast Asia (Sanchez et al. 2018). Four species of *Fejervarya* occur in Thailand, including *F. limnocharis* (Gravenhorst, 1829), *F. multistriata*

(Hallowell, 1861), *F. orissaensis* (Dutta, 1997), and *F. triora* Stuart et al, 2006. Three additional *Fejervarya* species occur in adjacent countries, including *F. iskandari* Vieth et al. 2001, *F. sakishimensis* Matsui et al., 2007, and *F. kawamurai* Djong et al., 2011.

Fejervarya cancrivora and *F. moodiei* differ from all of these species by having the following combination of characters: (1) medium to large body size (vs. small to medium, SVL about 30–40 mm in males for *F. iskandari*, *F. kawamurai*, *F. limnocharis*, SVL about 40–55 mm in males for *F. multistriata*, *F. orissaensis*, *F. triora* [Dutta 1997; Matsui et al. 2007; Chuaynkern et al. 2009; Djong et al. 2011]); (2) webbing formula: I1–11/2II1–2III1–2IV2–1V (vs. I0–1II0–11/2III0–11/2IV11/2–0V in *F. vittigera*, I1–2II1–2III1–22/3IV22/3–11/2V in *F. limnocharis*, I1–2II1–2III1–22/3IV21/3–1V in *F. iskandari*, I1–2II1–2III11/2–22/3 IV22/3–1V in *F. multistriata*, I1–2II1–21/2III11/2–3IV3–11/2V in *F. sakishimensis*, I1–2II1–21/3III11/2–3IV3–1V in *F. kawamurai*); (3) having triangular or rectangular dark brown blotches covering vocal sacs on both sides of throat (vs. black “M” shape across throat in *F. kawamurai*, *F. limnocharis*, *F. sakishimensis*, *F. triora*, *F. vittigera*); (4) having prepollax indistinct (vs. distinct in *F. kawamurai*, *F. iskandari*, *F. limnocharis*, *F. sakishimensis*, *F. triora*), and (6) having palmar tubercles indistinct (vs. distinct *F. kawamurai*, *F. limnocharis*, *F. sakishimensis*, *F. triora*).

Fejervarya moodiei differs from *F. cancrivora* by having: (1) SVL 42.7–62.7 mm in males, 50.0–81.8 mm in females (vs. 60.2–79.8 mm in males, 85.1–107.1 mm in females of *F. cancrivora*, Table 4; Appendix 2, 3); (2) indistinct, slightly raised inner tarsal ridge on tarsus (vs. distinct, strongly raised inner tarsal ridge on distal half or two-thirds of tarsus in *F. cancrivora*) (Fig. 5A–D); and (3) in body proportions (Table 4). In Thailand, *F. moodiei* appears to be closely associated with brackish water in or adjacent to mangrove forest, whereas *F. cancrivora* also occurs in freshwater wetlands.

Discussion

Our study clarifies that two species of crab-eating frogs (*Fejervarya cancrivora* complex) occur in mainland Southeast Asia: *F. moodiei* in coastal regions throughout mainland Southeast Asia, with replacement by *F. cancrivora* sensu stricto in extreme southern Thailand (on the Gulf of Thailand coast) and peninsular Malaysia. These findings corroborate those of Kurniawan et al. (2010; 2011) that the name *F. moodiei* is the correct name to apply to populations of the *F. cancrivora* complex throughout most of coastal mainland Southeast Asia. Our study provides the first molecular evidence that *F. raja* from southern Thailand represents only a large-bodied population of *F. cancrivora* sensu stricto, as suspected but untested by Iskandar (1998) and Kurniawan et al. (2010, 2011). Both *F. cancrivora* and *F. moodiei* have wide geographic distributions that span coastlines of both mainland and insular Southeast Asia (Fig. 1), a likely testament to their remarkable tolerance of salt and brackish water (e.g., Gordon et al. 1961; Balinsky et al. 1972; Wright et al. 2004; Hopkins and Brodie 2015). Although our findings of two Southeast Asian frog species having wide geographic distributions is inconsistent with many recent analyses of other taxa (e.g., Stuart et al. 2006; Aowphol et al. 2013; Geissler et al. 2014; Phimmachak et al. 2015; Wogan et al. 2016; Sheridan and Stuart 2018), the conserved

morphology of the *F. cancrivora* complex has long hindered accurately understanding species diversity and distributions of these frogs, as evidenced by the conflicting interpretations of experienced systematic herpetologists (e.g., Smith 1930; Inger 1954; Taylor 1962). Hence, the integrative taxonomic approach used here that incorporated both molecular and morphological data, including from topotypes and name-bearing type specimens, respectively, proved to be imperative for resolving these uncertainties.

This study provides a basis for revising the identifications of historical and contemporary records (both museum vouchers and literature descriptions) of crab-eating frogs to improve the finer-scale details of the geographic ranges, as well as the natural histories, of *F. cancrivora* and *F. moodiei* in mainland Southeast Asia. Our sampling did not reveal *F. cancrivora* and *F. moodiei* to occur in sympatry, but did find the two species to occur in shrimp ponds that were separated by only approximately 4.5 air-km (or 5.2 km following the river course) along the Pak Phanang River in Pak Phanang District, Nakhon Si Thammarat Province, Thailand (Fig. 1; Appendix 1). The Pak Phanang locality of *F. moodiei* (8°19.850'N, 100°11.870'E) lies closer to the river mouth and has higher saltwater intrusion than does the Pak Phanang locality of *F. cancrivora* (8°17.454'N, 100°11.229'E) that lies further upstream of a complex system of water gates and irrigation canals that were constructed in the 1960s to reduce saltwater intrusion and facilitate rice production (Boromthananarat et al. 1991). It is not known if the two species were separated at these shrimp ponds because the two localities are coincident with the boundaries of their geographic ranges, or if the two species differ in saltwater tolerance and other aspects of their ecology. Future sampling to clarify the fine-scale partitioning of the two species where their ranges come into contact is warranted.

Acknowledgments

This research was supported by the Center of Excellence on Biodiversity (BDC), Office of Higher Education Commission, Thailand (BDC-PG4-160022). The research protocol was approved by the Institutional Animal Care and Use Committee, Kasetsart University, Thailand (project number OACKU00459). Alan Resetar (FMNH), Sunchai Makchai (THNHM), and Stephen Rogers, Jennifer Sheridan and Kaylin Martin (CM) facilitated the study of specimens in their care. David S. McLeod provided helpful suggestions with the morphological study. Attapol Rujirawan assisted with statistical analyses and provided photographs. Attapol Rujirawan, Korkwan Termprayoon, Natee Ampai, and Piyawan Puanprapai assisted with field work. David S. McLeod and Guinevere O. U. Wogan improved the manuscript.

References

Aowphol A, Rujirawan A, Taksintum W, Arsirapot S, McLeod DS (2013) Re-evaluating the taxonomic status of *Chiromantis* in Thailand using multiple lines of evidence (Am-

- phibia: Anura: Rhacophoridae). *Zootaxa* 3702(2): 101–123. <https://doi.org/10.11646/zootaxa.3702.2.1>
- Balinsky JB, Dicker SE, Elliott AB (1972) The effect of long-term adaptation to different levels of salinity on urea synthesis and tissue amino acid concentrations in *Rana cancrivora*. *Comparative Biochemistry and Physiology Part B: Comparative Biochemistry* 43(1): 71–82. [https://doi.org/10.1016/0305-0491\(72\)90203-9](https://doi.org/10.1016/0305-0491(72)90203-9)
- Bickford D, Lohman DJ, Sodhi NS, Ng PKL, Meier R, Winker K, Ingram KK, Das I (2006) Cryptic species as a window on diversity and conservation. *Trends in Ecology and Evolution* 22(3): 14–155. <https://doi.org/10.1016/j.tree.2006.11.004>
- Boromthanasart S, Cobb S, Lee V (1991) Coastal Management in Pak Phanang: A Historical Perspective of the Resources and Issue. In: Boromthanasart S, Cobb S, Lee V (Eds) Chapter 3. Freshwater: a prime concern. Coastal Resources Institute, Prince of Songkla University, Hat Yai, 22–33.
- Brown RF, Siler CD, Olivers CH, Welton LJ, Rock A, Swab J, Weerd MV, van Beijnen J, Jose E, Rodriguez D, Jose E, Diesmos AC (2013) The amphibians and reptiles of Luzon Island, Philippines, VIII: the herpetofauna of Cagayan and Isabela Provinces, northern Sierra Madre Mountain Range. *ZooKeys* 266: 1–120. <http://doi.org/10.3897/zookeys.266.3982>
- Brown RM, Stuart BL (2012) Patterns of biodiversity discovery through time: an historical analysis of amphibian species discoveries in the Southeast Asian mainland and adjacent island archipelagos. In: Gower DJ, Johnson KG, Richardson JE, Rosen BR, Rüber L, Williams SL (Eds) *Biotic Evolution and Environmental Change in Southeast Asia*. Cambridge University Press, 348–389. <https://doi.org/10.1017/CBO9780511735882.016>
- Chan-ard T (2003) *A Photographic Guide to Amphibians in Thailand*. Darnsutha Press Co. Ltd., Bangkok, 175 pp. [In Thai]
- Che J, Hu JS, Zhou WW, Murphy RW, Papenfuss TJ, Chen MY, Rao DQ, Li PP, Zhang YP (2009) Phylogeny of the Asian spiny frog tribe Painei (Family Dicroglossidae) sensu Dubois. *Molecular Phylogenetics and Evolution* 50: 59–73. <https://doi.org/10.1016/j.ympev.2008.10.007>
- Che J, Pang J, Zhao H, Wu GF, Zhao EM, Zhang YP (2007) Molecular phylogeny of the Chinese ranids inferred from nuclear and mitochondrial DNA sequences. *Biochemical Systematics and Ecology* 35: 29–35. <https://doi.org/10.1016/j.bse.2006.09.003>
- Chen LQ, Murphy RW, Lathrop A, Ngo A, Orlov NL, Ho CT, Somorja ILM (2005) Taxonomic chaos in Asian Ranid frogs: an initial phylogenetic resolution. *Herpetological journal* 15: 231–243.
- Chuaynkern Y, Chuaynkern C (2012) A checklist of amphibians in Thailand. *Journal of Wildlife in Thailand* 19(1): 163–211. [In Thai]
- Chuaynkern Y, Salangsingha N, Makchai S, Inthara C, Duengkhae P (2009) *Fejervarya trionra* (Amphibia, Ranidae): first description of the adult male and recent distribution records. *Alytes* 27(1): 13–24.
- Christy MY, Clark CS, Gee DEI, Vice D, Vice DS, Warner MP, Tyrrell CL, Rodda GH, Savidge JA (2007) Recent records of alien anurans on the Pacific island of Guam. *Pacific Science*. 61(4): 469–484. [https://doi.org/10.2984/1534-6188\(2007\)61\[469:RROAAO\]2.0.CO;2](https://doi.org/10.2984/1534-6188(2007)61[469:RROAAO]2.0.CO;2)
- Darriba D, Taboada GL, Doallo R, Posada D (2012) jModelTest 2: more models, new heuristics and parallel computing. *Nature Methods* 9(8): 772. <https://doi.org/10.1038/nmeth.2109>

- Djong TH, Matsui M, Kuramoto M, Belabut DM, Yong HS, Nishioka M, Sumida M (2007) Morphological divergence, reproductive isolating mechanism, and molecular phylogenetic relationships among Indonesia, Malaysia, and Japan population of the *Fejervarya limnocharis* complex (Anura, Ranidae). *Zoological Science* 24: 1197–1212. <https://doi.org/10.2108/zsj.24.1197>
- Djong TH, Matsui M, Kuramoto M, Nishioka M, Sumida M (2011) A new species of the *Fejervarya limnocharis* complex from Japan (Anura, Dicroglossidae). *Zoological Science* 28: 922–929. <https://doi.org/10.2108/zsj.28.922>
- Dubois A, Ohler A (2000) Systematics of *Fejervarya limnocharis* (Gravenhorst, 1829) (Amphibia, Anura, Ranidae) and related species. 1. Nomenclatural status and type-specimens of the nominal species *Rana limnocharis* Gravenhorst, 1829. *Alytes* 18: 15–50.
- Dutta SK (1997) A new species of *Limnonectes* (Anura: Ranidae) from Orissa, India. *Hamadryad* 22(1): 1–8.
- Evans BJ, Brown RM, McGuire JA, Supriatna J, Andayani N, Diesmos A, Iskandar D, Melnick DJ, Cannatella DC (2003) Phylogenetics of Fanged Frogs: Testing Biogeographical Hypotheses at the Interface of the Asian and Australian Faunal Zones. *Systematic Biology* 52(6): 794–819. <https://doi.org/10.1093/sysbio/52.6.794>
- Frost DR (2019) Amphibian Species of the World: an Online Reference Version 6.0. <http://research.amnh.org/vz/herpetology/amphibia/> [accessed 26-03-2019]
- Geissler P, Poyarkov NA Jr, Grismer L, Nguyen TQ, An HT, Neang T, Kupfer A, Ziegler T, Böhme W, Müller H (2014) New *Ichthyophis* species from Indochina (Gymnophiona, Ichthyophiidae): 1. The unstriped forms with descriptions of three new species and the redescriptions of *I. acuminatus* Taylor, 1960, *I. youngorum* Taylor, 1960 and *I. laosensis* Taylor, 1969. *Organisms, Diversity & Evolution* 15(1): 143–174. <https://doi.org/10.1007/s13127-014-0190-6>
- Gordon MS, Schmidt-Nielsen K, Kelly HM (1961) Osmotic regulation in the Crab-eating Frog (*Rana cancrivora*). *Journal of Experimental Biology* 38(3): 659–678.
- Gravenhorst JLC (1829) *Deliciae Musei Zoologici Vratislaviensis. Fasciculus primus. Chelonios et Batrachia.* Leopold Voss, Leipzig 1, 41 pp.
- Hasan M, Islam MM, Khan MdMR, Alam MS, Kurabayashi A, Igawa T, Kuramoto M, Sumida M (2012) Cryptic anuran biodiversity in Bangladesh revealed by mitochondrial 16S rRNA gene sequences. *Zoological Science* 29: 162–172. <https://doi.org/10.2108/zsj.29.162>
- Hasan M, Islam MM, Md Khan MdMR, Igawa T, Alam MS, Djong HT, Kurniawan N, Joshy H, Sen YH, Belabut DM, Kurabayashi A, Kuramoto M, Sumida M (2014) Genetic divergences of South and Southeast Asian frogs: a case study of several taxa based on 16S ribosomal RNA gene data with notes on the generic name *Fejervarya*. *Turkish Journal of Zoology* 38: 389–41. <https://doi.org/10.3906/zoo-1308-36>
- Harikrishnan S, Vasudevan K (2018) Amphibians of the Andaman & Nicobar Islands: distribution, natural history, and notes on taxonomy. *Alytes* 36(1–4): 238–265.
- Hopkins G, Brodie ED Jr (2015) Occurrence of Amphibians in Saline Habitats: A Review and Evolutionary Perspective. *Herpetological Monographs* 29: 1–27. <https://doi.org/10.1655/HERPMONOGRAPHS-D-14-00006>
- Husson F, Le S, Pagès J (2017) *Exploratory Multivariate Analysis by Example Using R* (2nd edn). Chapman and Hall/CRC Press, New York, 262 pp.

- Lê S, Josse J, Husson F (2008) FactoMineR: An R Package for Multivariate Analysis. *Journal of Statistical Software* 25(1):1–18. <https://doi.org/10.18637/jss.v025.i01>
- Inger RF (1954) Systematics and zoogeography of Philippine amphibia. *Fieldiana Zoology* 33(4): 183–531. <https://doi.org/10.5962/bhl.title.5571>
- Islam MM, Kurose N, Khan MMR, Nishizawa T, Kuramoto M, Alam MS, Hasan M, Kurniawan N, Nishioka M, Sumida M (2008) Genetic divergence and reproductive isolation in the genus *Fejervarya* (Amphibia: Anura) from Bangladesh inferred from morphological observations, crossing experiments, and molecular analyses. *Zoological Sciences* 25(11): 1084–1105. <http://doi.org/10.2108/zsj.25.1084>
- Iskandar DT (1998) The Amphibian of Java and Bali. Research and Development Centre for Biology-LIPI and GEF Biodiversity Collections Project, Indonesia, 117 pp.
- Kotaki, M, Kurabayashi A, Matsui M, Khonsue W, Djong TH, Tandon M, Sumida M (2008) Genetic divergence and phylogenetic relationships among the *Fejervarya limnocharis* complex in Thailand and neighboring countries revealed by mitochondrial and nuclear genes. *Zoological Science* 25: 381–390. <http://doi.org/10.2108/zsj.25.381>
- Kotaki M, Kurabayashi A, Matsui M, Kuramoto M, Djong TH, Sumida M (2010) Molecular phylogeny of the diversified frogs of genus *Fejervarya* (Anura: Dicroglossidae). *Zoological Science* 27: 386–395. <https://doi.org/10.2108/zsj.27.386>
- Kumar S, Stecher G, Li M, Knyaz C, Tamura K (2018) MEGA X: Molecular Evolutionary Genetics Analysis across computing platforms. *Molecular Biology and Evolution* 35: 1547–1549. <https://doi.org/10.1093/molbev/msy096>
- Kurniawan N, Djong TH, Islam MM, Nishizawa T, Belabut DM, Sen YH, Wanichanon R, Yasir I, Sumida M (2011) Taxonomic status of three types of *Fejervarya cancrivora* from Indonesia and other Asian countries based on morphological observations and crossing experiments. *Zoological Science* 28: 12–24. <https://doi.org/10.2108/zsj.28.12>
- Kurniawan N, Djong TH, Maidliza T, Harmidy A, Hasan M, Igawa T, Sumida M (2014) Genetic divergence and geographic distribution of frogs in genus *Fejervarya* from Indonesia from mitochondrial 16S rRNA gene analysis. *Treubia* 41: 1–16. <https://doi.org/10.14203/treubia.v41i0.361>
- Kurniawan N, Islam MM, Djong TH, Igawa T, Daicus MB, Yong HS, Wanichanon R, Khan MdMR, Iskandar DT, Nishioka M, Sumida M (2010) Genetic divergence and evolutionary relationship in *Fejervarya cancrivora* from Indonesia and other Asian countries inferred from allozyme and mtDNA sequence analyses. *Zoological Science* 27: 222–233. <https://doi.org/10.2108/zsj.27.222>
- Matsui M, Panha S, Khonsue W, Kuraishi N (2010) Two new species of the “*kublii*” complex of the genus *Limnonectes* from Thailand (Anura: Dicroglossidae). *Zootaxa* 2615:1–22. <https://doi.org/10.11646/zootaxa.2615.1.1>
- Matsui M, Toda M, Ota H (2007) A new species of frog allied to *Fejervarya limnocharis* from southern Ryukyus, Japan (Amphibia: Ranidae). *Current Herpetology* 26: 65–79. [https://doi.org/10.3105/1881-1019\(2007\)26\[65:ANSOFA\]2.0.CO;2](https://doi.org/10.3105/1881-1019(2007)26[65:ANSOFA]2.0.CO;2)
- Nutphud W (2001) Amphibia of Thailand. Amarin Printing and Publishing Public Co. Ltd., Bangkok, Thailand, 320 pp. [in Thai]
- Palumbi SR (1996) Nucleic acids II: the polymerase chain reaction. In: Hillis DM, Moritz C, Mable BK (Eds) *Molecular Systematics*. Second edition. Sinauer Associates, Inc. Sunderland, Massachusetts, 205–247.

- Phimmachak S, Aowphol A, Stuart BL (2015) Morphological and molecular variation in *Tyloporosus* (Caudata: Salamandridae) in Laos, with description of a new species. *Zootaxa* 4006(2): 285–310. <https://doi.org/10.11646/zootaxa.4006.2.3>
- R Development Core Team (2017) R: A language and environment for statistical computing. R Foundation for Statistical Computing, Vienna. <http://www.r-project.org>
- Rambaut A, Drummond AJ, Xie D, Baele G, Suchard MA (2018) Posterior summarisation in Bayesian phylogenetics using Tracer 1.7. *Systematic Biology* 67(5): 901–904. <https://doi.org/10.1093/sysbio/syy032>
- Ronquist F, Teslenko M, Van Der Mark P, Ayres DL, Darling A, Höhna S, Larget B, Liu L, Suchard MA, Huelsenbeck JP (2012) MrBayes 3.2: efficient Bayesian phylogenetic inference and model choice across a large model space. *Systematic Biology* 61: 539–542. <https://doi.org/10.1093/sysbio/sys029>
- Sanchez E, Biju SD, Islam MM, Hasan M, Ohler A, Vences M, Kurabayashi A (2018) Phylogeny and classification of fejevaryan frogs (Anura: Dicroglossidae). *Salamandra* 54(2): 109–116.
- Savage JM, Heyer WR (1967) Variation and distribution in the tree-frog genus *Phyllomedusa* in Costa Rica, central America. *Beiträge zur Neotropischen Fauna*. Stuttgart 5: 111–131. <https://doi.org/10.1080/01650526709360400>
- Sheridan JA, Stuart BL (2018) Hidden species diversity in *Sylvirana nigrovittata* (Amphibia: Ranidae) highlights the importance of taxonomic revisions in biodiversity conservation. *PLoS ONE* 13(3): e0192766. <https://doi.org/10.1371/journal.pone.0192766>
- Smith M (1927) Contributions to the herpetology of the Indo-Australian Region. *Proceedings of the Zoological Society of London* 1927: 199–225. <https://doi.org/10.1111/j.1096-3642.1927.tb02255.x>
- Smith MA (1930) The reptilia and amphibia of the Malay Peninsula. A supplement to G. A. Boulenger's reptilia and Batrachia, 1912. *Bulletin of the Raffles Museum*. Singapore 3: 96–97.
- Stuart BL, Chuaynkern Y, Chan-ard T, Inger RF (2006a) Three new species of frogs and a new tadpole from eastern Thailand. *Fieldiana Zoology New Series* 111: 1–19. [https://doi.org/10.3158/0015-0754\(2006\)187\[1:TNSOFA\]2.0.CO;2](https://doi.org/10.3158/0015-0754(2006)187[1:TNSOFA]2.0.CO;2)
- Stuart BL, Inger RF, Voris HK (2006b) High level of cryptic species diversity revealed by sympatric lineages of Southeast Asian forest frogs. *Biology Letters* 2: 470–474. <http://doi.org/10.1098/rsbl.2006.0505>
- Sumida M, Kondo Y, Kanamori Y, Nishioka M (2002) Inter- and intraspecific evolutionary relationships of the rice frog *Rana limnocharis* and allied species *R. cancrivora* inferred from crossing experiments and mitochondrial DNA sequences of the 12S and 16S rRNA genes. *Molecular phylogenetics and evolution* 25: 293–305. [https://doi.org/10.1016/S1055-7903\(02\)00243-9](https://doi.org/10.1016/S1055-7903(02)00243-9)
- Taylor EH (1920) Philippine Amphibia. *The Philippine Journal of Science* 16: 213–359.
- Taylor EH (1962) The amphibian fauna of Thailand. *The University of Kansas Science Bulletin* 43: 265–599.
- Vieth M, Kosuch J, Ohler A, Dubois A (2001) Systematics of *Fejervarya limnocharis* (Gravenhorst, 1829) (Amphibia, Anura, Ranidae) and related species. 2. Morphological and molecular variation in frogs from the Greater Sunda Islands (Sumatra, Java, Bornea) with the definition of two species. *Alytes* 19(1): 5–28.

- Wogan GOU, Stuart BL, Iskandar DT, McGuire JA (2016) Deep genetic structure and ecological divergence in a widespread human commensal toad. *Biology Letters* 12: 20150807. <http://doi.org/10.1098/rsbl.2015.0807>
- Wright P, Anderson P, Weng L, Frick N, Wong WP, IP YK (2004) The crab-eating frog, *Rana cancrivora*, up-regulates hepatic carbamoyl phosphate synthetase I activity and tissue osmolyte levels in response to increased salinity. *Journal of Experimental Zoology* 301A(7): 559–568. <https://doi.org/10.1002/jez.a.54>

Appendix I

Specimens examined.

- Fejervarya cancrivora* (Gravenhorst, 1829): **Indonesia**, Java: CNHM 131093, 131100, 131105–09, 161102, 191098, 313095, FMNH 131108, 131111; West Java, Cianjur FMNH 256688 (neotype); **Thailand**, Nakhon Si Thammarat Province: FMNH 174052–53; Pak Phanang District: (8°17.454'N, 100°11.229'E) ZMKU AM 01507–13; THNHM 25499; Narathiwat Province, Su-Ngai Kolok District: THNHM 19221, 20754; Tak Bai District: THNHM 19722–23, 19726–28, 19764–71; Pattani Province, Nong Chick District: THNHM 15623, 21248–49; Phatthalung Province: CNHM 175923–26; Khuan Khanun District: (7°45.580'N, 100°9.446'E): ZMKU AM 01415–26, 01427–29, (7°44.127'N, 100°8.635'E) ZMKU AM 01430–34; Pak Phayun District: THNHM 19852–57; Songkhla Province: THNHM 04332, 04955–56
- Fejervarya moodiei* (Taylor, 1920): **Malaysia**: CNHM 161312; **Philippines**, Northern Luzon: FMNH 161693, 161697; Luzon, Manila: CM 3724 (holotype); **Thailand**: Chonburi Province: FNHM 190532, THNHM 04919–21, Mueang Chonburi District: THNHM 06408–12; Chumphon Province, Moo Ko Chumphon National Park: THNHM 01030–33; Krabi Province, Ko Lanta District (7°35.702'N, 99°4.272'E): ZMKU AM 01405–14, Mueang Krabi District (8°4.502'N, 98°55.506'E): ZMKU AM 01487–90; Nakhon Si Thammarat Province, Khanom District (9°12.760'N, 99°50.969'E): ZMKU AM 01435–41; Pak Phanang District (8°19.850'N, 100°11.870'E): ZMKU AM 01464–79; Narathiwat Province, Tak Bai District: THNHM 19720–21, 19724–25; Phang-nga Province, Mueang Phang-nga District (8°25.998'N, 98°30.973'E): ZMKU AM 01390–98; Phatthalung Province, Songkhla lake: THNHM 04332–33; Phuket Province, Mueang Phuket District (7°54.522'N, 98°24.425'E): ZMKU AM 01376–83, 01399–404; Prachuap Khiri Khan Province, Kui Buri District (12°8.143'N, 99°57.737'E): ZMKU AM 01491–92, Sam Roi Yot District: ZMKU AM 01368–71; Ranong Province, Kra Buri District (10°19.435'N, 98°45.894'E): ZMKU AM 01372–75, 01480–86, Suk Samran District: THNHM 25736; 26002, 26016; Rayong Province, Klaeng District THNHM 14252–64, (12°42.164'N, 101°41.634'E): ZMKU AM 01514–20; Samut Prakarn Province, Phra Pradaeng District, Bang Krachao Sub-district: THNHM 26075–78; Satun Province, La-ngu District (6°51.861'N, 99°45.484'E): ZMKU AM 01493–

506; Songkhla Province, Songkhla lake: THNHM 02403–05; Surat Thani Province, Ko Samui District (9°33.220'N, 100°3.327'E): ZMKU AM 01384–89; Mueang Surat Thani District, Makhm Tia Sub-district: THNHM 05857–58; Trat Province, Ko Chang District (12°0.178'N, 102°22.639'E): ZMKU AM 01442–63; Klong Yai District: THNHM14292–94; Mueang Trat District: THNHM 16631–36, 24452; Trang Province, Kantang District, Ko Libong: THNHM 02249.

Appendix 2. Morphological measurements (mm) of adult male specimens of *Fejervarya*. Data are given as mean and standard deviation, followed by range in parentheses.

Characters	<i>F. cancrivora</i>	<i>F. cancrivora</i> Indonesia	<i>F. cancrivora</i> (previously	<i>F. moodiei</i> (previously
	neotype	and Malaysia	<i>F. raja</i>) Thailand	<i>F. cancrivora</i>) Thailand
	N = 1	N = 4	N = 26	N = 30
SVL	66.9	74.6 ± 3.8 (71.4 – 79.8)	71.0 ± 5.7 (60.2–78.9)	51.4 ± 5.4 (42.7–62.7)
HL	25.6	29.7 ± 1.1 (28.6 – 31.0)	29.1 ± 2.1 (24.5–32.4)	20.5 ± 1.8 (17.3–25.0)
HW	23.7	26.2 ± 1.6 (24.37 – 27.9)	26.6 ± 2.3 (22.0–30.5)	17.7 ± 1.8 (14.4–22.1)
STL	19.1	22.0 ± 0.6 (21.3– 22.8)	21.56 ± 1.4 (18.4–23.7)	15.4 ± 1.4 (13.3–18.8)
NS	4.3	4.9 ± 0.2 (4.7–5.2)	5.2 ± 0.4 (4.5–6.0)	3.8 ± 0.40 (3.1–4.7)
SL	10.5	11.7 ± 0.7 (11.0–12.6)	12.2 ± 0.7 (10.8–14.1)	8.4 ± 0.8 (6.8–10.2)
NTL	14.8	17.1 ± 0.78 (16.2–18.1)	16.6 ± 1.2 (14.2– 18.2)	12.0 ± 1.0 (10.5 –14.4)
EN	6.0	6.9 ± 0.5 (6.6–7.6)	6.7 ± 0.5 (5.6–7.6)	4.5 ± 0.4 (3.6–5.2)
TEL	2.3	3.2 ± 0.2 (3.08 – 3.4)	2.7 ± 0.6 (1.9–3.7)	1.7 ± 0.4 (1.2–2.8)
TD	5.1	5.2 ± 0.5 (4.6–5.7)	5.1 ± 0.4 (4.2–6.0)	4.1 ± 0.4 (3.3–4.9)
IN	2.8	3.9 ± 0.1 (3.8–3.9)	3.5 ± 0.4 (2.9–4.4)	2.5 ± 0.4 (1.9–3.5)
EL	6.6	6.9 ± 0.6 (6.1–7.4)	7.0 ± 0.7 (5.5–8.6)	5.9 ± 0.6 (4.8–7.1)
IOD	3.0	3.4 ± 0.2 (3.1–3.6)	3.5 ± 0.5 (2.7– 4.4)	3.2 ± 0.4 (2.5–3.8)
UEW	4.9	6.4 ± 0.4 (6.07 – 6.83)	5.9 ± 0.7 (4.9–7.3)	4.2 ± 0.5 (3.2–5.1)
HAL	16.2	18.00 ± 0.9 (16.9–19.1)	17.5 ± 1.2 (15.5–19.5)	12.7 ± 1.4 (10.6–15.7)
FAL	13.1	15.0 ± 0.9 (14.1–16.0)	13.6 ± 0.9 (11.5–15.0)	10.2 ± 1.2 (8.2–12.2)
THIGHL	30.2	34.7 ± 2.8 (31.6–38.0)	34.1 ± 2.8 (29.1–39.1)	23.4 ± 2.7 (19.0–29.3)
TL	34.5	38.4 ± 2.1 (36.5–41.4)	37.0 ± 3.0 (30.7 – 42.7)	24.44 ± 2.73 (19.84 – 30.3)
FOL	37.2	39.8 ± 1.0 (38.6–40.7)	38.35 ± 2.5 (30.7–43.3)	26.6 ± 3.1 (21.5–32.9)
TFOL	56.3	59.8 ± 1.4 (58.4–61.3)	56.2 ± 4.1 (48.7–62.8)	38.6 ± 4.6 (30.4–48.1)
1FL	13.8	14.3 ± 0.8 (13.3–15.0)	13.3 ± 1.1 (11.6–16.1)	9.4 ± 1.3 (7.2–12.4)
IMTL	4.1	3.9 ± 0.5 (3.5– 4.5)	4.3 ± 0.4 (3.2–5.2)	3.0 ± 0.5 (1.9–4.0)
ITL	12.4	13.2 ± 1.3 (11.3–14.3)	13.3 ± 1.0 (11.9–14.9)	9.2 ± 1.4 (7.0–11.3)
HL/HW	1.1	1.1 ± 0.0 (1.1–1.2)	1.1 ± 0.0 (1.0–1.2)	1.2 ± 0.0 (1.1–1.2)
IOD/HW	0.1	0.1 ± 0.0 (0.1–0.1)	0.1 ± 0.0 (0.1–0.2)	0.2 ± 0.2 (0.1–0.2)
SL/HL	0.4	0.4 ± 0.1 (0.4–0.4)	0.4 ± 0.0 (0.4– 0.5)	0.4 ± 0.0 (0.4–0.5)
EL/HL	0.3	0.2 ± 0.0 (0.2–0.3)	0.2 ± 0.0 (0.2–0.3)	0.3 ± 0.0 (0.2–0.3)
NS/EN	0.7	0.72 ± 0.1 (0.6–0.8)	0.8 ± 0.1 (0.7–0.9)	0.8 ± 0.1 (0.7–1.0)
EL/SL	0.6	0.6 ± 0.0 (0.6–0.6)	0.6 ± 0.0 (0.5–0.7)	0.7 ± 0.1 (0.6–0.8)
EL/EN	1.1	0.0 ± 0.1 (0.9–1.1)	1.0 ± 0.1 (1.0–1.2)	1.3 ± 0.2 (1.0–1.6)
IN/IOD	0.9	1.1 ± 0.1 (1.1–1.3)	1.0 ± 0.2 (0.8–1.5)	0.8 ± 0.1 (0.5–1.2)
TD/EL	0.8	0.8 ± 0.1 (0.6–0.8)	0.7 ± 0.1 (0.6–0.9)	0.7 ± 0.1 (0.6–0.8)
TEL/EL	0.3	0.5 ± 0.1 (0.4–0.6)	0.4 ± 0.1 (0.3–0.5)	0.3 ± 0.1 (0.2–0.4)
FAL/HAL	0.8	0.9 ± 0.0 (0.9–1.0)	0.8 ± 0.0 (0.7–0.9)	0.8 ± 0.1 (0.7– 0.9)
THIGHL/TL	0.9	0.8 ± 0.0 (0.8–0.9)	0.8 ± 0.0 (0.7–0.9)	1.0 ± 0.0 (0.9–1.1)
FOL/TL	1.1	1.0 ± 0.0 (1.0–1.1)	1.0 ± 0.0 (1.0–1.1)	1.1 ± 0.1 (0.9–1.2)
IMTL/TL	0.1	0.1 ± 0.0 (0.1–0.1)	0.1 ± 0.0 (0.1–1.1)	0.2 ± 0.0 (0.9–0.2)

Appendix 3. Morphological measurements (mm) of adult female specimens of *Fejervarya*. Data are given as mean and standard deviation, followed by range in parentheses.

Character	<i>F. moodiei</i>	<i>F. cancrivora</i>	<i>F. cancrivora</i>	<i>F. moodiei</i>
	CM 3724 Holotype <i>N</i> = 1	Indonesia and Malaysia <i>N</i> = 2	(previously <i>F. raja</i>) Thailand <i>N</i> = 12	(previously <i>F. cancrivora</i>) Thailand <i>N</i> = 32
SVL	73.3	93.9 ± 7.0 (93.0–98.0)	95.5 ± 3.5 (107.1–85.1)	69.0 ± 10.1 (50.0–81.8)
HL	29.8	35.3 ± 1.1 (34.5–36.1)	37.5 ± 2.0 (34.2–41.6)	27.1 ± 4.0 (19.2–33.0)
HW	27.3	28.0 ± 1.1 (27.2–28.7)	36.2 ± 2.3 (31.8–39.4)	24.5 ± 4.1 (17.2–30.9)
STL	22.4	35.1 ± 1.1 (34.3–35.9)	28.1 ± 1.4 (25.5–29.9)	20.1 ± 2.8 (14.6–23.6)
NS	5.3	5.9 ± 0.3 (5.7–6.1)	6.9 ± 0.6 (5.8–8.1)	4.9 ± 0.7 (3.5–6.1)
SL	11.4	15.2 ± 0.3 (14.9–15.4)	16.3 ± 1.0 (14.8–18.3)	11.1 ± 1.6 (7.9–13.2)
NTL	17.1	22.1 ± 0.8 (21.5–22.6)	21.5 ± 1.4 (19.0–24.1)	15.6 ± 2.2 (11.3–18.2)
EN	6.2	8.6 ± 0.3 (8.4–8.8)	9.0 ± 0.7 (7.9–10.4)	6.0 ± 0.8 (4.3–7.2)
TEL	3.8	5.2 ± 0.9 (4.6–5.9)	4.5 ± 0.8 (3.6–6.1)	3.0 ± 0.8 (1.4–4.0)
TD	5.8	6.4 ± 0.6 (5.6–6.8)	6.5 ± 0.6 (5.7–7.6)	4.9 ± 0.6 (3.8–5.7)
IN	3.3	4.1 ± 0.2 (4.0–4.2)	4.7 ± 0.6 (3.9–5.7)	3.2 ± 0.5 (2.2–4.0)
EL	6.7	7.5 ± 0.2 (7.4–7.6)	8.5 ± 0.7 (7.7–9.7)	6.9 ± 0.7 (5.4–8.4)
IOD	3.1	4.4 ± 0.5 (4.0–4.8)	4.8 ± 0.5 (4.0–5.7)	3.9 ± 0.64 (2.9–5.4)
UEW	5.9	7.4 ± 0.4 (7.1–7.7)	7.5 ± 0.7 (6.3–8.4)	5.4 ± 0.8 (4.2–6.9)
HAL	17.0	22.5 ± 1.5 (23.4–21.5)	22.5 ± 1.9 (19.6–26.1)	16.5 ± 2.3 (12.0–19.6)
FAL	12.9	17.6 ± 0.3 (17.4–17.8)	17.6 ± 1.4 (15.4–20.1)	13.0 ± 2.2 (9.2–16.4)
THIGHL	34.4	40.5 ± 4.6 (37.2–43.7)	43.8 ± 2.8 (40.0–48.8)	29.9 ± 4.3 (21.6–35.8)
TL	35.7	46.4 ± 0.5 (46.0–46.7)	48.0 ± 4.1 (42.6–54.9)	31.9 ± 4.5 (23.1–37.0)
FOL	40.2	48.5 ± 0.7 (48.0–49.0)	49.2 ± 3.9 (43.6–54.7)	34.8 ± 5.0 (24.6–42.7)
TFOL	57.2	73.5 ± 1.7 (72.3–74.7)	73.1 ± 7.7 (64.2–86.2)	49.9 ± 7.0 (35.4–58.8)
IFL	13.6	18.2 ± 0.6 (17.7–18.6)	17.8 ± 1.4 (15.2–20.3)	13.0 ± 2.1 (9.2–15.8)
IMTL	4.4	4.9 ± 0.5 (4.6–5.3)	5.7 ± 0.5 (4.9–6.4)	4.1 ± 0.7 (2.9–5.4)
ITL	14.8	16.7 ± 0.2 (16.5–16.9)	17.5 ± 1.9 (13.8–20.5)	12.4 ± 1.8 (8.5–15.2)

